

AD-A148 082

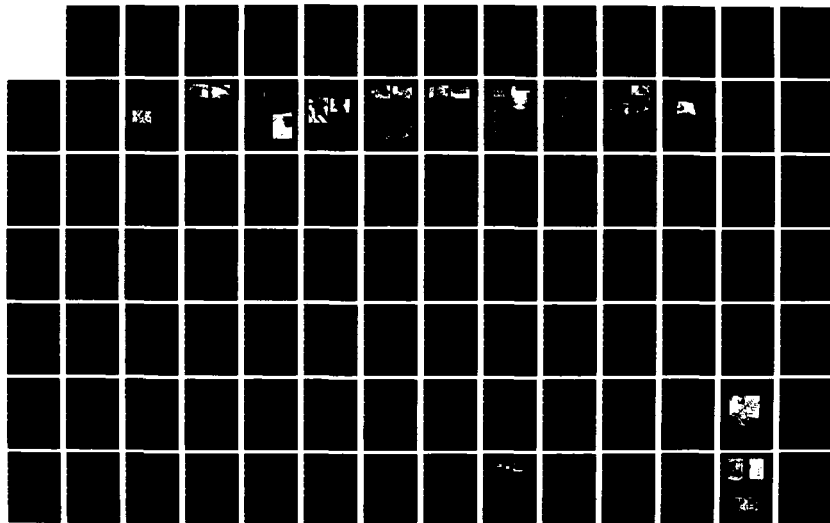
THE SHOCK AND VIBRATION BULLETIN PART 1 KEYNOTE ADDRESS  
INVITED PAPERS PA. (U) NAVAL RESEARCH LAB WASHINGTON DC  
SHOCK AND VIBRATION INFORMAT. SEP 78 BULL-48-PT-1

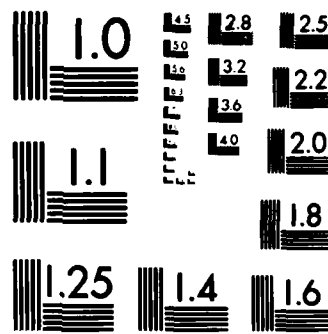
1/2

UNCLASSIFIED

F/G 20/11

NL





MICROCOPY RESOLUTION TEST CHART  
NATIONAL BUREAU OF STANDARDS-1963-A

# THE SHOCK AND VIBRATION BULLETIN

## Part 1

Keynote Address, Invited Papers, Panel Sessions,  
Modal Test and Analysis

SEPTEMBER 1978

A Publication of  
THE SHOCK AND VIBRATION  
INFORMATION CENTER  
Naval Research Laboratory, Washington, D.C.



Office of  
The Director of Defense  
Research and Engineering

Approved for public release; distribution unlimited.

84 11 26 195

AD-A148 082

THIS FILE COPY

**SYMPOSIUM MANAGEMENT**

**THE SHOCK AND VIBRATION INFORMATION CENTER**

Henry C. Pusey, Director  
Rudolph H. Volin  
J. Gordon Showalter  
Barbara Szymanski  
Carol Healey

**Bulletin Production**

Graphic Arts Branch, Technical Information Division,  
Naval Research Laboratory



**Bulletin 48**  
**(Part 1 of 4 Parts)**

# **THE SHOCK AND VIBRATION BULLETIN**

**September 1978**

**A Publication of  
THE SHOCK AND VIBRATION  
INFORMATION CENTER  
Naval Research Laboratory, Washington, D.C.**

**The 48th Symposium on Shock and Vibration was held at the Von Braun Civic Center, Huntsville, Alabama on October 18-20, 1977. The U.S. Army Missile Research and Development Command, Redstone Arsenal, Huntsville, Alabama was the host.**

**Office of  
The Director of Defense  
Research and Engineering**



## CONTENTS

### PAPERS APPEARING IN PART 1

#### Keynote Address

KEYNOTE ADDRESS .....	xi
Dr. John L. McDaniel, Deputy/Technical Director, U.S. Army Missile Research and Development Command, Redstone Arsenal, AL	

#### Invited Papers

SHOCK RESPONSE RESEARCH AT THE WATERWAYS EXPERIMENT STATION .....	1
Colonel John L. Cannon, U.S. Army Engineer Waterways Experiment Station, Vicksburg, MS	

TECHNICAL INFORMATION RESOURCES FOR THE SHOCK AND VIBRATION COMMUNITY .....	11
E.J. Kolb, U.S. Army Material Development and Readiness Command Alexandria, VA	

EARTHQUAKES, THEIR CAUSES AND EFFECTS .....	19
R.M. Hamilton, U.S. Geological Survey, Reston, VA	

#### Panel Sessions

SOFTWARE EVALUATION .....	23
DATA MANAGEMENT .....	31

#### Modal Test and Analysis

FORCE APPORTIONING FOR MODAL VIBRATION TESTING USING INCOMPLETE EXCITATION .....	39
G. Morosow, Martin Marietta Corporation, Denver, CO R.S. Ayre, University of Colorado, Boulder, CO	

<b>ON THE DISTRIBUTION OF SHAKER FORCES IN MULTIPLE-SHAKER MODAL TESTING</b> .....	49
W.L. Hallauer, Jr. and J.F. Stafford, Virginia Polytechnic Institute and State University, Blacksburg, VA	
<b>MODAL CONFIDENCE FACTOR IN VIBRATION TESTING</b> .....	65
S.R. Ibrahim, Old Dominion University, Norfolk, VA	
<b>A BUILDING BLOCK APPROACH TO THE DYNAMIC BEHAVIOR OF COMPLEX STRUCTURES USING EXPERIMENTAL AND ANALYTICAL MODAL MODELING TECHNIQUES</b> .....	77
J.C. Cromer and M. Lalanne, Institut National des Sciences Appliques, Villeurbanne, France	
D. Bonnetcase and L. Gaudriot, Metravib, Ecully, France	
<b>TRANSFER FUNCTION APPLICATIONS TO SPACECRAFT STRUCTURAL DYNAMICS</b> .....	93
J.R. Fowler, Hughes Aircraft Co., El Segundo, CA	
E. Dancy, Hewlett-Packard Co., Los Angeles, CA	
<b>LOAD TRANSFORMATION DEVELOPMENT CONSISTENT WITH MODAL SYNTHESIS TECHNIQUES</b> .....	103
R.F. Hruda and P.J. Jones, Martin Marietta Corporation, Denver, CO	
<b>REDUCED SYSTEM MODELS USING MODAL OSCILLATORS FOR SUBSYSTEMS (RATIONALLY NORMALIZED MODES)</b> .....	111
F.H. Wolff and A.J. Molnar, Westinghouse R&D Center, Pittsburgh, PA	
<b>CHARACTERIZATION OF TORPEDO STRUCTURAL MODES AND RESONANT FREQUENCIES</b> .....	119
C.M. Curtis, R.H. Messier, and B.E. Sandman, Naval Underwater Systems Center, Newport, R.I. and	
R. Brown, Bolt, Beranek and Newman, Cambridge, MA	
<b>LAGUERRE FUNCTION REPRESENTATION OF TRANSIENTS</b> .....	137
G.R. Spalding, Wright State University, Dayton, OH	

## **PAPERS APPEARING IN PART 2**

### **Isolation and Damping**

<b>SPECIFICATION OF DAMPING MATERIAL PERFORMANCE</b> D.I.G. Jones and J.P. Henderson, Air Force Materials Laboratory, Wright-Patterson AFB, OH
<b>A REDUCED-TEMPERATURE NOMOGRAM FOR CHARACTERIZATION OF DAMPING MATERIAL BEHAVIOR</b> D.I.G. Jones, Air Force Materials Laboratory, Wright-Patterson AFB, OH

**COMPUTERIZED PROCESSING AND EMPIRICAL REPRESENTATION OF  
VISCOELASTIC MATERIAL PROPERTY DATA AND PRELIMINARY  
CONSTRAINED LAYER DAMPING TREATMENT DESIGN**

L. Rogers and A. Nashif, Air Force Flight Dynamics Laboratory,  
Wright-Patterson AFB, OH

**NEW STRUCTURAL DAMPING TECHNIQUE FOR VIBRATION CONTROL**

B.M. Patel and G.E. Warnaka, Lord Kinematics, Erie, PA  
D.J. Mead, The University Southampton, United Kingdom

**VIBRATIONS OF A COMPRESSOR BLADE WITH SLIP AT THE ROOT**

D.I. G. Jones, Air Force Materials Laboratory, Wright-Patterson AFB, OH  
A. Muszyńska, Institute of Fundamental Technological Research,  
Polish Academy of Sciences, Warsaw, Poland

**RESPONSE OF A HELICAL SPRING CONSIDERING HYSTERETIC AND  
VISCOUS DAMPING**

P.F. Mlakar and R.E. Walker, U.S. Army Engineer Waterways Experiment  
Station, Vicksburg, MS

**DAMPING OF AN ENGINE EXHAUST STACK**

J.J. DeFelice, Sikorsky Aircraft, Stratford, CT  
A.D. Nashif, Anatrol Corporation, Cincinnati, OH

**MULTI-VARIABLE OPTIMIZATION FOR VIBRATION ISOLATION OF  
ROAD VEHICLES**

E. Esmailzadeh, Arya Mehr University of Technology, Tehran, Iran

**ISOLATION MOUNTS FOR THE HEAO-B X-RAY TELESCOPE**

H.L. Hain, Lord Kinematics, Erie, PA  
R. Miller, American Science and Engineering, Inc. Cambridge, MA

**Impact**

**BIRD IMPACT LOADING**

J.S. Wilbeck, Air Force Materials Laboratory, Wright-Patterson AFB, OH

**FREQUENCY RESPONSE AND DIFFERENTIATION REQUIREMENTS  
FOR IMPACT MEASUREMENTS**

A.S. Hu and H.T. Chen, New Mexico State University, Las Cruces, NM

**STRUCTURAL RESPONSE OF EARTH PENETRATORS IN  
ANGLE-OF-ATTACK IMPACTS**

J.D. Colton, SRI International, Menlo Park, CA

**SCALING AND PREDICTION OF IMPACT PUNCTURE OF SHIPPING  
CASKS FOR RADIOACTIVE MATERIALS**

W.E. Baker, Southwest Research Institute, San Antonio, TX

**FINITE ELEMENT ANALYSIS OF MULTICOMPONENT STRUCTURES  
IN RIGID BARRIER IMPACTS**

J.K. Gran, L.E. Schwer, J.D. Colton and H.E. Lindberg,  
SRI International, Menlo Park, CA

Blast

**TESTING PIPING CONSTRAINT ENERGY ABSORBERS FOR REACTOR  
CONTAINMENT APPLICATIONS**

R.C. Yaeger and R.C. Chou, Franklin Institute Research Laboratories,  
Philadelphia, PA

**PREDICTION OF CONSTRAINED SECONDARY FRAGMENT VELOCITIES**

P.S. Westine, Southwest Research Institute, San Antonio, TX  
J.H. Kineke, Jr., Ballistic Research Laboratories, Aberdeen, MD

**IMPEDANCE TECHNIQUES FOR SCALING AND FOR PREDICTING  
STRUCTURE RESPONSE TO AIR BLAST**

F.B. Safford, Agbabian Associates, El Segundo, CA  
R.E. Walker, U.S. Army Waterways Experiment Station, Vicksburg, MS  
T.E. Kennedy, Defense Nuclear Agency, Washington, DC

**PROBABILISTIC FAILURE ANALYSIS OF LINED TUNNELS IN ROCK**

D.A. Evensen and J.D. Collins, J.H. Wiggins Company, Redondo Beach, CA

**PAPERS APPEARING IN PART 3**

Structural Analysis

**A SOURCE OF LARGE ERRORS IN CALCULATING SYSTEM FREQUENCIES**

R.M. Mains, Washington University, St. Louis, MO

**RESEARCH METHOD OF THE EIGENMODES AND GENERALIZED  
ELEMENTS OF A LINEAR MECHANICAL STRUCTURE**

R. Fillod and J. Piranda, Laboratoire de Mécanique Appliquée,  
Besancon, France

**CALCULATION OF NATURAL FREQUENCIES AND MODE SHAPES OF  
MASS LOADED AIRCRAFT STRUCTURES**

P.W. Whaley, Air Force Flight Dynamics Laboratory,  
Wright-Patterson AFB, OH

**ROCKET MOTOR RESPONSE TO TRANSVERSE BLAST LOADING**

N.J. Huffington, Jr. and H.L. Wisniewski, U.S. Army Ballistic Research  
Laboratory, Aberdeen Proving Ground, MD

**EXPERIMENTAL AND THEORETICAL DYNAMIC ANALYSIS OF  
CARBON-GRAPHITE COMPOSITE SHELLS**

A. Harari and B.E. Sandman, Naval Underwater Systems Center, Newport, RI

**USE OF SHOCK SPECTRA TO EVALUATE JITTER OF A  
FLEXIBLE MANEUVERING SPACECRAFT**

W.J. Kacena, Martin Marietta Corporation, Denver, CO

**BUCKLING OF EULER'S ROD IN THE PRESENCE OF  
ERGODIC RANDOM DAMPING**

H.H.E. Leipholz, University of Waterloo, Waterloo, Ontario, Canada

**WAVE PROPAGATION IN A CYLINDRICAL SHELL WITH  
JOINT DISCONTINUITY**

A. Harari, Naval Underwater Systems Center, Newport, RI

**RESPONSE TO MOVING LOADS OVER A CRYSTALLINE HALF-SPACE**

S. De, Old Engineering Office, West Bengal, India

**ADJUSTMENT OF A CONSERVATIVE NON GYROSCOPIC MATHEMATICAL  
MODEL FROM MEASUREMENT**

L. Bugeat, R. Fillod, G. Lallement, and J. Piranda, Laboratoire de  
Mecanique Appliquee, Besancon, France

**FIRST-PASSAGE FAILURE PROBABILITY IN RANDOM VIBRATION  
OF STRUCTURES WITH RANDOM PROPERTIES**

N. Nakagawa, and R. Kawai, Kobe University, Kobe, Japan  
K. Funahashi, Kawasaki Heavy Industries, Ltd. Kobe, Japan

**Fatigue**

**FRACTURE MECHANICS APPLIES TO STEP-STRESS FATIGUE UNDER  
SINE/RANDOM VIBRATION**

R.G. Lambert, General Electric Company, Utica, NY

**RANDOM FATIGUE DAMAGE APPROACH TO MACHINERY MAINTENANCE**

T.S. Sankar and G.D. Xistris, Concordia University, Montreal, Quebec, Canada  
G.L. Ostiguy, Ecole Polytechnique, Montreal, Quebec, Canada

**PAPERS APPEARING IN PART 4**

**Vibration Testing**

**A MATHEMATICAL METHOD FOR DETERMINING A LABORATORY  
SIMULATION OF THE CAPTIVE-FLIGHT VIBRATIONAL  
ENVIRONMENT**

S. Ogden, Pacific Missile Test Center, Point Mugu, CA

**ACOUSTICS OR SHAKERS FOR SIMULATION OF CAPTIVE  
FLIGHT VIBRATION**

A.M. Spandrio and M.E. Burke, Pacific Missile Test Center, Point Mugu, CA

**AUTOMATIC ENVIRONMENTAL CONTROL SYSTEM FOR MISSION  
PROFILE TESTING**

R. Schilken, Pacific Missile Test Center, Point Mugu, CA

**BROAD-BAND MECHANICAL VIBRATION AMPLIFIER**

R.T. Fandrich, Harris Corporation, Melbourne, FL

**STABILITY AND FREQUENCY RESPONSE OF HYDRO-MECHANICAL  
SHAKERS IN VIBRATION RIGS**

S. Sankar, Concordia University, Montreal, Canada

**MIL-STD-781C RANDOM RELIABILITY TESTING PERFORMED BY  
USING ACOUSTIC COUPLING**

S.M. Landre, Harris Corporation, Melbourne, FL

**CONSERVATISM IN RANDOM VIBRATION ANALYSIS AND TESTING**

T.L. Paez, Sandia Laboratories, Albuquerque, NM

**INCANDESCENT LAMP LIFE UNDER RANDOM VIBRATION**

C.J. Beck, Jr., Boeing Aerospace Company, Seattle, WA

**Instrumentation**

**ANGULAR VIBRATION MEASUREMENT TECHNIQUES**

P.W. Whaley and M.W. Obal, Air Force Flight Dynamics Laboratory,  
Wright-Patterson AFB, OH

**HIGH FREQUENCY GROUND VIBRATION MEASUREMENT**

H. Nolle, Monash University, Clayton, Victoria, Australia

**THE RECIPROCITY CALIBRATION OF VIBRATION STANDARDS  
OVER AN EXTENDED FREQUENCY RANGE**

R.R. Bouche, Bouche Laboratories, Sun Valley, CA

**A NON-CONTACTING BETA BACKSCATTER GAGE FOR EXPLOSIVE  
QUANTITY MEASUREMENT**

P.B. Higgins, F.H. Mathews and R.A. Benham, Sandia Laboratories,  
Albuquerque, NM

**DATA ACQUISITION SYSTEMS FOR THE IMMEDIATE FUTURE**

J.F. Schneider, Air Force Weapons Laboratory, Kirtland AFB, NM

**Loads and Environments**

**THE VIBRATION RESPONSE OF THE PHOENIX MISSILE IN THE F-14  
AIRCRAFT CAPTIVE-FLIGHT ENVIRONMENT**

M.E. Burke, Pacific Missile Test Center, Point Mugu, CA

**SOME DYNAMIC RESPONSE ENVIRONMENTAL MEASUREMENTS  
OF VARIOUS TACTICAL WEAPONS**

W.W. Parmenter, Naval Weapons Center, China Lake, CA

**TURBULENT-BOUNDARY-LAYER EXCITATION AND RESPONSE THERETO  
FOR A HIGH-PERFORMANCE CONICAL VEHICLE**

C.M. Ailman, McDonnell-Douglas Astro. Corp. Employee for this work.  
Currently an independent researcher in Los Angeles, CA

**CALCULATION OF ATTACH POINT LOADS DUE TO POSSIBLE COMBUSTION  
INSTABILITY IN THE SPACE SHUTTLE SOLID ROCKET BOOSTERS**

F.R. Jensen and D.T. Wang, Hercules Inc., Magna, UT

**Tracked Vehicles**

**HULL VIBRATORY POWER FLOW AND RESULTING INTERIOR NOISE  
ON THE M113A ARMORED PERSONNEL CARRIER**

P.E. Rentz, Bolt Beranek and Newman, Canoga Park, CA

**REDUCING TRACKED VEHICLE VIBRATION AND NOISE HARDWARE  
CONSIDERATIONS**

R.B. Hare and T.R. Norris, FMC Corporation, San Jose, CA

**THE USE OF AN EARTH BERM TO REDUCE THE ENVIRONMENTAL  
NOISE IMPACT OF THE TEST TRACK AT DETROIT ARSENAL**

N.D. Lewis, U.S. Army Environmental Hygiene Agency,  
Aberdeen Proving Ground, MD

**PAPERS APPEARING IN THE SUPPLEMENT**

**ANALYSIS OF ACOUSTIC COATINGS BY THE FINITE  
ELEMENT METHOD**

Anthony J. Kalinowski, Naval Underwater Systemc Center,  
New London, CT

**DEVELOPMENT AND VALIDATION OF PRELAUNCH SHOCK CAPABILITY  
FOR THE NAVY TOMAHAWK CRUISE MISSILE**

W.M. Dreyer, R.E. Martin, R.G. Huntington, General Dynamics  
Convair Division, San Diego, CA



## KEYNOTE ADDRESS

### KEYNOTE ADDRESS

John L. McDaniel  
U.S. Army Missile Research and Development Command  
Redstone Arsenal, AL

Adequate testing is an essential step in the development process. Much of the success in developing better weapons and delivering them to the soldier is due to insistence that they survive adequate environmental tests. Designers scream that their sophisticated hardware is being torn up but testing continues because the real world on the battlefield is the wrong place to find design weaknesses. Designers should analyze and simulate the environments which their components will have to endure before they are incorporated into missile and rocket systems. Certainly the analysis of the response of these components to the shock and vibration stimuli is significant to their survival. Testing in the US Army Missile Research and Development Command (MIRADCOM) laboratories, to the shock and vibration criteria which have been developed and continuously updated, reveals how well the analysis has been done. This booklet will discuss shock and vibration from the Army viewpoint and highlight some areas where improvements in test methods would be especially helpful.

In February 1977 the US Army Missile Command (MICOM) was divided into two new commands: the US Army Missile Material Readiness Command (MIRCOM) and the US Army Missile Research and Development Command (MIRADCOM).

MIRCOM, the readiness command, as the name implies, has responsibility for production of missile and related hardware, supplying this material to the troops in the field. It is responsible for material maintenance until it is obsolete and must be replaced. MIRCOM is commanded by MAJ GEN Louis Rachmeler.

MIRADCOM is the research and development side of the house at Redstone and is responsible for missile research and development management, the Missile Intelligence Agency, and the in-house laboratories. MAJ GEN Charles F. Means is the commander of MIRADCOM.

These two commands, teamed with the US Army Missile and Munitions Center and School, also located at Redstone, work together to develop, produce, maintain, and train soldiers in the use of the weapons necessary for the modern army to defend itself against outside threats to the security of the United States.

MIRADCOM has the in-house, "hands on" technical expertise and facilities. It supports the production side in

requalification of new production hardware, modification and improvement of existing systems, and incorporation of new developments into fielded systems. However, MIRADCOM is primarily involved with the development of new advanced systems.

MIRADCOM has full responsibility for the development and initial procurement of all Army missile systems. A quick look at some of the new systems will illustrate the challenge of developing realistic shock and vibration analysis and simulation testing of missiles. PERSHING II is an extremely accurate long-range missile system currently in advanced development. PERSHING II will provide improved military effectiveness against the complete target spectrum, while limiting collateral effects to the military target.

The accuracy for PERSHING II is obtained by the use of a terminally guided reentry vehicle, which contains both the guidance and warhead. The terminal guidance approach for PERSHING II utilizes a radar area correlation process which compares a live target scene from a scanning radar with a stored reference scene of the target area.

The tactical reentry vehicle will use the current PERSHING solid propellant boosters and can be accommodated by present PERSHING IA ground equipment with minor modifications.

The VIPER system is a short-range, manportable, anti-tank weapon. The tactical round consists of a free-flight in-tube burning rocket which is packaged, sealed, and transported in an expendable launcher that also serves as the tactical storage container. This system satisfies the operational requirement to provide a higher hit probability, greater lethality, longer effective range, and increased reliability. The VIPER weapon will be capable of being treated as a round of ammunition, will be maintenance free, capable of long term storage without significant degradation, and will be relatively immune to worldwide environmental conditions.

The general support rocket system (GSR) is envisioned to be a modular, multiple rocket launcher system designed to provide rapid, nonnuclear, indirect fire support against time-sensitive targets. The rocket will be unguided and will have a high degree of accuracy. The launcher loader will be a self-propelled tracked vehicle with the capability to support multiple rocket launchers. The fire control equipment will be part of the launcher loader vehicle. The rocket pod will

serve as a shipping container, a storage container, as well as a launch pod for the rocket.

The mission of GSRS is to provide field artillery fires in general support of a division of corps by delivering large volumes of effective firepower in a very short time against critical, time-sensitive targets with a variety of warhead options and without the necessity to mass large numbers of weapons and men.

**HELLFIRE** - The HELLFIRE weapon system will consist of the HELLFIRE missile system, laser designators, communication network, and scout and attack helicopters. Ground designation and scout helicopter designation provide the attack helicopter with a launch-and-leave capability. Fire-and-forget missile/seeker configurations will allow target acquisition and firing from the attack helicopter without the assistance of any type of target designation.

The HELLFIRE missile system will include a helicopter launcher missile equipped with a terminal homing seeker and a shaped charged warhead. The missile configuration will have the capability for modular seeker replacements.

The HELLFIRE modular missile system is designed to defeat hardpoint targets in the forward battle area over a wide operating envelope of speed, flight profiles, and attack scenarios.

**STINGER** - STINGER is the shoulder-fired member of the family of short range air defense (SHORAD) weapons protecting the field army units. The system will normally be employed to provide low-altitude air defense for units operating near the forward edge of the battle area. The system may also be employed to provide air defense for vital areas when no other ground-based air defense means are available. The complete STINGER weapon system consists of the weapon round, battery coolant unit, identification friend or foe, containers, and support and training equipment.

The US ROLAND is an all-weather, low-altitude, command-to-line-of-sight (CLOS) air defense weapon system designed to perform the SHORAD mission. Salient features of the US ROLAND are as follows:

1. A missile can be launched at an attacking aircraft in a matter of seconds.
2. Each fire unit contains 10 missiles that can be fired during the course of a single mass raid.
3. The fire unit is mounted on the self-propelled, M109 tracked vehicle.
4. The surveillance radar can perform target search during fire unit movement.
5. The fire unit can halt and fire at attacking aircraft within seconds after target detection while on the move.
6. The fire unit can move from a deployed position within seconds after receiving a march order.

The modularity of the fire unit provides potential for usage on a variety of platforms in the future. The system is almost identical to the European version of the system. Almost all components will be fully interchangeable. One major difference is the mounting of the air defense components into a self-contained module which can be removed from the vehicle.

A broad spectrum of land combat and air defense, ranging from shoulder fired infantry weapons to long range nuclear missiles is being developed. As a result, there are wide variations in environmental criteria. These operational environments and some of the types of simulated tests used to develop and produce these systems will be summarized in the following paragraphs.

MIRADCOM must concern itself with two types of transportation and handling: the commercial or logistical transportation from point of manufacture to the final use area and the field or tactical transportation associated with training and combat.

Anyone who has used the US mail or commercial freight lines is well aware of the problems associated with this form of transportation. Military equipment shipped by commercial truck, rail, air, or ship fares no better. In World War II, it was found that more than half of the equipment arrived at the scene of operations in either a damaged or unusable condition due to handling and transportation induced shock and vibration. All Army equipment is packaged in an attempt to protect it from damage by loading, transporting, or accidental dropping. All containers used for Army equipment are designed and tested to this anticipated environment.

For example, within the last 18 months at MIRADCOM, a new 18,000 force-lb shaker and a high performance shock machine were purchased. The shaker sustained over \$2000.00 in damages in shipment from the manufacturer. The shock machine was so badly damaged in a train derailment that it was returned to the manufacturer.

Those who procure military equipment should be aware that the commercial shipment and the shock and vibration problems associated with this environment cannot be overlooked.

During the other form of transportation referred to as field or tactical use, the Army has a large number of shock and vibration problems to overcome. Some systems while still packaged for commercial transportation may be transported by military truck, tracked vehicle, or helicopter before they are removed from their protective containers. Once the item is removed from its container, it may be mounted to a helicopter, tank, truck, trailer, or man carried. Each of these forms of field use has a unique vibration and shock environment that must be considered when it is designed. Self-induced shock and vibration during equipment use can be severe and must not be discounted.

Obviously, each system fielded by the Army is unique to its environment; each system must be tested differently. The environment for a helicopter mounted missile is different from that experienced by a man carried weapon.

Some of the tests that may be used at MIRADCOM to see that this toughness is built in may be a series that starts with a design verification test on prototype hardware to make modal studies, determine dynamic response, and conduct preflight vibration tests to ensure basic integrity.

Later in the development cycle, prequalification tests may be conducted to apply military standard shock and vibration tests to hardware representative of production type items is an effort to discover any design deficiencies prior to full qualification and subsequent production.

Next, safety tests are conducted in which these items are overstressed with shock and vibration to determine if any hazards to the field troops exist due to extreme environments. Safety tests will also be conducted at normal vibration or shock levels to satisfy requirements for a flight release on new designs for equipment to be installed on aircraft.

Qualification tests are conducted to insure that the equipment will meet those environments anticipated in world-wide development. These items are tested in larger samples than previous tests for statistical confidence and consist of a full sequence of shipping, handling, field, and operational tests.

When a system is fielded and in the hands of the combat troops, continual testing is still required. This program is called "fly-to-buy." The fly-to-buy plan has been very successful from the Army's standpoint in assuring the Army that the hardware bought is reliable, and maintains the standards developed into it. These tests may be called first article tests, lot acceptance, or production verification; but in essence, it means that for each production lot, a sample is taken, environmentally treated, and operated. If these tests are successful, then the lot is accepted.

Since weapons undergo this wide diversity of stimuli, MIRADCOM is confronted with the difficult problem of establishing shock and vibration tests which are realistic and adequate to insure survival in the real world. All criteria are important: the first, because inadequate tests mean inadequate weapons for the soldier; the second, because excessive requirements drive up weight and costs.

There is an expression "a good test is worth a thousand expert opinions." It is not all that simple until it is determined just what a "good test" is. A good test was once defined as "one which fails equipment which will fail in service and will not fail equipment which is satisfactory for service."

Many times project managers will very comfortably specify a procedure, curve, and figure from a military standard and then move on to what they think are more important things. The result is often a waste basket full of parts and a frantic cry for help. This is never a good test. The solution is proper analysis and simulation prior to testing.

Another important consideration is how the vibration community can best communicate this complex and specialized technology to managers in a form most useful to them in selecting requirements and establishing test specifications.

The answers to these questions should be an important part of this symposium's theme. From the Army's standpoint (at MIRADCOM) this technology should be used efficiently so that it transfers to cheaper, lighter, and more reliable equipment in the field. Of course, MIRADCOM along with anyone else in the development process, is always constrained by the state-of-the-art, cost, schedules, and standardization. Much of the time, aspirations are not realized. All that is accomplished here should be directed toward something constructive whether it is better military hardware, advancing the state-of-the-art, or creating a better life style for all.

MIRADCOM has an excellent shock and vibration capability which is used as a means of staying abreast of what is going on in the entire shock and vibration community. The technology has been moving rapidly in the past few years and gatherings like this symposium are valuable. Close coordination and communication help to prevent wasting resources and resolving problems someone else has already solved.

In any technical endeavor there is always room for improvement. There are two areas that deserve increased attention.

The first one is a way this community can best communicate vibration and shock to a manager in a form more useful to him in developing hardware. There are military specifications which are used almost universally in establishing initial requirements but may not always be applicable to the product being developed. These specifications are sometimes overly severe when interpreted literally and can lead to laboratory failures which are not reproducible in the field. General specifications have been used for many years at Redstone with much success, but sometimes it is difficult to apply a general standard specification to a sophisticated design intended for specialized use.

Tests that have been proposed to circumvent this problem and tailored to a particular system or subsystem have in some cases been worse due to the cost and time involved. These tests generally require extensive facilities such as multiple shakers or computer control systems, thus few groups can perform them. This really becomes a problem when new subsystems or components are developed and need qualifying. Another disadvantage to tests of this type is that they are difficult to describe in, and interpret from, a procurement document.

A second challenge is one of data exchange and presentation. The Army fields equipment which is transported by a multitude of commercial and tactical ground and airborne vehicles. Many government agencies and contractors have conducted field tests on most of these vehicles and have recorded and analyzed hours and hours of data. It would obviously be of immense value to everyone involved to have all of these data compiled at one location and made available to participating members of the shock and vibration community. MIRADCOM's dynamics people have received many inquiries from project managers looking for such information. For example, a project manager may want to know if he can install his system in a "Y" vehicle without conducting a large scale measurement and test program even though the system was originally designed for the "X" vehicle. Such

questions could be handled much better if immediate reference could be made to a document presenting summarized data from both the "X" and "Y" vehicles.

These are the challenges for future developments in the field of shock and vibration systems.

## INVITED PAPERS

### SHOCK RESPONSE RESEARCH AT THE WATERWAYS EXPERIMENT STATION

Colonel John L. Cannon  
U.S. Army Engineer Waterways Experiment Station  
Vicksburg, Mississippi

#### Background

The Waterways Experiment Station (WES) was established in 1929, two years after the most devastating flood ever to strike on the lower reaches of the Mississippi River basin. The Waterways Experiment Station is located in Vicksburg, Mississippi, which is situated midway between Memphis and New Orleans. An aerial view of the Waterways Experiment Station, (Figure 1) gives some idea of the physical plant located on 600 acres of beautifully wooded areas that have been recognized this past year as an arboretum by the Garden Clubs of Mississippi.

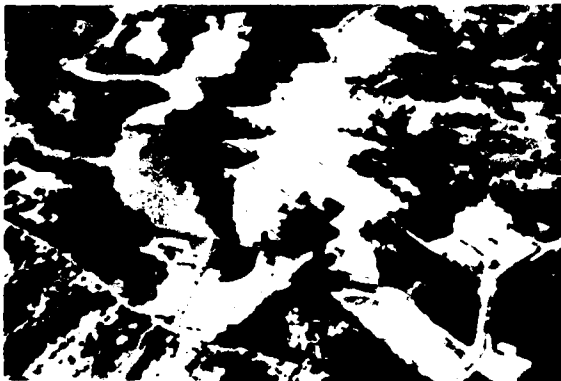
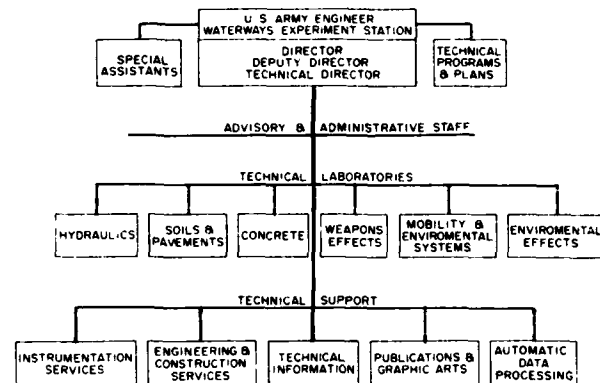


Figure 1 - Aerial view of Waterways Experiment Station

The original technical responsibilities of WES involved hydraulic engineering with the physical model being the principle tool for early investigators. Since then the technical mission has grown and now includes research in soils, concrete, mobility, weapons effects and environmental engineering. The technical missions are accomplished by six technical laboratories, (Figure 2). The administrative and supporting technical staff, i.e., Instrumentation, ADPC, Shops, etc., are also shown. Our current strength is about 1400 employees.

#### Shock Response Research

Today, I would like to discuss the shock and vibration work done at the Waterways Experiment Station primarily in the Weapons Effects, Soils and Pavements, and Hydraulics



JULY 75

Figure 2 - Technical missions of the Waterways Experiment Station

**Laboratories.** As the origin of the Waterways Experiment Station WES was based on the use of physical models for hydraulic studies, we have employed this tool to other fields, coupled with theoretical studies as well as complex laboratory and prototype testing. I have selected several projects that will serve to exemplify the shock response research conducted.

#### Dams

**North Fork Dam.** This 150-foot-high, 620-foot-long (crest length) arch dam is located on the North Fork River in Northern California several miles upstream from the site of the Auburn Dam now under construction, (Figure 3).

A 1/24-scale model dam was constructed and subjected to vibratory loads; in one case, two mechanical vibrators were placed on the crest and vibrated in-and-out of phase with each other, (Figure 4). A large hydraulic shaker was also used to excite the base of the model dam for comparison with results obtained from the tests using vibrators on the crest. Shaking the dam at its base more nearly represents the loadings that might be induced by an actual earthquake. Vibration tests similar to those on the model were conducted on prototype.

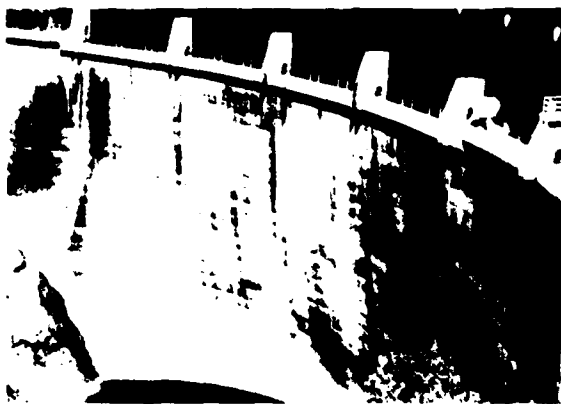


Figure 3 - North Fork Dam



Figure 4 - Vibration test of 1/24 scale model North Fork Dam

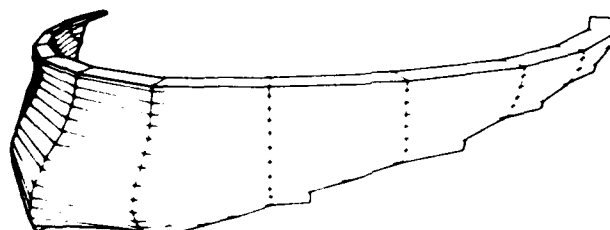


Figure 5 - Finite element model of perfectly fixed dam

In addition to the model and prototype tests, finite element calculations were made for the case where the dam was considered perfectly fixed, (Figure 5) and another where the dam was considered to be tied to the foundation material, (Figure 6).

The mode shapes for model results scaled to prototype compared very favorably, (Figure 7). The finite element prediction also compared favorably with test results, (Figure 8). Note that the predictions for the finite element code that included the foundation material compared best with the experimental results.

In addition, the damping factors for the dam with the reservoir full and empty were determined as well as the participation of the water mass in influencing the natural frequency of the dam for various modes of vibration.

A comparison of the calculated natural frequencies, those measured on the prototype, and the model results scaled to the prototype, show excellent agreement and, therefore, add to the confidence in the role of both the physical and analytical model in making predictions, (Figure 9).

As a result of the near failure (Figure 10) of the lower San Fernando Dam during the San Fernando Earthquake of 9 February 1971, the Corps of Engineers has been reevaluating its hydraulic fill dams. The Waterways Experiment Station

has been assisting Districts in performing seismic analysis of these structures. Shown Figure 11 is the finite element grid of Fort Peck Dam that was used in the computerized portion of the dynamic analysis of the Fort Peck Dam.

Controlling the high-velocity flow that occurs in some sluiceways in hydraulic structures can cause flow-induced hydroelastic vibrations. These vibrations can cause substantial damage to even massive structures. An example of such damage occurred at Libby Dam on the Kootenai River, see Figure 12. In this case, severe cavitation damage occurred along the floor and walls of the sluice and shock-type noises came from the gate, see Figure 13 and 14. The sluice was repaired, the control valve was instrumented with accelerometers and pressure transducers were installed in the sluice floor, see Figures 15 and 16. The test results showed no correlation between the flow-induced vibration of the control gate and the large pressure fluctuations along the floor of the sluice. Since the alternate reason for the large pressure fluctuation involved the slope of the sluice (which causes low pressures to exist along the sluice floor) and the roughness of the floor (which causes large turbulent fluctuations in the flow) the problem was further studied by means of hydraulic model tests, see Figure 17. The results of these tests indicate that an aerator could be placed in the sluice so as to eliminate the cavitation damage in the sluice and that the gate vibration could be prevented by limiting the gate opening or modifying the intake roof shape and; hence, the problem was solved through the use of a model.

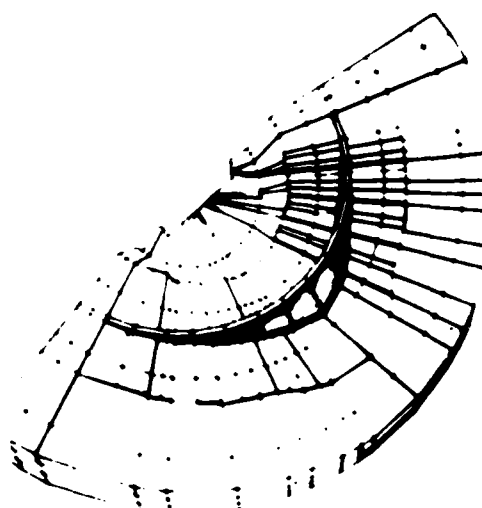
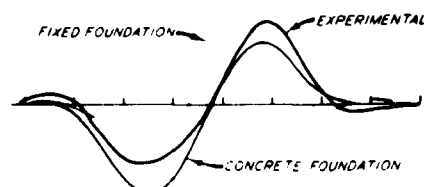
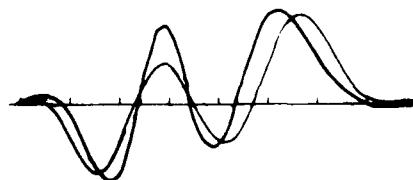


Figure 6 - Finite element model of dam tied to foundation material



1<sup>ST</sup> ASYMMETRIC MODE

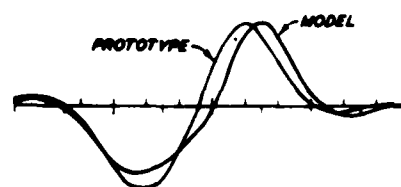


2<sup>ND</sup> ASYMMETRIC MODE

Figure 8 - Comparison of experimental and analytical normalized mode shapes, reservoir full

MODE	NATURAL FREQUENCY, Hz		
	FULL SCALE	MODEL (SCALED)	ANALYTICAL (SCALED)
1	-	-	5.17
2	5.80	4.29	5.08
3	6.30	6.12	6.29
4	7.47	7.29	7.58
5	8.53	10.10	-

Figure 9 - Comparison of natural frequencies



MODE 2

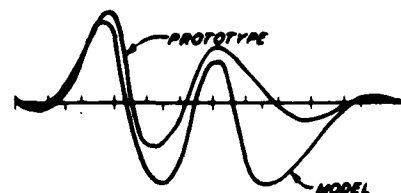


Figure 7 - Comparison of normalized full scale and model mode shapes, radial crest deflections



Figure 10 - Lower San Fernando Dam

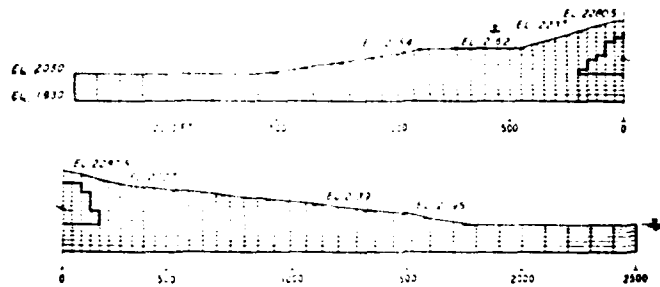


Figure 11 - Finite element dynamic analyses, Fort Peck Dam



Figure 12 - Libby Dam

#### Structures

The shock and vibration transmissivity characteristics of the Perimeter Acquisition Radar (PAR) building, was studied by conducting model tests. The building is 125 feet high, 194 feet wide at its base, has walls that are 6 feet thick at the base, and floors that are 3 feet thick, see Figure 18.

A 1/12-scale model of the prototype was constructed and tested in the DIAL PACK Event (500-tons of HE) conducted at the Suffield Experimental Station in Canada, see Figure 19. Interface surface pressures as well as internal acceleration and strain were measured.

After the DIAL PACK Event, tests were conducted by systematically placing mechanical vibrators on the outside

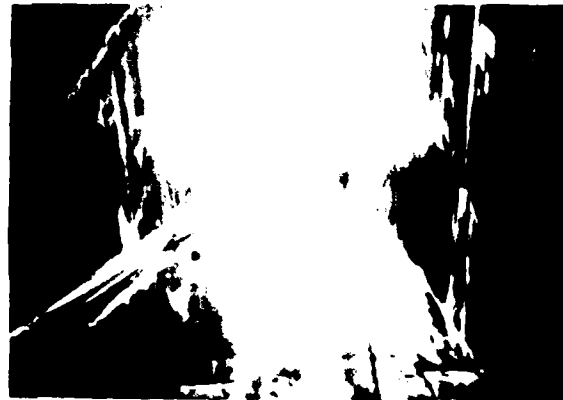


Figure 13 - Damage to floor and walls of sluice of Libby Dam

roof and walls of the structure so that the entire external surface was mapped and the signals recorded by accelerometers located at fixed locations within the structure produced signatures indicating how energy was transferred from an external location to an internal location, (Figure 20). This signature is called the transfer function and relates some external location to an internal location for a range of frequencies, (Figure 21).

By knowing the transfer function for all the patches over the entire surface of the structure, it was possible to engulf the structure with the actual DIAL PACK airblast load, apply the appropriate transfer function and predict the transient acceleration of particular points within the structure, (Figure 22).

Comparisons of predicted (using the transfer functions) and measured results of the DIAL PACK tests, are in close agreement thereby giving some confidence in the use of transfer function, (Figure 23).

Vibration tests were then conducted on the prototype; however, it was not practical to map the entire structure because of the size of the vibrator and the building. Therefore, by verifying the principle of reciprocity, it was also possible to map the walls, (Figure 24). First the vibrator was placed on the roof as shown, and a measurement made at a point on one of the floors. Then the drive point and measuring point





Figure 14 Damage to floor and walls of sluice of Libby Dam



Figure 15 Installation of pressure transducers in sluice floor, Libby Dam

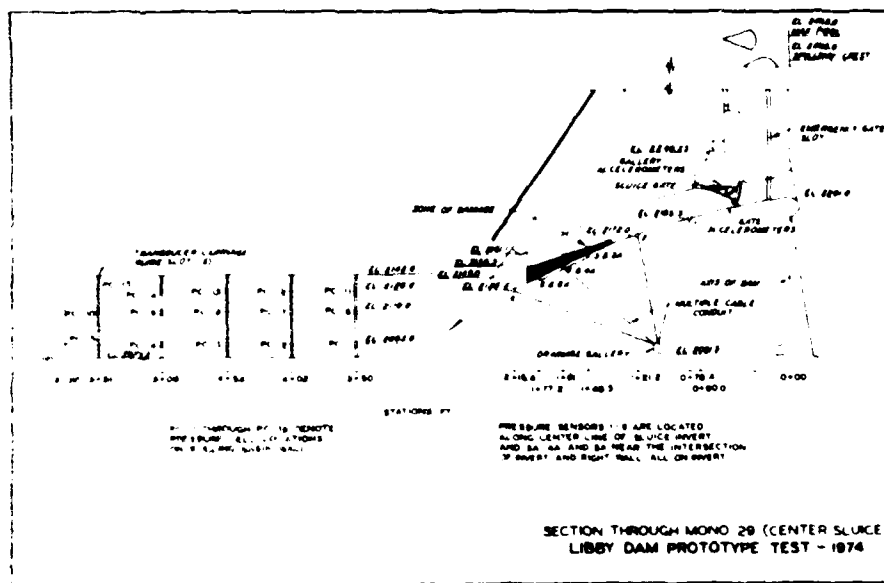


Figure 16 Instrumentation in sluice of Libby Dam

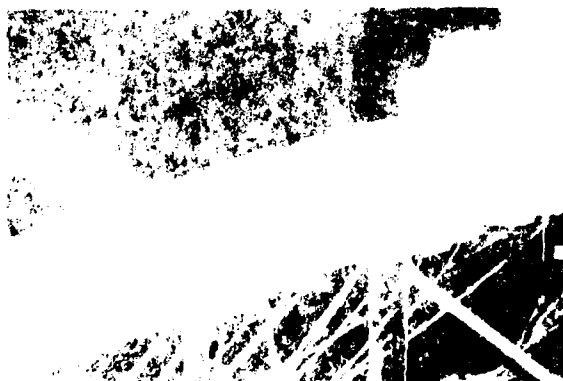


Figure 17 Close-up view of concrete model test of Sluice of Libby Dam



Figure 18 Perimeter acquisition radar (PAR) site



Figure 19 - One-twelfth scale model of perimeter acquisition radar building

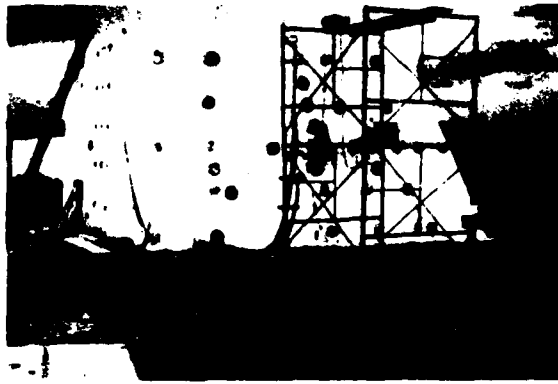


Figure 20 - Arrangement for measuring transfer function on wall of scale model perimeter acquisition radar building

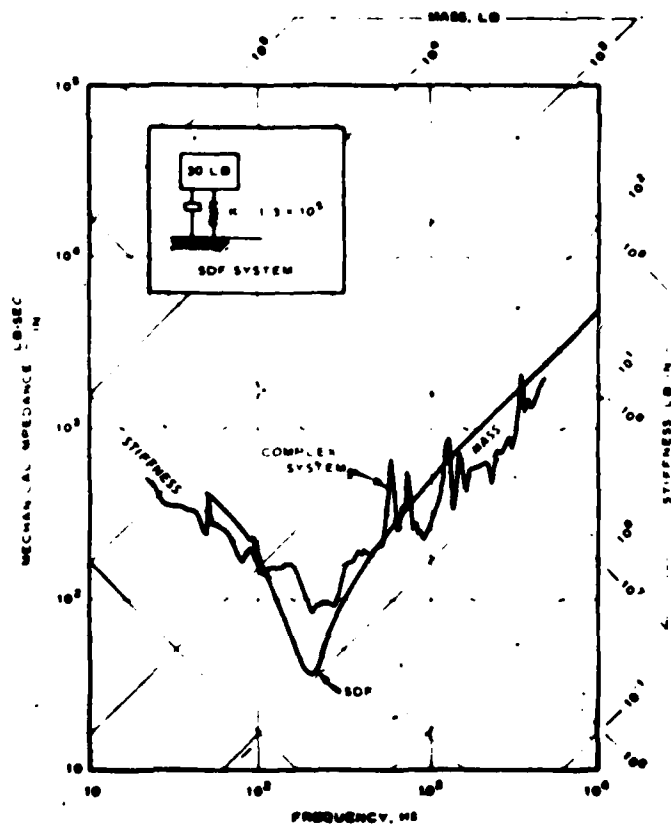
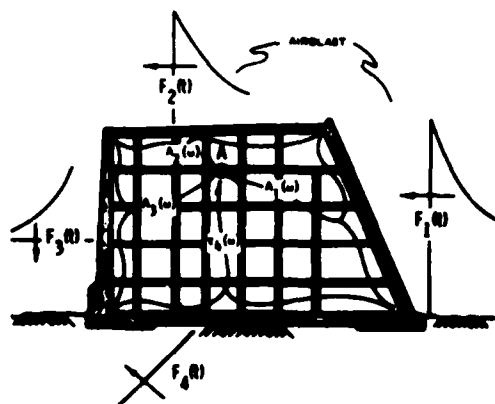
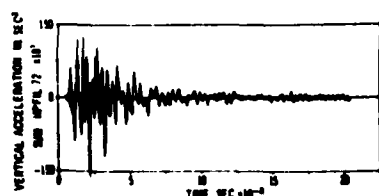


Figure 21 - Typical transfer function

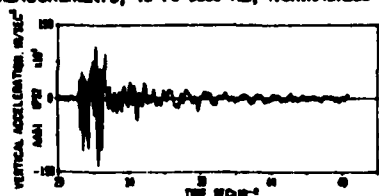


RESPONSE AT POINT A =  $R_A(t)$   
 $R_A(t) = R_A(t) = \sum F_1(t) A_1(t) + F_2(t) A_2(t) + F_3(t) A_3(t) + F_4(t) A_4(t) + \dots$

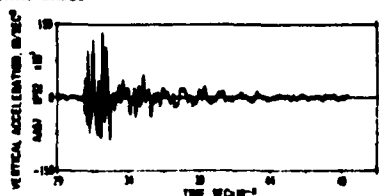
Figure 22 - Schematic load and transmission paths for scale model perimeter acquisition radar building



PREDICTED ACCELERATION-TIME HISTORY MODEL PARB FIFTH FLOOR CENTER FROM 21 ACCELERATION ACCEPTANCE MEASUREMENTS AND 3 AIR-BLAST MEASUREMENTS, 72 TO 3000 HZ, NORMALIZED



MODEL PARB ACCELERATION RECORD AA 51, EVENT DIAL PACK, FIFTH FLOOR NEAR CENTER, 72 HZ TO 3 KHZ, NORMALIZED



MODEL PARB ACCELERATION RECORD AA 57, EVENT DIAL PACK, FIFTH FLOOR NEAR CENTER, 72 HZ TO 3 KHZ, NORMALIZED

Figure 23 - Predicted and measured motions on fifth floor of model perimeter acquisition radar building

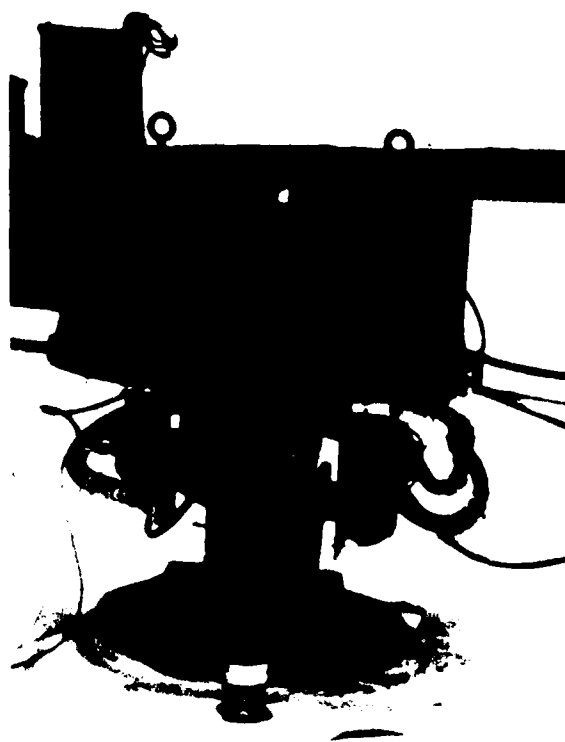


Figure 24 - Vibration input on roof of perimeter acquisition radar building

were interchanged; i.e., the vibrator was placed on the floor and the measurement made at the former drive point on the roof.

A comparison of records for such a situation shows that reciprocity does exist for both the model and prototype, (Figure 25). Thus, the transfer function could be obtained without placing the vibrators on the external walls of the prototype.

It was also shown that the transfer function for the model can be scaled to the prototype condition, see Figure 26.

By using these functions, it was possible to predict the acceleration response within the prototype structure at selected points for a variety of external airblast loads.

#### Equipment Fragility

During the same timeframe of the PAR prototype testing, a test series was conducted on the shock isolation platforms of the complete SAFEGUARD System. The areas of these rectangular platforms range from 15 sq ft to more than 3000 sq ft, and the isolated weight ranges from 1400 lb to 284,000 lb. Shown in Figure 27 is one of the typical large platforms with the shock isolators on the left. The shock

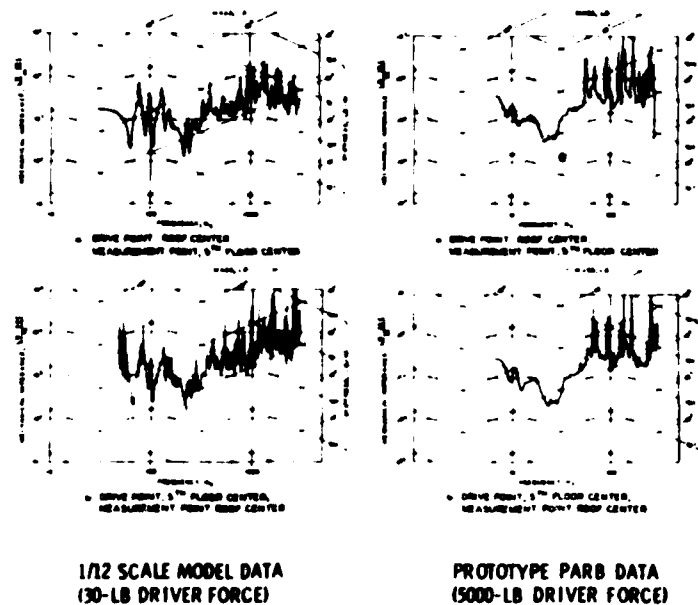


Figure 25 - Comparison of mechanical impedance records for scale model and prototype perimeter acquisition radar

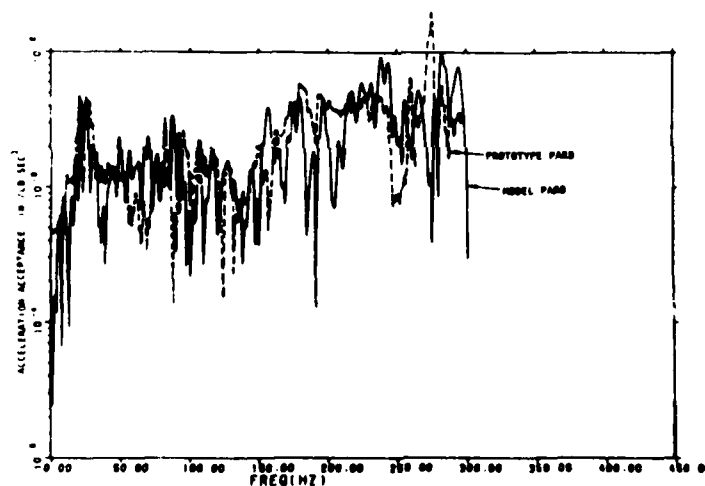


Figure 26 - Comparison between scale model and prototype perimeter acquisition radar building transfer functions

isolators were of a variety of types (undamped mechanical springs, friction damped mechanical springs and pneumatic).

The Waterways Experiment Station developed techniques for shock testing these platforms in-place under full operation. The test consisted of a high-frequency pulse train and a drop test. The pulse tests were at threat level in order to test electronic equipment to high-frequency inputs and the drop test was used to evaluate the rattle space design as well as the low frequency of response of the cable system.

The techniques developed were successful in applying

threat magnitude motion to the platforms. Under the threat motions, none of the platform-mounted electronics failed to perform their function. We now have techniques that can be used to test an operational weapon system to the full threat loads.

Recently, we fabricated an inertial mass transportable vibrator that can be programmed to provide a constant force throughout a specific frequency range. Forces exceeding 50,000 pounds can be achieved through a limited portion of the overall frequency spectrum from 0 to 200 Hz. The dual moving masses have combined weight of 12,000 pounds and



Figure 27 Shock isolation platforms for SAFEGUARD system



Figure 29 Scale model reinforced concrete arch for underground command and control center

can be accelerated to approximately 5 g. Since the actuator is servo controlled, complex waveforms can be duplicated in addition to the more common sine wave forcing functions. In the inertial mass configuration, the vibrator system can be used to excite extremely large prototype or model structures so that a dynamic performance assessment can be made, see Figure 28. (It should be noted, however, that the actuator assembly is top mounted to facilitate removal for testing in the conventional reaction mass mode. In all cases, the system is hydraulically powered by a 70 gpm supercharged pump, supplied by approximately 250 amp, 440 volt, 3-phase electric power.)

#### Buried Structures

A model buried arch for use as a command and control center was recently subjected to the shock effects detonations simulating near misses of conventional bombs. A view of the arch before being covered with soil is shown in Figure 29. The test plan is shown in Figure 30. It was interesting to note that the vertical acceleration across the entire floor

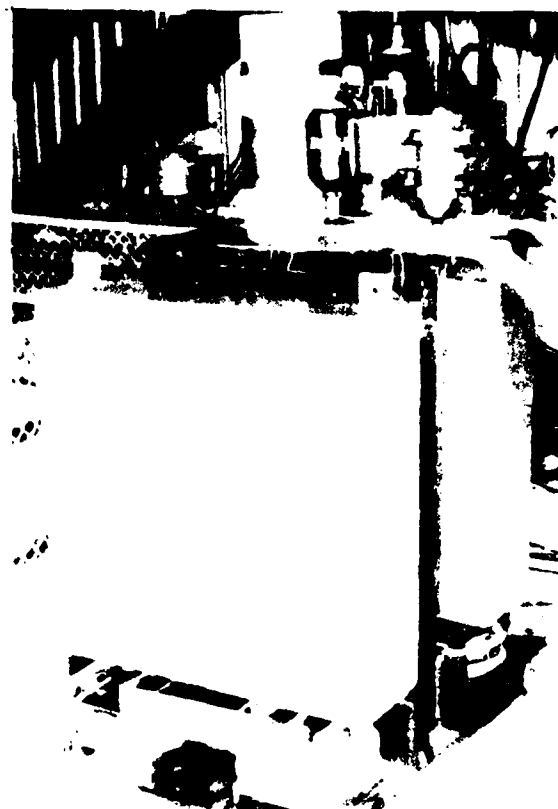


Figure 28 - Transportable vibrator for exciting large structures

slab attenuated very slightly and no noticeable attenuation occurred for the horizontal acceleration across the floor indicating the structure moved as a rigid body. Procedures were developed for predicting the acceleration levels within the structures from free-field values predicted at the leading edge of the structure. The close-in charge, 21 pounds located 3 feet from the arch, caused a significant breach, see Figure 31.

#### Conclusions

In summary, we have used physical models, mathematical models, and vibration tests to determine the response of real systems to shock and vibratory loads. Such approaches using state of the art analytical and testing techniques have made it possible to solve difficult design problems as well as verify the capability of systems to function when subjected to transient forces resulting from earthquakes and turbulent water flow as well as shocks produced by the detonation of explosives.

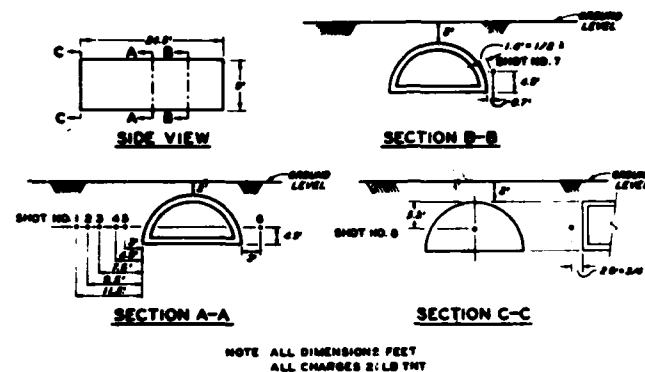


Figure 30 — Test plan for scale model reinforced concrete arch



Figure 31 — Explosive test damage to scale model reinforced concrete arch

## TECHNICAL INFORMATION RESOURCES FOR THE SHOCK AND VIBRATION COMMUNITY

Edward J. Kolb  
Principal Technical Information Officer  
U.S. Army

Let us first consider how information has come to be a technical discipline over the past 10 years, and where we are in the state-of-the-art in this field.

In 1957, the International Geophysical year was heralded by the world's first earth satellite vehicle, Sputnik. It was the successful accomplishment of many disciplines that enabled the achievement of Sputnik and these, in turn, brought about the information "explosion." Sputnik was possible because the technical parameters necessary to achieve success with an earth satellite vehicle were simultaneously available to us. These included: escape velocity boosters, high vacuum technology, world-wide telemetry, automatic data processing, techniques for assimilating vast amounts of information synoptically, and many others. This information could be forwarded on line to a central control facility and a feedback signal could correct an off-normal condition. Ever since this epic period, information has been mushrooming to the point where the management of information has indeed become a discipline in its own right.

Figure 1 shows what has happened to the workforce in the United States and how it relates to the information domain. You see that roughly 75 percent of the workforce, in the beginning of the century, was devoted to agricultural pursuits. This continued until around 1940 when it began to taper off to the point where today only 5 percent of the U.S. workforce is involved in agriculture. (We must be eating a lot less.) The reason for this dramatic shift is because we are doing a much better job in agricultural productivity. What is the rest of the workforce doing? The industrial revolution absorbed much of the nonagricultural workforce. Since the 1940s, the muscle-intensive society of agriculture and industry has yielded to a brain-intensive workforce. In other words the goods-business society of pre-war times has become a services-business of post war times. Seventy percent of the entire U.S. workforce (which is 85 million people) is now devoted to services industries, most of which involves information activities.

Figure 2 presents the growth of information storage techniques (derived by Dr. Marvin Camras at Illinois Institute of Technology in Chicago, the "father" of magnetic recording). This shows the progress of two-dimensional storage media expressed in square centimeters.

The top of this figure shows the punched card, with a minimum storage capacity, followed by illustrations of increasing storage. Microfilms are listed in the lower right-hand corner. Think of microfilms as a micro storage not

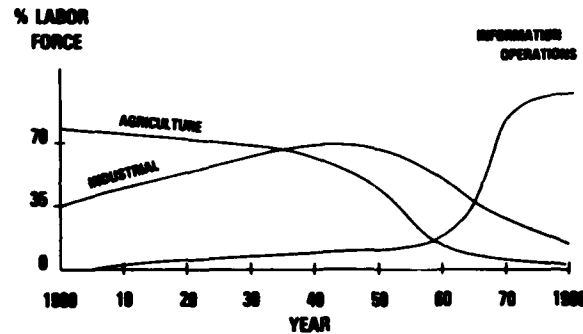


Figure 1 - United States Workforce

necessarily limited to films. If you will scan the media mentioned in this figure, you will see that the increasing "bin" storage is moving us into an enormous information handling capacity.

Figure 3 shows a similar growth rate but illustrates storage in the third dimension. This relates the maximum practical limit of storage capacity to the DNA molecule.

Figure 4 shows the shrinking work week as a result of the industrial revolution. We see that from 1890 through 1970 we have moved from a daylight-hours work day to something less than 40 hours per week. This has been made possible because of the industrialization and the information transfer process.

Figure 5 relates energy resources to the same period of time as shown above. Animals were used heavily up through the 1930s as a primary source of energy. Human energy played a large part also in the early mid-century. Following this, however, these sources have fallen to a mere 5 percent of our current energy use. Electromechanical energy use has continually risen to the point where it now accounts for 90 percent of our current production.

Consider now the "personal-interaction" aspect of information exchange. The overall concept illustrated in Figure 6 portrays organizational communications structure. The top diagram in this figure depicts the organizational communications of the 40s and pre-40s. The boss or the president delegated work down through his organization - the top-down-only approach. The next step in communications involved some cross talk as in the next diagram of Figure 6. The bench level people and worker-bees began to talk to each

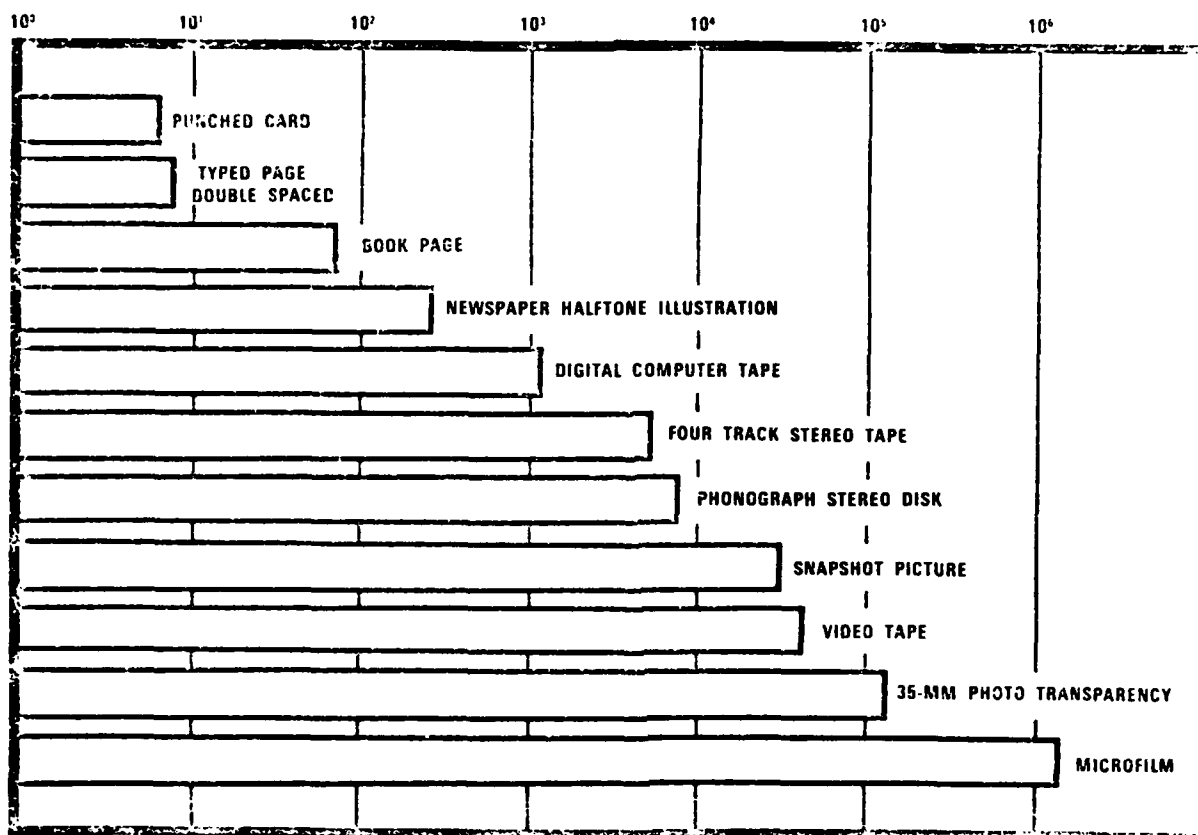


Figure 2 - Gross Area Information Density

other across the organization. Then we developed patterns involving vertical feedback. Soon, some of the bosses began to listen to their men. Finally, we have reached the stage where the top men talk to the bench level men and vice versa all the way through the structure. This is depicted by the rosette of arrows (Figure 6).

We turn now (Figure 7) to what's happening in communications in the 1974-1984 timeframe. If we look at the media such as telephones, TV sets, radios, two-way transmitters, cable television, computers in use, etc., we find a tremendous increase in 10 years. Figure 8 shows the increase in channel capacity for signal energy forwarding systems. A further example of improvement in signal carrying capacity is given in the optical fiber development. These fibers, one-fifth the thickness of human hair, can do the work of 10,000 ordinary telephone wires or serve as a television cable to transmit 8,000 different channels at the same time.

The disciplines of communications and of computers are gradually coming together as noted in this time line from 1930 to 1980 (see Figure 9).

Let's turn now to the question of where shock and vibration information can be found. Back in 1968, the President's executive office had a committee known as COSATI—the Committee on Scientific and Technical Information. This committee established 22 categories of technical

disciplines in which all technical information could be subdivided. None of those areas referred specifically to shock and vibration. The categories were much more general like engineering, physical science, computer science, etc. If papers indexed under these 22 COSATI categories were actually on the subject of shock and vibration, then the burden is on the inquirer to know the broader COSATI index term under which they are filed. This can be frustrating to the inquirer because he may not know the terms which are in the file which are related to his subject field.

Let me now turn to the subject of journals and their growth since 1960. If one depends upon text books for technical information, he is resigned to information which is 3 to 5 years old because it takes that long to get books into print. Text books are only useful for the layman or neophyte. Those who work at the forefront of technology cannot seek current information from text books but instead must look for state-of-the-art information from the journal literature and in conference proceedings. There are about 35,000 technical journals currently being printed. That is a sizable information resource available for reference when we are seeking specific information. The costs of generating this information, storing, packaging, retrieving, and accessing it are continuing to concern us. Look particularly at the cost rise from 1974 through 1980 (see Figure 10). Look also at what is happening in the computer storage area in terms of cost. Fortunately, it is continually diminishing and at the



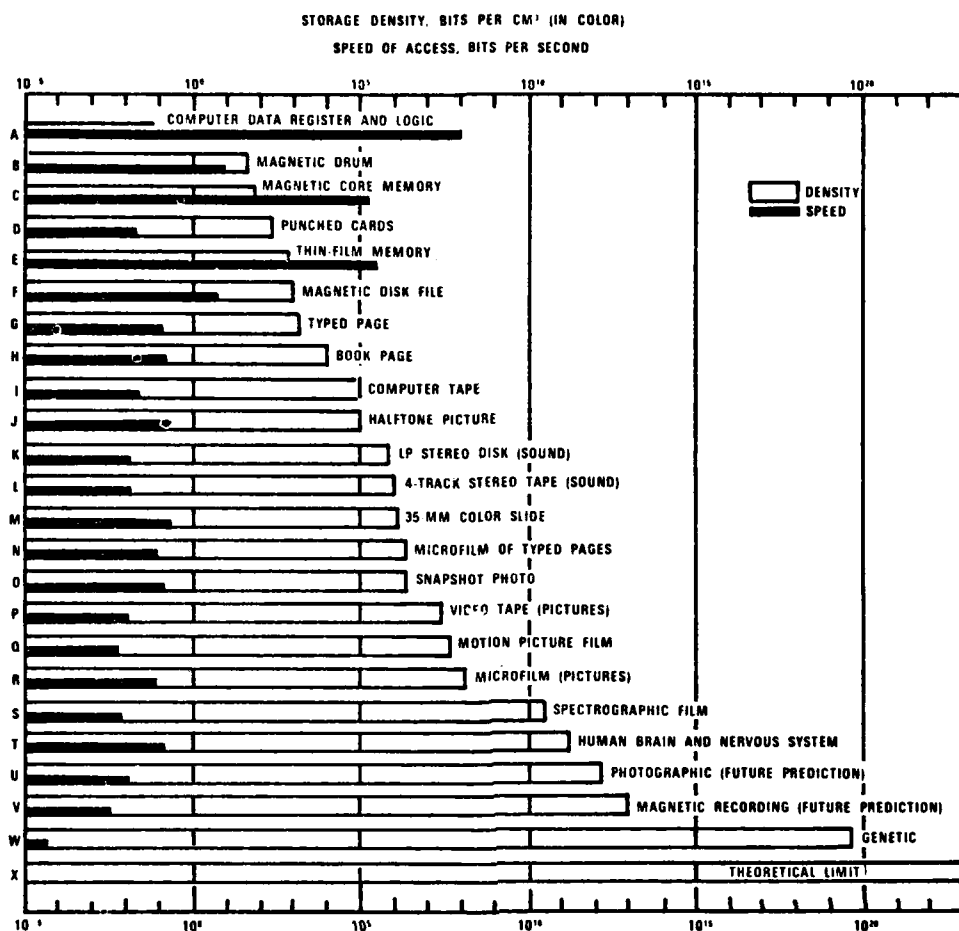


Figure 3 - Information Storage Density and Speed of Access to Information

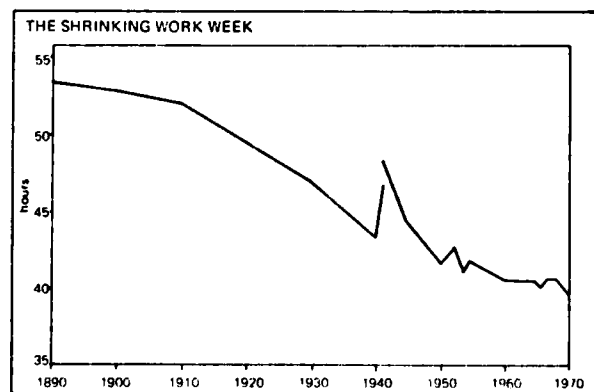


Figure 4 - Shrinking Work Week

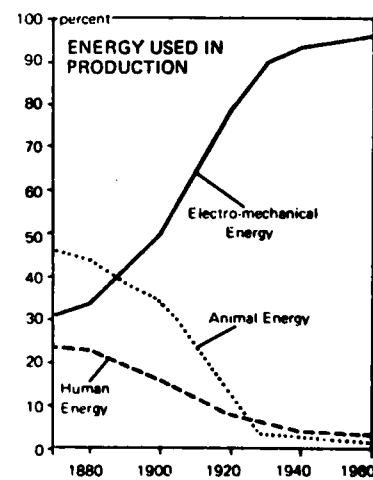


Figure 5 - Energy Used in Production

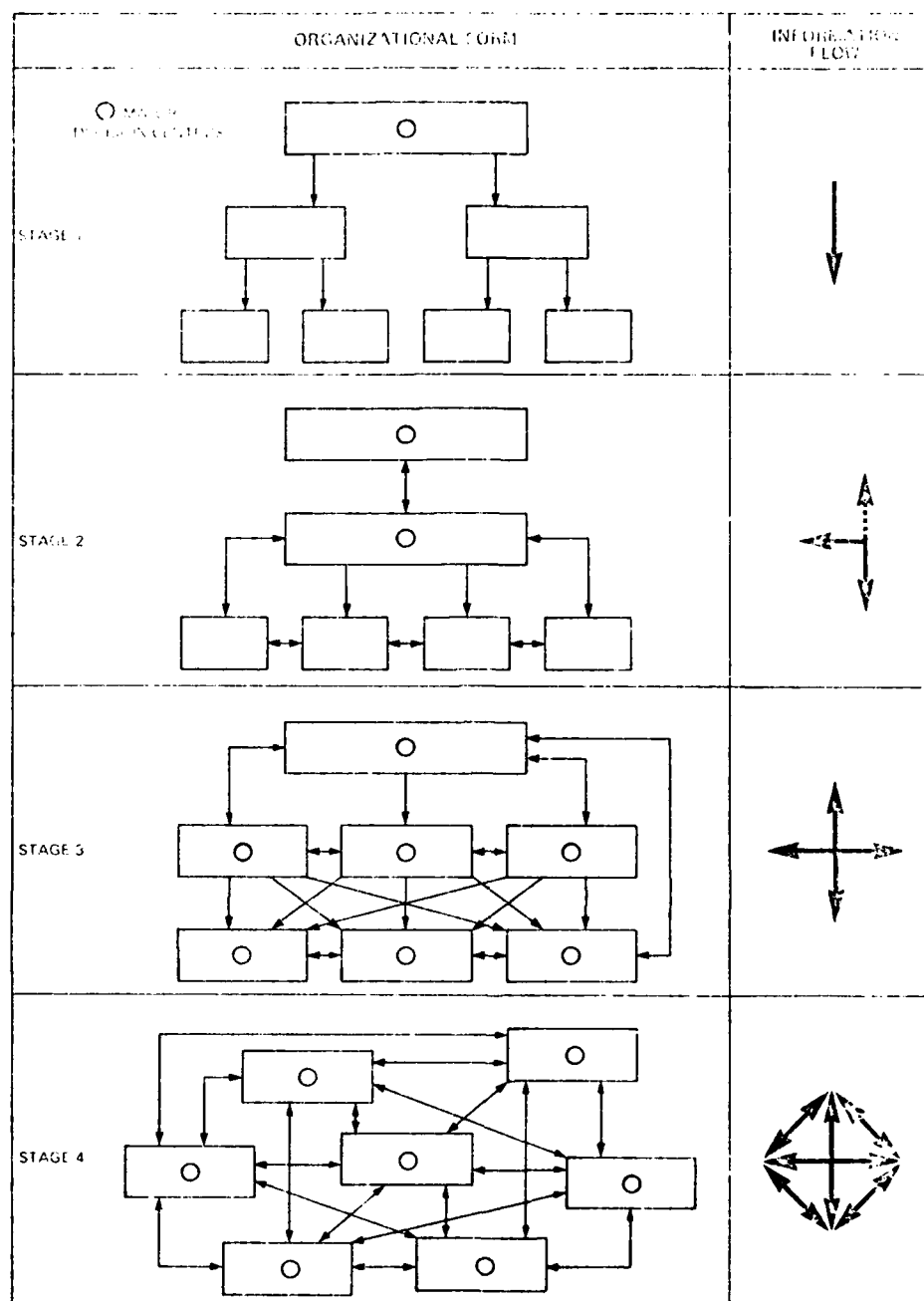


Figure 6 — Effects of Information Technology on Corporate Organization

same time the computer access speed is regularly increasing. There are a lot of other disciplines that are helping us out in all of this. Integrated circuitry, time measuring devices, recording and storage devices, display techniques, communications improvements are some examples.

The number of bibliographic references that are accessible through computer file searching is continually growing. Around a million searches were made in 1975 and that was

before Scorpio (the Library of Congress computerized reference file) was operational.

Computers will continue to play an increasing major role as the costs diminish. The distribution of computers in the world is represented in Figure 11.

There are about a quarter million computers in the United States. Notice that the countries—U.S., Canada,

	1974	1984
TELEPHONE INSTALLED	145 MILLION	203 MILLION
TV SETS IN USE	117 MILLION	200 MILLION
RADIOS IN USE	383 MILLION	600 MILLION
TWO-WAY TRANSMITTERS	10 MILLION	20 MILLION
CATV SUBSCRIBERS	8 MILLION	30 MILLION
COMPUTERS IN USE	80,600	285,000
DATA TERMINALS	960,000	7 MILLION
FACSIMILE SETS	60,000	182,000

Figure 7 - Communications in 1974-1984 Timeframe

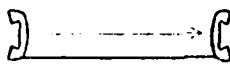
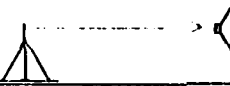
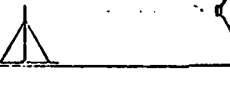
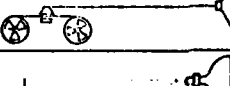
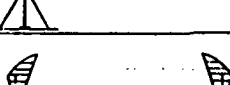
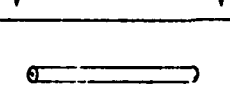
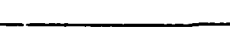
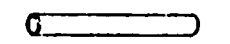
CHANNEL		CHANNEL BANDWIDTH (HERTZ)	CHANNEL CAPACITY (BITS PER SECOND)
TELEPHONE WIRE (SPEECH)		3,000	60,000
AM RADIO		10,000	80,000
FM RADIO		200,000	250,000
HIGH-FIDELITY PHONOGRAPH OR TAPE		15,000	250,000
COMMERCIAL TELEVISION		6 MILLION	90 MILLION
MICROWAVE RELAY SYSTEM (1,200 TELEPHONE CHANNELS)		20 MILLION	72 MILLION
L-5 COAXIAL-CABLE SYSTEM (10,800 TELEPHONE CHANNELS)		57 MILLION	648 MILLION
PROPOSED MILLIMETER-WAVEGUIDE SYSTEM (250,000 TELEPHONE CHANNELS)		70 BILLION	15 BILLION
HYPOTHETICAL LASER SYSTEM		10 TRILLION	100 BILLION

Figure 8 - Channel Capacities for Signal Energy Forwarding Systems

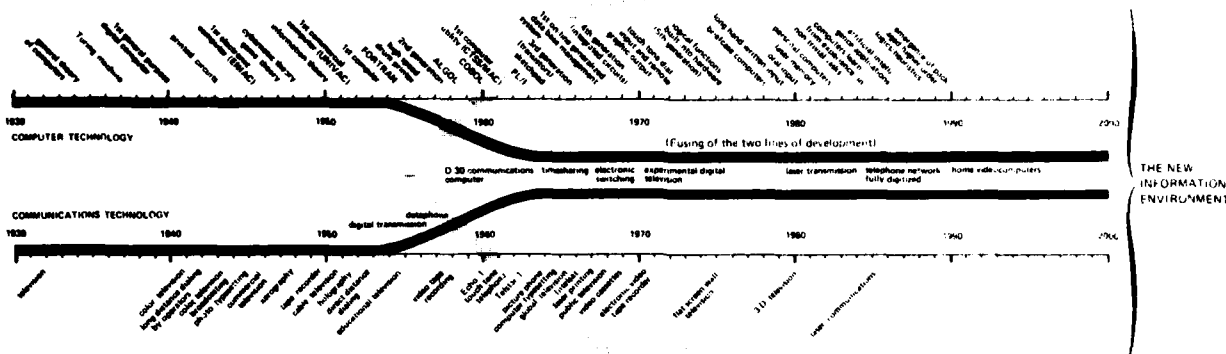


Figure 9 — Communications and Computer Technologies

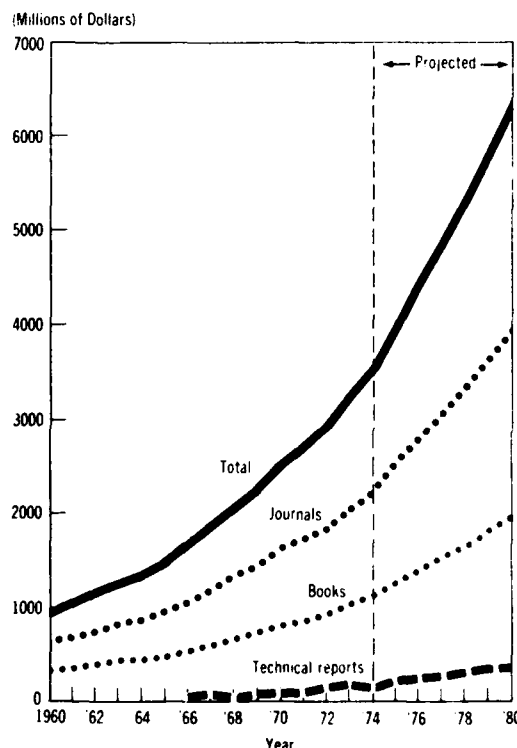


Figure 10 — Estimated Total Cost of Assimilation of Scientific and Technical Literature

Western Germany, U.K., France, and the Netherlands—are actively using computers. These same six countries (in that order) generate most of the world's technical information. Further evidence of the growing proliferation of computers is that they are being netted together to further extend their usefulness. This is a map (Figure 12) of the U.S. which depicts the Defense Department ARPANET being managed by the Defense Communications Agency and enabling computers to "talk" to other computers with wide separation.

Now, I would like to move to the subject of centrally

storing and retrieving information generated by DOD and their contractors.

The Defense Documentation Center (DDC) (a part of Defense Logistics Agency) is as a central repository of technical reports (except special classified) generated under DOD sponsorship. The DDC maintains four "information" banks. The DD Form 1634 bank maintains the information of the future program plan of the work that has not yet been undertaken. A second information bank is the work unit data or the DD Form 1498. This is information on what is currently being done or on-going DOD-sponsored R&D. A third information bank is the technical reports and this contains all final reports on DOD-sponsored R&D. The fourth information bank is the Independent Research and Development (IR&D) information. If you want to know about anything in any of these banks that relates to shock and vibration, you should be able to get it by using the keywords "shock and/or vibration" (or closely related words) in your input inquiry. There are several commercial data banks which serve as repositories of information in scientific, medical, legal, engineering, demographic, actuarial, etc., fields. These service organizations usually supply bibliographies or abstracts as their output but the day is fast approaching when we will be able to get full text from these information banks.

One point worth emphasizing is how you can learn about universities leading the field of shock and vibration (or any other topic). At least one of the commercial data banks maintains a file on Doctoral Dissertations. If you query that file over a period of time for doctoral work relating to shock and vibration, you will soon learn the most active universities in this field. You then only need to contact that university and ask to be put on their mailing list for their technical reports distribution.

Certainly, mention should be made of the information analysis centers. The Federal Government sponsors 122 of these centers of which 21 are in the Department of Defense. These are centers of excellence in specialized subjects and are maintained by experts who reformat assorted published literature, abstract, index, publish, alert, and distribute information, as well as answer specific questions and or solve problems in the subject of their speciality. Fees may be charged for the services rendered but much of their service is without charge.

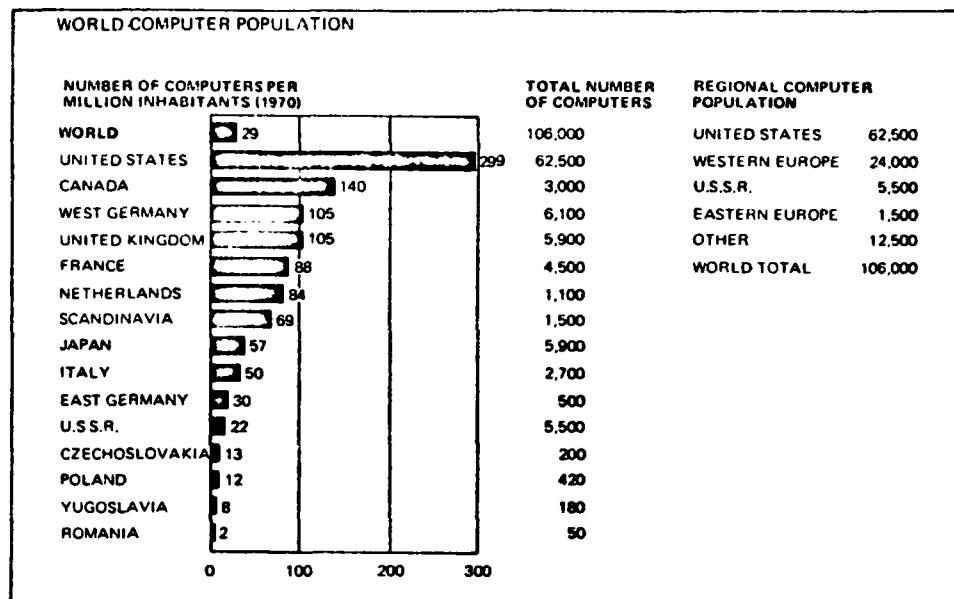


Figure 11 - World Computer Population

**ARPANET GEOGRAPHIC MAP, SEPTEMBER 1977**

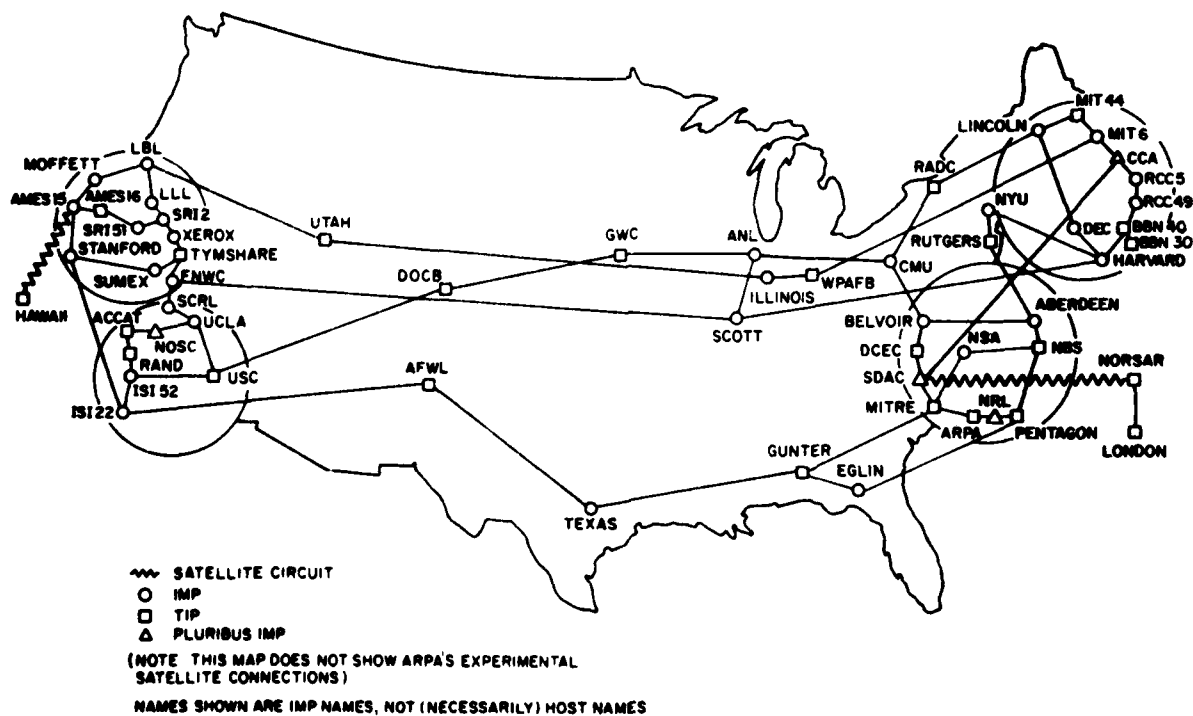


Figure 12 - Department of Defense ARPANET

Another resource for shock and vibration information is the Smithsonian Science Information Exchange (SSIE), Washington, D.C. They collect "who's doing what" information from federal agencies, contractors, state and local governments, non-profit institutions, associations, foundations, and universities. The problem they have with maintaining a complete data file is that input to their service is voluntary. Ongoing work may not be in their file simply because the organization doing the work did not input the information.

A particularly notable commercial resource for literature information is the Institute for Scientific Information in Philadelphia. They provide a number of services associated with optimizing the access to the literature. For example, their "citation index" will provide you with reference to every journal article which mentions a given author. They also provide "contents" pages of all scientific publications plus another service provides an original copy of any article you request from a journal publication. They offer many other valuable services.

The Ohio College Library Center (OCLC) can provide extensive services to the shock and vibration community. They have a network of (now) over a thousand libraries who are linked to their computer. This means that references to the collections of each of these libraries can be shared. Further, the cataloging for all 1,000 of these libraries'

collections can be centrally accomplished (by automatic data processing).

Another good resource for information can be found in the Gale Research Company publications. For example, they publish an encyclopedia of associations that list over 13,000 and briefly describe their functions. Of these, at least 10 percent relate to science and technology which may concern the military and of these probably half or about 500 relate to shock and vibration. If we look into these 500 associations, we can probably learn much more of what is going on than was revealed by the previously mentioned sources.

Many new technologies are coming along which will significantly improve the information access and transfer process. These include displays, direct computer information input, computer output microform, information networking, computer composition and formatting, automated selective dissemination of information, portable microform devices, etc. This just indicates a very few. The important thing is that much is being done to store, forward, access, reformat, and issue information. The day is rapidly coming when the information user will need only to describe his requirement or ask the question and he will be overwhelmed with information from which he may select his best answer. Think of what an improvement that will afford in time, accuracy, validity, and alternatives, when we can do so much more than supply books; but can supply information.

## EARTHQUAKES: THEIR CAUSES AND EFFECTS

Dr. Robert M. Hamilton  
Chief, Office of Earthquake Studies  
U.S. Geological Survey

During the 1950's, our understanding of the nature of the Earth's topography expanded greatly. One of the major findings was that the floor of the ocean is not a smooth plain—it has great topographic relief. In fact, the relief of the ocean basins is greater than that of the continents. The floors of the oceans are lined with ridges and mountain ranges, one of the most prominent being the midoceanic ridge of the Atlantic Ocean. Down the axis of this Mid-Atlantic Ridge is a valley; the ridge also contains many off-sets.

One of the other major findings of the 1950's and early 1960's, which grew partly out of the effort to tell the difference between earthquakes and underground nuclear explosions, was that the world's seismicity is very tightly concentrated in certain zones. Starting in Iceland, one of the zones runs down the middle of the Atlantic Ocean, almost equidistant from the continents on either side. When plotted on a bathymetric map, this line of epicenters is coincident with the axial canyon of the Mid-Atlantic Ridge. Further, offsets in the line of epicenters correspond closely to offsets in the Mid-Atlantic Ridge.

I will discuss the seismicity in other parts of the world later, but for now, let me note that the seismicity on continental boundaries, for example along the western coast of South America, increases in depth from near surface at the coast to more than 600 km inland.

The ocean ridge system continues into the Pacific, where it is not as well defined. The ridge system in the eastern Pacific Ocean is referred to as the East Pacific Rise. It extends through the Gulf of California.

The ocean basins also have deep trenches, located along the island arcs. The trench along the Aleutian arc and the trenches along the western margin of the Pacific Ocean are examples. These trenches are closely related to the zones of inclined seismicity.

Another essential piece of information derived during the 1960's has to do with the magnetization of rocks. When a magnetometer is towed behind a ship, sometimes the orientation of the magnetic field is in a normal direction—that is, the sensor will line up in the direction of the Earth's present magnetic field—but sometimes it is reversed. Through extensive surveys, bands of normal and reverse magnetization of the ocean floor were discovered; these bands are approximately parallel to the ridge system.

Piecing these clues together, scientists derived a new understanding of the Earth. The new concept has various

names: plate tectonics, continental drift, and sea-floor spreading. According to this new concept, the outer shell of the Earth, the lithosphere, is able to move laterally at rates on the order of 10 cm a year. Previously, most of the crustal movement was thought to be vertical. In this new view, the inner part of the Earth, below 100 km and down to a few hundred km, is in a near-molten state, not actually liquid. Magma rises from this zone along the midoceanic ridges, which are areas of separation of the Earth's crust. The magma is intruded into the outer shell of the Earth or extruded to form islands like Iceland and the Azores as it cools. In this manner, new crust, the outer shell of the Earth, is formed. As the material cools, it acquires the orientation of the Earth's magnetic field at the time. The rocks that are cooling today, therefore, are acquiring what we call the normal orientation of the Earth's magnetic field; those that cooled millions of years ago would have acquired a different direction. As the crustal rocks cool and move away from the midoceanic ridge, in effect, they constitute a tape recording of the magnetic history of the Earth.

Because the Earth has essentially a fixed circumference, if new crust is being formed along the ocean ridge and moving out—and this is happening worldwide along all the mid-ocean ridge systems—obviously something has to give, and in places, the plates collide. One such place is the coast of South America. When this happens, one plate either gravitationally sinks or is forced down into the interior of the Earth. The zones of collision are places of high stress, so earthquakes result. As a plate plunges into the Earth's interior, it melts, and the lighter fractions of the melt rise. Some of the melt is extruded onto the surface of the Earth to form volcanoes, which is why lines of volcanoes often parallel the trenches and zones of seismicity. It is also why the circumference of the Pacific Ocean is often referred to as "the ring of fire."

In summary, the vast majority of earthquakes take place where plates collide, where plates are formed and move apart, and where plates slip past each other. The understanding of the Earth known as plate tectonics certainly represents a major intellectual achievement. We now understand the movements of the outer shell of the Earth over about the last 200 million years. We know that the rocks on the floor of the ocean along the East Pacific Rise are newborn; they are still being created today. Because they are farther from the ridge, rocks of the northwest Pacific Ocean are more than 160 million years old. In effect, we have a history of the Earth's movement over this period as recorded in the rocks.

One of the major boundaries between the plates lies along the west coast of North America. The San Andreas

fault in California is part of this boundary, along which the Pacific plate moves northwest toward the Aleutian Islands relative to North America. The rate of movement is about 6 cm a year. This movement can be measured by surveying or by wires stretched across the fault. Los Angeles is moving closer to San Francisco at the rate of several centimeters a year, and in about 10 million years it will be a suburb of San Francisco. I recently spoke to the Commonwealth Club in San Francisco and mentioned this. They were shocked to learn that Los Angeles was coming their way, but I assured them that if they only waited 50 million years, Los Angeles will have passed them by and will have arrived at the southern coast of Alaska. There it will be carried into the interior of the Earth and melted down to appear again in a future volcanic eruption.

California is not the only State in the United States that is prone to earthquakes. The area of greatest seismicity is the Aleutian Islands. Much of the Eastern United States has experienced earthquakes in the past. Southeastern Missouri experienced three very strong earthquakes in 1811 and 1812. Strong earthquakes took place near Boston, Massachusetts, in the Cape Ann area in 1755; in Charleston, South Carolina, in 1886; and in the St. Lawrence River Valley on the Canadian border.

People often wonder why the Eastern United States should be considered to have high seismic risk when admittedly, this area has a relatively low rate of earthquake occurrence. One factor is that the crust of the Earth in the Eastern United States is older. Consequently, it transmits seismic waves much more efficiently. Also, in the East, a larger percentage of the houses are of unreinforced masonry construction, whereas in the West, wooden frame structures, which resist earthquakes well, are more common. An argument, therefore, can be made that the earthquake threat to the Eastern United States is much higher than one would expect from the history of the rate of earthquake occurrence.

Now let us turn away from the causes of earthquakes and consider the topic of earthquake prediction, in which significant advances have been made in recent years. The Chinese in February 1975 successfully predicted a large earthquake near the city of Haicheng in northeast China. Almost certainly, tens of thousands of lives were saved as a result. A demonstration that the Chinese have not completely solved the prediction problem, however, is shown by the earthquake in July 1976, at Tangshan, where reportedly more than 600,000 people were killed. That quake was not predicted.

A variety of phenomena are monitored in the search for earthquake precursors:

- land deformation
- seismicity
- electrical resistivity
- magnetic field
- gravity
- strain
- fault slippage
- water level or pressure in wells
- geochemical properties of ground water
- animal behavior

The conclusion from this monitoring is that earthquakes do have precursors. Observations have been sufficient in recent years and throughout history to provide convincing evidence that anomalous changes do indeed take place before an earthquake begins. The major uncertainty now is whether precursors are regular enough in nature to provide a reliable basis for earthquake prediction.

On October 7, 1977, the President signed the Earthquake Hazards Reduction Act of 1977, providing for a major expansion in earthquake studies. Part of that program will be an intensive effort to try to record earthquake precursors and to develop an earthquake-prediction system. As yet, we cannot assert that a prediction system capable of providing useful warnings can be achieved, but many people believe that this can be done.

As a part of the earthquake-prediction program, we are currently focusing attention on a land uplift in southern California. In December 1975 we found out that the land in the area north and east of Los Angeles had risen by as much as 45 cm (about a foot and a half) in the period 1959 to 1974. This rise was a basis for concern because sometimes such an uplift precedes earthquakes, as in the 1964 earthquake in Niigata, Japan. We also know that land uplifts have taken place that have not been followed by earthquakes.

The southern California area is of particular concern to us because the last break in the section of the San Andreas fault from San Bernardino north was in 1857, that is, 120 years ago. There should be high stress in that area now, which could produce a magnitude-8 earthquake. Another basis for concern is that in the 70 years before the 1906 San Francisco earthquake, a half dozen major earthquakes took place in the northern California region, which indicated that stresses had built up to the level where the crust started to fail; in the 70 years after 1906, no such earthquakes took place. In southern California, a long period with few earthquakes followed the 1857 earthquake. Then the Kern County earthquake took place in 1952, and the San Fernando earthquake, in 1970; these earthquakes could be indicative of a buildup of stress.

This situation in the region of the uplift is very complicated, and we cannot pretend to know everything that is going on. At this stage, we have no evidence that a major earthquake is imminent.

My final topic is earthquake control, one of the more exciting aspects of earthquake studies. In the early 1960's, Denver began to have earthquakes. Denver had never had any significant earthquake activity in the past. A consulting geologist in the area, Mr. David Evans, said that the earthquakes were being caused by a well at the Rocky Mountain Arsenal near Denver where waste water was being pumped into the ground. The initial reaction was disbelief, but later, this explanation was found to be almost certainly correct. The convincing evidence was a close correlation between the rate of water injection and the rate of earthquake occurrence.

After this realization, efforts were made to find another such situation, which was discovered at Rangely oil field in northwestern Colorado. That oil field is a classic anticlinal



structure. The field is undergoing secondary recovery involving water flooding. The water pressure is high around the perimeter of the field and low in the middle. Earthquakes were taking place where a fault intersected the zone of high fluid pressure. We obtained access to four wells in the area and undertook an experiment to try to turn off the earthquake activity, to turn it back on again, and then to turn it off. This was successfully done.

The understanding that has come out of this work is fundamental in understanding the nature of earthquakes. When rock is under stress, the main reason that a fault in the rock does not slip is because the frictional strength of the rock in the fault zone is greater than the stress on the fault. As fluid is injected into a fault, it changes the effective stress on the fault. The fluid is not exactly a lubricant, but it reduces the frictional strength of the rock in the fault zone, permitting slip to take place.

## PANEL SESSIONS

### SOFTWARE EVALUATION

Moderator: Dr. J. Gordan Showalter  
Shock and Vibration Information Center, Washington, D.C.

Panelists: Dr. Robert Nickell, Pacifica Technology, Del Mar, CA  
Dr. Walter Pilkey, University of Virginia, Charlottesville, VA  
Mr. E.J. Kolb, Headquarters, U.S. Army Development and  
Readiness Command, Alexandria, VA

Mr. Showalter: This panel is composed of members of the Interagency Software Evaluation Group (ISEG). Dr. Perrone, who is the chairman of this group and who was instrumental in setting up the Interagency Software Evaluation Group (ISEG) was not able to attend this panel session which is a progress report on the activities of this group over the last few months. One does not like to work in a vacuum too long and this session is an attempt to get feedback from the users of computer programs, which probably includes most of the audience. We intend to outline how ISEG proposes to have software evaluated and we want your reactions to these proposals. If someone has any criticisms of the way we in ISEG are going about setting up this evaluation procedure or if we are not doing something we should be doing then hopefully this will be brought out in this panel discussion. We want comments on a proposed list of structural mechanics computer programs which are under consideration for evaluation. We also want to get your feelings on how you would like to see computer programs evaluated; if at all.

Mr. Nickell, (Pacifica Technology): I don't think I have to dwell on the need for some kind of focusing of effort in the software area. For those of you who are either analysts working with programs that use analytical techniques or those of you who are managing programs where analytical techniques are a strong component of the problem, I characterize the problem emotionally with a couple of key words. For the managers I think the key word is uncertainty. First, you are uncertain whether you will get any results and second whether the results will be meaningful. For the analyst I think the key word is a combination of frustration and exhilaration before you plunge back into the depths of frustration again on your next project. Emotional descriptions however don't get us very far. We seek a rational approach to the problem.

People have developed a kind of a rational approach to the software problem over the last 10 years by focusing on those things that they could actually touch. The key word here is focus; everyone is trying to bring the problem into focus so they can discern the grain of what is going on. The first efforts that took place were what might be called information gathering. If we have a problem let us gather data and find out how big the problem is, what the shape of it is,

or how it tastes, smells and feels. This resulted in a number of surveys that were conducted by a few Federal Agencies and Professional Societies that were aimed at producing this kind of data. One of our panel members who could not attend today, Dr. Michael Gaus from the National Science Foundation, was responsible for funding at least two of these surveys which were designed to examine the attitudes of the users, the attitudes of the managers, and the extent to which software is documented, used and transmitted. So, the information has been gathered to some extent.

The next step to bring the problem into focus is to transmit the information that we have to the people without any information. I believe that part is also under control; each agency has their own approach to that problem. The Energy Research and Development Administration, now the Department of Energy, has the Argonne Code Center in Argonne, Illinois, the National Aeronautics and Space Administration (NASA) has the Computer Software Management Information Center (COSMIC) at the University of Georgia, The National Science Foundation (NSF) has their NICE center, and finally there is the NISEE group at Berkeley, California that serves the earthquake engineering community. You also have a series of efforts by the Navy through the Office of Naval Research (ONR) and some of the Navy Laboratories; Symposia organized to describe the characteristics of software and determine how much it is being used. These Navy efforts have culminated in a Software Series that Walt Pilkey will describe to some extent. So the problem is in focus to that degree.

Now we are ready to take the next step and this step will be quite tentative; this is one reason why we organized this panel session. This is an attempt to use the Federal "Sunshine Laws", all of these smoke filled rooms are beginning to fill us up with unhealthy atmospheres. We are now ready to tell you what we have been thinking about for the past 6 months and we are ready to hear what you have to say.

I will describe our current concept of this ISEG effort. We don't intend that it will be the limiting point for the focusing of effort. There are a number of Federal Agencies who have taken the problem essentially to its ultimate and

who have established software centers, where there is common control of software and where there is a place where people can use the best software that is available in a particular field. The prime example of that is in the area of Magnetic fusion research, the former Energy Research and Development Administration through their division of physical research has created the center at the Lawrence Livermore Laboratory, where all of the controlled fusion research calculations were supposed to be performed. They bought a 4th generation computer and began to set up all of the software they thought was the best in the land. Of course one of the first things which happened was that two of the largest components of the controlled thermonuclear fusion research program pulled out, namely the laser and the electron beam people so now it is called the Magnetic Fusion Research Group. Parochialism is our constant enemy in this problem. We do not intend to do that we are talking about the evaluation of the software that is currently on the market and is being used.

ISEG stands for Interagency Software Evaluation Group. There have been some casual as well as determined members of this group. The most notable contributors have been the members of each of the armed service branches, Army, Navy and the Air Force; we also have representatives from the former Energy Research and Development Administration (now the Department of Energy), the National Science Foundation (NSF) and the US Nuclear Regulatory Commission (NRC). On occasion we have had other individuals drop in for brief periods of time, but this has been the main cadre of individuals who are interested in the problem of software evaluation.

Our purpose is to formalize the critical evaluation of applications or engineering oriented software. We are not interested in systems software, we don't intend for that to be part of our program. We will develop criteria for the evaluation of software and we will carry this out in practice by actually evaluating as much software as money and time will permit. The justification, is the next step beyond information dissemination; we are interested in pursuing cost effective use of software. We are not the limit point we are merely trying to make the next step.

We have chosen three tasks for ourselves:

1. Select software within budget constraints.
2. Develop the criteria by which this software is to be evaluated. This is primarily my job with help from a community of scholars.
3. Find the contractors who will perform the evaluation.

Implied in all of this is a fourth step which is to make sure the contractors do what they have agreed to do.

The evaluation criteria that we have been working on appeared in rough draft form in May 1977. A second draft appeared in July 1977 and now we have a third iteration. We see it breaking up into four (4) parts.

First we will screen the programs to find out if they can be moved from the machine where they are resident to the machine of the contractor that we have selected to do the

evaluation. The contractors that we choose will not be the developers of that particular software nor will they be strong opponents or proponents of that software; we are interested in balanced evaluation therefore we may have to move software from a resident machine to non-resident machine. We don't want our contractors to spend a year and \$40K just to get the software up and running. Therefore we have a screening procedure to determine whether the software is fit to be moved from one machine to another.

The second item is program architecture. There are many people, especially in the armed services, who feel that if you can't describe it you shouldn't use it. So one of the efforts will be to come up with two types of descriptions of the program architecture.

Thirdly there is an advanced evaluation procedure which includes energy checks, mesh discretization checks, ways of measuring the efficiency of different programs, ways of measuring the convergence of algorithms and the like. Finally there is a summary which will provide directions not only for the developers of software but perhaps even for hardware vendors.

The screening criteria contain five items in the chain. The first I call availability. That really means the ability to move software from one machine to another. Is it really available to somebody on a different machine or in a different environment? Second does the theory in the program manifest itself in a set of verification examples? Third is it adequately documented so that we can proceed to step two? Then there are two non mandatory items; the first is configuration control, that is can the program be altered in the way in which it does its job so that we can do different things to measure its efficiency? And second has it been used by a sufficient number of people? That is also non mandatory, we will not throw out a program because it hasn't been used by many people besides its developer but we would like to have it that way.

Program architecture is split into two parts. There is a functional description, which is the way the discretization is done in space and time or the order of the approximation in space and time; it also includes the solution methods such as eigenvalue and eigenvector extraction methods and all other kinds of descriptions that would be necessary to try to put the code in context with other codes of its type. Second, there is the programming description which includes things such as how modular is it and how are the modules constructed? How are the file structures created? How are the sub programs designed and the calling sequences created? How is the storage and the use of common files handled and many other things that would be vital to an organization that is thinking about putting a program up on their own machine and putting time and money into maintaining it.

In the advanced evaluation state we are concerned about those things which should be done in preanalysis to screen the problems that the user creates. This includes energy checks, namely what is the mesh effort required for a given mesh and how hard does it have to work in order to produce results. This also includes convergence of all kinds, nonlinear problems, configuration control if

possible, and efficiency. We think of efficiency in two different ways. If we intend to compare the efficiency of two different codes we want them to solve a problem that has exactly the same number of degrees of freedom, the same size bandwidth, and we want to check their solution efficiency that is the first item. Second, we would like to have them do a stated problem with a given error and see how efficiently they can solve it regardless of how they do it; that is called library efficiency. Finally we want to compare the overall general capability of the program to do a variety of problems. That gives you a very general overview of the ISEG effort and the way in which we perceive the criteria we will use for evaluating the software that we have identified to date. A set of programs has been identified by two branches of the armed services. The Navy and the Air Force have in fact identified the codes in a rank list that they wish to have evaluated.

Mr. Pilkey, (University of Virginia): I thought I would talk about something related to this evaluation effort and also talk about alternative approaches to the proposed ISEG evaluation. Let me go back in time a little bit, perhaps some of you know that the Shock and Vibration Information Center did attempt an entirely different sort of evaluation and it culminated in a book called Shock and Vibration Computer Programs. It is an attempt, without specific funding to match program against program or to go into great depth, to review the available software for solving prescribed problems in shock and vibration. In this case one looked toward authorities in the area, people who were using programs to solve prescribed problems, and we asked them to evaluate the programs and to state precisely the availability conditions of all programs whether they were commercial programs, free programs or government programs. So then it is an effort at having people who are using particular programs say what they think of them and hopefully in a disciplined logical fashion. It is a reasonably thick book and it contains a great deal of information about many programs. That same effort is being continued in something called the Structural Mechanics Software Series in which we again asked people working in particular areas such as rotating shafts, building designs, bridge designs, random vibration, or whatever to evaluate all of the programs that are available. But the shortcomings and drawback to this sort of activity is that the people who are involved don't necessarily have the opportunity to use every program. So they collect information on the programs then they attempt to discern tradeoffs between the programs and ascertain the relative merits of various programs and then put it in writing. This culminates in the software series which is a series of books that come out once every six months for each volume.

There is a second activity. The software series has linked itself to several national computer networks. Usually time sharing networks, but in one case a batch network. This allows people to submit computer programs to the software series instead of technical papers, but in the same fashion as a technical paper. The programs are then evaluated, and if the reviewers think they are worthy of being placed on the national networks then the developer of the program gets free computer time to place his program on the network and it becomes publicly available. We have done many programs this way and this includes most recently SAP V, the TAB system WHAM, which is a finite element shock

analysis program, BOSOR and many other programs like this. Thus there are two activities that belong within the framework of the software series.

But the ISEG effort is doing something quite different, especially in magnitude, because we are talking about securing funding to look at the specific programs in depth and to look at them in a very logical and a very controlled fashion and the control resides with Bob Nickell. The effort is to examine specific programs.

Our goal is to stimulate discussion on what directions ISEG should take, whether they are aimed in the right direction now, what kind of evaluations would be the most valuable or the most useful. Let me propose a possible orientation of ISEG which could be done within the framework but it is not really in the direction that we are aiming at at the moment. At the moment we intend to take particular programs, such as NASTRAN, and have a contractor look at the program and evaluate their capabilities, in the form that Bob had on the Board and do this in great depth. Another contractor would look at the MARC program, for example, and all of these would be done under the supervision and the direct control of Bob Nickell. That is the key to this effort; it would be controlled, it would be regulated and we would see to it that when it came down to looking at the economy and the efficiency of the different programs that they are evaluated on a fair basis. An alternate approach is to evaluate certain capabilities within the general purpose programs. Examples include random vibration capabilities, rotating shaft capabilities, they aren't necessarily available in general purpose programs, nonlinear material capabilities, nonlinear analysis, the nonlinear geometry capabilities, transient dynamics capabilities, or shells or revolution capabilities. One contractor would evaluate the random vibration capabilities in all of the programs and another contractor would evaluate the shells of revolution capabilities of all the programs and then they would try to discern, distinguish, and evaluate the program from that basis rather than having one contractor look at each program. The end result could be the same if they are properly controlled. That is in terms of results that are useable to the technical community, it is possible that both of them could lead to results if they are properly written, properly displayed, and properly publicized. Both of them could be used such that if a user had a particular problem the results of this type of evaluation could be used to determine which program is the best for the problem. It is possible that the alternative of having one contractor look at many things would lead to results that would make it somewhat easier to discern what program would be best for solving the problem.

Mr. Kolb, (U.S. Army Development and Readiness Command): During my talk in the opening session I discussed a trend in the ratio of the cost of hardware to the cost of software over a period of roughly twenty years since 1955. The hardware development is pretty well defined now to the point where virtually all of the expenses in computer oriented end products are vested in the cost of the software. This gives us great concern and there are a number of entities within the Army, which I represent, that are vesting a considerable amount of money in software orientation and software improvement and so on.

In the technical information program for the Army I have three hundred thousand dollars per year vested in the

sole purpose of doing R&D in computer program improvement. We want to optimize those dollars and we want to optimize everyone's computer programs; one of the ways that we propose to do this is to sponsor collective concentrated evaluation efforts such as this to determine the viability, applicability and so on because everyone goes off in their own way developing their own programs to do their own things and it is incumbent upon us to optimize those investments.

We are in the process of justifying sponsorship of this kind of effort so that one can go to a central source and get evaluation type information on his software materials. I currently have on my desk three applications for sponsorship of three different Army organizations that want to become a world center of software information. This is three currently, but in the past three or four years we have had others and therefore there are many people in many different laboratories who are gathering all kinds of software information and they think that this should be collated and coordinated into a center. There is enough interest in this that we feel that we better do something about closing in on it so everyone doesn't go off spending their own money. The storage space is increasing like 100 fold over the same period, 1955 to 1975, and the cost of storage is coming way down therefore we envision that we should put a great deal of effort into evaluating some of the materials that are coming out of this computer effort.

Mr. Nokes, (Draper Laboratory): I am wondering about the scheme of having one contractor evaluate each individual computer program; how do you get around the problem of the existing published summaries of what works with the computer program? You have one contractor he knows that a certain program works for all the cases he has tried but he doesn't know if it works better or worse than any other program. I have one program that I am using now and I am basically quite happy with it. But I would really like to know if other ones work better. With that scheme it seems as if you are leaving the tough part of the work to the one who has to evaluate the overall program.

Mr. Nickell: My understanding was that in the advanced evaluation phase they will all do the same problem. Each contractor will do the same problem with their particular code. They will do efficiency examples, convergence examples, energy check examples, do mesh discretization examples, and they will all do the same one. So there will be a comparison in the overall summary of the report.

Mr. Nokes: To the extent that all the programs can do the same examples?

Mr. Nickell: That is correct. They will all be able to do some examples.

Mr. Nokes: On the other hand having the one vendor evaluate ten different programs will be expensive. That means one has to learn to run ten programs, just to do his particular cases. It would be more valuable that way, but whether you can afford it is another thing.

Mr. Nickell: There is overhead connected with having

any organization use a piece of software and if you have them use ten pieces of software that multiplies the overhead by a factor of ten.

Mr. Nokes: That is why we use only one.

Mr. Nickell: Before you get your first useful result you have to factor in the overhead. That was one of the reasons for going to this scheme.

Mr. Pilkey: What is the overhead?

Mr. Nickell: I once worked in an organization where there were hidden costs of the order of about 25 man years to implicitly maintain all of the structural codes that were being used by about 100 analysts that we had in the organization. That is a substantial cost if you do a strict cost accounting on it.

Mr. Nokes: It appears that it is a fair amount of money even for the codes that are better set up to be portable and that are easy put up on "a new machine".

Mr. Nickell: At best it takes a few days.

Mr. Pilkey: It is clear to me that control that would be exercised by Bob Nickell, or whoever is running this will make this proposed ISEG evaluation meaningful. Certainly that is essential to seeing that the evaluations are meaningful.

Mr. Nokes: I suppose I should mention that I would be very interested in having this type of evaluation. We continually run into the problem, where someone wanders in and suggests we use so and so's code instead of the one we are using. We have no real answer. We don't have enough money to attempt to purchase it or lease it and put it up and try it to find out whether it even works.

Mr. Nickell: Would it be useful to have a document available that had the results from ten or twelve such programs that had examples with which you can compare your code?

Mr. Nokes: Yes, because even if it only had three or four examples at least there would be a way of comparing my code, as it exists, with the other one and I would have some sort of objective measure of whether I am using a reasonable code.

Mr. Pilkey: You say that you will evaluate NASTRAN, as you know there are various versions of NASTRAN, there is a public version and there is a private version. Will that create a problem? Will you have problems trying to identify what you will call NASTRAN? If you locate some shortcomings in one version of NASTRAN you will have problems with those contractors that say "well our version doesn't have that drawback".

Mr. Nickell: The first question relates to how to identify which version of NASTRAN you will evaluate? That was accomplished by asking the services themselves to pick out the particular version that they wanted to evaluate. The Navy picked out their version 15.3 and we talked to the Air Force and they said "we are trying to use version 16.0 we

don't like it: we prefer to use the Navy's version 15.3 for the evaluation studies"; we got a commonality so it turned out not to be a problem because everybody seemed to concur about which version should be evaluated. The second question related to what happens if you discover flaws in a particular piece of software; won't the developer run right out and fix them? The answer is you bet! In fact that is the one thing that we really hope will happen. Some developers simply do not understand that their program doesn't do as much for their neighbors and perhaps this will be a stimulus to many of them to put out better software. We don't expect this field to stand still, we expect it to keep moving very rapidly and we expect to be providing some impetus to the improvement of software. That means that our results will be dated, but that is part of life, it is a living thing.

Mr. Dyrdaahl, (Boeing Co.): We have made a great deal of use of Dr. Pilkey's book to select programs when we were in a big hurry. What about the schedule of ISEG? What kind of timing are we talking about? Will I be retired before you get everything evaluated?

Mr. Nickell: I understand that the people from the armed services will go ahead with the first two parts of the evaluation procedure on about six or nine different codes during fiscal year 1978. We intended to complete phases three and four and the summary in fiscal year 1979 so in two years we expect to have gone through our first six to nine codes.

Mr. Kiefling, (Marshall Space Flight Center): What do you perceive as the critical problems that you will be evaluating? Before you look for the answer you should know what the problem is. I am sure that there are dozens of codes that will solve linear stress, and the like but are you looking for nonlinear material programs? Are you looking for complex eigensolvers that will handle the rotating shaft? How do you rate the problems?

Mr. Nickell: If I understand your question what specific features of programs are we trying to focus on?

Mr. Kiefling: Yes.

Mr. Nickell: As I understand it the services haven't perceived the problem in quite that detail yet. They see a general problem. Their codes are not fully documented. They are not quite sure of the limitations on some software. They are not sure what the eigenvalue extractors will do. They are not sure what the stability limits of the integration operators are. They are not sure what the convergence rate of the elements are. Those are problems on their codes that they use on a everyday basis. So I see the problem as much more generic than specific. Maybe we should focus somewhat more on specifics and that may pop up more later. If you have ideas on that we would welcome them.

Mr. Kiefling: I would also like to know if anybody has come up with a size definition? What is a large problem or a small problem or a medium problem? Every so often I see the eigensolution for a large problem in the literature and the largest one that they do is maybe 240 degrees of freedom. We routinely do things like that as test cases on small problems.

Mr. Nickell: 240 eigenvalue sounds like a big problem to me. I guess there is supposed to be an answer to that question. Does anybody know what the definition of large is? Bigger than a bread box, smaller than a house?

Mr. Sepcenko, (Planning Research Corporation): I was going to answer the gentlemen that 240 degrees of freedom is probably quite a substantial eigenvalue structural problem because we recently found that NASTRAN level 16 doesn't do it too well with the first six rigid body modes. I guess the problem is probably known because we knew that level fifteen and so on didn't do this problem very well and we saw the importance in some papers of having those rigid body modes extracted in a modal analysis. Hopefully this will be evaluated. I have a comment. I got an impression that the government agencies will have all of the available programs evaluated as a result of this evaluation. I further suspect that the contractors may be so obliged to use these particular programs in some contracts to cut down the cost. At the same time I have a feeling that many proprietary programs which may be substantially more powerful than the available programs will not be evaluated at all.

Mr. Nickell: That is a very serious problem. The intent of the evaluation exercise was not to lead to the standardization of the use of software in contractual negotiations, but you can never tell what will happen and that is a serious danger to fall into. It can get out of hand. In regard to proprietary software not being evaluated, I think some of the armed services have purchased proprietary software and in the cases where the purchased proprietary software is being used heavily it will be evaluated. That is if they show up on the list of heavily used codes they will be evaluated even though they are proprietary. That raises a very touchy issue about how we select a contractor but we think we have managed to solve that problem. We have identified some contractors who are not the developers and they have no strong proponent feeling toward the software but yet they have it available. In fact many of them have it available and they are sort of against it.

Mr. Robins, (University of Michigan): We have been developing the type of computer programs which deal with simulation of crash victim dynamics mostly in the automotive restraint area. If you are familiar with that there are a few fairly large scale programs floating around on this topic and we are faced with many of the same problems that Walt Pilkey outlined pretty well; should one look a single program, go through it and detail all of its features and its documentation, or should one look across the various programs for the way they solve particular physical problems, or can they solve various physical problems? These are both very important and very useful things to do I think but there are several contractors and several government agencies mainly in the transportation area that have different kinds of models. We have about five or six fairly large computer programs that simulate human dynamics, some of our colleagues at other groups and competitors have similar stables of programs and so the automotive industry and government agencies of various sorts are trying to use these things. But we are not sure that one can even compare these programs very well except on a very simple basis and there is a subcommittee of a Society of Automotive Engineers committee which is trying to discuss commonality between these programs and we have simply

taken the approach does a particular computer program have something called a valid solution to a problem? That is, given an experiment does the program work? We sort of jumped across this big description between programs and have many problems with this. We are trying to develop the scales of validation of how well a particular computer program actually predicts the various physical variables; we are also trying to develop scales of how well experimental data, for example a time dependent trace is match by predictions and if it is wrong what is wrong. Has this group ever thought about how well a particular structural model may duplicate the physical event as one of the primary indicators?

Mr. Nickell: There has been about five or six years of history of people trying to define validation. As I recall the first attempt to define validation occurred during a Pressure Vessel and Piping meeting in 1969. There we decided that a validation consisted of at least two parts, one of which was called verification and the other was called qualification. The verification part is will the software generate a theoretical solution that is consistent with the theory on which the program was written? That is, if it is a viscoelastic program does it produce a result for a simple viscoelastic problem? Can you put in the right viscoelastic law and have it reproduced? If it is metallic creep will it do that? If it is cracking in concrete can it do that? If it is linear dynamics will it do that? Then there is the part about qualification and that gets into the experimental area. You would like to have qualification examples for which you have absolute and utter faith in the solution whether it is experimental or closed form but in most cases you only have an experiment of often somewhat dubious integrity. But over the years we have accumulated some experimental results that match the solutions several programs have produced reasonably well, then that becomes sort of a standard qualification example. The Pressure Vessel and Piping Division of the American Society of Mechanical Engineers has published about three volumes of these various experiments that we give to people in order that they can try-out their inelastic programs or whatever they happen to have; so there is a big and growing concern about so called qualification examples of the type you mentioned that represent real physical behavior. Whether we will include any of those in our exercise is still open for discussion.

Mr. Robins: I would like to go a little further in this same direction if I might. You said that some experimental results matched reasonably well but this is the problem that we are trying to overcome; we do not want to use a term like reasonably well we want to actually develop quantitative measures of the correlation between the experimental event, which may be of dubious quality, and the analytical event which also may be of unknown quality. Has there been an attempt to develop quantitative correlation measures?

Mr. Nickell: If there has I am not aware of it. Typically the reason why an inelastic analysis has problems matching experimental results is because of such things as variability in the properties of the material. In fact I have not seen anybody try to come up with a quantitative assessment of the effects of inhomogeneous properties, the anisotropic properties, of the effect of heat to heat variation, on the experimental response. They have a great deal of qualitative data but not quantitative data.

Mr. Eshleman, (Vibration Institute): I think if you got into qualification at this point you would be making a mistake because first the programs should be evaluated on what they do automatically; anytime you get into experimental-analytical matching, or qualification, you get into engineering, you get into art, and one does it better than another. One person can model something very cleverly with the existing program where another person may not have that capability and so you get into engineering which is a gray area in this kind of an evaluation.

Mr. Nickell: This is the "old saw" about the good engineer using the bad program to get a good result and the poor engineer using a terrific program to get a bad result. That is why we have tried to really control the operation in these efficiency comparisons so that everybody does the same thing and it is not user dependent. I agree with your assessment of that situation. I have known many people who have done fabulously well with programs that have all kinds of faults in them and if they were used by another person they would lead them down the "primrose path"; that is what we are trying to avoid. We also want to avoid the so called subroutine answer syndrome namely that somebody has a code somewhere which generates numbers that are remarkably close to an experiment but in fact no one is really quite sure whether that is the only result it will ever get.

Mr. Showalter, (SVIC): These manuals and documentation will probably run through my hands at least once in this whole procedure. When you review many of them, you find out which ones are poorly documented and which ones are well documented. Does anyone have feelings about the quality of the documentation that they have seen, especially on the large structural programs? Is there room for standardizing some of the documentation? Have you been buffaloed by some of it yourself like I have on the large structures programs?

Mr. Eshleman: I don't know much about the large structural programs but the documentation of the rotating machinery and the shock isolation programs that I am familiar with has been bad all around. I don't think that one person could pick up the program and use it without extensive learning. I suggest that you should have a format for documentation.

Mr. Nickell: In your opinion the concern about documentation is not a "red herring"?

Mr. Eshleman: Not at all! That is a real problem and I believe that to achieve some sort of universal usage the first thing is documentation.

Mr. Nickell: This is a question of perception. If you talk to the developers, they will generally tell you, quietly in the back room when they are not in public, that documentation is a "red herring". This is propaganda that is put out by managers, it is really meaningless, and in fact the users are having no problems at all. A better perception of the problem is needed. The users, on the other hand, are stumbling their way through the user's manuals and they are groping with trying to solve their particular problem. I am not sure whether they are having trouble or not.



Voice: Every user that I have talked to is having trouble.

Mr. Nickell: The American Nuclear Society began an effort about five years ago to develop a set of three level documentation standards. They published what was virtually a book, it had about 85 or 90 pages representing the description of the standards by which the documentation was supposed to be judged. It received severe criticism just because of its sheer bulk. I am not sure whether anyone else has had the temerity to try to establish documentation standards since but it is a novel idea.

Voice: One of the most annoying things I have found in the documentation of some of the programs has been the practice of documenting a feature prior to its being coded and then not bothering to code it.

Documenting things like having a conical shell element when in fact it is a cylindrical shell element; if it goes to a flat cone it doesn't work. There seem to be several instances where documentation was written ahead of time if not in fact published, and nobody bothered to fix it for the things they didn't code. It would be particularly helpful if it could be pointed out which features aren't in a program. I have spent time learning to use a code, which is always expensive in manpower, only to find that the feature I was using that code for did not exist.

Mr. Morosow, (Martin Marietta): Unless you work the program to its capability you may not have a valid comparison, in fact you won't be able to evaluate the capability of the program. Let me give you an example. Some years back on the Skylab program the intent was to perform a buckling analysis of a shell which was a skin stringer type of shell with some parts monocoque and a fairly large system with many degrees of freedom. NASTRAN at that time said "yes we can do it", other programs said "yes we can do it," our own program said "Yes we can do it." The net result was that we did not get any results until we finally searched out a program that was basically a finite difference program, and I don't want to even tell who has it and they were able to solve it. Everybody else claimed that they could do it. I am afraid that sometimes you have to stretch the program to really see whether it has that capability or not.

Voice: Can I ask you a question about that? It was not just a matter of economics then? The capability was not here?

Mr. Morosow: We did not get the solution. Buckling is a fairly complex mode. It is a difficult representation it is much more difficult than getting eigenvalues.

Mr. Nickell: So, establishing the absolute limits of a particular piece of software also should be part of it.

Mr. Paladino, (Naval Sea Systems Command): I would like to see your group really provide a set of guidelines for all of the software. If you are not familiar with the program you can misuse it, or use a very complicated system which is costly. Give the user some guidelines so he doesn't get lost. There will be many new people coming into this field and

don't let them use a complicated program if they don't have too.

Mr. Nickell: Do I understand you to say that you want guidelines on modeling?

Mr. Paladino: Yes, and also the limitations on programs. It is a very sophisticated program don't let someone use it because it will be very expensive. Perhaps you can get the same answer from a different program that is not as complicated and is much simpler to use. The Navy modified the original NASTRAN because they couldn't afford it. Now it is cheaper to use and we get good results.

Mr. On, (Goddard Space Flight Center): I would like to address the question of selecting contractors to evaluate the various programs. Generally you have to go to a contractor that has some expertise in the use of the program and that almost limits you back to the person who developed the program. So to start with you already have a built-in bias in the evaluation. Ideally you would like to go to an independent contractor who was not related to the development of the program. In such a case like that the contractor may not have the expertise and the familiarity with the use of the program.

Mr. Nickell: Do you really believe that? I have observed that there are literally dozens of small firms, and some large ones, around the country who are using software that they did not write and who have become absolutely expert at using not only those codes but a variety of other programs just like it. They are also expert at making judgements about which software they want to use in any given situation. I know many consulting firms that use all kinds of proprietary codes that they didn't write but they have good judgement about which one to pick for which problem. Is it your feeling that these people don't exist?

Mr. On: We have been users of NASTRAN and there are a couple of versions of NASTRAN; we have used it for about ten years and there are still some problems that NASTRAN level 16 won't solve as well as the McNeal Schwindler version of NASTRAN. We only learned this by experience.

Mr. Pilkey: We assume that we will find contractors that can evaluate other people's codes and under no circumstances would we select a contractor who developed the code to evaluate his own code. Do you think that is dangerous? Do you think we will have trouble?

Mr. On: I really think you will have a bias in a contractor's evaluation.

Mr. Pilkey: We believe that properly controlled there will be no bias.

Mr. On: I want to wish you a lot of luck.

Mr. Curtis, (Hughes Aircraft): Frankly I don't think the problem is as bad as you indicate. In my department we use whatever program we can that will get the job done as economically as possible. We have access through terminals



to a variety of programs such as STARDYNE, SAP and the various versions of NASTRAN. There are people who have used all of these programs and we are certainly unbiased, we don't want to develop programs we would like to have them available to us. There are people who are not only objective but who are very critical of these various programs. I have two comments. First, the discussion has been about evaluating the difference between programs but it seems to me that running the same program on two different computers may not yield equivalent results. I am not sure what you would be evaluating in that case. Second, most of you probably know that NASTRAN can handle orthotropic materials whereas a more economical program that we often use cannot. If I have a more economical program and I need to examine orthotropic effects I am not sure how I would evaluate it if I need to take orthotropy into account. It really doesn't matter how efficient or inefficient that program is, if it is the only one that can do that, or the only one available to me that does that, then it makes no difference.

Mr. Nickell: Let me answer your second comment first.

It would be clearly pointed out in the functional description that will be provided for each code that such a code could not handle orthotropic properties; but if that program then turned out to be very efficient in comparison with other codes I would suspect that the developer would be stimulated to add that feature if it were crucial to his business. I agree that you should use the most efficient program for your particular problem and you should determine that on the basis of the functional description of the code and your problem. In regard to your first comment a great deal of documented evidence indicates that some programs run very well on some machines and some run very poorly on others but that has not been part of our study. In every case we will use the program on a machine which is roughly its host, that is the machine for which it was developed. For example we will not try to run a code that was developed for a CDC machine on a UNIVAC machine or vice versa. That may mean if you have a UNIVAC machine you may wish to use this code, and we are not going to address that question.

## DATA MANAGEMENT

Moderator: Major David R. Spangler, Defense Nuclear Agency  
Washington, DC

Co-Moderator: Mr. Edward J. Martin, General Electric/Tempo  
Santa Barbara, CA

Panelists: Mr. Glen Wadleigh, General Dynamics/Convair Division  
San Diego, CA  
Mr. Clarence A. Davidson, Sandia Laboratories  
Albuquerque, NM  
Mr. Wilbur Rinehart, National Oceanic Atmospheric Administration  
Boulder, CO  
Mr. James A. Malthan, Agbabian Associates  
El Segundo, CA

**Major Spangler (Defense Nuclear Agency):** This is the panel discussion on data management; hopefully we will be able to provide some insight into a number of existing systems that are in being to address data management for specific user communities. The systems that we have represented here range from the very specific that are pertinent to one company, to those that range over a wide spectrum of users, different communities and varying requirements. These presentations should give you some appreciation of the variety of problems that exist when you range from small communities to very large ones and we want to stimulate discussion on how we can better manage the data in these various systems. We would like to provide a brief discussion of the capabilities of these systems that different organizations, communities or groups have established. We want to learn how they address the problem of data management pertinent to the shock and vibration community, and the floor will be open for discussion of other requirements, other existing systems that you might be aware of, and any interface that might be able to be achieved between these types of systems. Some of you might know of other requirements that need to be addressed but aren't being addressed.

The reason for this panel discussion is obvious. It recognizes that a great portion of our budgets and our efforts in the shock and vibration community should be, or are addressing the best and most efficient use of the data that we are accumulating or that is in existence. I think we have to be constantly aware that we not only generate new information and new data, but once we have gained the new data we should utilize it properly.

**Mr. Wadleigh (General Dynamics/Convair Division):** Within the past few years at Convair we have developed a data management system specifically for handling our environmental vibration data. We have chosen a particular 7-tier hierarchy to store our data and we derive our data from flight vehicles and from our laboratories. We store most of our data such as our power spectral densities, shock spectra, or acoustic data in the frequency domain rather than

in the time domain. All of our original data were recorded on analog tape in the time domain and we have processed those data into the frequency domain for storage into this data system. Our most detailed breakdown of data is clear down at one particular function residency. We can also store with more general levels, and our most general description is by vehicle type, then we can be more specific and categorize data by zone, by measurement type, measurement number, and flight period. These data can be recovered in any one of those levels and we can produce lists or reports from textual information that we have stored. We can also retrieve the actual X-Y data, we can plot each of the functions, we can plot multiple functions, and we can operate on those functions.

We had a large collection of data that we have gathered for some 15 or so years when we started this system in the early 70's, and we had no inventory of it. It is very difficult to go back through our data and find which vehicle had which particular measurement or how the vibration in the propulsion zone on that vehicle compared to the same data on a different vehicle. The data were recorded on individual pages of miscellaneous flight reports, they were all plotted to different scales, the frequency scales were different, some were semi-log some were log, so this system was designed to get us a common data base from which we could retrieve and plot on a common basis. We have a workable data management system that will provide the fast answers to very specific questions. It was very expensive to develop but we now have about 1000 arrays of launch vehicle data and about 500 arrays of laboratory data stored in this library. This one particular bank contains some 750,000 60 bit words. I am told that it only requires a quarter to one third of the standard reel of "mag" tape, so we have a long way to go before we are really pushing our system. It is a general purpose data management program with particular aerospace applications, and I expect we will use it for several years.

**Major Spangler:** As you can see we have started with a specific system, one that was initiated because of a

requirement within an organization for recurring design or systems needs. We will go from a specific single user to a broader system that serves a number of users and a number of different disciplines.

Mr. Davidson (Sandia Laboratories): From the moment of its manufacture equipment or cargo is exposed to an environment. This exposure affects the useful life of that item in inverse proportion to the protection given by the design considerations whenever it was manufactured and the environments that it sees during storage, transport, handling, and use. It is useful and economical to have a central store of measured environmental data available to your engineering staff since they don't have to "reinvent the wheel" each time they need environmental data. It is also a time saver for the engineer who has a problem either with test or designing an article for shipment.

We have two data banks at the Sandia Laboratories. We have a Department of Defense data bank that is sponsored by the Defense Nuclear Agency and it covers the conventional and nuclear ordnance items. We have a transportation data bank that is sponsored by the Environmental Control Technology Branch in the Department of Energy and it is for the Department of Energy users, private industry, educational institutions, foreign countries, or whoever would like to use it. The first data bank for normal environments was started in 1959. We added the abnormal environments for weapons in 1973, and in 1974 we were asked to start a transportation bank for radioactive materials. We added storage, dissemination and special studies to that bank in 1976 and 1977 to cover all energy materials, we didn't limit ourselves to radioactive materials.

The purpose of the second data bank is for transportation, and that is the one that I will describe. We store criteria for shipping container design to support the functions of the test engineers. We are concerned with both normal and abnormal environments. Normal environments generally have a low intensity but they occur frequently in nearly every shipment, whereas the abnormal environments have a very low frequency of occurrence but they have a very high intensity; the latter category mostly concerns accidents. In order to index our information and make it available to people in the transportation area, we have elected to divide the environments into 12 categories and some are both normal and abnormal. Our retrieval system and our storage system are based on these 12 categories. Three factors operate to limit the number of environments for which abnormal levels require consideration. For instance, humidity, you can't get above 100%; so when you protect for the normal you protect for the abnormal. Acoustic noise might be abnormal if it causes structural damage. Another example of protecting against the effect of an abnormal environment is the entry of water into an item during a downpour or an immersion, it is the same as if it is in a drizzle, you don't want that to happen. The data bank is structured with the input and the responses to the 12 environments. We define input as that activity that goes into the vehicle, and the response is the way that the cargo or equipment reacts. Some are normal and others are abnormal. There are some examples of the useful parameters that we would like to have with regard to abnormal environments. For earthquakes, we would like to

have the time histories, for impact we would like to have vehicle velocity and so forth.

We have a number of data sources. The information that we collect, abstract, and store comes from industry, from other government agencies, from activities within the Sandia Laboratories; when we don't have data, or if we have made a search and determined that the data appears not to be available, we go out and make the measurements and then bank that information. Most of you may have used one or more of these data sources that I spoke of at one time or another. In the central file of the data bank, you will find a store of information on transportation from all of the various government agencies, industry, and private institutions that provide data. The people that use this information are many of the same people that provide information. These consist of industry, schools, institutions and government contractors. Foreign countries are also beginning to use this information.

The data are computerized and they are entered into the file randomly without regard to title. We assign a number to each entry; the first four digits tell what environment it is, the last three digits give the number of cards available on the subject. We have broken it down by the type of transport, whether impact or crushing occur within that particular environment, and also whether it is input or response. We publish an index which is available to those who have requested data or to anyone who might like to use the bank within the realm of our time to recover the information. It is a very stable system. We average anywhere from 30 to 45 requests a month for data from sources outside of the Sandia Laboratories; we also have a branch in Livermore, California and they also provide information. We have one central input in Albuquerque, but both the satellite data bank at Livermore and the main data bank at Albuquerque provide information to those who request it.

Major Spangler: We are presenting a rather diverse group of data management systems because the Shock and Vibration community is a very diverse group. We have an interest in different bits of data relating to shock and vibration for many reasons, so we have tried to present a broad spectrum of systems that address these problems. One of the ideas that we want to impart is the difficulty having once gained all the information and having it available, of letting the user know about it and how he can retrieve it. In some of the following presentations you will find more about the methods that have been used for actually disseminating the information, making it available, and also making the user aware of its existence.

Mr. Rinehart (National Oceanic Atmospheric Administration): The National Oceanic Atmospheric Administration (NOAA) is in the Department of Commerce. Around 1970, we established the Environmental Data Service and it is funded separately from our other research activities at NOAA so it doesn't have to compete for its money, outside of the top level of our agency. This has provided a continuum of our archiving meteorological data or solid earth geophysical data. There are six data centers in the Environmental Data Service. I am associated with the National Geophysical Solar Terrestrial Data Center in Boulder, Colorado, and there are

two divisions that primarily provide data to users, the Solid Earth Data Services Division and the Solar Terrestrial Physics Division that handle mostly upper atmosphere physics, or ionosphere type information. In the Solid Earth Data Services Division, we handle seismological, marine geology, geophysical, and geomagnetic data. I am in the Environmental Hazards Branch.

We have a number of data bases; the HDF is the Hypo-Center Data File that presently contains about 130,000 locations of earthquakes ranging in time back to about 1700. In the near future it will be over 200 thousand with data that we have obtained from the Chinese primarily through the efforts of Dr. Hamilton whom you heard yesterday. We also have data from Eastern Europe and the Balkan areas that go back to around 2000 BC, some biblical references there I guess. The effect file is a file of data that refers to the isoseismal maps that Dr. Hamilton mentioned in his talk. The effect file has taken the literature and coded it so that for any place name in the United States we have some indications of the intensity of shaking at that city for earthquakes over a time history.

SM stands for strong motion, and I want to address that because it is somewhat closely related to the shock and vibration data. Since about 1928 there have been seismic instruments that are triggered by earthquakes. You do not see the initial key wave, the compressional wave, but you do see many of the succeeding damaging earthquake waves and we get our data primarily from the Seismic Engineering Branch of the United States Geological Survey in Menlo Park, California. There are a large set of data from 1928 to 1971 that have been digitized by a contractor that has a flying spot scanner for digitizing these seismic entries. These data are all reduced to digital values and they can be used in design spectra by engineers and also the nuclear siting engineers. The San Fernando earthquake in February 1971 produced about 300 records that were digitized by the California Institute of Technology, and they are also available. We also get digital data from foreign countries. I recently received the data for the Bucharest earthquake, that occurred in the summer of 1977.

Our users are primarily engineers who are interested in environmental impact statements or nuclear plant siting, seismologists, or seismological engineers who are doing research in building design or building response; they use the digital information as the input forcing functions to their models. The entire data center received 10 thousand requests a year but the Solid Earth Geophysics probably handles about six or seven thousand of these requests. They are world wide since we are not only a federal government agency, but we are also the world data center for solid earth geophysics which means that the Russians or the Chinese will contribute data to us and we send it back to them. We also have a large collection of earthquake damage photographs and I noticed that Dr. Hamilton used a few of them yesterday. We have a catalog of these in case people need these for illustrating their talks or publications. We make maps and searches from the Hypo-Center data file. A person will ask us to search around a certain spot, or give us the latitude and longitude where he wants a map made, and we can do that. We are also starting to get digital data. The Geological Survey has installed about 15 digital stations in the world and their readings are re-

corded on cassette tapes that are sent in to their laboratory in Albuquerque. Then they are sent on to an ARPA facility in Alexandria, VA which currently makes copies and distributes them to researchers. We are archiving the copies but so far we have no authority to pass them out. One of the problems is that we have many people who ask for data and we send them a data tape; most of the time we send them 2400 feet of tape and often there is only 100 feet of data on it. It is no big deal because the tape is relatively cheap these days, but we are starting to get into some new technology. We will use a Tektronix 4051 which is a "smart terminal" that has up to 32 thousand words of storage, it has a cassette tape recorder, and it uses the Basic or Extended Basic language. We can use it to provide data. There are other manufacturers that build "smart terminals" that have floppy discs in them. We can provide data, and we can also provide programs that unblock the data or even analyze the data. Thus if a person wants us to provide a program that produces a velocity response spectrum and that also does the graphics right on the scope, we could do this. But it is necessary that one has the same type of equipment that we do, so we are investing into a number of these kinds of small terminals that will be able to serve us in a new way.

Mr. Malthan (Agabian Associates): I would like to give you some indication of where we have been in the development of the Defense Nuclear Agency Master File of Ground Shock, Air Blast, and Structural Response Data. I would also like to give you some indication of where we stand today and perhaps try to make some projections of where we think we are going to go with this system. Following World War II you may recall that the United States engaged in a relatively large number of atmospheric nuclear tests and that continued more or less uniformly until 1958 when the United States and Russia entered into a moratorium in which they voluntarily agreed to cease all atmospheric tests. That continued for several years and then you may recall that Russia went into a series of very large scale atmospheric tests. The United States responded in kind until 1963 when the Official Test Ban Treaty was signed. I believe the United Kingdom was also involved. This treaty banned all atmospheric nuclear tests. That left the United States in somewhat of a dilemma in the continuing development of its nuclear weapons effects technology and a number of alternatives were available to us. We could conduct high explosive field tests on a very large scale up to 500 tons of equivalent TNT, we could continue to conduct underground nuclear tests, we could conduct specialized tests using large scale blast generators or shock tubes, or we could perform calculations.

I would like to discuss primarily the proliferation of the high explosive field tests which began almost immediately after the treaty was signed and which continue on even until today. In 1972, the Defense Nuclear Agency decided that some effort should be made to consolidate this high explosive data into some file so that researchers could use it. If all worked well, perhaps we could work back and start looking at some of the old nuclear data. The purpose of this program was to collect the raw data from the various organizations which had conducted the tests, reformat this data into a consistent format, establish some sort of a universal identification system that researchers could readily identify and use, prepare directories so that researchers could locate the data that they needed, retrieve any piece of data for these researchers on their demand, perform some sort of a signal processing on that data if

required, and present the data to them in some raw or processed form as they dictate it. The data could be on tape, plots, punched cards, or on a print-out. If it were necessary or desirable their processed data could also be stored so that it could be called up in the future. Eventually, we hoped that we could go into a period of disseminating the capabilities of the system to a wider user group to increase its use and to establish procedures for the use of that system in the future. We also wanted to develop some sort of cost guidelines so that the individual researchers could make some estimate of the cost of utilizing the system.

The data that are in the master file are composed of ground-motion data, stress and strain data, air blast data, and a very minor amount of structural data. It is all time series data, except the coded data which is the high explosive information. There are presently 5 thousand channels of data on tape and that comprises about 45 reels of full tape. The system which is used to implement the master file consists of five basic modules. The editor subroutine accepts raw data and reformats it into a consistent format. The update data takes the data from the editor and builds a master file from it and constructs a directory. An extract program allows the data to be retrieved from the master file according to some processing request supplied by cards. A data processing module allows the data to be processed in many different ways, using standard time series analysis techniques. A post processor module allows the processed data to either be output as plots on tape or cards. It can also have the processed data returned to the master file through the update program so that it too becomes a part of the master file.

Eventually we developed cost guidelines, one of which we called the simplified usage guidelines which allows a researcher to make some kind of estimate of the computer time and labor required to process a given number of channels of data. This particular kind of format is based on some average file located at some average location on a reel of tape, comprising some representative type of processing sequences. There are a series of more elaborate algorithms that were developed for more specific kinds of processes which can be used by individual researchers to develop more exact estimates of the computer time and the labor required to do very specific kinds of operations for both single and multiple files. That brings us up to date as to where the system is today.

Let us take a look at where we think we will go in the future. It is presently a little nebulous exactly where we are going to go. In October 1976 we conducted a two day seminar in Los Angeles in which all Defense Nuclear Agency contractors who might presumably have some interest in this master file plus a number of other researchers, who had an interest in other activities and who might also be interested in this system, were invited to attend. We went into great detail about how the system was constructed, how it was to be used, its capabilities, and so forth. At that time the Defense Nuclear Agency made a public offer that those who would be interested in using this system could do so free of charge in order to familiarize themselves with the system. Over a period of the next several months a number of organizations requested us to process data, and we did that for them. Then finally in July 1977 a group which had been formed earlier by Defense Nuclear Agency known as the Data

Analysis Working Group (DAWG) also had a meeting in Los Angeles which extended for one day and many of those who attended the seminar were also invited to attend this committee meeting. The purpose of this meeting was to answer some questions which had to do with the future of the archive. At this meeting two particular distinctions were made between an archive and a library. An archive is defined as a safe depository, or a permanent depository for original data generally thought to be on analog tape. Any associated information might be applied to it, such as calibrations, log sheets, drilling logs, diaries, or anything that might reflect and add information to the data that were collected. And this particular data was thought not to require immediate turnaround. As a matter of fact, most people would be satisfied if the turnaround were on the order of a week to several months. On the other hand, a library was conceived to be an active storage of both raw and processed data on digital tape; it should be in engineering units and immediately available for researchers. To facilitate its use it should have quick turnaround which is measured in terms of days or weeks. Four questions were asked in the Data Analysis Working Group Meeting which had convened in July 1977. 1) Is there a need for an archive and/or a library? 2) What services should be provided by those archives or libraries? 3) What data should be in the archives or library? 4) Where should these two functions be located? The conclusions reached by that group of users were that all of the field test data should be archived together with related information so that a researcher in the future could obtain analog data, the auxiliary information with it, and reanalyze it if desired. It was thought that there was no real recommendation to establish a library but it was felt that if one were established it would motivate increased data analysis by researchers which was considered to be a positive factor for its establishment. The cost of such a library was then and is now still unknown. A positive factor though is that if it could be established at a government facility then it would be cost effective in the sense that it would be readily accessible and there would be no penalty for low usage. If the library were properly established that in itself would motivate increased use. The library should contain both raw and corrected data and almost everyone agreed that there should be no processing capability associated with either the archive or the library. In fact, when people retrieve data from either the archive or the library they should do their own processing and almost all agreed that is the way to do it; that is, they didn't want some other organization processing their data. Finally it was felt that users should be consulted in planning either the archive or the library as it developed, so that users desires could be factored into the development of these two functions. Finally the recommendation made by the Data Analysis Working Group was to take immediate steps to stop the destruction, loss, and deterioration of existing data. We are referring primarily to the nuclear data and, believe it or not, there has been some loss both from losing the data and the deterioration of the material to the point where it is not useable. A data archive should very definitely be established. The analog tapes and other auxiliary information in that data archive should be at DASLAC. The Defense Nuclear Agency should entertain plans for developing a data library and if the library is established it should be located at a government facility, preferably at the Defense Nuclear Agency computer which at the present time is in Albuquerque, N.M. The Data Analysis Working Group established a priority list of data to

be added to the master file and topping the list was the old nuclear data which was in dire jeopardy of being lost and then following that, new and current HE tests should be added to the file. If a question of priorities arose then ground shock should take priority over air blast information, higher yield data should take precedent over lower yield data, and finally if there were funds available then structures data should be added to the file. The Data Analysis Working Group also recommended that it be used as a committee to guide activities for the development of the library and presumably also of the archive. At the present time, I believe that the Defense Nuclear Agency is acting on these recommendations.

**Major Spangler:** Our last presentation will branch out not only into data management but perhaps provide more knowledge about information management which may be of interest to many of you in the audience.

**Mr. Martin (General Electric/Tempo):** DASIAC is an information bank that may be of some peripheral interest to the Shock and Vibration community. It is an information activity which General Electric has operated for the Defense Nuclear Agency for over 15 years. It is one of the information analysis centers sponsored by the Defense Nuclear Agency. The subject scope is nuclear weapons effects, simulations, and related topics. It is similar to the shock and vibration group that is sponsoring this meeting. It sort of crosses classical disciplines and provides a variety of information services for the Defense Nuclear Agency contractors and other Department of Defense people when they are bonafide and established. It has an information collection of books, technical reports, data from past nuclear weapons tests and simulation efforts, and computer generated data files. The instrumentation records are in the form of picture films, oscilloscope films, strip charts, a wide variety of a heterogeneous nature. Our customers are primarily contractors interested in weapons effects and for you this means impulsive loading so there is a small overlap between the Shock and Vibration community and our subject interest.

The people in our community use many of the tools for predicting the response that the Shock and Vibration community has developed and they have probably supported the forcing functions for hardened systems that many of you may have worked on. We have a broad variety of people who use the center. We are prepared to do something for those who develop the handbooks on which design engineers base their work, those who contribute and also use the center, and those who are merely users who need to know an answer, and we may only see them once. Our users are primarily sponsored researchers we see very few individual seekers after truth. We provide the usual bibliographic type services; we provide summaries of our data base, special compilations, limited publication services, and a variety of miscellaneous information services such as the distribution of certain well used nuclear weapons effects computer codes. Our data management process is very simple. We have data that are of a very heterogeneous nature, and as I pointed earlier, the use of any single file is rather small so we can't afford to build a computer system to retrieve and display a single gaged record. If somebody wants that sort of thing we go to the shelf pull it off and say here it is.

I would like to discuss the various data management approaches, perhaps pick up some of the threads that were mentioned yesterday in the invited papers, and perhaps get a little idea of the data management techniques that the Shock and Vibration community has developed. I want to make a distinction between data and useful information. There are people who say "we have data up the kazoo," what they need is little information. We are in a situation where we can generate many more numbers than we can usefully handle both in experiments and computer code predictions. I think one way of handling these things is in the systems that Glen Wadleigh and Jim Malthan described. The computer is used as a housekeeping and bookkeeping system that not only retrieves the data for you, if experimental records are stored, but it may also perform various operations on the data to translate it into meaningful information for the user. I think all these things are methods of data management. The direct numerical retrieval of data includes the retrieval of experimental data arrays, the strong motion data of the National Oceanic and Atmospheric Administration bank, our blast and ground shock data bank, and the vibration data bank at Convair. The Defense Nuclear Agency has been involved in the development of files of various physical constants that consists of non-experimental material that has been evaluated. A best value is put on a computer tape and you can get these; this is another sort of numerical retrieval. Finally there is another data bank. The Defense Nuclear Agency and the Army sponsors one where the Harry Diamond Laboratories accumulates and retrieves a limited number of parameters of data on the response of transistors to radiation effects. I think that the direct numerical retrieval of data is in good shape. That is there is a great deal of work to be done but at least the factors can be analyzed. You can say that one person has done it better or worse, and that their use or demand is measurable and can be compared with the expense of setting up the data bank. You can determine if there is enough call to do all of the record processing. Throughout the scientific community we are generating reams and reams of numbers. With these, it is at least possible when you talk about retrieving numerical data, to sort of get some handle on whether it's an economic activity.

Document retrieval is the second form that is directly numerical, and this is what Mr. Kolb mostly talked about. I do not think that this is in very good shape. He mentioned something about the three year half life of published scientific information. I think this means that the half that is thrown out after three years is probably junk to begin with. We are at sea in paper! But some of this is required by contractual obligations and the person who sponsors research wants his pound of flesh. So the experimenter, reluctantly or not, writes up his inch and three quarters of paper and sends it in. Then it is duplicated 23 times and sent to some people, the Defense Documentation Center, the National Technical Information Service, and it gets into various data banks. We see the kinds of curves that Mr. Kolb showed us are growing. I would like to pose some possible ways in a community where this sort of thing could possibly be handled. The March 1977 issue of the Shock and Vibration Digest had an editorial on review papers. This picks up the theme that Dr. Lewis M. Branscomb wrote in an editorial in "Science" several years ago; that is there are implications for funding agencies to spend a little more time reviewing what they are doing instead of simply going ahead and doing something.



There are things that the agencies might do instead of requiring contractual reports. Perhaps if there is any significance to the work, that is if it is anything that should be published, it should be submitted in the form of an article to the proper professional journal where the author's peers can evaluate it and it may or may not be published. Within the allocation of federal funds, a certain measure of peer review exists. This meeting is one example. I was appalled when Mr. Kolb said that he expected a truckload of references when he tapped out shock and vibration on his terminal. I can't imagine how anybody would want a truckload of references about anything! It seems that this is what we want to avoid. However I can't personally complain because the truckloads of references provide a job or a little bit of insurance for me. But I think we are seeing a build up or an entropy in the scientific and engineering field where for each dollar spent in research less is spent in actual search and more is spent in documentation and shuffling papers back together. Some of this is consistent with the graphs Mr. Kolb presented where it showed that back in the "old days" half of the work force was doing reasonable work but now 95% of the people are doing what he called information services. Maybe there is a certain amount of feather-bedding in this, it provides work, and certainly many of us would be out of it if it was just honest work done. However, still being involved in it one would like to see some improvement in documentation as far as possible. So many of our problems are future problems. It is implied, especially in the engineering and scientific community, that there is a technological fix and that we can escape the seemingly inescapable growth problems because we will figure out something to do. Well if you look at this sort of growing entropy in the research effort, you come to the conclusion that there may not be a technological fix because we have this growing bunch of people and the research dollar buys less and less research.

**Major Spangler:** This afternoon you have heard a description of a number of different attempts within the Shock and Vibration community to address data management. I think Ed Martin has said that we should be careful to make the best use of all of this data, convert it into useful information, and make it available to everyone in the proper form.

**Mr. Kennedy (Defense Nuclear Agency):** We have heard references to some biblical data and I know of the shambles that the nuclear data base is in right now as far as actually putting it into a computer. What are your thoughts on taking the existing data as it stands, be it in the Bible, oscillographs, or what not, and actually putting it into a computer? This seems to be a big bottleneck and a large cost factor especially for nuclear data.

**Mr. Malthan:** While it may take months or perhaps years to find the data, and even if it takes longer to digitize and reformat it, it is the kind of thing that can be worked out so that the problem doesn't seem to be very severe. That is you can get the data into the computer, but now what? One of the great surprises in the Defense Nuclear Agency work was that people didn't use it! There are 5000 channels of very pertinent information addressing problems of great uncertainty; for example, there is information in the master file that would provide some enlightenment on cratering. Why didn't they use the master file even when you offered to search it for them free of charge? There are probably a

number of reasons for that. First, and one that I have never stated before, is the "but it's not invented here" syndrome; that is if someone hasn't devised this procedure himself then he is skeptical about using someone else's ideas and I can see some of that. Second, it would have been nice had the researchers come to this conclusion that they needed this data and would have given some sort of guidance to the Defense Nuclear Agency to do this. As a matter of fact the reverse occurred. The Defense Nuclear Agency was the one that decided that the master file should be created and that the researchers would almost surely flock to that data to use it, and that didn't happen. There are other criticisms; it is too cumbersome, you have to walk across the room, you have to pick up a phone in order to get the data out, sometimes it is slow coming out, and by the time someone gets the data he wanted he has forgotten why he wanted it. A number of these issues come to light but somehow it leads to the fact that even if you had a master file created of all this data, I am not really sure if it would be used. To some extent, it is easier to go out and run a new test.

**Mr. Rinehart:** The Geological Survey digitized all of the strong motion data since there were only 2000 records. There is a vast quantity of data there that will never be used, I know that. We get two requests a month for strong motion data and usually we send this out on punched cards. I also have another data file that comes in digital fashion and so far we have no requests for it; we have advertised it in the journals and we sent out fliers. I suspect it will be an important thing in earthquake predictions since it is ultra long period seismic data and perhaps the researchers are not aware of it yet. As far as going to the Bible or any other source, usually I get data from people who are interested in a particular area. It might be a Yugoslavian who wanted to study the Balkan area and so he had to go to any source he could find. There is a scholar in London who looked into earthquakes back to the year 2000 B.C. and he read the Odyssey and found one earthquake there. So these data come to us usually in listings which we simply have to have key punched.

**Major Spangler:** One of the general conclusions that we came to as a panel is that there are a number of other information centers that exist that haven't been discussed. One of the things that has been experienced in attempting to provide an information center for a broad spectrum of users is the fact that you can't dictate the user going to that file or that information center and using it. Many of these very broad spectrum information centers have languished from the standpoint of the number of users or any requirement for them and they are having a very difficult time making it just because people don't go to the file; it is trouble. It is more difficult than going to something you have in-house, running a new test, or a new idea that you can readily sell because it is identifiable. It is very difficult to sell analysis of past data. So the broad spectrum data management centers appear to have had some difficulties whereas some of the more particular systems, such as those that have been discussed in a couple of instances here, have done quite well because the users have actually demanded or provided the requirement for setting up that particular system and they have also shown that there is a user need. I think that is a problem that we have noticed across the board.

**Voice:** With regard to computerizing all of the data sources, you can put a wealth of data in the computer but if people don't have terminals available, or if they don't request the information, then they are not using it and I think you are fighting a losing battle to keep it on the computer. At today's costs, even for disc storage of information, it will run up your cost to operate that data center. So if you don't have a rather large user area where you are getting requests, and if they don't have to have fast turnaround where you can give them the data within an hour or two manually, they would only get it 60 or 70 minutes faster if they had a terminal. They may not even get it that fast if the terminal is

down. I think you have to weigh this in your data centers of the future as well as data centers that are currently in existence. Recently we have heard of two or three data centers that were operational on the computer, and they are just about to be sold off. They will shut them down because they don't have enough users to justify the cost for the computers and terminals that are involved in the data bank operations these days. So that is something to consider when you set up data bank or when you have data that have been taken either by analog or some other means you want to convert it to a data center.



## MODAL TEST AND ANALYSIS

### FORCE APPORTIONING FOR MODAL VIBRATION TESTING USING INCOMPLETE EXCITATION

G. Morosow  
Martin Marietta Corporation  
Denver, Colorado

R. S. Ayre  
University of Colorado  
Boulder, Colorado

A technique is presented for determining the shaker forces necessary to isolate a mode during a modal vibration test. The approach requires no prior knowledge of the model and is particularly usable for structures with high modal density.

#### INTRODUCTION

A modal vibration test, or a modal survey as it is sometimes referred to, is a test imposed on a structure with the purpose of establishing or estimating its modal parameters. A modal vibration test is performed by applying one or more exciters or shakers to the structure being tested and then driving it sinusoidally, randomly or by a specified transient force. In general, the testing can be done in either the frequency domain or the time domain. The material presented in this paper pertains to sinusoidal testing only.

From a practical point of view it is difficult, if not impossible, to achieve pure resonance in a test. A pure mode exists only if damping forces are in equilibrium with the applied forces at each point throughout the structure. Because in a real structure the dissipative forces are distributed continuously throughout the structure, it is impossible to achieve a strict equilibrium between applied and damping forces everywhere in the structure if only a finite number of exciters is used. Continuous aerospace structures can be represented reasonably well by dynamic models on the order of several hundred degrees of freedom. It would be impractical and physically impossible to use that many exciters. The practical limit is, perhaps, ten to sixteen exciters, but more commonly six. In this case the damping forces throughout the structure will not be cancelled at their points of origin and the condition for the existence of a true

normal mode will not be achieved.

The method presented in this paper is based on the multiple exciter, tuned dwell approach originally developed by Lewis and Wrisley (1)\*. Their intent was to:

produce in a complex structure, by means of adjustable forces, oscillations that consist essentially of one natural mode.

The majority of modal vibration tests performed during the last 10-15 years was based on the Lewis and Wrisley approach. In general, an iterative adjustment of force ratios and the excitation frequency is used to minimize the phase differences among various points on the structure and to bring all the displacement or acceleration measurements into quadrature with the excitation forces. It is basically a manual, iterative phase-optimization process which is laborious and time consuming. Much depends upon the degree of skill of test personnel and their familiarity of the structure.

Several papers on shaker force apportioning were published in Europe. Specifically, in 1968 Deck (2) published a paper on the subject using a semiautomated method to obtain a phase coherence. Prior to this in 1964 deVries (3) discussed the problem of determining the excitation forces.

\* The numbers shown in parentheses are the references given at the end of the paper.

He considered this problem to be the most difficult:

Determining the excitation forces is at the same time the most important and the most difficult problem in vibration testing.

With  $n$  available exciters it is possible to eliminate  $(n-1)$  modes. This statement is, however, of very little practical value because the modes can be eliminated only for one certain distribution (a priori unknown) of excitation forces, the study of which would necessitate a displacement of the exciters, and would be impossible to achieve in the event that certain elements of the structure should be inaccessible.

He developed an approach using additional artificial damping supplied by the shakers to complement nonproportional damping and to convert it to proportional damping. In this way he decoupled the system of equations and eliminated one source of error. There is no discussion regarding the errors due to incomplete excitation or higher mode interaction.

Jamison and Tao (4) developed an approach for shaker force apportioning using pretest analysis as a basis. They formulated an optimization problem using a Lagrange multiplier technique. In this approach modal displacements must be known.

Asher (5) suggested an approach whereby an experimentally determined admittance matrix is used to determine the natural frequencies and the force ratios required to obtain the best approximation to a corresponding natural mode.

However, the methods discussed cannot guarantee that a usable mode will be obtained under all circumstances. The most important factor is a judicious placement of shakers. Unless a great number of shakers is available where for each mode the "optimum" subset is used, the skill of the test conductor may mean the difference between a successful test and a set of unusable data.

The method proposed does not alleviate the shaker placement problem. However, it provides the test director with a set of shaker force ratios for the mode to be isolated for the shaker locations specified. An error in modal displacements can also be assessed providing, thus, a criterion for terminating the iterative process.

#### THE PROBLEM

There are three sources of error in experimental modal data if the number of

shakers is small in comparison to the total number degrees of freedom. The first error stems from the fact that if the force ratios are not proportional to the damping or dissipative forces present at each shaker attachment point, a residual phase lag will be present in the modal displacements.

The second source of error comes from the interference of neighboring modes with the mode excited. Each mode responds to a sinusoidal excitation at any frequency. This response is small unless the excitation frequency is in the immediate vicinity of the mode's resonant frequency as shown in Figure 1. Even though this response is relatively small at the frequency of the mode to be excited, it adds to the distortion of data and must, therefore, be removed.

The third source of error is damping at the mass points that is not proportional to either the mass or stiffness matrix terms. We call this nonproportional damping. In this case, although the modal mass and stiffness

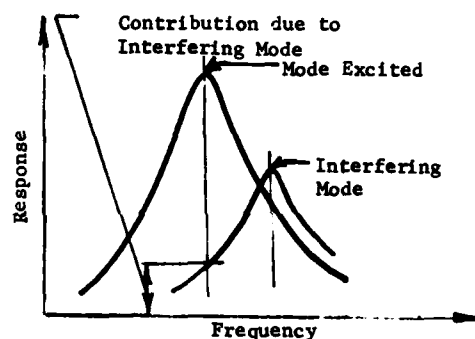


Figure 1. Modal Interference

matrices are diagonal, the modal damping matrix is not. This provides coupling forces among the modes, and all modes will respond to some extent to an excitation apportioned to excite a single mode.

The approach taken in this paper tends to remove, intrinsically, the first two sources of error. The case of nonproportional damping is not considered in this study. The method proposed uses an iterative scheme that suppresses the undesired responses in the modes with frequencies in close proximity to the desired mode. This approach uses only experimental data and is independent of knowledge of the analytical model. The process consists of obtaining the dynamic influence coefficient matrix by performing frequency sweeps with one shaker at a time. Then, using such an experimental influence coefficient or admittance matrix, an iterative process is initiated using

a digital computer. The process is terminated when a set of shaker forces is found which produces natural mode shapes that contain the least possible contamination with other modes.

#### APPROACH

In the derivation of the method, certain assumptions were made. These are:

- the model is linear and, therefore, the superposition of modal responses holds;
- only proportional damping is considered;
- all shaker forces are phase-coherent, i.e., they are in phase or 180 degrees out of phase among themselves; and
- the approach is derived for a discrete system. By inference the method is applicable to continuous systems.

The modal equations of motion in the frequency domain are

$$(-\omega_x^2 \begin{bmatrix} 1 \end{bmatrix} + \begin{bmatrix} 1 + jg \end{bmatrix} \omega_n^2) \{ \xi(\omega) \} = \{ Q(\omega) \} \quad (1)$$

where  $\omega_x$  is the driving frequency and  $\omega_n$  is the natural frequency. The modal masses have been normalized to unity by the following transformation

$$\begin{bmatrix} \phi \end{bmatrix} \begin{bmatrix} M \end{bmatrix} \begin{bmatrix} \phi \end{bmatrix}^T = \begin{bmatrix} 1 \end{bmatrix} \quad (2)$$

and similarly

$$\begin{bmatrix} \phi \end{bmatrix} \begin{bmatrix} K \end{bmatrix} \begin{bmatrix} \phi \end{bmatrix}^T = \begin{bmatrix} \omega_n^2 \end{bmatrix} \quad (3)$$

The modal coordinates  $\xi$  are related to the discrete coordinates  $q$  by the transformation

$$\{ \xi(\omega) \} = \begin{bmatrix} \phi \end{bmatrix} \{ q(\omega) \} \quad (4)$$

The modal matrix  $\begin{bmatrix} \phi \end{bmatrix}$  is a square  $n \times n$  matrix relating  $n$  modes to  $n$  structural locations. Although either viscous or hysteretic damping can be used, hysteretic damping  $g$  was selected as more representative for engineering structures. Finally, the vector  $\{ Q \}$  is the vector of generalized or modal forces.

Equation (1) can be written in its complex modal admittance form

$$\{ \xi(\omega) \} = ( \begin{bmatrix} H_R(\omega) \end{bmatrix} + j \begin{bmatrix} H_I(\omega) \end{bmatrix} ) \{ Q(\omega) \}, \quad (5)$$

where

$$\begin{bmatrix} H_R(\omega) \end{bmatrix} = \begin{bmatrix} \frac{-\Omega^2 (1-\Omega^2)}{(1-\Omega^2)^2 + g^2} \end{bmatrix} \quad (6)$$

$$\begin{bmatrix} H_I(\omega) \end{bmatrix} = \begin{bmatrix} \frac{g \Omega^2}{(1-\Omega^2)^2 + g^2} \end{bmatrix} \quad (7)$$

$$\text{and } \Omega = \omega_x / \omega_n$$

The subscripts R and I define the real and imaginary parts of the complex admittance matrix.

The transformations

$$\{ \xi(\omega) \} = \begin{bmatrix} \phi \end{bmatrix} \{ \ddot{q}(\omega) \} \quad \text{and} \quad (8)$$

$$\{ Q(\omega) \} = \begin{bmatrix} \phi \end{bmatrix}^T \{ F(\omega) \}, \quad (9)$$

where  $\{ F(\omega) \}$  is the vector of discrete applied forces, yield the admittance form of the equations of motion in discrete coordinates

$$\{ \ddot{q}(\omega) \} = ( \begin{bmatrix} D_R(\omega) \end{bmatrix} + j \begin{bmatrix} D_I(\omega) \end{bmatrix} ) \{ F(\omega) \} \quad (10)$$

where

$$\begin{bmatrix} D_R(\omega) \end{bmatrix} = \begin{bmatrix} \phi \end{bmatrix} \begin{bmatrix} H_R(\omega) \end{bmatrix} \begin{bmatrix} \phi \end{bmatrix}^T \quad \text{and} \quad (11)$$

$$\begin{bmatrix} D_I(\omega) \end{bmatrix} = \begin{bmatrix} \phi \end{bmatrix} \begin{bmatrix} H_I(\omega) \end{bmatrix} \begin{bmatrix} \phi \end{bmatrix}^T \quad (12)$$

Finally, because a linear system is considered, the actual amplitude of motion is irrelevant and the following normalized form of the force vector can be used:

$$\{ F(\omega) \} = a \{ \alpha(\omega) \} \quad (13)$$

where the largest amplitude of  $\{ \alpha(\omega) \}$  is normalized to unity. Equation (13) can be written in terms of coincidental and quadrature components such that

$$\{ \ddot{q}_R(\omega) \} = a \begin{bmatrix} D_R(\omega) \end{bmatrix} \{ \alpha \} \quad \text{and} \quad (14)$$

$$\{ \ddot{q}_I(\omega) \} = a \begin{bmatrix} D_I(\omega) \end{bmatrix} \{ \alpha \} \quad (15)$$

An example showing the total, coincidental and quadrature response components is shown in Fig. 2. Both the real (coincident) and the imaginary (quadrature) admittance matrices contain complete information about the system. However, the quadrature admittance matrix, evaluated at a resonance, contains large numerical terms in comparison to the coincident admittance matrix which in many cases has terms

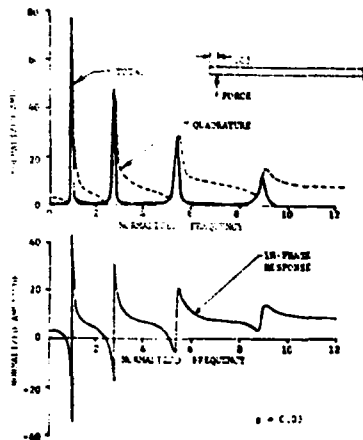


Figure 2. Frequency Response of a Uniform Beam (Ref. 9)

close to zero; the quadrature admittance matrix is better conditioned and, therefore, easier to work with, especially if the data is experimental and contains noise.

There is only one unique force vector  $\{\alpha_i\}$ , called the modal force vector\*, that will excite only one natural mode  $\{\phi_i\}$ . If we remove some of the shaker forces from  $\{\alpha_i\}$  and replace them with zeros, the resulting vector  $\{\alpha_i^0\}$  is no longer a proper vector to excite a natural mode and the ensuing response vector  $\{\tilde{q}_i\}$  will contain responses of other modes. A complete set of modal force vectors, one for each mode, consists of  $n$  independent vectors. Any arbitrary force vector can be expressed in terms of these vectors. An incomplete force vector can be considered to be an arbitrary vector and, therefore, may be expressed as a linear combination of modal force vectors

$$\{\alpha_i^0\} = \gamma_1 \{\alpha_1\} + \dots + \gamma_n \{\alpha_n\} \quad (16)$$

\* also known as principal force vector.

where  $\gamma_i$  is a weighting factor. If a substitution of Eq. (16) into (15) is made, the following expression is obtained,

$$[D_I(\omega_{ni})] \left( \gamma_1 \{\alpha_1\} + \dots + \gamma_n \{\alpha_n\} \right) = \{\tilde{q}_i\} \quad (17)$$

Each modal forcing vector  $\{\alpha_i\}$  is related to a modal displacement vector  $\{\phi_i\}$  by

$$\gamma_i [D_I(\omega_{ni})] \{\alpha_i\} = \{\phi_i\} \quad (18)$$

and similarly,

$$\gamma_j [D_I(\omega_{nj})] \{\alpha_j\} = \{\phi_j\} \quad (19)$$

The contributions of spurious modes ( $j \neq i$ ) to the mode excited ( $i$ ), are usually small for two reasons. First, the factors  $\gamma_j$  are small, and second, the product of the admittance matrix with the forcing vector is also small for all but the  $i$ th term, Eq. (18). If the modal density is high, the terms of the kernel matrix  $[H_I(\omega_{ni})]$ , Equation (12), corresponding to the modes close to the mode  $i$  become correspondingly larger and, therefore, the contributions of spurious modes, Equation (19) are also larger. This makes it more difficult to isolate a mode if the modal density is high.

The arguments presented above let us write the following equation relating the response to the excitation by an incomplete modal force vector

$$\begin{matrix} [D_I(\omega_{ni})] & \{\tilde{\alpha}_i\} & \approx & \{\tilde{\phi}_i\} \\ n \times s & s \times 1 & & n \times 1 \end{matrix} \quad (20)$$

Several items must be noted in this equation. Firstly, the normalizing constant has been omitted and the vectors  $\{\tilde{\alpha}_i\}$  and  $\{\tilde{\phi}_i\}$  have been normalized by forcing the dominant term to unity. Secondly, the order of the forcing vector has been reduced to be consistent with the number of shakers used,  $s$ . Thirdly, a symbol tilde ( $\sim$ ) has been introduced to designate an approximation to the correct modal force and the modal displacement vectors.

We select now a number  $(r-1)$  which designates the number of modes to be suppressed. Conversely,  $r$  means the number of modes to be suppressed plus one mode to be isolated.

The next step is assemble a rectangular modal displacement approximation matrix by applying  $r$  equations

$$\begin{matrix} \text{nxr} & \text{sxr} & \text{nxr} \\ \left[ \bar{D}_I(\omega_{ni}) \right] & \left\{ \tilde{\alpha}_i \right\} & \longrightarrow \left[ \tilde{\theta} \right] \end{matrix} \quad (21)$$

Although one admittance matrix would suffice to obtain the needed information, the use of  $r$  matrices (one for each resonant frequency within the range of zero to  $r$  modes) provides a better numerical accuracy, especially when working with experimental numbers.

Now that the first approximation to the modal matrix is obtained, we will use it to construct an iterative process to refine the initial estimate of the  $\{\tilde{\alpha}_i\}$ . The equation used is the one relating the discrete and modal forces

$$\begin{aligned} \left\{ Q_i \right\} &= a \left[ \tilde{\theta} \right]^T \left\{ \alpha_i \right\}, \\ a \left\{ \alpha_i \right\} &= \left[ \tilde{\theta} \right]^{-T} \left\{ Q_i \right\} \end{aligned}$$

where  $T$  means inverse of a transpose.

For the case on hand this equation becomes

$$\left\{ \tilde{\alpha}_i \right\} = \left( \left[ \tilde{\theta} \right]^T \right)^x \left\{ Q_i \right\}$$

where the symbol  $x$  means a pseudoinverse.

Because the size of the modal force vector  $\{Q_i\}$  is  $r$ , reflecting the number of modes to be excited and suppressed, the size of matrices  $\{\tilde{\theta}\}$  and  $\{\tilde{\alpha}_i\}$  must be adjusted accordingly. This means that the error is corrected only at shaker location points. No control over the rest of the structure is actively exercised. However, as explained below, the errors are monitored at all instrumented points of the structure. The pseudoinverse, (ref. 6 and 7), is the necessary tool to obtain an inverse of a rectangular matrix. If more modes are suppressed than the number of shakers,  $r > s$ , the system presents a least square solution. If on the other hand,  $r < s$ , the solution is an optimal solution, ref. 7.

To obtain a better estimate for  $\{\tilde{\alpha}_i\}$ , we purge the contribution of the modes to be suppressed by requiring that  $\{Q_i\}$  consists of zeros except for the term relative to the mode

to be isolated,

$$\begin{aligned} \left\{ Q_i \right\} &= \left\{ \delta_{ij} \right\} \text{ where } \delta_{ij} = 1 \\ &\text{for } i = j \\ &\text{and } \delta_{ij} = 0 \\ &\text{for } i \neq j. \end{aligned}$$

By specifying the position of unity in the Kronecker delta matrix, to coincide with the location of the mode to be excited, a new approximation for the excitation of that mode is obtained.

The process described is an iterative technique. It involves a computation of an approximate modal matrix, assuming an initial trial force vector. Then the contributions of higher modes are purged and a new force vector is obtained. This new vector is applied to the original Eq. (21) and the process is repeated. The convergence is monitored by computing an error at each cycle. The discussion of an error computation will follow.

To facilitate comprehension of the scheme all pertinent steps and equations are summarized and presented below.

- (1) Determine real and imaginary admittance matrices from test at all resonant frequencies of interest,  $[D_R(\omega_{ni})]$  and  $[D_I(\omega_{ni})]$ .
- (2) Select an initial trial vector for exciter force ratios  $\{\tilde{\alpha}\}^{(1)*}$  consistent with the mode being excited.
- (3) Perform the following computation

$$\begin{matrix} \text{nxrxr} & \text{sxrxr} & \text{nxrxr} \\ \left[ D_I(\omega_{ni}) \right] & \left\{ \tilde{\alpha}_i \right\}^{(1)} & = \left\{ \tilde{\theta} \right\}^{(1)} \end{matrix} \quad (22)$$

$$i = 1, 2, \dots, r$$

- (4) Assemble a complete modal matrix  $\left[ \tilde{\theta} \right]^{(1)}$  and delete rows where no exciters are present. The superscript (1) means first iteration.

$$\begin{matrix} \text{nxrxr} & \text{sxrxr} \\ \left\{ \tilde{\theta} \right\}^{(1)} & \longrightarrow \left[ \tilde{\theta} \right]^{(1)} = \left[ \left\{ \tilde{\theta}_1 \right\}^{(1)} \dots \left\{ \tilde{\theta}_r \right\}^{(1)} \right] \end{matrix} \quad (23)$$

- (5) Invert the matrix in (23) either by a regular inversion or by a pseudoinverse process

\* A concept of three-dimensional matrices is introduced here. For example,  $n \times s \times r$  means a number of rows ( $n$ ) by a number of columns ( $s$ ) by a number of matrices ( $r$ ).

TABLE 1  
Mode Isolation Process for 18-Degree-of-Freedom System

NORMALIZED MODAL FORCES, $\{Q\}$					
Iteration No. →	1	2	3	4	5
Mode Excited → ①	1.00+0	1.00+0	1.00+0	1.00+0	1.00+0
2	8.14-5	4.21-8	1.71-9	1.77-9	1.77-9
3	2.54-5	2.29-8	1.59-9	1.58-9	1.58-9
Modes Suppressed	4	9.49-7	5.27-8	2.28-9	2.32-9
5	4.50-6	7.02-9	3.09-9	3.54-9	3.54-9
6	4.14-6	7.46-9	6.22-9	6.19-9	6.18-9
7	-4.04-6	-1.73-6	-1.74-6	-1.74-6	-1.74-6
8	-9.11-7	3.87-8	4.44-8	4.45-8	4.45-8
9	-7.29-7	-2.30-7	-2.34-7	-2.34-7	-2.34-7
10	1.99-6	5.17-7	5.09-7	5.09-7	5.09-7
11	9.83-7	-1.77-6	-1.77-6	-1.77-6	-1.77-6
Modes Not Suppressed	12	7.70-6	8.16-6	8.16-6	8.16-6
13	2.98-6	3.28-6	3.27-6	3.27-6	3.27-6
14	3.85-6	3.00-6	3.00-6	3.00-6	3.00-6
15	3.14-7	-1.59-6	-1.59-6	-1.59-6	-1.59-6
16	1.60-6	1.33-6	1.32-6	1.32-6	1.32-6
17	1.10-7	-1.25-6	-1.25-6	-1.25-6	-1.25-6
18	1.85-6	2.24-6	2.24-6	2.24-6	2.24-6
NORMALIZED SHAKER FORCES, $\{\alpha\}$					
Mass Point Number	3	1.00+0	2.56-1	2.55-1	2.55-1
6	1.00+0	3.79-1	3.80-1	3.80-1	3.80-1
9	1.00+0	7.04-1	7.05-1	7.05-1	7.05-1
12	1.00+0	6.58-1	6.58-1	6.58-1	6.58-1
15	1.00+0	1.00+0	1.00+0	1.00+0	1.00+0
18	1.00+0	5.73-1	5.74-1	5.74-1	5.74-1
ERROR INDICATOR, $\epsilon_0$					
	2.97-4	2.49-5	2.50-5	2.50-5	2.50-5
ERROR INDICATOR, $\epsilon_j$					
	1.44-2	7.19-4	7.17-4	7.17-4	7.17-4

Notes: 1. Damping  $g = 0.05$

Six shakers are used.

TABLE 2  
Modal Parameters for the System With the Coupler

Natural Frequency, $\omega_{ni}$ , Hz					Structural Damping, $g$		
Case	A	B	C	D	1	2	3
Mode 1	8.13	8.13	8.09	7.99	.05	.25	.05
Mode 2	16.22	11.95	8.77	8.35	.05	.25	.25
Mode 3	24.17	24.06	23.8	23.69	.05	.25	.05
Mode 4	32.00	26.25	24.8	24.72	.05	.25	.25
Mode 5	39.54	39.13	38.8	38.75	.05	.25	.05
Mode 6	46.90	41.18	40.5	40.44	.05	.25	.25
Coupler $\kappa_c$	1	1/10	1/100	1/1000			

Note: The 12 cases investigated were formed by taking one letter and one number. For example, B2 case.

$$\begin{matrix} \left( \begin{bmatrix} \tilde{\varphi} \end{bmatrix}^x \right)^{(1)} & = & \left( \begin{bmatrix} \tilde{\varphi} \end{bmatrix}^{(1)} \left( \begin{bmatrix} \tilde{\varphi} \end{bmatrix}^T \right)^{(1)} \right)^{-1} \begin{bmatrix} \tilde{\varphi} \end{bmatrix}^{(1)} \\ \text{sxrxl} & & \text{sxrxl} \quad \text{sxrxl} \end{matrix} \quad (24)$$

- (6) Compute a new approximation to the forcing vector  $\{\tilde{\alpha}_1\}^{(2)}$  using the following recursive formula

$$\begin{matrix} \left\{ \tilde{\alpha}_1 \right\}^{(2)} & = & \left( \begin{bmatrix} \tilde{\varphi} \end{bmatrix}^x \right)^{(1)} \left\{ Q_1 \right\} \\ \text{sxlxr} & & \text{sxrxl} \quad \text{rxlxr} \end{matrix} \quad (25)$$

The position of the unity in the matrix  $\{Q_1\}$  is determined by the position of the mode to be isolated and remains fixed for the duration of the iteration process.

- (7) Repeat the process using Eq. (22).

If one observes Eq. (24), it becomes apparent that the solution exists only if  $s \leq r$ , otherwise the matrix product in the parentheses becomes singular and the inverse does not exist. A different type of a pseudoinverse can be used in this case representing a minimization problem.

The error in modal displacements can be evaluated by an application of Eq. (14). At resonance, if a correct modal force vector is used,

$$\begin{bmatrix} D_R(\omega_{ni}) \end{bmatrix} \left\{ \alpha_i \right\} = \left\{ 0 \right\} \quad (26)$$

If an incomplete force vector is used in Eq. (26), specifically  $\{\tilde{\alpha}_1\}$ , which is obtained from  $\{\alpha_i\}$  by inserting zero terms at locations where there are no shakers, Eq. (26) becomes

$$\begin{bmatrix} D_R(\omega_{ni}) \end{bmatrix} \left\{ \tilde{\alpha}_1^0 \right\} = \left\{ \beta \right\} \quad (27)$$

The error vector  $\{\beta\}$  represents a measure of errors in modal displacements. To obtain a convenient single number  $\epsilon_\beta$  as a measure of error, a root-sum-square of individual terms can be used

$$\epsilon_\beta = \left( \left\{ \beta \right\}^T \left\{ \beta \right\} \right)^{\frac{1}{2}} \quad (28)$$

Another measure of error  $\epsilon_\varphi$  used in examples presented below is based on the difference of modal displacements as calculated by this algorithm and by analysis, assuming that analysis produces correct mode shapes:

$$\left\{ \Delta \varphi \right\} = \left\{ \varphi_E \right\} - \left\{ \varphi_A \right\} \quad (29)$$

$$\epsilon_\varphi = \left( \left\{ \Delta \varphi \right\}^T \left\{ \Delta \varphi \right\} \right)^{\frac{1}{2}} \quad (30)$$

#### ANALYTICAL SIMULATION

Two examples have been selected to demonstrate the technique. These involve an analytical simulation of the test. The physical properties are shown in Fig. 3. Six shakers are used. Mode 1 is isolated, modes 2 through 6 are suppressed. Table 1 shows the iterative process for five iteration cycles. For the first iteration cycle all six shaker forces were arbitrarily set in phase at unity amplitude. For this simple example convergence occurs after the second iteration cycle. In computing the error indicator the coincidental acceleration vectors were normalized to be consistent with the normalized quadrature vectors.

Another example consists of an 18-degree-of-freedom mass-spring model with a coupler in the middle. Fig. 4 shows its physical characteristics. The intent here was to obtain closely spaced pairs of natural frequencies. These are shown in Table 2. The results are shown graphically in Fig. 5 for two cases of coupler stiffness,  $\kappa_c = 1/1$  and  $1/100$ . The resolution of the computer plots is not sufficient to show the double peaks for the  $\kappa_c = 1/100$  case except for the first mode. After five iteration cycles most of the higher mode contributions disappear.

Several factors affect the convergence rate and the minimum attainable error. The most important is the number of shakers in comparison with the total number of degrees of freedom. Also, the lower modes converge faster than higher modes as shown in Fig. 6. In some cases, especially for higher modes, oscillations in the convergence curves occur. No explanation for this phenomenon is offered.

A number of simulations was performed varying structural damping, the number of shakers, the number of modes suppressed, etc. More comprehensive discussion of these parametric studies is offered in ref. (8). The following conclusions were reached:

The algorithm performs well under conditions found during the actual testing. In cases investigated, structural damping coefficients of 0.1 produced acceptable convergence. Also, a general conclusion is that as more modes are used in the suppression process, less suppression is obtained. Optimum results are obtained if the number of modes suppressed is equal to the number of shakers less one. Some analyses were performed with random errors introduced into the admittance matrices simulating experimental error. Also errors in the natural frequencies

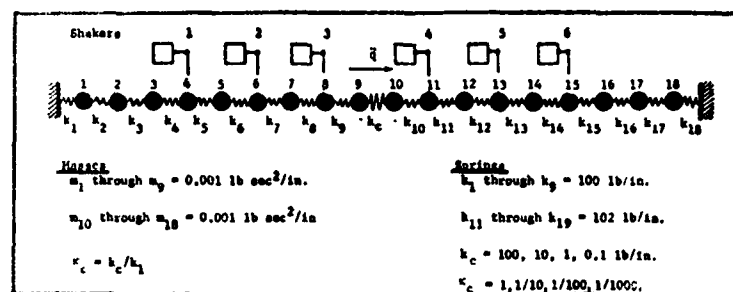


Figure 3. Physical Parameters

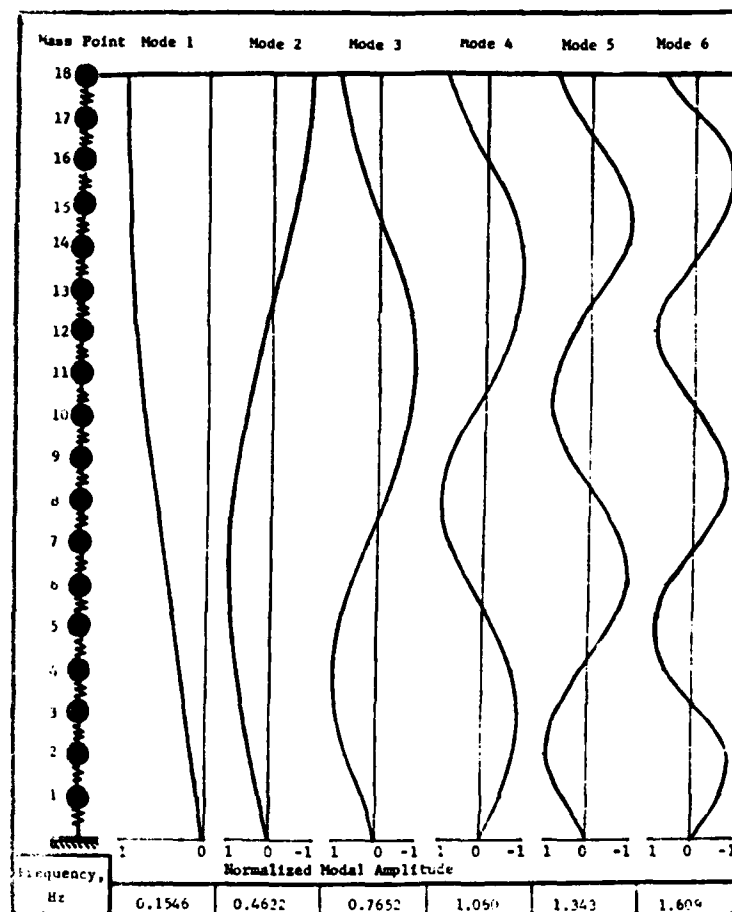


Figure 4. Modal Parameters



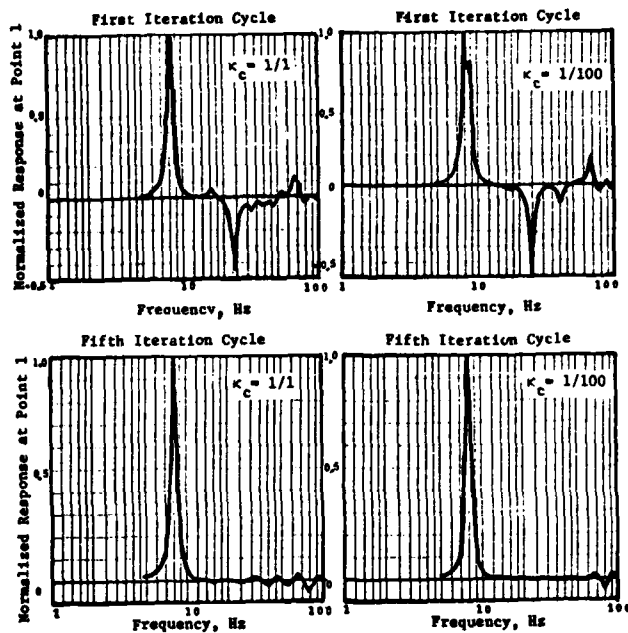


Figure 5. Frequency Response for First and Fifth Iteration Cycle

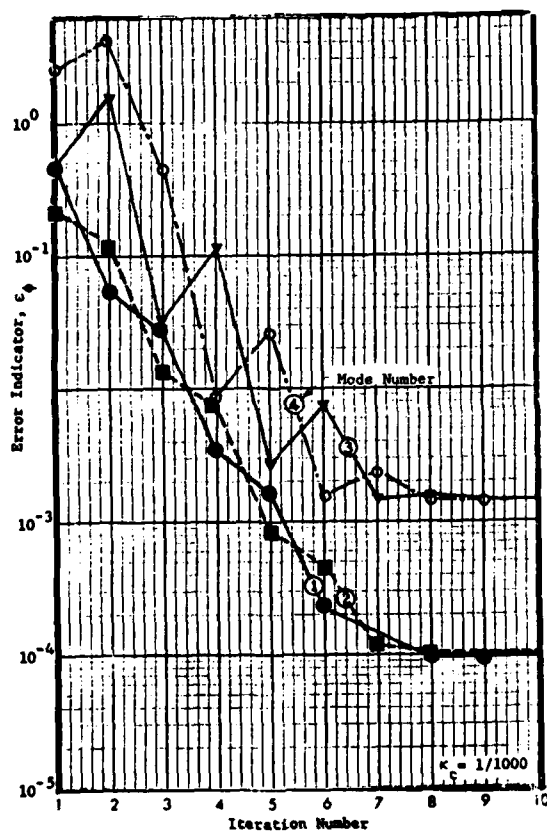


Figure 6. Error vs Iteration Number

were simulated to investigate the convergence. In all cases where the errors did not exceed  $\pm 10\%$  the convergence was satisfactory.

The examples shown demonstrate the basic feasibility of the algorithm. However, the real proof lies in using the actual test data. This work is being done at the present time. The results will be presented at a later date.

#### REFERENCES

1. Lewis, R. C., and Wrisley, D. L., "A System for the Excitation of Pure Natural Modes of Complex Systems", Journal of the Aeronautical Sciences, (November 1950), pp. 705-723.
2. Deck, A., "Methods Automatique D'Appropriation Des Forces D'Excitation Dans L'Essai d'une Structure D'Avion", Communication presente au Congres UROMECH 22, (September 15-16, 1970).
3. de Vries, G., "The Problem of Determining the Excitation Forces in Vibration Testing", NASA TT F-348, La Recherche Aerospaciale No. 102, (1964), pp. 43-49.
4. Jamison, G. T., and Tao, K. M., "Preliminary Shaker Sizing and Location Study for Determining Free-Free Modes in the Mated Vertical Ground Vibration Test", Northrop Services Inc., TN-250-1386, (December 1974).
5. Asher, G. W., "A Method of Normal Mode Excitation Utilizing Admittance Measurement", Proceedings of IAS National Specialist Meeting on Dynamics and Aeroelasticity, (November 1958).
6. Greville, T. N. E., "The Pseudoinverse of a Rectangular or Singular Matrix and its Application to the Solution of Systems of Linear Equations", SIAM Review, Vol. 1, No. 1, (January 1959), pp. 38-43.
7. Ibanez, P., "Force Appropriation by Extended Asher's Method", SAE Aerospace Engineering and Manufacturing Meeting, Paper No. 760873, (November 1976).
8. Morosow, G., Thesis: "Exciter Force Apportioning for Modal Vibration Testing Using Incomplete Excitation", University of Colorado, Boulder, Co., 1977.
9. Stahle, C. V., Jr., "Phase Separation Techniques for Ground Vibration Testing", Aerospace Engineering, (July 1962), p. 56.

ON THE DISTRIBUTION OF SHAKER FORCES  
IN MULTIPLE-SHAKER MODAL TESTING

W. L. Hallauer, Jr. and J. F. Stafford  
Virginia Polytechnic Institute and State University  
Blacksburg, Virginia 24061

The method proposed by Asher for structural dynamic modal testing by multiple-shaker sinusoidal excitation is reviewed, and its theory and application are discussed in detail. Numerical results from simulated modal testing on mathematical structural models are presented to illustrate the strengths and weaknesses of the method. The characteristics of these models include damping which couples the normal modes and closely spaced modes. Numerical techniques required for implementation of the method are described. A procedure is suggested for replacing actual mechanical tuning with calculations employing transfer function data.

## I. INTRODUCTION

Structural dynamic modal testing by means of multiple-shaker sinusoidal excitation requires some method for specifying shaker forces so as to isolate or tune individual modes of vibration. Asher [1], expressing doubt that other methods available or proposed at the time (1958) were capable of separating closely spaced modes, proposed a quantitative method which both detects natural frequencies and provides the force distributions for multiple-shaker tuning. The method uses only experimental transfer function data as input and, in principle, is capable of tuning any mode, regardless of the degree of modal density.

Asher was unable to apply his method successfully in modal testing due to equipment limitations. Furthermore, he stated that implementation of the method would require the development of data acquisition and processing equipment to handle experimental transfer function data. These practical obstacles evidently discouraged attempts to apply Asher's method in the laboratory throughout the 1960's. Nonetheless, the method was considered promising and was discussed extensively by several authors, notably Bishop and Gladwell [2] and Craig and Su [3]. Finally, in 1974 the practical usefulness of Asher's method was demonstrated by application in the MODALAB test facility, as described by Smith et al [4], Stroud et al [5], and Hamma et al [6].

The objectives of this paper are (i) to review and discuss in detail the theory underlying Asher's method, (ii) to present numerical results developed from computer simulation of modal testing on relatively simple structural

models, some of which have closely spaced modes, and (iii) to discuss some aspects of the practical application of the method. Our computer simulation models are similar to those of Craig and Su [3]; however, whereas they represented structural damping as the proportional or non-coupling type, we have accounted for the more realistic type of damping which couples the normal modes of vibration.

The computer simulation results demonstrate instances of both success and failure of Asher's method. In many cases, it detects all modes and provides force distributions which effectively separate the modes so that mode shapes may be measured accurately. However, it is also possible that Asher's method may provide poor tuning, miss modes, or even introduce false modes.

The distribution of excitation on a test specimen encompasses both spatial distribution or position (location and direction) and force-amplitude distribution of the mechanical shakers. However, Asher's method addresses directly only the problem of force-amplitude distribution; the shaker positions must already have been selected before Asher's method is applied. The positioning of exciters is usually based on the judgment and experience of test and analysis engineers. To date, very little quantitative study has been devoted to the positioning problem and, although important, it is not the primary concern of this paper.

## II. THEORETICAL BACKGROUND

Consider a linear structural system having  $n$  degrees of freedom, the time-dependent

responses of which make up the  $n \times 1$  column matrix  $\underline{x}$ . (Notation is listed at the end of the paper.) The system is excited by a set of sinusoidally varying forces having coherent phases, i.e., all having  $0^\circ$  or  $180^\circ$  phase,

$$\underline{f} = \underline{F} \cos \omega t = \text{Re} \{ \underline{F} e^{i\omega t} \} \quad (1a)$$

It is assumed that all starting transients have decayed away, so the response is steady-state sinusoidal,

$$\underline{x} = \text{Re} \{ \underline{X} e^{i\omega t} \} \quad (1b)$$

Response amplitude vector  $\underline{X}$  is generally complex, reflecting the facts that response is usually not in phase with excitation and that each response may have a different phase. Having equations (1a, b), we may treat the problem as one in which  $\underline{F}$  is the input,  $\underline{X}$  the output, and their linear relationship is completely defined by the  $n \times n$  transfer function matrix  $[H(\omega)]$ ,

$$\underline{X} = [H(\omega)] \underline{F} \quad (2)$$

It will be necessary to distinguish between the in-phase ( $0^\circ$  or  $180^\circ$ ) portion and the out-of-phase ( $\pm 90^\circ$ ) portion of response in the forms, respectively, of the coincident-response matrix  $[C(\omega)]$  and the quadrature-response matrix  $[Q(\omega)]$  defined by

$$[H(\omega)] = [C(\omega)] + i [Q(\omega)] \quad (3)$$

All structures considered in this paper are assumed to be discretized to  $n$  degrees of freedom, so that the governing matrix equation of motion for steady-state sinusoidal excitation and response is

$$[m]\ddot{\underline{x}} + [c(\omega)]\dot{\underline{x}} + [k]\underline{x} = \underline{F} \cos \omega t \quad (4)$$

System inertia, damping and stiffness matrices,  $[m]$ ,  $[c(\omega)]$  and  $[k]$  respectively, are assumed to be real, symmetric, and positive-definite. The representation of damping by an arbitrarily frequency-dependent term is rather general. In particular, it encompasses any combination of the standard viscous and hysteretic types; if  $[b]$  and  $[d]$  are, respectively, the constant viscous and hysteretic damping matrices, then  $[c(\omega)] = [b] + 1/\omega [d]$ . Damping matrix  $[c(\omega)]$  is not necessarily diagonalized by the standard normal mode transformation; i.e., if  $[\phi]$  is the modal matrix of normal modes, then  $[\phi]^T [c(\omega)] [\phi]$  is not necessarily diagonal. If the product is not diagonal, then  $[c]$  is called a coupling damping matrix since it couples the otherwise uncoupled normal equations of motion.

The frequency response solution for arbitrary linear damping  $[c(\omega)]$  has been established by application of the characteristic phase-lag theory of Fraeijs de Veubeke [7,8]. The summary here follows primarily the developments in English by Bishop and Gladwell [2] and Bishop *et al* [9].

To solve equation (4) for frequency response, references [2] and [9] develop a frequency-dependent eigenvalue problem,

$$\omega [c(\omega)] \underline{\psi} - \tan \theta ([k] - \omega^2 [m]) \underline{\psi} = 0 \quad (5a)$$

At each driving frequency  $\omega$  there are  $n$  eigen-solutions, each consisting of real mode shape  $\underline{\psi}_r(\omega)$  and real phase-lag angle  $\theta_r(\omega)$ , which is calculated from the actual eigenvalue  $\tan \theta_r$ .

With these quantities known, the associated force-amplitude vectors  $\underline{\Gamma}_r(\omega)$ ,  $r = 1, 2, \dots, n$ , are calculated from

$$\underline{\Gamma}_r = \cos \theta_r ([k] - \omega^2 [m]) \underline{\psi}_r + \omega \sin \theta_r [c(\omega)] \underline{\psi}_r \quad (5b)$$

Each vector  $\underline{\Gamma}_r(\omega)$  is that amplitude distribution of coherently phased forces,

$$\underline{f} = \underline{\Gamma}_r \cos \omega t$$

which produces responses in all degrees of freedom having the same phase lag  $\theta_r$ ,

$$\underline{x} = \underline{\psi}_r \cos (\omega t - \theta_r)$$

Solutions  $\underline{\psi}_r(\omega)$ ,  $\theta_r(\omega)$  and  $\underline{\Gamma}_r(\omega)$  may be termed collectively the  $r$ th frequency-dependent "characteristic phase-lag mode".

Equation (5a) is valid provided  $\theta \neq \frac{\pi}{2}$ . However, if  $\theta_s = \frac{\pi}{2}$  for the  $s$ th mode, then equations (5a,b) reduce, respectively, to

$$([k] - \omega_s^2 [m]) \underline{\psi}_s = 0 \quad (6a)$$

$$\underline{\Gamma}_s = \omega_s [c(\omega_s)] \underline{\psi}_s \quad (6b)$$

The only solution to equation (6a) is the normal mode solution. Hence if  $\omega = \omega_s$ , the  $s$ th undamped natural frequency, then the  $s$ th characteristic phase-lag mode shape becomes the  $s$ th normal mode shape,

$$\underline{\psi}_s(\omega_s) = \underline{\phi}_s \quad (7a)$$

and the responses of all degrees of freedom in that mode are in quadrature with the excitation,

$$\theta_s = \frac{\pi}{2} \quad (7b)$$

and, finally, the excitation has the particular form,

$$\underline{\Gamma}_s(\omega_s) = \omega_s [c(\omega_s)] \underline{\phi}_s \quad (7c)$$

The characteristic phase-lag modes represent a specific type of forced response, so they do not give directly an equation of the type (2) expressing response due to arbitrary excitation, from which  $[H(\omega)]$  may be written. However, at each excitation frequency the set of vectors  $\underline{\Gamma}_r$ ,  $r = 1, 2, \dots, n$ , is linearly independent, so any arbitrary force amplitude distribution  $\underline{F}$  of coherently phased forces may

be expressed as a linear sum of the  $\underline{r}_r$ ,

$$\underline{F} = \sum_{r=1}^n \lambda_r \underline{r}_r$$

By using this expansion, orthogonality conditions which are easily derived from equations (5a,b), and the principle of superposition for linear systems, references [2] and [9] derive the frequency response transfer function matrix in the form

$$[H(\omega)] = \sum_{r=1}^n (R_r + iI_r) \underline{\psi}_r \underline{\psi}_r^t \quad (8a)$$

where

$$R_r = \frac{\beta_r}{\alpha_r^2 + \beta_r^2}, \quad I_r = \frac{-\alpha_r}{\alpha_r^2 + \beta_r^2} \quad (8b)$$

$$\alpha_r = \omega \underline{\psi}_r^t [c] \underline{\psi}_r,$$

$$\beta_r = \underline{\psi}_r^t ([k] - \omega^2 [m]) \underline{\psi}_r$$

It is worth repeating for emphasis that the modal vectors  $\underline{\psi}_r$  are frequency-dependent, quite unlike modal vectors for normal or complex modes. Equation (8a) applies for almost any type of linear damping that one might wish to consider, so it is quite useful for discussion of the nature of solutions. However, it is somewhat impractical for numerical studies because it requires the solution of eigenvalue problem (5a) at each excitation frequency of interest. None of the numerical results in this paper have been calculated from equation (8a).

The coincident-response matrix defined by equation (3) is of particular interest. It may be expressed either as a sum, from equation (8a),

$$[C(\omega)] = \sum_{r=1}^n R_r \underline{\psi}_r \underline{\psi}_r^t \quad (9a)$$

or as a matrix product,

$$[C(\omega)] = [\psi] [R] [\psi]^t \quad (9b)$$

where  $[\psi]$  is the square modal matrix of  $\underline{\psi}_r$  vectors and  $[R]$  is the diagonal matrix whose  $k$ th diagonal element is  $R_k$ . From equation (9b) the determinant of  $[C(\omega)]$  is

$$\det [C(\omega)] = (\det [\psi])^2 \prod_{r=1}^n R_r \quad (10)$$

An important conclusion may be inferred from equation (10), namely,

$$\det [C(\omega_s)] = 0, \quad s = 1, 2, \dots, n \quad (11)$$

That is, the coincident-response matrix is singular at each undamped natural frequency. This is so because, from equations (6a), (7a), and (8b),  $\beta_s(\omega_s) = 0$  so  $R_s(\omega_s) = 0$ . Another interpretation of this singularity is seen by expressing the  $k$ th column of the coincident-response matrix as

$$\underline{C}_k(\omega) = \sum_{r=1}^n R_r \psi_{kr} \underline{\psi}_r \quad (12)$$

where  $\psi_{kr}$  is the  $k$ th element of  $\underline{\psi}_r$ . When  $\omega \neq \omega_r$ ,  $r = 1, 2, \dots, n$ , each column  $\underline{C}_k$  is a sum of the  $n$  linearly independent vectors  $\underline{\psi}_r$ , so that  $[C]$  is not singular. However, when  $\omega = \omega_s$ , the  $s$ th undamped natural frequency, then  $R_s(\omega_s) = 0$  so equation (12) becomes

$$\underline{C}_k(\omega_s) = \sum_{\substack{r=1 \\ r \neq s}}^n R_r \psi_{kr} \underline{\psi}_r \quad (13)$$

In this case, each column  $\underline{C}_k$  is a sum of only  $n - 1$  linearly independent  $n$ -dimensional vectors, so the  $n$  columns of  $[C(\omega_s)]$  are linearly dependent and the matrix is singular.

Another important conclusion is

$$[C(\omega_s)] \underline{r}_s(\omega_s) = 0, \quad s = 1, 2, \dots, n \quad (14)$$

This can be proved by substituting equations (9a) and (7c) into the left-hand side of (14), applying the following orthogonality condition derived in references [2] and [9],

$$\underline{\psi}_r^t [c(\omega)] \underline{\psi}_s = 0 \quad \text{for } r \neq s$$

and, finally, using  $R_s(\omega_s) = 0$ .

In view of results (11) and (14), the equation

$$[C(\omega)] \underline{F} = 0 \quad (15)$$

may be regarded as a non-standard eigenvalue problem having  $n$  eigensolutions. The  $r$ th eigenvalue is the  $r$ th undamped natural frequency, and the associated eigenvector is the amplitude distribution of coherently phased forces required to tune exactly the  $r$ th undamped normal mode in quadrature phase with the excitation.

Asher [1] first stated results (11) and (14) and proposed the interpretation of equation (15) as an eigenvalue problem. Bishop and Gladwell [2] rigorously established the mathematical validity of those results. Craig and Su [3] established the same conclusions with a short and direct derivation. We have presented this review rather than simply restating the conclusions for the following reasons: to provide a summary for readers unfamiliar with the characteristic phase-lag

theory; to extend the scope of Bishop and Gladwell's results to include a more general form of damping (They regarded their results as applicable only for viscous or hysteretic damping, but the extension is almost trivial.); finally, to represent the coincident-response matrix in the new forms (9b) and (12), which expedite interpretation of results.

### III. ASHER'S METHOD

Asher's method is based on the theoretical results contained in equations (11) and (14). The method can be described with reference to those equations in the context of an idealized modal test on a discrete  $n$ -degree-of-freedom linear structure with arbitrary linear structural damping. The test begins with measurement of the  $n \times n$  frequency response transfer function  $[H(\omega)]$  over the entire modal spectrum of the structure. This data may be assembled by applying excitation and measuring response at each degree of freedom, with the use of either incremental sine-sweep excitation for direct measurement or broadband excitation and calculation by digital time series analysis. (See Hamma et al [6] and Brown et al [10] for contrasting views on the merits of these two testing methods.) Next, the coincident-response matrix  $[C(\omega)]$  is extracted as the real part of  $[H(\omega)]$ , and  $\det [C(\omega)]$  is plotted over the entire modal spectrum. Exactly  $n$  zero crossings of  $\det [C(\omega)]$  are found, and the frequencies at which they occur are, from equation (11), the undamped natural frequencies of the structure, even though damping is present. Next, the relative force-amplitude distributions for tuning all modes are determined as the solutions  $r_s(\omega_s)$ ,  $s = 1, 2, \dots, n$ , of equation (14). Each vector  $r_s(\omega_s)$  is equal to any one of the identical (to within constant multiples) columns of the adjoint matrix  $\text{adj} [C(\omega_s)]$ . This relatively simple solution procedure is predicated on the availability of  $[C]$  at the exact zeros of  $\det [C]$ ; otherwise, interpolation is required. Finally, each of the  $n$  modes is tuned exactly in a multiple-shaker sine dwell. For the  $s$ th mode, the shakers are set to produce the forces

$$f = r_s(\omega_s) \cos \omega_s t$$

Then the response is measured to be

$$x = \phi_s \cos (\omega_s t - \frac{\pi}{2})$$

The response-amplitude distribution  $\phi_s$  is the exact mode shape of the  $s$ th undamped normal mode, again, even though the structure is damped.

A short digression on the tuning step is in order. Normally a narrow-band sine sweep about  $\omega_s$  with fixed force-amplitude distribution is more useful than a sine dwell. If damping is hysteretic and non-coupling, then the locus of each complex response is a perfect

circle on a co-quad plot in the complex plane, from which modal damping as well as the mode shape component may be determined (Kennedy and Pancu [11]). Moreover, if damping is viscous and non-coupling, the co-quad plot is still nearly circular. Even if damping couples the normal modes, a co-quad plot is useful for indicating the presence of a true mode; however, as shown by the simulation study results of Section V, damping coupling of closely spaced modes may give co-quad plots which are somewhat difficult to interpret in light of our expectations based on non-coupling damping.

Returning to Asher's method, we may state that in principle it is capable of measuring exactly every undamped natural frequency and the associated real mode shape of an ideal discrete structure with  $n$  degrees of freedom and linear damping. The method uses only experimental data as input; no estimated data such as a mass matrix is required.

Actual modal testing of real hardware is, of course, much more complicated than the idealized testing of a perfect discrete structure described above. The practical realities are that any continuous structure has an indefinitely large number of degrees of freedom, and that sensing and exciting equipment can be applied at only a relatively small number of locations on the structure. It is feasible therefore to measure only a  $p \times p$  incomplete coincident-response matrix  $[C^*(\omega)]$ , where  $p < n$ . It is clearly not possible to satisfy the exact equations (11) and (14), so the most reasonable alternative course for practical application of Asher's method is to seek useful solutions to the analogous equations,

$$\det [C^*(\omega)] = 0 \quad (16a)$$

$$[C^*(\omega)] r^* = 0 \quad (16b)$$

where  $r^*$  is a  $p \times 1$  vector of force amplitudes corresponding to the  $p$  available shaker locations. As we shall demonstrate with the simulation study results, use of equations (16a,b) can lead to the following possible consequences, listed in order of decreasing desirability: (i) a zero of  $\det [C^*]$  may occur close to but not exactly at a natural frequency, and the force vector  $r^*$  will effectively tune the corresponding mode; (ii) a zero of  $\det [C^*]$  may occur close to a natural frequency, but the vector  $r^*$  will not adequately isolate the mode from interfering modes; (iii) a zero of  $\det [C^*]$  may be totally unrelated to any of the natural frequencies; (iv)  $\det [C^*]$  may have no zero in the vicinity of a natural frequency.

Mathematical justification is quite limited for the proposition that the solutions of equations (16a,b) will represent accurate natural frequencies and effective tuning force-amplitude distributions. With the definition of the characteristic phase-lag  $p \times 1$  truncated modal vectors  $\psi_r^*$ ,  $r = 1, 2, \dots, n$ , and

the corresponding  $p \times n$  modal matrix  $[\psi^*]$ , equation (9b) gives

$$[C^*(\omega)] = [\psi^*] [R] [\psi^*]^t$$

The degrees of freedom deleted from each  $\psi_r$  to form  $\psi_r^*$  are, of course, the degrees of freedom missing from  $[C^*]$ . Since  $[\psi_r^*]$  is not square, it is not possible to write a simple equation for  $\det [C^*]$  analogous to equation (10) for  $\det [C]$ . Hence, it is difficult if not impossible to predict, in a precise mathematical sense, how closely the zeros of  $\det [C^*]$  approximate the true natural frequencies. It is perhaps even more difficult to assess mathematically the tuning effectiveness of a force-amplitude solution  $r^*$  to equation (16b). Bishop and Gladwell [2] stated without proof several interesting results regarding the numbers of zeros of  $\det [C^*]$  and their lower and upper bounds ( $\omega_1$  and  $\omega_n$ ). These results are possibly the most precise mathematical statements that can be made regarding the solutions of equations (16a,b).

Despite the absence of firm mathematical justification, application of equations (16a,b) often leads to surprisingly good results. This frequent success can be partially explained, at least physically if not mathematically, on the basis of the following result from equations (7): forced vibration in a pure normal mode at its undamped natural frequency is characterized by all response being in quadrature phase with the excitation. The physical consequence of equations (16a,b) being satisfied at some frequency  $\omega'$  is that the  $p$  degrees of freedom represented in  $[C^*]$  are constrained to respond exactly in quadrature phase with the  $p$  forces. The  $n - p$  unforced degrees of freedom are, of course, not so constrained. But if  $\omega'$  is close to a natural frequency and if the  $p$  shakers are located at positions appropriate to tune the mode, then it is reasonable to expect, and it often happens, that the unforced degrees of freedom having significant modal energy will "cooperate" by responding nearly in quadrature phase with the forces. In such a case, the entire structure vibrates in a close approximation to the true normal mode.

In discussing equations (16a,b), we have assumed that the  $p$  response locations are identical to the  $p$  excitation locations. However, in the spirit of the quadrature-response explanation given above, it is permissible that the response and excitation locations differ. Stroud et al [5] and Ibanez [12] made this observation and, in addition, described approaches for which the number of responses measured need not equal the number of exciters.

#### IV. COUPLING DAMPING MATRICES

Although most analytical studies using standard modal analysis assume that damping

does not couple the normal modes, there seems to be no reason to expect that the dissipative mechanisms of the actual structures should have this very special and desirable characteristic. Hence, damping matrices which couple the normal modes have been used in calculations of the results to be presented in Section V.

But how does one specify numerically the elements of coupling damping matrix  $[c]$ , which is required for calculation of the frequency response solution? Since structural damping is always dissipative and since dashpot elements are analogous to spring elements in mechanical models, it seems reasonable to expect that  $[c]$  should be symmetric and positive-definite. Beyond that, however, there is apparently no information available to guide one in selecting physically reasonable element values for damping matrices of continuous structures. We therefore have used the concept of a coupled modal damping matrix with unit diagonal elements (Hasselman [13]) to derive an equation for calculating a coupling damping matrix. The equation is based on an assumption about the nature of damping rather than on actual measurements of damping, so the resulting matrices may be regarded as plausible but not necessarily physically representative.

For a damping matrix  $[c_n]$  which does not couple the undamped normal modes, we have by definition

$$[\phi]^t [c_n] [\phi] = [G]$$

where  $[G]$  is the diagonal generalized damping matrix. For example, if damping is a combination of non-coupling viscous and hysteretic types, then

$$[c_n] = [b] + \frac{1}{\omega} [d]$$

so that

$$[G] = [B] + \frac{1}{\omega} [D] \quad (17)$$

where the  $r$ th diagonal elements are calculated from

$$\begin{aligned} B_r &= 2 M_r \zeta_r \omega_r \\ D_r &= M_r \omega_r^2 g_r \\ M_r &= \phi_r^t [m] \phi_r \end{aligned} \quad (18)$$

and  $\zeta_r$  and  $g_r$  are, respectively, the standard viscous damping ratio and hysteretic damping constant for the  $r$ th mode. Although  $[G]$  is diagonal for non-coupling damping, in general the modal vectors are not normalized so as to make it the unit or identity matrix. However, if the modal vectors are re-normalized in the form

$$\hat{\phi}_r = \frac{1}{\sqrt{G_r}} \phi_r, \quad r = 1, 2, \dots, n$$

or

$$[\hat{\phi}] = [\phi] [G^{-1/2}] \quad (19)$$

then there follows

$$[\hat{\phi}]^t [c_n] [\hat{\phi}] = [1] \quad (20)$$

We may regard the unit matrix in this equation as the uncoupled unit modal damping matrix.

Consider now the inverse problem, namely, calculating the damping matrix given the undamped normal modes and the modal damping constants, which would normally be  $\zeta_r$  and/or  $g_r$ ,  $r = 1, 2, \dots, n$ . In this case,  $[G]$  is calculated from equations (17) and (18), and equation (20) is post- and pre-multiplied by  $[\hat{\phi}]^{-1}$  and its transpose, respectively, to give

$$[c_n] = [V]^t [1] [V] \quad (21)$$

where

$$[V] = [\hat{\phi}]^{-1} \\ = [G^{1/2}] [\phi]^{-1} \quad (22)$$

Equation (21) by itself has no particular value since a damping matrix is certainly not required for a frequency response solution if damping does not couple the normal modes and if modal data, including structural damping constants, are given. However, the form of equation (21) does provide the model for calculation of a plausible coupling damping matrix.

If damping couples the normal modes, then the modal damping matrix will certainly not be the unit matrix of equation (20). It is reasonable to expect, though, that the modal damping matrix should have the appearance of a properly normalized experimental mass orthogonality matrix (See, for example, Stroud et al [5].); that is, the coupled modal damping matrix, denoted  $[1c]$ , should be symmetric and should have unit diagonal elements, with at least some non-zero off-diagonal elements to represent coupling between modes. Then, by analogy with equation (21), we define the physical coupling damping matrix associated with the degree of modal coupling in  $[1c]$  and with the uncoupled modal damping in a given  $[G]$  to be

$$[c] = [V]^t [1c] [V] \quad (23)$$

where  $[V]$  is evaluated from equations (17), (18) and (22). We have no rational basis at present for choosing the off-diagonal elements of  $[1c]$ . Our usual procedure is to specify positive numbers less than 1 and then judge our choice to be satisfactory or unsatisfactory on the basis of the physical plausibility of the consequent frequency response calculations.

Methods are available for calculating the frequency response of a system with coupling damping which is either purely viscous or purely hysteretic. For viscous damping, we have used

the solution of Foss [14] based on a complex eigenvalue problem devised by Frazer et al [15]. Miramand et al [16] recently presented an efficient computational form of this solution. For hysteretic damping, we have used the solution established by Bishop and Johnson [17].

## V. NUMERICAL SIMULATION OF MODAL TESTING

Simulation studies with mathematical models having non-coupling damping were conducted previously by Bishop and Gladwell [2], Craig and Su [3], and Stafford [18] (an unpublished thesis). Bishop and Gladwell examined only the zeros of  $\det [C^*]$  and demonstrated the occurrence of a good mode indication (a zero very close to a natural frequency), a false mode indication (a zero distant from all natural frequencies), and a missed mode (no zero in the vicinity of a natural frequency). In a more detailed study, Craig and Su examined the zeros of  $\det [C^*]$  and the quality of sine dwell tuning achieved by  $r^*$  force-amplitude distributions. Stafford included plots of  $\det [C^*(\omega)]$  and examined the quality of narrow-band sine-sweep tuning achieved by  $r^*$  distributions; tuning quality was demonstrated by both co-quad response plots and modal energy calculations.

Although not included in previously published simulation studies, plots of  $\det [C^*(\omega)]$  are quite informative, certainly much more so than listings of zero-crossing frequencies. A few determinant plots calculated from experimental data appear in the papers by Smith et al [4] and Stroud et al [5]. But those plots demonstrate only good mode indications. Since false mode indications and missed modes also exhibit informative characteristic forms on coincident-response determinant plots, several examples of such plots are included in the present results.

All results presented here have been calculated for coupling damping. Both hysteretic and viscous damping were considered, but there appear to be no distinguishing differences in the determinant or response plots. The effects of substantial coupling appear very clearly on co-quad response plots, which also indicate the quality of modal tuning.

A particular advantage of computer simulation of modal testing is that the parameters of the mathematical structural model are known precisely and can even be designed to produce desired characteristics such as high modal density and nodes at certain degrees of freedom. Hence, an absolute standard is available against which to judge the simulated test results and, furthermore, failures of the test method can often be attributed directly to some specific cause. The models described and the results presented here have been selected to demonstrate the consequences of applying Asher's method in situations which are typical



of actual hardware testing; our expectation is that these results will provide guidance for the interpretation of real data.

#### V.1 MODELS 5H AND 5V

These two models are structurally identical but have different damping matrices. The structure, a cantilevered plane grid with five degrees of freedom, is illustrated in Figure 1. It is similar to Craig and Su's [3] model structure. Five discrete masses are located in the  $\alpha - \beta$  plane at rigid right-angle joints connecting the bars, and the degrees of freedom are vertical ( $\gamma$ ) translations of the masses. The mass values, which are the elements of the diagonal mass matrix, are listed as follows in order from 1 to 5: 1.259 kg (0.007191 lb-sec<sup>2</sup>/in), 1.385 (0.007911), 2.096 (0.01197), 0.3447 (0.001968), 1.613 (0.009213). (All calculations for models 5H and 5V were made in the primary units of pounds, inches and seconds.) The eight identical bars are assumed massless and flexible only in vertical bending and torsion. Each bar has 0.254 m (10.0 inch) length and 6.35 mm (0.25 inch) diameter. Bar material has Young's modulus  $E = 68.9$  GPa ( $10.0 \times 10^6$  psi) and shear modulus  $G = 27.6$  GPa ( $4.0 \times 10^6$  psi).

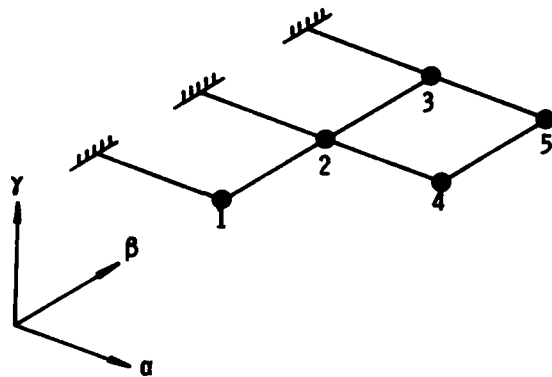


Fig. 1 Structure of Models 5H and 5V

The undamped normal mode solution is listed in Table 1. The structure was designed to have its third and fourth natural frequencies within 4% of each other by means of an optimization procedure (Hallauer *et al* [19]). Damping values  $g_r$  and  $\zeta_r$  for the third and fourth modes were selected (see below) so as to make these modes closely spaced in the sense that they be separated by less than one half-power bandwidth.

Coupling damping matrices for these models were calculated from equation (23). Model 5H has hysteretic damping, and its  $[d]$  matrix was calculated from a  $[lc]$  matrix with all off-diagonal elements equal to 0.15. The hysteretic modal damping values  $g_r$ , listed in order from 1 to 5, are 0.025, 0.035, 0.05, 0.04, 0.02. Model 5V has viscous damping with  $\zeta_r = 0.025$

for each mode, and its  $[b]$  matrix was calculated from the following coupled modal damping matrix:

$$[lc] = \begin{bmatrix} 1.0 & 0.3 & 0.1 & 0.0 & 0.0 \\ & 1.0 & 0.3 & 0.1 & 0.0 \\ & & 1.0 & 0.3 & 0.1 \\ & & & 1.0 & 0.3 \\ & & & & 1.0 \end{bmatrix}$$

#### V.2 MODEL 11H

This model consists of a beam subject to vertical bending and torsion and an attached spring-mass oscillator. It is illustrated in Figure 2. A massless flexible beam of length  $\ell$  is attached to supports at points A and B. These supports provide boundary restraint such that the beam is simply-supported relative to bending in the  $\gamma$  direction and clamped relative to torsion. Discrete masses 1 - 5 are uniformly spaced along the beam at intervals of  $\ell/6$ ; masses 6 - 10 are suspended from the beam in the  $\alpha - \beta$  plane by rigid massless links, each having length  $e$ ; mass 11 is suspended vertically from mass 4 by a spring with stiffness constant  $k$ . The eleven degrees of freedom are vertical ( $\gamma$ ) translations of the masses. For numerical evaluation, the equations describing

TABLE 1

Undamped normal modes of models 5H and 5V						
r	1	2	3	4	5	
$\omega_r$ (rad/sec)	10.908	32.055	53.500	55.409	94.924	
(mass)						
$\phi_r$	(1)	0.126	0.943	-0.380	-0.595	0.121
	(2)	0.232	0.479	-0.075	0.478	-0.712
	(3)	0.337	-0.165	-0.703	0.320	0.217
	(4)	0.773	1.000	1.000	1.000	1.000
	(5)	1.000	-0.281	0.195	-0.342	-0.130

this model were written in dimensionless form. The dimensionless mass values, stated relative to the summed total  $M_0$  of the beam and link

masses, are 0.18 for masses 1 - 5, 0.02 for masses 6 - 10, and 0.07 for mass 11. The other dimensionless parameters are  $\frac{e}{l} = \sqrt{0.1}$ ,  $\frac{GJ}{EI} =$

$0.01 \pi^2$ , and  $\frac{k_l^3}{EI} = 5.5$ , in which  $EI$  and  $GJ$  are beam bending and torsional stiffnesses, respectively.

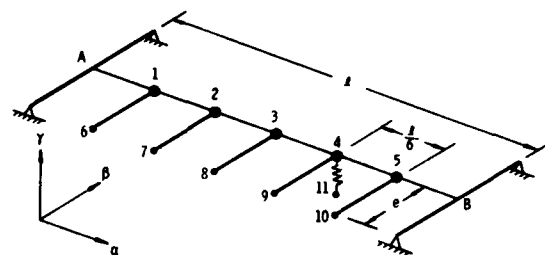


Fig. 2 Structure of Model 11H

The first five normal modes of model 11H are listed in Table 2. The dimensionless natural frequencies are defined as

$$\bar{\omega}_r = \omega_r \sqrt{\frac{M_0 l^3}{EI}}$$

The hysteretic damping matrix for this model was calculated from equation (23) with a  $[1c]$  matrix having all off-diagonal elements equal to 0.2 and with  $g_r$  for each mode equal to 0.02.

### V.3 RESULTS AND DISCUSSION

Coincident-response determinant plots for model 5H are shown on Figures 3a, b, c, in solid curves for all masses excited and in dashed curves for only masses 1 and 5 excited. In the vicinity of natural frequencies, these curves usually have the form typical of the coincident component of a transfer function. Each curve is normalized to the determinant having largest absolute value in the frequency range of the graph. With this normalization scheme, it is typical that the lowest mode dominates and higher modes may be lost within the amplitude resolution of the graph. Thus the 94.9 rad/sec mode is not evident on Figure 3a, so a re-normalized expanded-scale plot, Figure 3b, must be made. (A simple way to indicate on Figure 3a at least the zero crossing of the high mode is to plot the reciprocal of the determinant, which for data at discrete frequencies would have finite positive and negative peaks adjacent to the crossing.) The  $\det [C]$  curves on Figures 3a, b have zero crossings exactly at the undamped natural frequencies, in accordance with theory.

Figure 4 represents the consequences of applying Asher's method with complete excitation (i.e., all masses forced) to isolate the higher of the two close modes of model 5H. The normalized tuning force-amplitude distribution  $\bar{F}$  ( $= r$  in this case) was calculated from  $[C(\omega_q)]_r = 0$ . This distribution was then applied to the model in a 3 rad/sec narrow-band sine sweep to determine the co-quad curves of compliance  $\bar{X}_i$  of each mass. ( $X_3$  was omitted to reduce plot clutter.) Conjugates were plotted where appropriate to reduce graph size. The starting frequency in the sweep is indicated

TABLE 2

First five undamped normal modes of model 11H						
r	1	2	3	4	5	
$\bar{\omega}_r$	7.366	8.870	11.456	16.969	24.215	
(mass)						
$\phi_r$	(1)	0.155	0.009	-0.335	0.027	0.010
	(2)	0.270	0.013	-0.575	0.026	0.000
	(3)	0.316	0.009	-0.655	-0.002	-0.010
	(4)	0.278	0.001	-0.558	-0.029	0.000
	(5)	0.161	-0.001	-0.320	-0.028	0.010
	(6)	0.496	0.507	0.486	1.000	1.000
	(7)	0.862	0.874	0.851	1.000	0.000
	(8)	1.000	1.000	1.000	0.001	-1.000
	(9)	0.871	0.858	0.882	-0.999	0.000
	(10)	0.504	0.493	0.514	-0.999	1.000
	(11)	0.892	-0.984	0.828	0.011	0.000

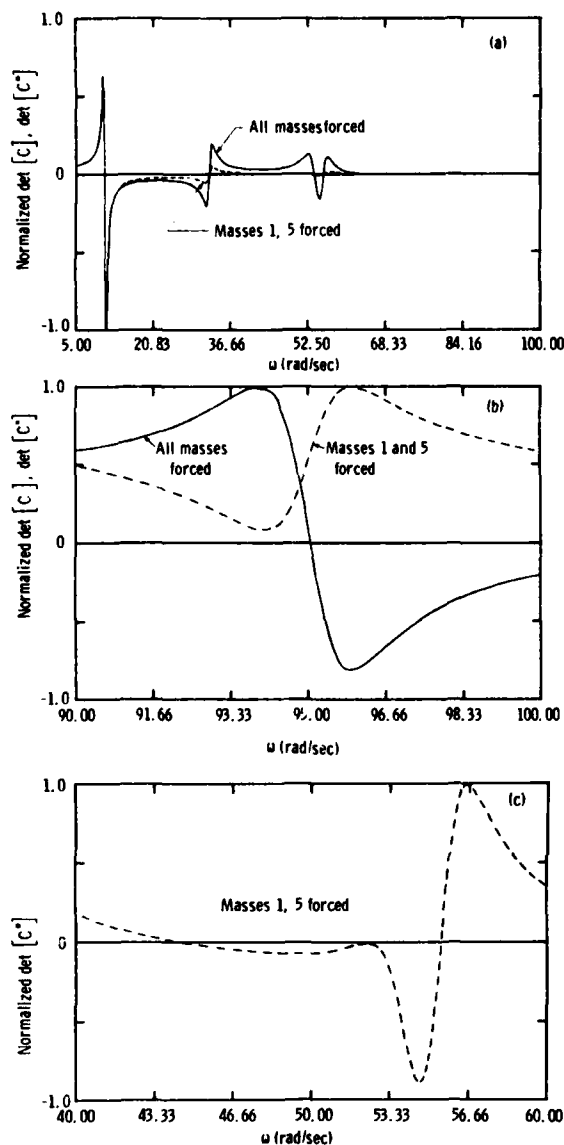


Fig. 3 Determinant plots for complete and incomplete excitation of model 5H: (a) 5-100 rad/sec, (b) 90-100 rad/sec, (c) 40-60 rad/sec

by an arrow for each response, and tic marks on response curves indicate increments of equal frequency. The test mode shape vector  $\bar{\phi}_4^*$  was calculated from the quadrature components of response at the determinant zero-crossing frequency; in this case it is the exact mode shape, in accordance with theory.

If damping had been non-coupling, each curve of the co-quad plot would be an arc of a perfect circle centered on the imaginary axis with its highest point passing through the origin (Kennedy and Pancu [11]). But coupling

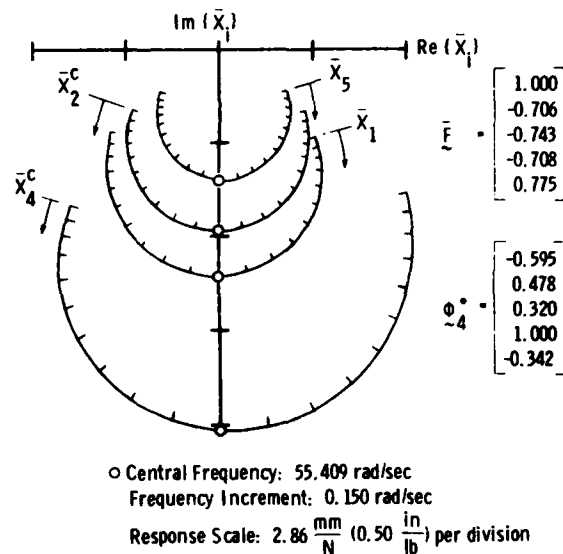


Fig. 4 Perfect tuning with complete excitation: co-quad plot for the fourth mode of model 5H with all masses forced in a 3 rad/sec narrow-band sine sweep

damping causes deviation from circular shape. In this case, coupling introduces obvious interference from the lower of the closely spaced modes. It should be noted that for coupling damping, the theory of Section II guarantees perfect mode tuning only at the natural frequency, with response in quadrature phase relative to excitation, even though all degrees of freedom are excited.

It is not unusual for the tuning force-amplitude distributions given by Asher's method to defy physical intuition. For example, the fundamental mode of model 5H has a typical first bending mode shape (Table 1) with all responses in phase, so we might expect that all tuning forces should also be in phase. But the normalized force vector for perfect tuning is

$$\bar{F} = \begin{bmatrix} -0.214 \\ -0.125 \\ 0.133 \\ 1.000 \\ 0.431 \end{bmatrix}$$

The explanation for this anomaly is that exciter forces appropriate for tuning a mode must cancel damping forces, which are not generally distributed spatially in accordance with mode shape.

The  $\det [C^*]$  dashed curves of Figures 3a, b, c exhibit good mode crossings at 10.909, 32.070 and 55.327 rad/sec, very close to the natural frequencies of the first, second and fourth modes, respectively. There is also a false mode crossing at 44.524 rad/sec. It is characteristic of lightly damped structures that good mode crossings have steep slopes and false mode crossings have relatively gentle

slopes. Hence, with the use of a determinant plot, distinguishing between good and false mode indications is usually a very easy matter.

Figures 3b, c show clearly that this  $\det [C^*]$  curve misses the third and fifth modes. But note that the curve has a relatively steep slope in the neighborhood of the natural frequency of each missed mode. This is another useful characteristic for lightly damped structures from which one can infer the presence of a mode even though there is no zero crossing.

Figure 5 is an example of the excellent tuning with incomplete excitation often provided by Asher's method. This tuning corresponds to the fourth-mode zero crossing at 55.327 rad/sec on Figures 3a, c for masses 1 and 5 forced. The  $5 \times 1$  vector  $\bar{F}^*$  on this figure is derived from the  $2 \times 1$   $\bar{r}^*$  vector, with zeros added for the unforced masses.

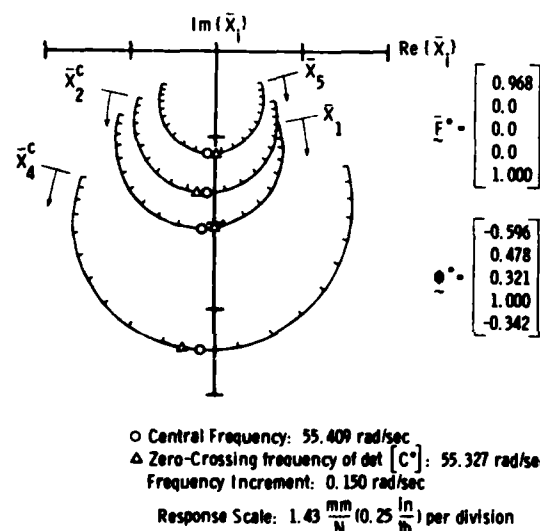


Fig. 5 Excellent tuning with incomplete excitation: co-quad plot for the fourth mode of model 5H with masses 1 and 5 forced in a 3 rad/sec narrow-band sine sweep

Coincident-response determinant curves for model 5V are shown on Figure 6. For comparison with model 5H response on Figure 4, the force-amplitude distribution and narrow-band response for perfect tuning of the fourth mode of model 5V are shown on Figure 7. Greater coupling is evident between the third and fourth modes of model 5V because the appropriate damping coupling element is 0.3, twice that of model 5H.

For masses 1, 3 and 5 excited, Figure 6 exhibits a false mode crossing at 44.764 rad/sec. The co-quad curves for a narrow-band sweep about that frequency with the appropriate force-amplitude distribution are shown in

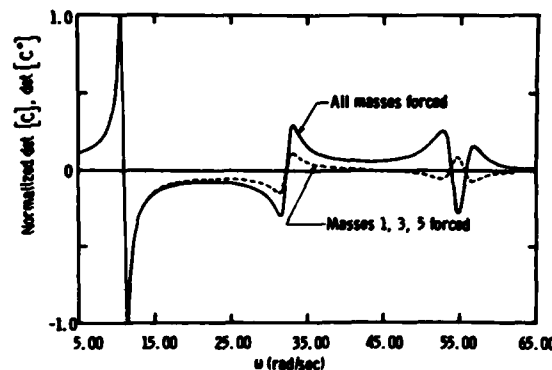


Fig. 6 Determinant plots for complete and incomplete excitation of model 5V

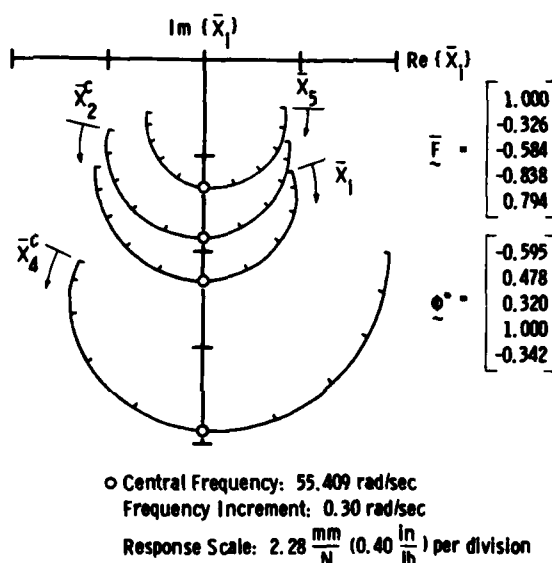


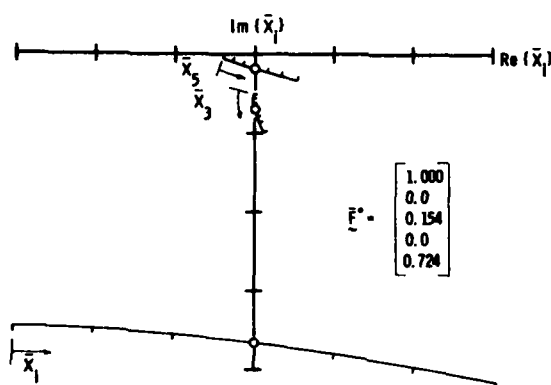
Fig. 7 Perfect tuning with complete excitation: co-quad plot for the fourth mode of model 5V with all masses forced in a 3 rad/sec narrow-band sine sweep

Figure 8. That response clearly bears no resemblance to a mode.

Good but not excellent tuning of the third mode of model 5V with incomplete excitation is illustrated by the co-quad curves of Figure 9. This tuning corresponds to the 53.395 rad/sec zero crossing on Figure 6 for masses 1, 3 and 5 forced.

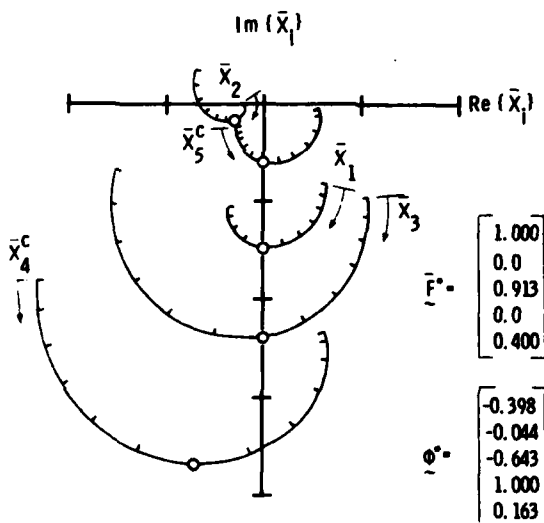
Mode shapes 2, 4 and 5 of model 11H listed on Table 2 have many node points on or near degrees of freedom. Hence, this model is useful for simulating the consequences of positioning shakers in nodal regions. Coincident-response determinant curves for model 11H are shown on Figure 10 for three different shaker

configurations.



Central Frequency: 44.764 rad/sec  
Frequency Increment: 0.45 rad/sec  
Response Scale: 0.0286  $\frac{\text{mm}}{\text{N}}$  (0.0050  $\frac{\text{in}}{\text{lb}}$ ) per division

Fig. 8 Attempted tuning of a false mode: co-quad plot for model 5V with masses 1, 3, 5 forced in a narrow-band sine sweep. Responses of masses 2 and 4 are far off scale.



Central Frequency: 53.395 rad/sec  
Frequency Increment: 0.25 rad/sec  
Response Scale: 1.14  $\frac{\text{mm}}{\text{N}}$  (0.20  $\frac{\text{in}}{\text{lb}}$ ) per division

Fig. 9 Good tuning with incomplete excitation: co-quad plot for the third mode of model 5V with masses 1, 3, 5 forced in a 3 rad/sec narrow-band sine sweep

Masses 1, 3 and 5 are essentially node points for modes 2, 4 and 5. It is not surprising, therefore, that excitation at those masses only results in a determinant curve which lacks zero crossings corresponding to modes 4 and 5

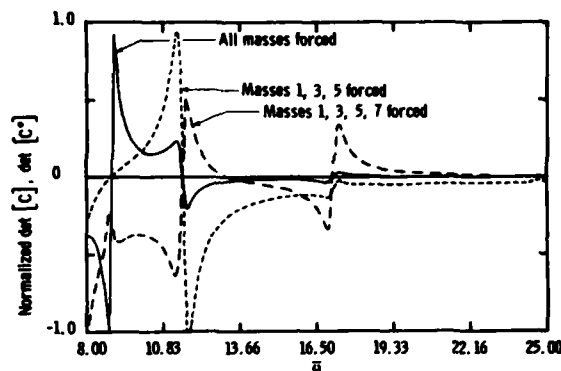


Fig. 10 Determinant plots for complete and incomplete excitation of model 11H. The frequency range of this graph excludes the first natural frequency.

(but still indicates their presence) and has a crossing at frequency 8.868 corresponding to mode 2 which one would normally dismiss as a false mode crossing due to its gentle slope. The dominant responses in the narrow-band sweep associated with the 8.868 crossing are shown on Figure 11. The presence of a mode is evident in that co-quad plot, but tuning is clearly very poor.

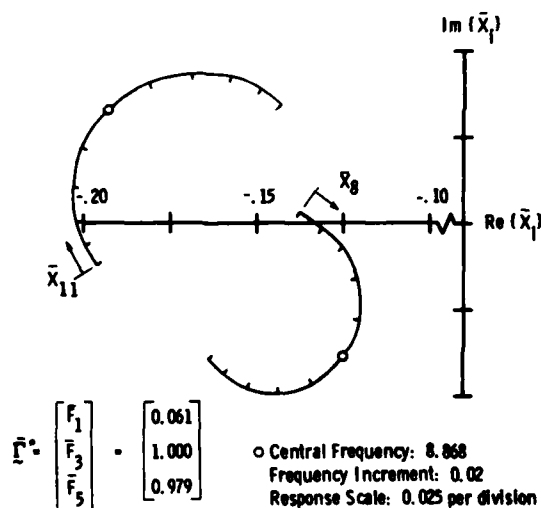


Fig. 11 Poor tuning with incomplete excitation: co-quad plot for the second mode of model 11H with masses 1, 3, 5 forced in a narrow-band sine sweep

When another exciter is added at mass 7, a good crossing results for mode 4, from which one can obtain excellent tuning. On the other hand, mode 2 is missed entirely, even though its mode shape has a large component at mass 7. Mode 5 is also missed, but this is to be expected since all excitation is in nodal regions.

By comparing missed modes on the determinant plots of Figure 3b and 10 with the associated mode shapes listed in Tables 1 and 2, we may infer the following rule of thumb: the presence of an obvious missed mode on a determinant plot indicates that the mode cannot be tuned with the given shakers (at least not in accordance with Asher's method) because too many of the shakers are positioned in nodal regions. Upon encountering such a situation in modal testing, one would be well advised to try a different shaker configuration. It appears that having some shakers in nodal regions may be helpful, or at least not harmful, for tuning, but clearly there must also be other shakers in regions of appreciable motion.

A circumstance not illustrated by our examples but which occurs occasionally is shown on Figure 12.

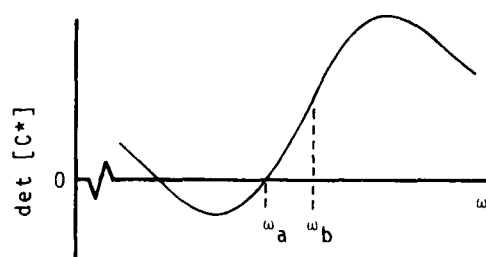


Fig. 12 Typical poor zero crossing

The determinant curve will have a zero crossing at  $\omega_a$ , which from the curve shape is obviously different than the natural frequency  $\omega_b$ . The force-amplitude vector resulting from the crossings at  $\omega_a$  will probably provide rather poor tuning. Again, a different shaker configuration may be required.

Finally, we note that higher structural damping manifests itself on coincident-response determinant plots in the form of gentler zero-crossing slopes, as illustrated by Figure 13. As a consequence, it may be difficult to distinguish between good and false mode crossings on the determinant plot for a heavily damped structure.

## VI. NOTES ON APPLICATION OF ASHER'S METHOD

For determinant evaluation, we have found the method of Crout (Hildebrand [20]), which employs triangular matrix decomposition, to be quite satisfactory. The algorithm is easily programmed, and execution is fast for determinants of order ten or smaller.

The usefulness of Asher's method is dependent in part upon how well the calculated force-amplitude distributions are able to tune modes. As discussed in Section V, the method itself fails in some cases due to its intrinsic

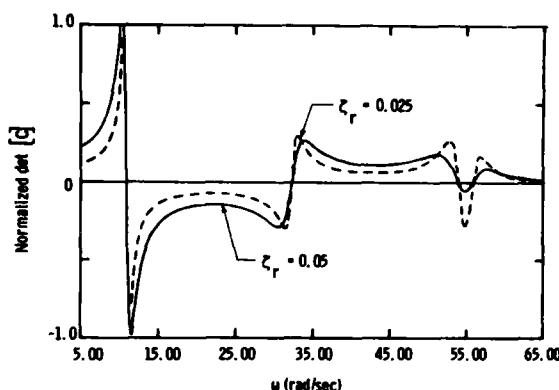


Fig. 13 Variation of determinant plots with damping level for model 5V with  $\zeta_r = 0.025$  and  $0.05$  in all modes

limitations. Another possible source of failure in applications is numerical inaccuracy in solutions of equations (16a, b). Accurate solution of equation (16b) for  $r^*$  is easy provided that  $[C^*]$  is indeed singular. Hence, it is essential to be able to determine the value of frequency  $\omega'$  for which  $D \equiv \det [C^*] = 0$  and, furthermore, to have accurate values for each element of  $[C^*(\omega')]$ . Our experience has been that errors in  $\omega'$  root solutions are amplified in the corresponding  $r^*$  solutions.

If transfer function data is available in equation form, as in a numerical simulation, then accurate solution is relatively easy. We have employed Newton's iterative method in the approximate form

$$\omega_{i+1}' = \omega_i' - D_i \left[ \frac{\omega_i' - \omega_{i-1}'}{D_i - D_{i-1}} \right] \quad (24)$$

The accuracy afforded by this equation in our application is limited only by computer precision.

On the other hand, if transfer function data is available only at discrete frequencies, then equation (24) is not immediately applicable. There are at least two approaches, interpolation and curve fitting, that might be used in this circumstance.

1. Interpolation. In this case, one should have available a graphics output display of the determinant plot, such as those reproduced in the paper by Stroud et al [5]. In the neighborhood of the zero crossing, that plot should resemble Figure 14. An interpolation equation should be developed for each transfer function using the appropriate number of data points surrounding the determinant zero crossing, e.g., two points for linear or four points for cubic interpolation. With the use of the

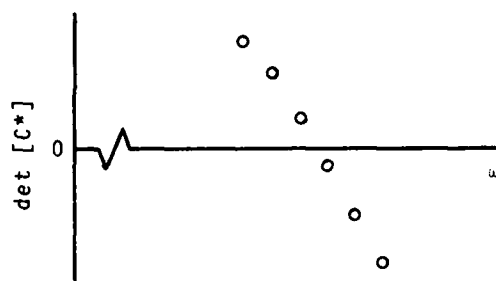


Fig. 14 Typical determinant plot at discrete frequencies near a zero crossing

interpolation equations, equation (24) may now be applied to determine the crossing frequency  $\omega'$ , and subsequently  $[C(\omega')]$  may be calculated. This approach should give good results if measured data is relatively clean; however, less satisfactory results can be expected for noisy data in the vicinity of the zero crossing.

2. Curve Fitting. There are several methods for fitting transfer function data, even noisy data, to analytical equations. After all elements of  $[C^*(\omega)]$  have been fit to equations, then equation (24) may be applied to calculate zero-crossing information. This approach obviously requires accurate curve fitting in the vicinity of modes.

As is discussed in Section III, a narrow-band sine sweep in the tuning step of Asher's method is preferable to a sine dwell. However, in a multiple-shaker sine sweep it is very difficult, due to interaction of specimen and shaker dynamics, to maintain constant amplitudes and phases of shaker force outputs. In view of this difficulty imposed by equipment performance, an acceptable alternative to actual mechanical tuning may be numerically simulated tuning with the use of experimental transfer function data and the excitation distribution calculated by Asher's method. For example, if  $k$  fixed motion sensors and  $m$  exciter locations are available on the specimen for a modal test, then one can measure with single-point excitation the corresponding  $k \times m$  experimental transfer function matrix  $[H_e(\omega)]$ .

Square sub-matrices of the real part of  $[H_e(\omega)]$  are evaluated by Asher's method to determine each test natural frequency  $\omega_j$  and the associated tuning force-amplitude  $m \times 1$  vector  $F_j^*$  (which is the  $p \times 1$  vector  $F^*$ , as previously defined, supplemented with  $m-1$  zero elements). Now a narrow-band sweep can be simulated numerically to give calculated co-quad plots of the  $k$  responses in the  $j$ th test mode simply by evaluating

$$X(\omega) = [H_e(\omega)] F_j^*$$

in a narrow band about  $\omega_j$ . This assumes either

that the frequency resolution of  $[H_e(\omega)]$  is sufficiently fine to provide several points in the narrow band, or that each element of  $[H_e(\omega)]$  is represented continuously by a curve-fit equation. If the test specimen behaves linearly, then all of the information that one might wish to determine about the  $k$  sensor responses from a multiple-shaker sine sweep or dwell is already contained in  $[H_e(\omega)]$ . So a multiple-shaker test is, in fact, redundant unless one wishes to determine additional information not available from the  $k$  sensors, such as an accurate map of nodal regions.

## VII. CONCLUDING REMARKS

Asher's method for modal testing by multiple-shaker sinusoidal excitation has been described in detail. Modal testing has been simulated numerically on mathematical structural models to illustrate the types of results that can be expected in practice. These results demonstrate that the method may succeed or it may fail depending, evidently, on the number and locations of exciters. Finally, numerical techniques required for implementation of Asher's method have been discussed, and a numerical alternative to actual multiple-shaker mechanical tuning has been suggested.

In view of the existence of efficient modern methods for characterizing structural modes by curve fitting of transfer function data, it might be contended that multiple-shaker tuning is no longer necessary. This is a reasonable contention only if modal density is low. As stated by Hamma et al [6] in their concluding remarks, curve fitting in frequency regions of high modal density can lead to inconsistent results. All curve-fit methods are based upon specific analytical models, all require an estimate of the number of participating modes, and most require at least initial estimates of some modal parameters. Hence, curve fitting is to some extent a subjective process, and for closely spaced modes it might lead to incorrect modal parameters or it might even miss modes. Clearly, the most important application of multiple-shaker testing by Asher's method is in separating closely spaced modes which cannot be adequately characterized by curve-fit methods.

## ACKNOWLEDGMENTS

This work has been sponsored by NASA Langley Research Center under Research Grant NSG 1276. A. G. Shostak calculated all results for the model with viscous damping. The authors make no claim to originality for the previously unpublished ideas and concepts appearing in this paper. For ideas related to practical implementation in particular, we are indebted to the first author's former associates, R. C. Stroud, S. Smith, G. A. Hamma, and R. C. Yee. We wish to thank the reviewers for their

helpful comments.

# BASIC NOTATION

$( )$	column matrix
$\text{Re } \{ \}$	real part of $\{ \}$
$\text{Im } \{ \}$	imaginary part of $\{ \}$
$[ ]^t, ( )^t$	transpose of $[ ]$ , $( )$
$( )^c$	complex conjugate of $( )$
$\det [ ]$	determinant of $[ ]$
$[C] = \text{Re } [H]$	coincident-response matrix
$[C^*]$	incomplete coincident-response matrix
$F$	force-amplitude vector
$\bar{F}, \bar{F}^*$	normalized $F$
$R_r$	constant defined by equation (8)
$[R]$	diagonal matrix of $R_r$ 's
$[V]$	matrix defined by equations (17), (18), (22)
$X$	complex response-amplitude vector
$\tilde{X}_i$	ith element of $X$
$\bar{X}$	compliance
$[b]$	viscous damping matrix
$[c(\omega)]$	structural damping matrix
$[d]$	hysteretic damping matrix
$f(t)$	time-dependent force vector
$\dot{g}_r$	hysteretic damping factor of the rth mode
$i = \sqrt{-1}$	
$[k]$	structural stiffness matrix
$[m]$	structural inertia matrix
$n$	total number of degrees of freedom
$p$	order of $[C^*]$
$x(t)$	time-dependent response vector
$\tilde{r}$	force-amplitude vector of rth characteristic phase-lag mode
$\tilde{r}^*$	tuning force-amplitude vector
$\tilde{r}$	viscous damping factor of the rth mode
$\phi_r$	phase lag of rth characteristic phase-lag mode
$[\psi]$	modal matrix of normal modes
$\psi_r$	rth column of $[\psi]$
$\psi^*$	test mode shape
$[\psi]$	modal matrix of characteristic phase-lag modes
$\psi_r$	rth column of $[\psi]$
$\omega$	excitation frequency
$\omega_r$	rth undamped natural frequency
$\omega$	dimensionless frequency; see Section V.2
$[lc]$	coupled modal damping matrix

# REFERENCES

1. Asher, G. W., "A Method of Normal Mode Excitation Utilizing Admittance Measurements", Proc. National Specialists' Meeting
2. Bishop, R. E. and Gladwell, G. M. L., "An Investigation into the Theory of Resonance Testing", Phil. Trans. of the Royal Society of London, Series A, Vol. 255, Mathematical and Physical Sciences, 1963, pp. 241-280.
3. Craig, R. R. and Su, Y. W. T., "On Multiple Shaker Resonance Testing", AIAA Journal, Vol. 12, No. 7, 1974, pp. 924-931.
4. Smith, S., Stroud, R. C., Hamma, G. A., Hallauer, W. L. and Yee, R. C., "MODALAB-A Computerized Data Acquisition and Analysis System for Structural Dynamic Testing", Proc. of the 21st International Instrumentation Symposium, Vol. 12, Philadelphia, Instrument Society of America, 1975, pp. 183-189.
5. Stroud, R. C., Smith, S. and Hamma, G. A., "MODALAB-A New System for Structural Dynamic Testing", The Shock and Vibration Bulletin, Bulletin 46, Part 5, 1976, pp. 153-175.
6. Hamma, G. A., Smith, S. and Stroud, R. C., "An Evaluation of Excitation and Analysis Methods for Modal Testing", SAE Paper No. 760872, Aerospace Engineering and Manufacturing Meeting, San Diego, 1976.
7. Fraeijs de Veubeke, B., "Dephasages caracteristiques et vibrations forcees d'un systeme amorti", Academie Royale de Belgique, Bulletin de la Classe des Sciences, 5e Serie-Tome XXXIV, 1948, pp. 626-641.
8. Fraeijs de Veubeke, B., "Comment on 'On Multiple-Shaker Resonance Testing'", AIAA Journal, Vol 13, No. 5, 1975, pp. 702-704.
9. Bishop, R. E. D., Gladwell, G. M. L. and Michaelson, S., The Matrix Analysis of Vibration, Cambridge University Press, 1965, Chapter 5.
10. Brown, D., Carbon, G. and Ramsey, K., "Survey of Excitation Techniques Applicable to the Testing of Automotive Structures", SAE Paper No. 770029, International Automotive Engineering Congress and Exposition, Detroit, 1977.
11. Kennedy, C. C. and Panco, C. D. P., "Use of Vectors in Vibration Measurement and Analysis", J. Aeronautical Sci., Vol. 14, No. 11, 1947, pp. 603-625.
12. Ibanez, P., "Force Appropriation by Extended Asher's Method", SAE Paper #760873,

on Dynamics and Aeroelasticity, Ft. Worth, Inst. of Aeronautical Sci., 1958, pp. 69-76.



Aerospace Engineering and Manufacturing Meeting, San Diego, 1976.

13. Hasselman, T. K., "Modal Coupling in Lightly Damped Structures", AIAA Journal, Vol. 14, No. 11, 1976, pp. 1627-1628.
14. Foss, K. A., "Co-Ordinates Which Uncouple the Equations of Motion of Damped Linear Dynamic Systems", Journal of Applied Mechanics, Vol. 25, 1958, pp. 361-364.
15. Frazer, R. A., Duncan, W. J. and Collar, A. R., Elementary Matrices, Cambridge University Press, 1946, p. 327.
16. Miramand, N., Billaud, J. F., Leleux, F. and Kernevez, J. P., "Identification of Structural Modal Parameters by Dynamic Tests at a Single Point", The Shock and Vibration Bulletin, Bulletin 46, Part 5, 1976, pp. 197-212.
17. Bishop, R. E. D. and Johnson, D. C., The Mechanics of Vibration, Cambridge University Press, 1960.
18. Stafford, J. F., "A Numerical Simulation of Multiple-Shaker Modal Testing", Master's thesis, Virginia Polytechnic Institute and State University, 1976.
19. Hallauer, W. L., Weisshaar, T. A. and Shostak, A. G., "A Simple Method for Designing Structural Models with Closely Spaced Modes of Vibration" submitted for publication, 1978.
20. Hildebrand, F. B., Methods of Applied Mathematics, 2nd ed., Prentice-Hall, 1965.

## MODAL CONFIDENCE FACTOR IN VIBRATION TESTING\*

Sam R. Ibrahim  
Department of Mechanical Engineering and Mechanics  
Old Dominion University, Norfolk, VA

The "Modal Confidence Factor", "MCF", is a number calculated for every identified mode for a structure under test. The MCF varies from 0.00 for a distorted, nonlinear, or noise mode to 100.0 for a pure structural mode. The theory of the MCF is based on the correlation that exists between the modal deflection at a certain station and the modal deflection at the same station delayed in time. The theory and application of the MCF is illustrated by two experiments. The first experiment deals with simulated responses from a two degree of freedom system with 20%, 40%, and 100% noise added. The second experiment was run on a generalized payload model. The free decay response from the payload model contained about 22% noise.

### INTRODUCTION

In modal vibration testing of complex structures, there exists some level of uncertainties as to the identified modal parameters in spite of the method of technique used to extract these modes. These uncertainties arise due to nonlinearity of structure under test, high coupling between closely spaced modes and or high levels of noise in the data used.

The theory and applications of a "time domain" modal test technique were presented in [1], [2], and [3]. The method uses free decay or, [4], random responses from a structure under test to identify its modal characteristics namely, natural frequencies, damping factors and mode shapes. The method was proved to be accurate, economical and insensitive to high levels of noise in the data. Furthermore the method can identify multi-modal (highly coupled) systems and modes that have very small contribution in the responses.

In [3], a method is presented to decrease the effects of high levels of noise in the data and thus improve the accuracy of identified parameters. This is done by using an oversized mathematical model. If the responses to be used are thought to have  $m$  number of modes, a math model to identify  $(m + n)$  modes is used. This gives  $n$  exits for noise and the  $m$  modes can be identified more accurately.

In this paper, the concept of Modal Confidence Factor (MCF) is developed. MCF is a

factor computed for every identified mode and this factor should be unity for any linear structural mode. Using this MCF, the clean structural modes can be separated from noise modes without leaving much chance for personal judgement.

The theory of the MCF is based on using the response of a station on the structure under test,  $x(t)$ , and the same response delayed  $\Delta\tau$ ,  $x(t + \Delta\tau)$ , (a transformed station), in the identification program. For every identified mode, the MCF is calculated as function of the modal deflections at the original station and the transformed station, the frequency and damping for that mode and the delay time  $\Delta\tau$ .

Simulated and experimental results are reported in support of the MCF theory developed in this paper.

It is important to note that although the MCF is developed to be used in conjunction with the "time domain" identification technique, the same concept can be adapted for use with other vibration identification techniques.

### BACKGROUND

#### 1. Time Domain Identification Technique:

This technique is fully described in [2] and [3]. It uses the free responses, (free decay), of a structure under test to identify its vibration parameters; namely frequencies, damping factors, and modal vectors in complex form.

\*This work is supported by NASA's Langley Grant No. NSG1459.

From the measured free responses of  $n$  stations on a structure under test, and assuming that the responses contain  $n$  modes, a matrix  $[A]$  is formed such that

$$[A] = \begin{bmatrix} [Y] \\ [Z] \end{bmatrix} \begin{bmatrix} [X] \\ [Y] \end{bmatrix}^{-1} \quad (1)$$

where,

$$\begin{aligned} x_{ij} &= x_i(t_j) \\ y_{ij} &= x_i(t_j + \Delta t) \\ z_{ij} &= x_i(t_j + 2\Delta t) \\ i &= 1, n \text{ and } j = 1, 2n. \end{aligned}$$

The eigen vectors of the  $[A]$  matrix are the modal vectors and the eigen values,  $\alpha_i$ , are related to the characteristic roots,  $\lambda_i$ , of the system through the equation

$$\alpha_i = e^{\lambda_i \Delta t} \quad (2)$$

This technique was originally developed such that for unique identification the order of the matrix  $[A]$  should be equal to twice the number of modes excited in the measured response vector  $\underline{x}$ .

In case of noisy data, two methods were presented in [3] to reduce the effect of noise on identified parameters. One of these methods was to use a mathematical model of order higher than the number of modes excited in the responses used for identification. The difference between the order of the mathematical model and the number of modes in the responses is merely an exit for the noise in the data. Using an oversized math model was proven to be very effective in reducing the effect of high levels of noise on identified parameters.

## 2. Transformed Stations

The time domain identification technique was developed to use the minimum amount of measuring channels. Any structure however complex can be identified using only two measuring stations at a time with one station kept as a reference station all the times. Due to this, a situation will arise when the number of modes excited in the measured responses is greater than the number of measuring stations. In such a case, it is not necessary to physically add measurement equipment and repeat the experiment; it is possible to use "assumed stations" for which the responses are generated using the response of the original, or real, stations. Indeed, if  $x(t)$  is the response of the  $p$  real

stations on a structure and  $m$  is number of modes in the response, the response at  $p$  assumed stations can take the form of  $x(t + \Delta\tau)$ . This can be shown by writing the response at time  $t_j$  as

$$\underline{x}(t_j) = \sum_{i=1}^{2m} R_i \psi_i e^{\lambda_i t_j} \quad (3)$$

and at time  $(t_j + \Delta\tau)$

$$\underline{x}(t_j + \Delta\tau) = \underline{\bar{x}}(t_j) = \sum_{i=1}^{2m} R_i e^{\lambda_i \Delta\tau} \psi_i e^{\lambda_i t_j} \quad (4)$$

where  $R_i$  is a constant associated with modal vector  $\psi_i$  and  $\lambda_i$  is the  $i$ th characteristic root. The two responses of equations (3) and (4) can be written as

$$\begin{bmatrix} \underline{x}(t_j) \\ \underline{\bar{x}}(t_j) \end{bmatrix} = \sum_{i=1}^{2m} R_i \begin{bmatrix} \psi_i \\ \bar{\psi}_i \end{bmatrix} e^{\lambda_i t_j} \quad (5)$$

where

$$\bar{\psi}_i = e^{\lambda_i \Delta\tau} \psi_i \quad (6)$$

Equation (5) may be considered to be the response vector for a system with  $2p$  stations and  $m$  modes. This procedure can be repeated to increase the apparent number of stations to  $3p, 4p, \dots$  etc.

## THEORY OF THE MODAL CONFIDENCE FACTOR

In a typical modal testing of a structure, if  $x(t)$  is the measured free responses from  $p$  station on the structure under test, new responses  $\underline{\bar{x}}(t) = \underline{x}(t + \Delta\tau)$ ,  $\underline{\bar{\bar{x}}}(t) = \underline{x}(t + 2\Delta\tau)$ ,  $\dots$  etc. will be generated to increase the apparent number of stations to be used in the identification program.

To calculate the "MCF" for a specific mode, one of the structure's stations will be arbitrarily specified together with the same station delayed in time  $\Delta\tau$ , say. If  $\lambda$  is the identified characteristic root for the mode,  $Q$  is the identified modal deflection at the chosen structure's station, and  $\bar{Q}$  is the identified modal deflection at the same station delayed

$\Delta\tau$ , these quantities can be used to calculate the "MCF" for the mode under consideration. From the theory of transformed stations discussed in the preceding section, the modal deflection expected at the transformed station should be:

$$\bar{Q}_{\text{expected}} = Q e^{\lambda \Delta\tau}$$

If the identified mode is a clean linear structural mode  $\bar{Q}$  should be equal to  $\bar{Q}_{\text{expected}}$ . Generally,

$$\bar{Q}_{\text{expected}} = \bar{Q} \times (\text{MCF}),$$

from which the equation for the "MCF" will be

$$\begin{aligned} (\text{MCF}) &= \left| \frac{\bar{Q}_{\text{expected}}}{\bar{Q}} \right| \times 100 \quad \bar{Q} > \bar{Q}_{\text{expected}} \\ &= \left| \frac{\bar{Q}}{\bar{Q}_{\text{expected}}} \right| \times 100 \quad \bar{Q}_{\text{expected}} > \bar{Q} \end{aligned}$$

## EXPERIMENTAL RESULTS

### 1. Simulated Experiment On A Two-Degree-of-Freedom System.

Free decay responses from the system shown in Fig. 1 were simulated on the CDC-6600 computer. Generated random numbers were added to the responses as noise. Three different noise levels were added such that the root mean square values of noise/signal ratio were 20%, 40%, and 100%. Fig. 2 shows the free decay responses  $x_1(t)$  and  $x_2(t)$  without noise and with three different levels of noise added.

The responses were used to identify the modal parameters of the system using the time domain technique described in [3]. Different orders for the math model were assumed. Math models of 2, 4, 6, 8 and 10 degrees of freedom were used. The "MCF" for different cases was calculated. Results are summarized in Tables 1 and 2. In Table 1 the "MCF" for the first two modes, the real system's modes, is quite high. For the rest of the modes "MCF" is low indicating non-structural modes or noise modes. The identified frequencies and damping factors are listed in Table 2 together with the percentage error. The errors in the identified parameters are much lower than the percentage of noise in the responses used for identification even in the case of 100% noise.

### 2. Generalized Payload Model

The payload model is shown in Fig. 3.

Sixteen accelerometers were fixed to the eight bulkheads; eight accelerometers on each side, Fig. 3. Two data groups were used. Data group one had accelerometers 1 to 8. Data group two had accelerometers 9 to 16 and accelerometer 8 as a common accelerometer for the two data groups. A random input was applied at station 8. The input was cut off and free responses from data group one were recorded on a tape recorder. The procedure was repeated for data group two. A two-way switch was used to cut off the random input and at same time generate a D.C. signal of about 1 volt. The start of the D.C. signal, recorded on a separate channel of the tape recorder, was used to determine the start of the free response.

The free responses were filtered to eliminate frequency components higher than 350 Hz and then digitized at a sampling rate of 2000 sample/second. Only 500 points for each channel were stored to be used as data for the identification program. This corresponds to a record length of 0.25 second.

The noise/signal ratio for the resulting data was estimated at about 22%. This estimate was based on comparing two responses from station 8 that were recorded simultaneously on two channels of the tape recorder. The root mean square of the two records, rms and RMS, were calculated and the noise/signal ratio was estimated using the following formula:

$$N/S = \sqrt{\frac{(\text{RMS} - \text{rms})^2}{\text{RMS} \times \text{rms}}}$$

Higher order response vectors were generated by delaying the responses of the original 17 stations 0.005 seconds and 0.01 seconds thus having the apparent number of stations to be 51. These responses were used as data for the time domain identification program. Three cases were studied for each of which the size of the mathematical model was different. Math model of 20, 30, and 40 degrees of freedom were used. Modal characteristics were identified together with the "MCF" for each mode. Table 3 lists the "MCF" for the three cases. In all the cases the "MCF" was consistently high for the first 11 modes and very low for the rest of the modes indicating 11 modes excited in the responses used. Table 4 lists the identified frequencies from the time domain technique together with frequencies identified using frequency sweep, "NASTRAN", and "FFT".

## CONCLUSIONS

The modal confidence factor "MCF" is a very powerful tool in the identification of modal characteristics of structures. It is specially useful when the data used has high levels of noise. The "MCF" can differentiate between a

real structural mode and a noise mode.

#### ACKNOWLEDGEMENT

The author is very grateful to personnel from the structural Dynamics Division at NASA's Langley Research Center for the help they offered during the preparation of this work.

#### REFERENCES

1. S.R. Ibrahim, and E.C. Mikulcik, "A Time Domain Modal Vibration Test Technique," Shock and Vibration Bulletin, Bulletin 43, Part 4, 1973.
2. S.R. Ibrahim, and E.C. Mikulcik, "The Experimental Determination of Vibration Parameters from the Free Responses," Shock and Vibration Bulletin, Bulletin 46, 1976.
3. S.R. Ibrahim, and E.C. Mikulcik, "A Method for the Direct Identification of Vibration Parameters from Time Domain Responses," Shock and Vibration Bulletin, Bulletin 47, 1977.
4. S.R. Ibrahim, "The Use of Random Decrement Technique for Identification of Structural Modes of Vibrations," Proceedings of the AIAA 18th Structures and Structural Dynamics and Materials Conference, March 1977.

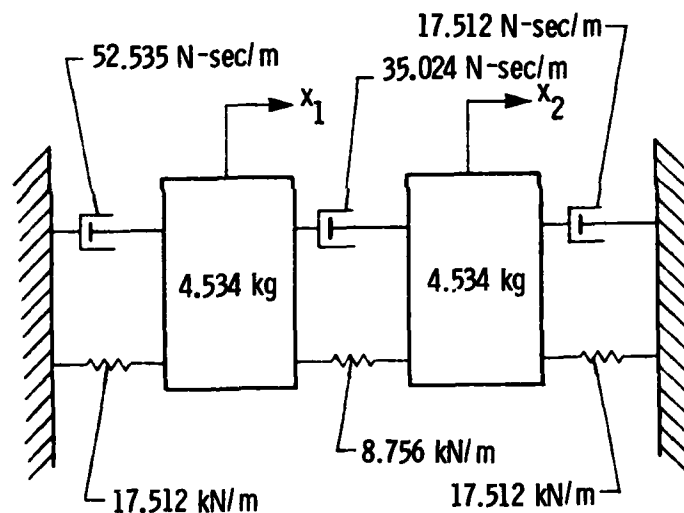


FIGURE 1. TWO-DEGREE-OF-FREEDOM SYSTEM

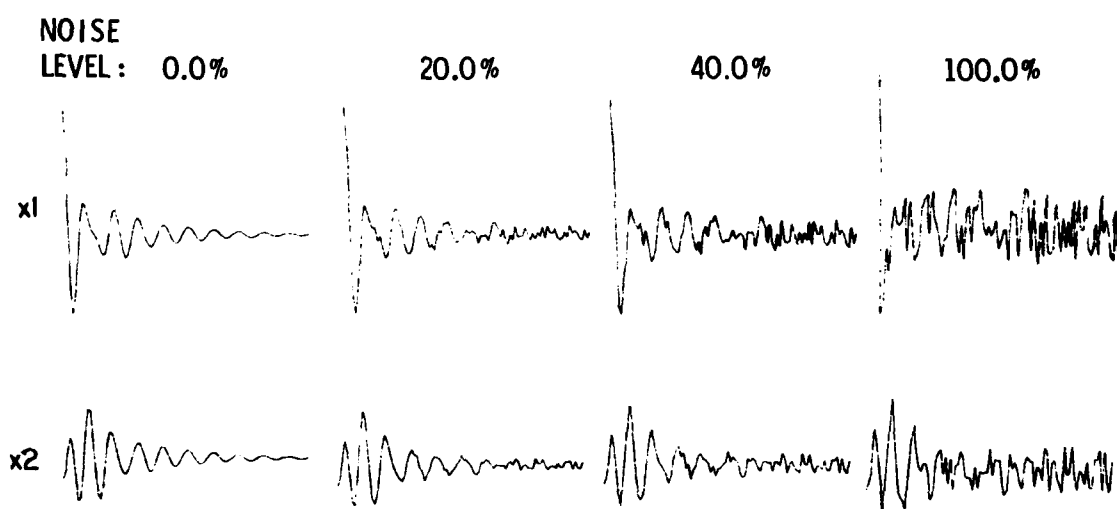


FIGURE 2. TWO-DEGREE-OF-FREEDOM RESPONSE

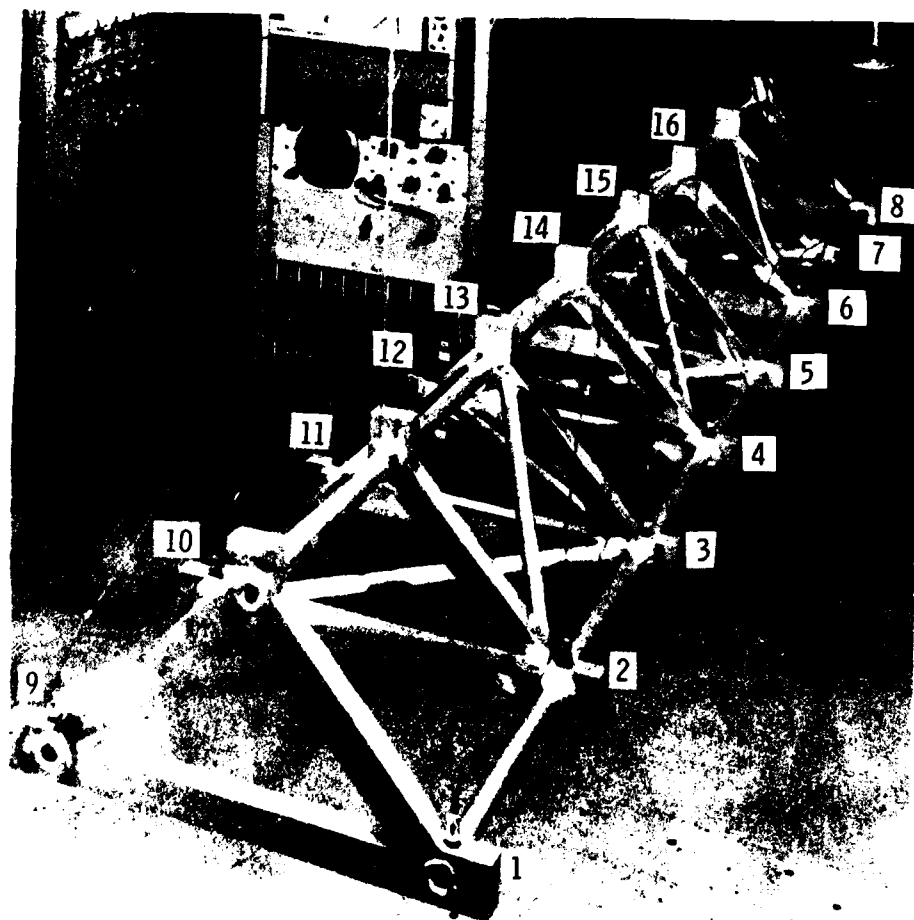


FIGURE 3. PAYLOAD MODEL

TABLE 1. "MCF" FOR THE TWO-DEGREE-OF-FREEDOM SYSTEM

NO. MODES	MCF								
	20 % NOISE				40 % NOISE				100 % NOISE
	NO. OF MODES				NO. OF MODES				NO. OF MODES
	4	6	8	10	4	6	8	10	10
1	90.0	98.3	98.7	99.6	81.7	93.7	96.4	97.7	89.9
2	96.7	96.4	96.3	92.3	98.0	93.6	97.1	89.6	70.4
3	32.0	24.2	26.0	20.4	30.8	24.5	25.5	21.5	19.6
4	8.2	15.0	6.0	45.2	5.6	16.5	5.1	44.0	22.0
5		10.6	10.4	17.8		14.6	10.3	16.2	38.9
6		0.2	8.6	17.5		4.0	9.2	16.3	8.2
7			4.6	7.1			4.4	6.6	7.1
8			3.6	8.7			3.3	8.8	12.0
9				8.9				7.4	1.6
10				0.1				0.1	3.0



TABLE 2. IDENTIFIED FREQUENCIES AND DAMPING FACTOR FOR THE TWO-DEGREE-OF-FREEDOM SYSTEM

PARAMETER	THEORETICAL	20% NOISE					40% NOISE				100%
	NUMBER OF MODES ASSUMED										
	2	4	6	8	10	4	6	8	10	10	
$f_1$	9.86	9.87	9.85	9.86	9.86	9.88	9.85	9.87	9.86	9.87	
% ERROR	-	0.1	0.1	0.0	0.0	0.2	0.1	0.1	0.0	1.1	
$\lambda_1$	6.2	5.9	6.4	6.3	6.4	6.0	6.8	7.0	6.8	9.7	
% ERROR	-	4.8	3.0	2.0	3.0	3.0	10.0	13.0	10.0	58.0	
$f_2$	13.79	13.68	14.09	13.78	13.79	13.60	14.36	13.82	13.9	14.38	
% ERROR	-	0.8	2.0	0.1	0.0	1.4	4.1	0.2	0.8	4.3	
$\lambda_2$	13.2	14.4	13.2	13.4	13.4	16.90	12.8	14.3	14.2	16.6	
% ERROR	-	9.8	0.0	1.5	1.5	28.0	3.0	8.3	7.6	25.8	

TABLE 3. "MCF" FOR PAYLOAD MODEL

	MCF								
	20 MODES		30 MODES			40 MODES			
	✓	X	✓	X		✓	X		
1	93.5	0.0	97.5	0.0	0.0	97.7	0.0	0.0	11.6
2	98.3	0.0	98.2	0.0	0.0	98.2	0.0	0.1	9.6
3	97.8	0.0	99.2	0.0	0.2	99.8	0.0	0.1	18.6
4	98.2	0.0	98.6	0.0	2.5	98.5	0.0	0.5	12.3
5	94.8	0.0	97.0	0.0	7.5	97.8	0.0	0.2	25.3
6	94.0	0.0	96.1	0.0	3.9	96.5	0.0	0.4	72.9
7	81.0	0.2	88.9	0.0	19.5	87.3	0.0	1.3	79.2
8	96.2	1.6	99.6	0.0	63.4	99.0	0.0	0.6	
9	75.6	31.2	89.0	0.0		92.0	0.0	1.6	
10	92.9		93.0	0.0		93.1	0.0	3.4	
11	97.9		98.0	0.0		97.9	0.0	3.3	

✓ GOOD MODE

X BAD MODE OR NOISE

TABLE 4. IDENTIFIED FREQUENCIES FOR THE PAYLOAD MODEL

MODE NO.	TIME DOMAIN			FREQUENCY SWEEP	'NASTRAN'	'FFT'
	20 D.O.F.	30 D.O.F.	40 D.O.F.			
1	74.2	74.2	74.1	74.6	73.4	74.1
2	78.7	78.7	78.7	79.7	80.1	78.8
3	119.9	119.8	119.8	120.7	117.3	119.6
4	156.6	156.6	156.6	158.5	158.9	156.5
5	162.1	161.9	161.9	163.1	159.9	161.6
6	216.0	216.4	216.4	219.2	218.6	216.5
7	245.4	245.4	245.2	246.7	244.6	245.0
8	258.9	259.2	259.3	?	253.1	259.0
9	260.1	260.6	261.0	263.7	-	261.0
10	280.9	280.9	280.9	283.7	283.0	281.0
11	325.3	325.3	325.3	325.0	-	325.0

## DISCUSSION

Voice: Isn't a factor a function of the delta T that you use in your formula?

Mr. Ibrahim: It is a function of delta T.

Voice: What delta T did you use?

Mr. Ibrahim: In delaying the response?

Voice: Yes.

Mr. Ibrahim: There are no constraints on the delta T that you use to delay your station.

Voice: Don't you have to use a number to do it? Don't you have to use a delta T in order to use the technique?

Mr. Ibrahim: Yes, I use it but there is no constraint on it. If your sampling frequency, or the time between two samples, is one millisecond you can delay your response three samples, five samples, or ten samples and use the same time. You will use a delta T of three thousandths, five thousandths, or ten thousandths. I tried using different delta T's and they gave me modal confidence factors of 97.6, 98.2, or 93.5. It is a function of the delta T. You use the delta T to get the "mcf", but there is no constraint on delta T.

# A BUILDING BLOCK APPROACH TO THE DYNAMIC BEHAVIOR OF COMPLEX STRUCTURES USING EXPERIMENTAL AND ANALYTICAL MODAL MODELING TECHNIQUES

J.C. Cromer, M. Lalanne  
Institut National des Sciences Appliquées  
Villeurbanne, France

D. Bonnecase, L. Gaudriot  
Métravib  
69130 Ecully - France

In the case of complex structures whose equations of motion cannot be obtained directly, even by finite element techniques, it may be possible to get their potential and kinetic energies from experiments. A building block approach taking into account constrained or unconstrained substructures is used. Components whose properties are determined by experiments are connected to those modeled by finite element techniques. In connection with theoretical formulations, experimental devices and procedures are presented. A new transfer function analyser system has been used. The constrained and unconstrained modal methods are applied first to a beam in bending in order to point out the experimental aspects of these techniques. The methods are then applied to a complex practical structure and agreement between experimental and theoretical results is shown to be good.

## INTRODUCTION

The formulation of the equations of motion is an important step in the dynamic analysis of structural systems. In the case of undamped structures, mass and stiffness matrices are needed. This is sometimes achieved by calculations using finite element techniques.

In the case of complex structures where dynamic modeling of the whole structure is impossible by a classical analytical approach, or generally a finite element approach, the global potential and kinetic energies may be obtained using a building block approach [6]. The structure is divided into interconnected components. Each of these can be analysed using either an analytical model or an experimental test procedure. By appropriate coupling the dynamic characteristics of each component, the kinetic and potential strain energies of the global structure is set up. Application of Lagrange's equation leads then to the differential equation system that can be used to predict the dynamical behavior of the structure.

Experimentally determined components are obtained according to a general method developed by Klosterman [1], ..., [5]. Throughout the experiments, components can be clamped (constrained modal methods) or free at the connection (unconstrained modal method).

Although the constrained modal method has already been presented [9], a synthesis of the theoretical formulation of both methods is presented in the paper. Here experimental aspects and limitations are pointed out, experimental devices and procedures are developed. Results are given for a cantilever beam in bending in order to evaluate the experimental aspects of these modal techniques.

Both methods have been tested on an industrial structure consisting of an horizontal plate (theoretically determined substructure) fixed on a foundation, to which a vertical cylinder is connected (experimentally determined substructure).

## SUBSTRUCTURE ANALYSIS AND DYNAMIC COUPLING

### Finite element analysis

The methods are presented in terms of two substructures and can be easily extended to many components.

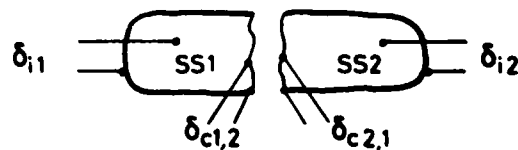


Fig. 1 : Structure decomposition

Let the degrees of freedom at the points of connection of the two components SS1 and SS2 be designated by the two vectors  $|\delta_{c1,2}|$  and  $|\delta_{c2,1}|$ , while the two vectors  $|\delta_{i1}|$  and  $|\delta_{i2}|$  are the others degrees of freedom of SS1 and SS2 respectively. Let us suppose that SS1 is analysed by finite elements and that  $T_1$  and  $U_1$  are respectively the kinetic and potential energy of this substructure.

From a classical finite element representation of SS1

$$2T_1 = \begin{vmatrix} \delta_{c1,2}^* \\ \delta_{i1}^* \end{vmatrix}^t \cdot \begin{vmatrix} m_{cc,1} & m_{ci,1} \\ m_{ic,1} & m_{ii,1} \end{vmatrix} \cdot \begin{vmatrix} \delta_{c1,2} \\ \delta_{i1} \end{vmatrix} \quad (1)$$

$$2U_1 = \begin{vmatrix} \delta_{c1,2}^* \\ \delta_{i1}^* \end{vmatrix}^t \cdot \begin{vmatrix} k_{cc,1} & k_{ci,1} \\ k_{ic,1} & k_{ii,1} \end{vmatrix} \cdot \begin{vmatrix} \delta_{c1,2} \\ \delta_{i1} \end{vmatrix} \quad (2)$$

A finite element representation of SS2 would be similar but, if we suppose, that only experimental tests can be performed to characterize SS2, the finite element expression of  $T_2$  and  $U_2$  will be transformed, using a modal basis where all formulations are expressed in terms of experimental data.

#### Unconstrained modal method

If SS2 is experimentally tested free at the connection modes, the modal basis used is :

$$\begin{vmatrix} \delta_{c2,1} \\ \delta_{i2} \end{vmatrix} = \begin{vmatrix} \psi_c \\ \psi_i \end{vmatrix} \cdot |\gamma(2)| = \begin{vmatrix} \psi_1, \psi_2, \dots, \psi_n \end{vmatrix} \begin{vmatrix} \gamma_1 \\ \gamma_2 \\ \vdots \\ \gamma_n \end{vmatrix} \quad (3)$$

The matrix  $|\psi|$  is composed of the "n" first eigenvectors used for the representation of SS2.  $|\psi|$  includes rigid body modes if they exist and the first elastic modes of vibration.

Using (3) : (1) and (2) become :

$$2T_2 = |\dot{\gamma}(2)|^t \cdot \hat{M}(2) \cdot |\dot{\gamma}(2)| \quad (4)$$

$$2U_2 = |\gamma(2)|^t \cdot \hat{K}(2) \cdot |\gamma(2)| \quad (5)$$

$\hat{M}(2)$  and  $\hat{K}(2)$  are the modal mass and stiffness matrices associated to the modal coordinates vector  $|\gamma(2)|$ .

If they are more than one rigid body modes, for example two ( $\omega_1 = 0$ ,  $\omega_2 = 0$ ) the orthogonality conditions are :

$$\begin{aligned} \psi_1^t \cdot K \cdot \psi_1 &= 0 \\ \psi_1^t \cdot M \cdot \psi_1 &\neq 0 \end{aligned} \quad (6)$$

$$\psi_2^t \cdot K \cdot \psi_2 = 0 \quad (7)$$

$$\psi_2^t \cdot M \cdot \psi_2 \neq 0$$

$$\psi_1^t \cdot K \cdot \psi_2 = 0 \quad (8)$$

$$\psi_1^t \cdot M \cdot \psi_2 \neq 0 \text{ (in general)}$$

Then the  $\hat{M}(2)$  mass matrix can have off diagonal terms. The rigid body modes are orthogonal if they are expressed using the principal inertia axis at the center of gravity of structure [8], [10].

The total kinetic and potential energies are :

$$2T = 2T_1 + 2T_2$$

$$2U = 2U_1 + 2U_2$$

and because of the condition at the connecting points :

$$\delta_{c1,2} = \delta_{c2,1} = |\psi_c| \cdot |\gamma(2)| \quad (9)$$

T and U become :

$$2T = \begin{vmatrix} \dot{\gamma}(2) \\ \delta_{i1}^* \end{vmatrix}^t \cdot \begin{vmatrix} \psi_c^t m_{cc,1} \psi_c + \hat{M}(2) & \psi_c^t m_{ci,1} \\ m_{ic,1} \psi_c & m_{ii,1} \end{vmatrix} \cdot \begin{vmatrix} \dot{\gamma}(2) \\ \delta_{i1} \end{vmatrix} \quad (10)$$

$$2U = \begin{vmatrix} \gamma(2) \\ \delta_{i1} \end{vmatrix} \cdot \begin{vmatrix} \psi_c^t k_{cc,1} \psi_c + \hat{K}(2) & \psi_c^t k_{ci,1} \\ k_{ic,1} \psi_c & k_{ii,1} \end{vmatrix} \cdot \begin{vmatrix} \gamma(2) \\ \delta_{i1} \end{vmatrix} \quad (11)$$

From Lagrange's equations, differential equation systems of the structures is easy to obtain. If they are no external forces :

$$\begin{vmatrix} \psi_c^t m_{cc,1} \psi_c + \hat{M}(2) & \psi_c^t m_{ci,1} \\ m_{ic,1} \psi_c & m_{ii,1} \end{vmatrix} \begin{vmatrix} \dot{\gamma}(2) \\ \delta_{i1}^* \end{vmatrix} + \begin{vmatrix} \psi_c^t k_{cc,1} \psi_c + \hat{K}(2) & \psi_c^t k_{ci,1} \\ k_{ic,1} \psi_c & k_{ii,1} \end{vmatrix} \begin{vmatrix} \gamma(2) \\ \delta_{i1} \end{vmatrix} = 0 \quad (12)$$

Then the first component is described by a finite element method, the second component is described from experimental tests: modal masses and stiffnesses and corresponding eigenvectors of SS2 tested free at the connection nodes.

#### Constrained modal method

This method has been presented previously [7], [9] and thus will be presented briefly. SS2 is clamped at the connection nodes. One has:

$$\begin{bmatrix} \delta_{c1,2} \\ \delta_{i2} \end{bmatrix} = \begin{bmatrix} 1 & 0 \\ 0 & \psi_i(2) \end{bmatrix} \begin{bmatrix} \delta_{c2,1} \\ \gamma(2) \end{bmatrix} \quad (13)$$

If the masses at the connection nodes are neglected the kinetic energy of SS2 is:

$$2T_2 = |\gamma(2)|^t \cdot |\psi_i| \cdot |m_{ii,2}| \cdot |\psi_i| \cdot |\gamma(2)| \quad (14)$$

$$2T_2 = |\gamma(2)|^t \cdot |M(2)| \cdot |\gamma(2)| \quad (15)$$

and the potential strain energy is:

$$2U_2 = \begin{bmatrix} \delta_{c2,1} \\ \gamma(2) \end{bmatrix}^t \cdot \begin{bmatrix} k_{cc,2} & k_{ci,2} \cdot \psi_i \\ \psi_i^t k_{ic,2} & k_{ii,2} \end{bmatrix} \cdot \begin{bmatrix} \delta_{c2,1} \\ \gamma(2) \end{bmatrix} \quad (16)$$

Modal forces  $|R(2)|$  at the constrained nodes of SS2 are given by:

$$|k_{ci,2} \cdot \psi_i| \cdot |\gamma(2)| = |F_c| = |R(2)| \cdot |\gamma(2)| \quad (17)$$

and  $k_{cc,2}$  can be expressed in form of:

$$|k_{cc,2}| = |K^*| + |R(2)| |K(2)|^{-1} |R(2)|^t \quad (18)$$

Where  $|K^*|$  is a supplementary stiffness matrix, experimentally determined if the set of connection nodes is a redundant one, ( $|K^*| \cdot |\delta_{c1,2}| = |F_c|$ ), otherwise  $|K^*| = 0$ , [7].

As for the unconstrained modal method,  $T$  and  $U$  for the global structure are obtained and:

$$2T = \begin{bmatrix} \gamma(2) \\ \delta_{ci,2} \\ \delta_{i1} \end{bmatrix}^t \cdot \begin{bmatrix} M(2) & & \\ & m_{cc,1} + m_{cc,2} & m_{ci,1} \\ & m_{ic,1} & m_{ii,1} \end{bmatrix} \cdot \begin{bmatrix} \gamma(2) \\ \delta_{ci,2} \\ \delta_{i1} \end{bmatrix} \quad (19)$$

$$2U = \begin{bmatrix} \gamma(2) \\ \delta_{ci,2} \\ \delta_{i2} \end{bmatrix}^t \cdot \begin{bmatrix} K(2) & R(2) \\ R(2)^t & K^* + R(2) \cdot K(2)^{-1} \cdot R(2)^t \end{bmatrix} \cdot \begin{bmatrix} \gamma(2) \\ \delta_{ci,2} \\ \delta_{i2} \end{bmatrix} + \begin{bmatrix} k_{ci,1} \\ k_{ii,1} \end{bmatrix} \cdot \begin{bmatrix} \gamma(2) \\ \delta_{i1} \end{bmatrix} \quad (20)$$

If the mass at the connection nodes of SS2 has to be used it can be taken in account by  $m_{cc,2}$ .

Then the first component is described by a finite element method the second component is described from experimental tests: modal masses, stiffness, forces and corresponding eigenvectors of SS2 tested clamped at the connecting nodes.

In the two methods the mass and stiffness matrices are expressed in a standard form used by most of the finite element computer programs.

#### EXPERIMENTAL ASPECTS AND LIMITATIONS

##### Unconstrained modal method

The experimentally determined modal parameters are:

- $\omega_i$ , natural frequencies
- $\psi_i$ , mode shape of the component
- $M_i$ , modal mass.

If often occurs that the connection area is free and thus free-free experimental tests have to be made. This is not always possible in fact but this method is very well adapted for light structures which belong for example to many of the aeronautical structures. Amongst the difficulties that have to be considered let us mention: rigid body mode determination.

The rigid body modes may be calculated, but they can also be determined experimentally. Knowing the effective mass and the center of gravity of the substructure a well chosen set of very low frequencies response leads, through an identification technique, to the required modal parameters of those constrained rigid body modes [8]. For diagonal modal matrices the axes are the principal inertia axes, at the center of gravity.

If the excitation direction is not straight towards the center of gravity, undesirable moments are perturbing the force measuring link. Several solutions have been successfully tested: introduction of a steel rod between excitation and structure (push-rod) or constrained steel rod sunken in a polymer sleeve [8].

The discontinuity of the stiffness between the connecting area and the inner part of the components (for example low rigidity of machinery connecting pads) may be very large. In the

dynamical behavior of the component alone these areas have very large amplitudes compared with the main part. These mode shapes singularities are not adapted to experimental measurements. The modal basis is composed of a large number of undesired natural modes (for example pads in phase or out of phase) which are of no interest in the global behavior. In general the connection of the components gives a high stiffness in this area.

#### Constrained modal method

The experimentally modal parameters are :  $\omega_i$ ,  $\psi_i$ ,  $M_i$  as in the unconstrained modal method and also  $R_i$  modal forces. Here the component has to be clamped at the connection nodes during the experimental tests. Two main difficulties have to be considered :

In the constrained area modal forces and moments related to the degrees of freedom of the connecting nodes (displacements or rotations) are not well experimentally determined. In fact, for most industrial structures, a good set of constrained modal forces without any measurement of moments, leads to a satisfactory dynamic behavior of the global structure. In our tests force measuring links are located in ball joints to cancel the unwanted effect of moments.

The problem of interaction between support and substructures, common to heavy structures,

is a limitation of the constrained modal method. The constrained boundary conditions are no more existing. The dynamic behavior of the component is related to the foundation. One of our future work will be to determine how to use identified data of a component, coupled to an active foundation, whose dynamic characteristics (component + foundation) have been previously determined.

#### Experimental devices and procedures

Measurement techniques and experiments have been developed by METRAVIB. The experimental approach is based upon the concept of a single shaker impedance technique. A general equipment has been developed : the "1191 Vibration Measurement and Analysis System". A transfer function analyser (Solartron) is associated to a mini computer (PDP 11/05 Digital Equipment) figure 2.

The mechanical transfer functions (X/F) are obtained and identified to an analytical development. The mini-calculator leads then to the best values of the required modal parameters, (figure 3).

Natural frequencies, damping coefficient, complex mode shapes, residual flexibility are obtained.

This equipment has been tested on several industrial existing structures. The experimental data of the complex structure presented in this paper were obtained likewise, (figure 4).

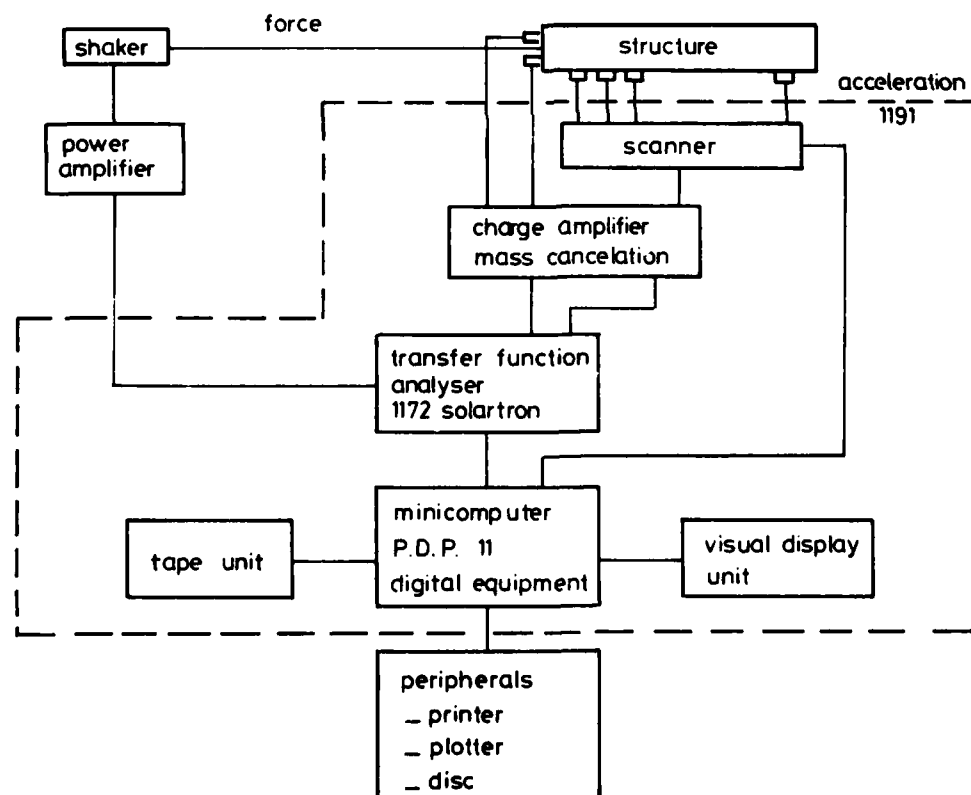


Fig. 2 : 1191 Vibration Measurement and Analysis System



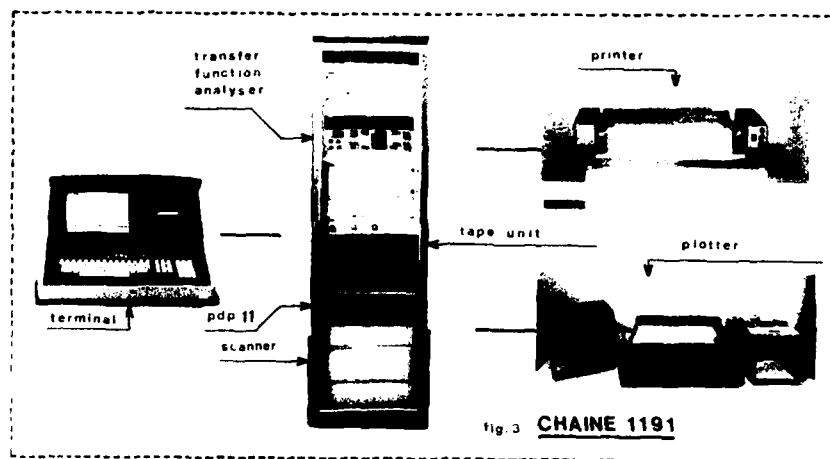


Figure 3

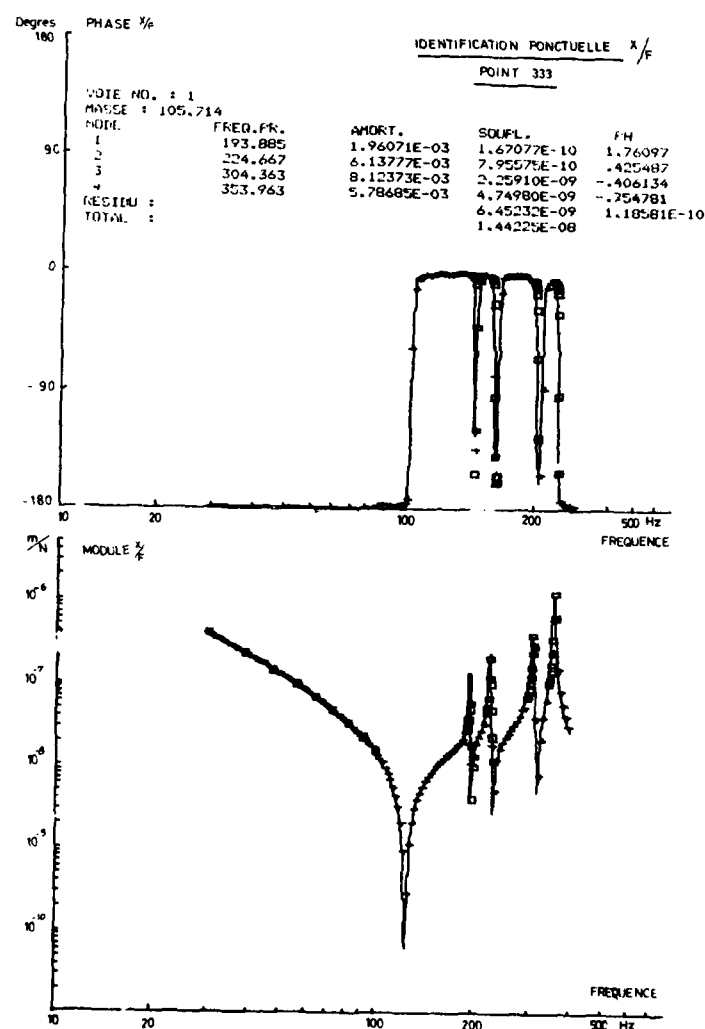


Figure 4 : representative sample of a response plot

## NUMERICAL CONSIDERATIONS

Two general programs have been developed using the Klosterman's building block approach for experimental constrained and unconstrained modal representations of components.

They are written in Fortran IV, specially adapted to CDC 7600 computers, and are also associated to a general finite element program, used for substructures represented by finite element techniques, (SAP IV), [24].

The lowest natural frequencies and corresponding eigenvectors of the complete structure are obtained by the simultaneous iteration method, [25].

## APPLICATION TO BEAMS

Both methods have been tested on simple examples consisting of beams in bending. Two types of end conditions are considered : clamped-free (figure 5) and clamped-clamped (figure 6).

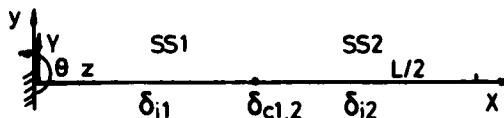
The first part of the beam (SS1 : first component), is always modeled by five beam element (analytically determined substructure). The second part of the beam (SS2 : second component) is modeled by constrained or unconstrained modal data (experimentally determined substructure). In a first step analytical data are substituted to experimental data to test the methods.

The accuracy of the description of the dynamic behaviour of the complete structure (SS1 + SS2) is good for both methods (table 1 and 2). The influence of each mode in the modal basis is shown (effect of even or uneven modes of SS2) and all modes have to be taken in the frequency range of interest. The best results are observed if the component modes are similar to those of the entire assembly (table 3).

Results concerning the constrained modal method have been presented in a previous paper [9] and are not given here.

As to experimental data quite large errors on modal data of SS2 do not affect significantly the resulting global behavior of the complete structure (table 4). The two techniques seem well adapted for experimental procedures and have to be tested on more complex structures.

Clamped free beam in bending (figure 5)



$$L=1m, h=0,01m, E = 2.10^{11}N/m^2, \rho = 7800 \text{ kg/m}^3$$

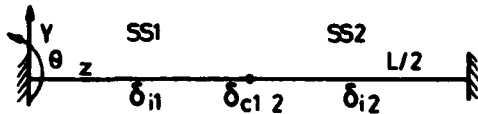
SS1 is modeled by a finite element technique, SS2 is either constrained or unconstrained.

$N_{hz}$	$N_1$	$N_2$	$N_3$	$N_4$	$N_5$
(1)	8.17	51.2	143.	281.	465.
(2)	8.17	51.2	143.	281.	466.
(3)	8.26	53.9	143.	298.	469.
(4)	8.25	54.3	144.	299.	469.
(5)	8.38	67.7	268.	632.	1110.
(6)	120.	297.	447.	745.	954.
(7)	8.26	53.5	143.	294.	467.

- |                                       |                                   |
|---------------------------------------|-----------------------------------|
| (1) Theoretical results               |                                   |
| (2) Finite elements results (SS1+SS2) |                                   |
| (3) SS1 5 Finite elements,            | SS2 2 rigid body modes            |
|                                       | 3 unconstrained elastic modes     |
| (4) SS1 5 F.E. diagonal mass matrix   | SS2 2 rigid body modes            |
|                                       | 3 unconstrained elastic modes     |
| (5) SS1 5 F.E. diagonal mass matrix   | SS2 2 rigid body modes            |
| (6) SS1 5 F.E. diagonal mass matrix   | SS2 3 unconstrained elastic modes |
| (7) SS1 5 F.E.                        | SS2 5 constrained elastic modes   |

Table 1 : Natural frequencies of the whole structure

Clamped-clamped beam in bending (figure 6)



$L=1m$ ,  $h=0.01m$ ,  $E=2.10^{11}N/m^2$ ,  $\rho = 7800 \text{ kg/m}^3$

SS1 is modeled by a finite element technique  
SS2 is either constrained or unconstrained

$N_{hz}$	$N_1$	$N_2$	$N_3$	$N_4$	$N_5$
(1)	52.	143.	279.	465.	693.
(2)	52.	143.	281.	466.	698.
(3)	52.1	142.	294.	467.	731.
(4)	54.	143.	295.	465.	731.
(5)	54.3	143.5	292.	466.	724.

- (1) Theoretical results  
 (2) Finite elements results (SS1+SS2)  
 (3) SS1 5 F.E. SS2 5 unconstrained modes  
 (4) SS1 5 F.E. diagonal mass matrix SS2 5 unconstrained modes  
 (5) SS1 5 F.E. SS2 5 constrained natural elastic modes

Table 2 : Natural frequencies of the whole structure

Influence of the number of modes of the modal basis

SS1 5 finite elements  
SS2 unconstrained modal basis ("n" first modes)

Clamped-clamped beam in bending

$N_{hz}$	TH	$n = 6$	$n = 5$	$n = 4$	$n = 3$	$n = 2$	$n = 1$
$N_1$	52.04	51.8	52.09	52.7	53.5	55.3	64.2
$N_2$	143.4	141.7	141.7	141.8	142.2	143.3	254.2
$N_3$	281.2	291.8	294.3	298.4	305.6	326.2	639.9
$N_4$	464.9	466.5	467.2	468.5	473.2	701.3	1207.9
$N_5$	694.5	724.7	731.9	744.4	774.9	1272.	1963.
$N_6$	970.	979.	981.	990.	1338.	2027.	3252.
$N_7$	1291.	1362.	1380.	1426.	2092.	3309.	4817.
$N_8$	1658.	1690.	1699.	2168.	3362.	4882.	7071.
$N_9$	2072.	2212.	2284.	3417.	4943.	7130.	9949.

Table 3 : Natural frequencies of the whole structure

Influence of the required experimental data  
Clamped-free beam with unconstrained modal  
data.

$N_{hz}$	(1)	(2)	(3)	(4)	(5)	(6)
$N_1$	8.17	8.26	8.32	8.16	8.28	8.28
$N_2$	51.26	53.9	57.7	49.8	53.7	55.5
$N_3$	143.4	142.9	143.5	142.9	135.5	146.1
$N_4$	281.2	298.4	324.9	302.8	297.3	298.2
$N_5$	464.8	468.8	517.3	468.5	460.1	473.5
$N_6$	694.5	744.6	704.9	755.3	742.9	740.6
$N_7$	970.7	989.6	1033.	989.4	982.9	994.6
$N_8$	1291.	1426.	1298.	1453.	1417.	1417.
$N_9$	1658.	2036.	2057.	2201.	2171.	2152.

- (1) Theoretical results
- (2) Exact analytical data
- (3) Displacement mode shapes, rotation neglected
- (4) Displacement and rotation introduced, but with 20 % error on rotation data
- (5) Displacement and rotation introduced, but with 20 % error on displacement data
- (6) Modal masses are analytically determined with arbitrary 20 % error

Table 4 : Natural frequencies of the whole structure

#### APPLICATION TO AN INDUSTRIAL STRUCTURE

A complex industrial example has been chosen to improve the constrained and unconstrained modal methods.

The structure studied here is a model of a gas diffusion column. The basic components are an horizontal plate supported at four points on an elastic foundation, on which a vertical cylinder is fixed by four connecting pads.

Two different connecting pads were tested :

- long pinned pads (figure 7)
- short rigid pads (figure 8)

The plate, first component of the structure, was determined theoretically. Experimental data of the dynamic behavior of the foundation were introduced as boundary conditions in the finite element representation of the steel plate. The agreement between finite element and experimental results is carefully checked in order to ensure a good analytical representation of this sub-structure, (table 5).

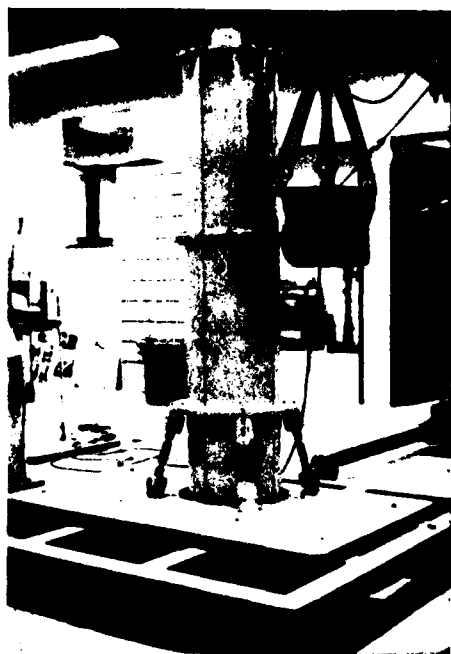


Figure : 7

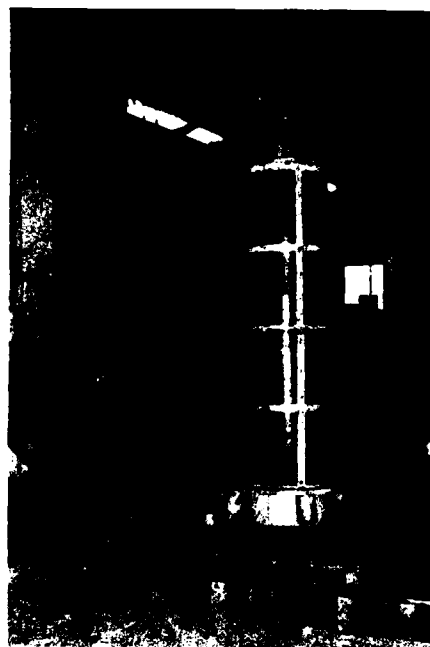


Figure : 8

$N_{hz}$	$N_1$	$N_2$	$N_3$	$N_4$	$N_5$	$N_6$	$N_7$
TH.	34.9	75.6	128.1	149.5	163.6	191.3	245.2
EXP.	35.	77.3	118.1	148.5	150.	193.8	246.5

Table 5 : Natural frequencies of the plate + foundation (finite element representation)

The calculated dynamic response of this component is good enough to be stored and utilized in the building block method.

The second component, column + connecting pads, because it is a complex structure was

tested experimentally.

All the dynamic characteristics needed in the constrained and unconstrained modal methods were exclusively determined from test data : figure 9 for example.

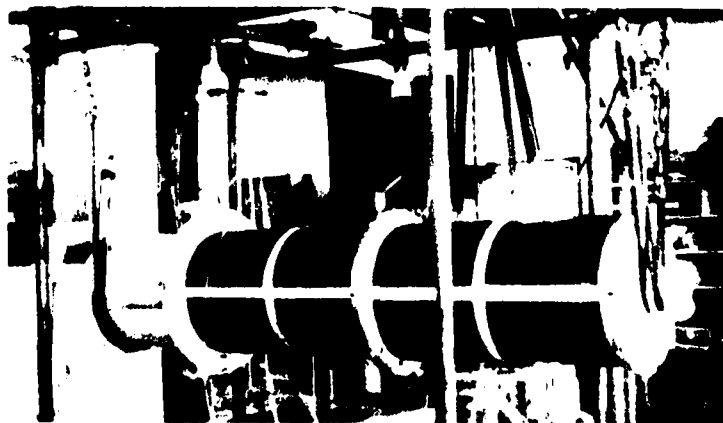


Figure 9 : Free-free test for the column

For the constrained modal method, the eight first constrained modes and modal data

were determined, (table 6).

	Pad 1	Pad 2	Pad 3	Pad 4	Modal mass
$N_1 = 28.4 \text{ Hz}$ $\omega_1 = 180 \text{ rad/s}$	- 5.5 $10^6 \text{ N/m}$	- 5.7 $10^5 \text{ N/m}$	+ 5.7 $10^5 \text{ N/m}$	+ 5.5 $10^6 \text{ N/m}$	$M_1 = 116 \text{ Kg}$
$N_2 = 31.6 \text{ Hz}$ $\omega_2 = 200 \text{ rad/s}$	+ 4.5 $10^5 \text{ N/m}$	- 6.7 $10^6 \text{ N/m}$	+ 6.7 $10^6 \text{ N/m}$	- 4.5 $10^5 \text{ N/m}$	$M_2 = 116 \text{ Kg}$
$N_3 = 40.9 \text{ Hz}$ $\omega_3 = 260 \text{ rad/s}$	- 1.7 $10^6 \text{ N/m}$	- 7.5 $10^6 \text{ N/m}$	+ 7.5 $10^6 \text{ N/m}$	- 1.7 $10^6 \text{ N/m}$	$M_3 = 116 \text{ Kg}$
$N_4 = 45.8 \text{ Hz}$ $\omega_4 = 290 \text{ rad/s}$	- 1.3 $10^7 \text{ N/m}$	- 2. $10^6 \text{ N/m}$	+ 2. $10^6 \text{ N/m}$	+ 1.3 $10^7 \text{ N/m}$	$M_4 = 116 \text{ Kg}$
$N_5 = 159.4 \text{ Hz}$ $\omega_5 = 10 \text{ rad/s}$	- 2. $10^7 \text{ N/m}$	- 2.5 $10^7 \text{ N/m}$	- 2.5 $10^7 \text{ N/m}$	- 2. $10^7 \text{ N/m}$	$M_5 = 116 \text{ Kg}$
$N_6 = 187. \text{ Hz}$ $\omega_6 = 1175 \text{ rad/s}$	1.4 $10^5 \text{ N/m}$	- 2.5 $10^7 \text{ N/m}$	2.5 $10^7 \text{ N/m}$	- 1.4 $10^5 \text{ N/m}$	$M_6 = 116 \text{ Kg}$
$N_7 = 191. \text{ Hz}$ $\omega_7 = 1200 \text{ rad/s}$	- 1. $10^7 \text{ N/m}$	- 4.5 $10^5 \text{ N/m}$	4.5 $10^5 \text{ N/m}$	1. $10^7 \text{ N/m}$	$M_7 = 116 \text{ Kg}$
$N_8 = 223. \text{ Hz}$ $\omega_8 = 1400 \text{ rad/s}$	- 1.3 $10^7 \text{ N/m}$	- 1. $10^7 \text{ N/m}$	- 1. $10^7 \text{ N/m}$	- 1.3 $10^7 \text{ N/m}$	$M_8 = 116 \text{ Kg}$

#### Vertical Modal Forces

$N_1, N_2$  "Rotation" of the cylinder  
 $N_3, N_4$  "Translation" of the cylinder  
 $N_5, N_6$  "Vertical modes" (symmetrical and antisymmetrical)  
 $N_7, N_8$  Main bending modes

Table 6 : Experimental data required for the constrained representation

For the unconstrained modal method, five rigid body modes were calculated and the first six elastic free-free modes of the column were measured. The orthogonality test for these six modes is :

$$\psi_i^T M \psi_j = \begin{vmatrix} 108 & 0 & 0 & 0 & -2 & 0 \\ & 108 & 0 & 0 & 0 & -2 \\ & & 108 & 2.5 & 0 & 0 \\ & & & 108 & 0 & 0 \\ & & & & 108 & 0 \\ \text{Symmetric} & & & & & 108 \end{vmatrix}$$

108 kg = mass of the cylinder without pads.

Experimental data required for the free-free representation of the column. Degrees of freedom (X Y Z  $\theta_x \theta_y$ ).

$$\begin{matrix} N_1 = 0 \text{ Hz} \\ M_1 = 116 \text{ Kg} \end{matrix} \quad |\delta_{C1,2}| = \begin{vmatrix} 1. & 0 & 0 & 0 & 0 \\ 1. & 0 & 0 & 0 & 0 \\ 1. & 0 & 0 & 0 & 0 \\ 1. & 0 & 0 & 0 & 0 \end{vmatrix}$$

$$\begin{matrix} N_2 = 0 \text{ Hz} \\ M_2 = 116 \text{ Kg} \end{matrix} \quad |\delta_{C1,2}| = \begin{vmatrix} 0 & 1. & 0 & 0 & 0 \\ 0 & 1. & 0 & 0 & 0 \\ 0 & 1. & 0 & 0 & 0 \\ 0 & 1. & 0 & 0 & 0 \end{vmatrix}$$

$$\begin{matrix} N_3 = 0 \text{ Hz} \\ M_3 = 116 \text{ kg} \end{matrix} \quad |\delta_{C1,2}| = \begin{vmatrix} 0 & 0 & 1. & 0 & 0 \\ 0 & 0 & 1. & 0 & 0 \\ 0 & 0 & 1. & 0 & 0 \\ 0 & 0 & 1. & 0 & 0 \end{vmatrix}$$

$$\begin{matrix} N_4 = 0 \text{ Hz} \\ M_4 = 55 \text{ Kg.m}^2 \end{matrix} \quad |\delta_{C1,2}| = \begin{vmatrix} 0 & 0.365 & -0.17 & 1. & 0 \\ 0 & 0.365 & 0.17 & 1. & 0 \\ 0 & 0.365 & 0.17 & 1. & 0 \\ 0 & 0.365 & -0.17 & 1. & 0 \end{vmatrix}$$

$$\begin{matrix} N_5 = 0 \text{ Hz} \\ M_5 = 55 \text{ Kg.m}^2 \end{matrix} \quad |\delta_{C1,2}| = \begin{vmatrix} -0.365 & 0 & 0.17 & 0 & 1. \\ -0.365 & 0 & 0.17 & 0 & 1. \\ -0.365 & 0 & -0.17 & 0 & 1. \\ -0.365 & 0 & -0.17 & 0 & 1. \end{vmatrix}$$

Modal masses and inertia are determined from very low frequency excitation tests for the five rigid body modes. The mode shapes on the connection nodes are calculated analytically.

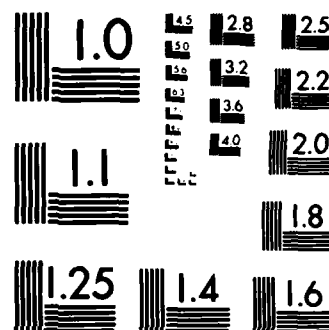
THE SHOCK AND VIBRATION BULLETIN PART 1 KEYNOTE ADDRESS  
INVITED PAPERS PA. (U) NAVAL RESEARCH LAB WASHINGTON DC  
SHOCK AND VIBRATION INFORMAT. SEP 78 BULL-48-PT-1

SHOCK AND VIBRATION INFORMAT. SEP 78 BULL-48-PT-1

F/G 20/11

NL

END



MICROCOPY RESOLUTION TEST CHART  
NATIONAL BUREAU OF STANDARDS-1963-A



Six first elastic natural modes of the cylinder (4 flexural and 2 vertical modes).

$$\begin{aligned} N_c &= 200 \text{ Hz} \\ M_c &= 116 \text{ Kg} \end{aligned} \quad |\delta_{c1,2}| = \begin{bmatrix} 0.558 & 0 & 0 & 0 & 0 \\ 0.558 & 0 & 0 & 0 & 0 \\ 0.558 & 0 & 0 & 0 & 0 \\ 0.558 & 0 & 0 & 0 & 0 \end{bmatrix}$$

$$\begin{aligned} N_c &= 200 \text{ Hz} \\ M_c &= 116 \text{ Kg} \end{aligned} \quad |\delta_{c1,2}| = \begin{bmatrix} 0 & 0.558 & 0 & 0 & 0 \\ 0 & 0.558 & 0 & 0 & 0 \\ 0 & 0.558 & 0 & 0 & 0 \\ 0 & 0.558 & 0 & 0 & 0 \end{bmatrix}$$

$$\begin{aligned} N_c &= 224 \text{ Hz} \\ M_c &= 116 \text{ Kg} \end{aligned} \quad |\delta_{c1,2}| = \begin{bmatrix} 0 & 0 & -0.305 & 0 & 0 \\ 0 & 0 & -0.305 & 0 & 0 \\ 0 & 0 & -0.305 & 0 & 0 \\ 0 & 0 & -0.305 & 0 & 0 \end{bmatrix}$$

$$\begin{aligned} N_c &= 285 \text{ Hz} \\ M_c &= 116 \text{ Kg} \end{aligned} \quad |\delta_{c1,2}| = \begin{bmatrix} 0 & 0 & -0.407 & 0 & 0 \\ 0 & 0 & -0.407 & 0 & 0 \\ 0 & 0 & -0.407 & 0 & 0 \\ 0 & 0 & -0.407 & 0 & 0 \end{bmatrix}$$

$$\begin{aligned} N_{1,0} &= 302 \text{ Hz} \\ M_{1,0} &= 116 \text{ Kg} \end{aligned} \quad |\delta_{c1,2}| = \begin{bmatrix} 0.066 & 0 & 0 & 0 & 0 \\ 0.066 & 0 & 0 & 0 & 0 \\ 0.066 & 0 & 0 & 0 & 0 \\ 0.066 & 0 & 0 & 0 & 0 \end{bmatrix}$$

$$\begin{aligned} N_{1,1} &= 302 \text{ Hz} \\ M_{1,1} &= 116 \text{ Kg} \end{aligned} \quad |\delta_{c1,2}| = \begin{bmatrix} 0 & 0.066 & 0 & 0 & 0 \\ 0 & 0.066 & 0 & 0 & 0 \\ 0 & 0.066 & 0 & 0 & 0 \\ 0 & 0.066 & 0 & 0 & 0 \end{bmatrix}$$

Data are performed using the new analyser system.

#### Complete system simulation results

The column with a constrained or unconstrained modal representation is connected to the plate throughout the long pinned or short rigid pads. Natural frequencies and mode shapes of the whole structure are computed and presented on table 7.

(1)	(2)	(3)	(4)
15.3	14.2	18.7	18.7
19.3	18.8	20.8	20.8
26.	27.9	25.2	25.3
34.3	35.9	21.9	21.9
37.3	38.		
105.	101.	97.1	97.5
163.	155.	198.	187.
181.	189.	135.	138.

Long connecting pads

(5)	(6)	(7)
19.	22.1	22.1
25.	32.7	32.7
33.	34.4	34.5
109.	129.	130.
165.	179.	187.
197.	201.	233.
205.	180.	228.

Short connecting pads

- (1),(5) experimental data
- (2) constrained cylinder with pads + plate + foundation
- (3),(6) unconstrained cylinder + plate with pads + foundation
- (4),(7) only rigid body modes are taken for the unconstrained modal basis of the cylinder.

Table 7 : Frequencies of the whole structure

Mode shapes of the global structure are shown on the following figures.

#### First case

Column with long pinned connection pads, fixed on the plate + foundation

- experimental results of the complete structure : figure 10,
- constrained column with long pinned pads (experiments) associated to the finite element representation of the plate : global mode shapes figure 11,
- unconstrained column without connecting pads (experiments) associated to the finite element representation of the plate + pads : figure 12.

#### Second case

Column with short rigid connecting pads, fixed on the plate + foundation

- experimental results of the complete structure (figure 13),
- unconstrained column without connecting pads (experiments) associated to the finite element representation of the plate + short rigid pads (figure 14).

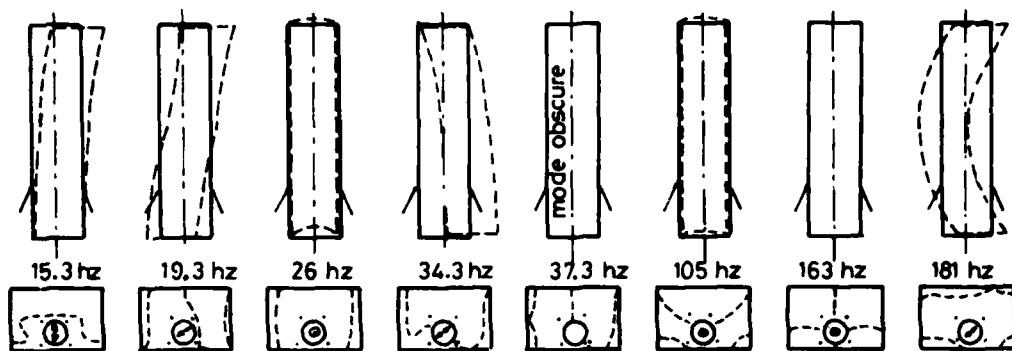


Fig. 10 : Experimental results . Column + long pinned pads + plate + foundation

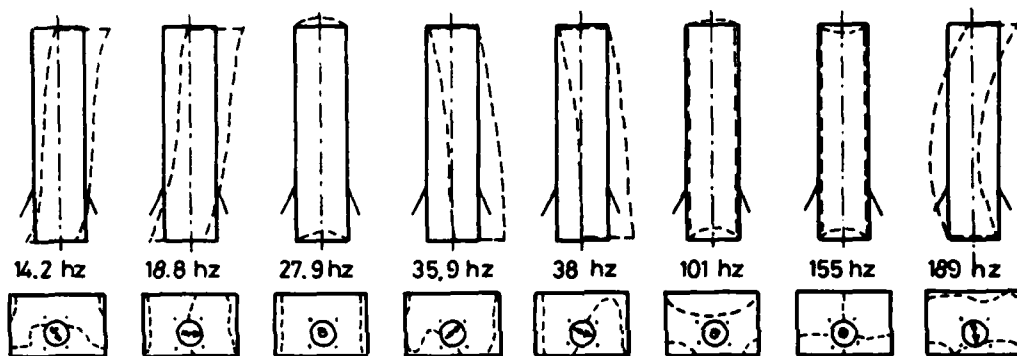


Fig. 11 : Computed results . Constrained column + long pinned pads + plate + foundation

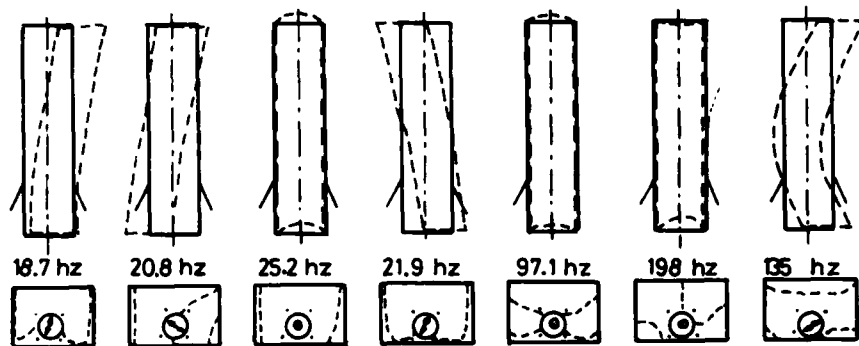


Fig. 12 : Computed results . Unconstrained column + plate with long pinned pads + foundation

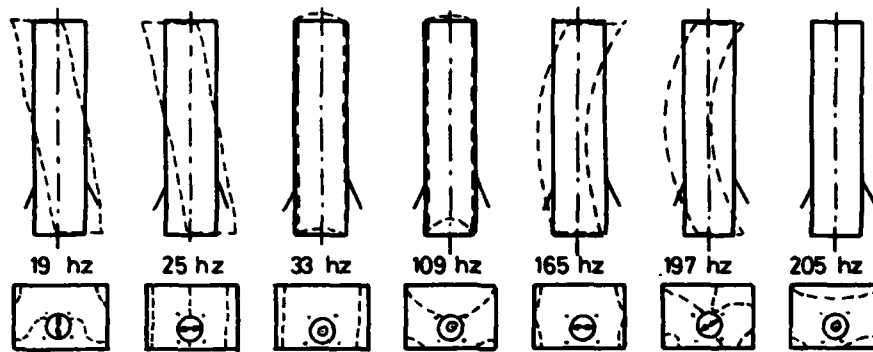


Fig. 13 : Experimental results . Column + short rigid pads + plate + foundation

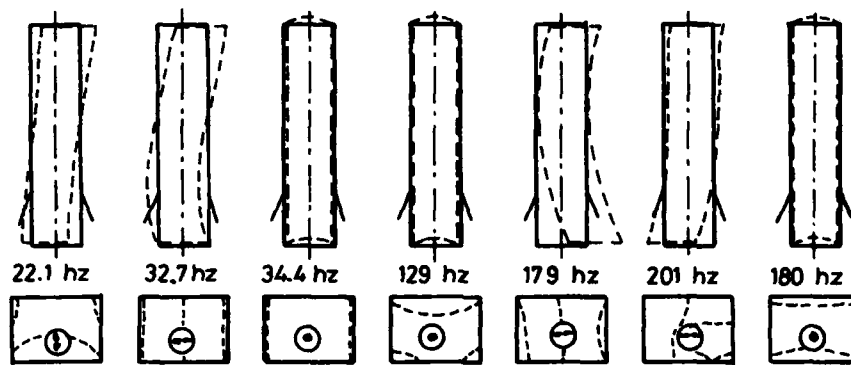


Fig. 14 : Computed results . Unconstrained column + short rigid pads + plate + foundation.

## DISCUSSION

Both methods have been applied successfully to the industrial test example. Two different connecting systems of the main components were tested. The constrained modal method seems better adapted to this particular structure. The constrained modal basis of the column is closer to the global behavior of the structure (figure 11) than the free-free mode shapes of the cylinder (figure 12).

Furthermore, the dynamical characteristics of the long pinned pads are difficult to calculate (column 3, table 7), the pads are included in the finite element modelisation. They are well represented by experimental data, (column 2, table 7).

Nevertheless, for the short rigid connecting pads, which are easily modelised by finite elements, the unconstrained modal method provides good results (column 6, table 7).

The influence of the rigid body modes are noticed at low frequencies and the free-free elastic modes shapes on the upper global modes considered (column 7, table 7).

As to experimental results, every calculated mode could be observed with the 1191 vibration measurement and analysis system. Some difficulties due to the particular interaction between the foundation and the mode shape of the plate at 163 Hz were encountered.

In general the results appear to be very satisfactory.

## CONCLUSION

Analysis of a complex structural dynamic system such as the one discussed in this paper is believed to be a significant test of Klosterman's building block methods. The constrained and unconstrained modal methods are being verified with scale model experimental data. Results indicate that the methods provide a realistic dynamic analysis of large and complex engineering structures.

## ACKNOWLEDGEMENTS

This work [7], [8] was supported by the Délégation Générale à la Recherche Scientifique et Technique, under contrats 73-7-1786, 75-7-1224, 75-7-1225. The authors are indebted to D.G.R.S.T. for permission to publish this paper.

## REFERENCES

- [1] A.L. KLOSTERMAN  
On the experimental determination and use of modal representation of dynamics characteristics. Ph. D. Thesis, 1971.
- [2] A.L. KLOSTERMAN, J.R. LEMON  
Dynamic design analysis via building block approach. Shock and Vibration Bulletin, n°42, Part 1, janvier 1972.

- [3] A.L. KLOSTERMAN, W.A. Mc CLELLAND, J.E. SHERLOCK  
Dynamic simulation of complex systems utilizing experimental and analytical techniques. A.S.M.E. 75-WA/Aero. 9, 1975.
- [4] A.L. KLOSTERMAN  
A combined experimental and analytical procedure for improving automotive systems dynamics. (S.A.E. n°72.0093), 1972.
- [5] J.C. DAVIES  
Modal modeling techniques for whicle shake analysis. (S.A.E. n° 72.0045), 1972.
- [6] M. LALANNE, P. BULAND  
Calcul des modes propres d'une structure par une méthode de sous-structures. Contrat C.N.E.S. 73/1039, 1973.
- [7] J.C. CROMER, M. LALANNE, D. BONNECASE, L. GAUDRIOT  
Comportement dynamique des structures complexes. Rapport final du contrat. D.G.R.S.T. 73-7-1786, 1973.
- [8] J.C. CROMER, M. LALANNE, D. BONNECASE, L. GAUDRIOT  
Comportement dynamique des structures complexes. Rapport final des contrats D.G.R.S.T. 75-7-1224 et 75-7-1225, 1975.
- [9] J.C. CROMER, M. LALANNE  
Dynamic behaviour of complex structures, using part experiment, part theory. Shock and Vibration Bulletin, n° 46, Part 5, 1976.
- [10] J.C. CROMER  
Modélisation semi-théorique, semi-expérimentale du comportement dynamique de structures complexes. Thèse de Docteur Ingénieur, 1977.

## GENERAL BIBLIOGRAPHY

- [11] C.E. KENNEDY, C.D.P. PANCU  
Use of vectors in vibration measurement and analysis. Journal of the Aeronautical Sciences, vol. 14, n° 11, nov. 1947.
- [12] W.C. HURTY  
Dynamic analysis of structural systems using component modes. A.I.A.A., vol. 3, n° 4, april 1965.
- [13] R.R. CRAIG, M.C.C. BAMPTON  
Coupling of substructures for dynamic analysis. A.I.A.A., vol. 6, n° 7, july 1968.
- [14] W.A. BENFELD, R.F. HRUDA  
Vibration analysis of structures by component mode substitution. A.I.A.A., vol. 9, n° 7, july 1971.
- [15] W.C. HURTY, J.D. COLLINS, G.C. HART  
Dynamic analysis of large structures by modal synthesis techniques. Computers and Structures, vol. 1, 1971.
- [16] R.M. HINTS  
Analytical methods in component modal syntheses. A.I.A.A., vol. 13, n° 8, august 1975.
- [17] C. SZU  
Vibration analysis of structures using fixed interface component modes. Shock and Vibration Bulletin, n° 46, Part 5, 1976.

- [18] E.J. KUJAR, C.V. STAHLÉ  
Dynamic transformation method for modal synthesis. A.I.A.A., vol. 12, 1974.
- [19] S. RUBIN  
Improved component-mode representation for structural dynamic analysis. A.I.A.A. vol. 13, 1975.
- [20] A. BERMAN  
Vibration analysis of structural systems using virtual substructures. Shock and Vibration Bulletin, n° 43, Part 2, 1973.
- [21] R.R. CRAIG, CHING-JONE CHANG  
Free interface methods of substructure coupling for dynamic analysis. A.I.A.A. Technical notes, novembre 1976.
- [22] R.L. GOLDMAN  
Vibration analysis by dynamic partitioning. A.I.A.A., vol. 7, 1969.
- [23] S.N. HOV  
Review of modal synthesis techniques and a new approach. Shock and Vibration Bulletin n° 40, Part 4, 1969.
- [24] K.J. BATHE, E.L. WILSON, F.E. PETERSON  
SAP IV, Berkeley, June 1973.
- [25] A. JENNINGS, D.L.R. ORR  
Application of the simultaneous iteration method to undamped vibration problems. International Journal for Numerical Methods in Engineering, vol. 3, 1971.
- [26] M. LALANNE, P. TROMPETTE, M.T. CHAMBAUD  
Recherche des valeurs propres et vecteurs propres par itérations simultanées. Rapport D.R.M.E., 1972.
- [27] G. FERRARIS, P. TROMPETTE  
Programme de calcul KFMW. Recherche de valeurs propres et vecteurs propres. Programme du Laboratoire de Mécanique des Structures, I.N.S.A., 1975.

#### SYMBOLS

- SSk substructure k
- $2U, 2T$  potential and kinetic energy of the complete structure
- $2U_k, 2T_k$  potential and kinetic energy of substructure k
- $\delta_{ck,l}$  connection degrees of freedom from component k to component l
- $\delta_{ik}$  inner degrees of freedom of component k
- $m_{(k)}, k_{(k)}$  finite element mass and stiffness matrices of component k with respect to connection node and inner nodes

$$m_{(k)} = \begin{bmatrix} m_{ci,k} & m_{ci,k} \\ m_{ic,k} & m_{ii,k} \end{bmatrix} ; k_{(k)} = \begin{bmatrix} k_{cc,k} & k_{ci,k} \\ k_{ic,k} & k_{ii,k} \end{bmatrix}$$

- $|\psi|$  set of eigenvectors

- $|y_{(k)}|$  modal coordinates of component k
- $M_{(k)}, K_{(k)}$  modal masses and stiffnesses of component k
- $\omega_i$   $i$ th natural pulsation
- $R_{(k)}$  set of modal external forces acting at the constrained area of component k
- $| \cdot |^o$  derivative with respect to time
- $| \cdot |^t$  matrix transposition symbol

## TRANSFER FUNCTION APPLICATIONS TO SPACECRAFT

### STRUCTURAL DYNAMICS\*

J. R. Fowler  
Hughes Aircraft Company  
El Segundo, California

E. Dancy  
Hewlett-Packard Company  
Los Angeles, California

Fast Fourier transform computed transfer functions are used for several spacecraft applications. An Intelsat IVA spacecraft was tested using several excitations and the resulting transfer functions are compared using modal frequencies and damping. An example of mass and stiffness computations from transfer functions is presented. Use of alternative reference points for the transfer functions is presented. An example of the use of slight changes in transfer functions to detect failures is shown.

#### PURPOSE

The term "transfer function" as traditionally used in the structural dynamics field refers to the amplitude ratio and phase relation between two measurements on a slowly swept sinusoidally vibrated structure. One of the measurements would normally be the force input and the other a response location of interest. Modal studies have traditionally been run using a force signal as the input and an accelerometer signal as the response. The resulting transfer functions are typically displayed in a co-quad plot form and then used to identify the modal frequencies and amplitudes. With the development of the fast Fourier transform processors, the basic definition of a transfer function is unchanged, but the excitation signals that may be used are greatly expanded.

The purpose of this paper is to illustrate the power of this capability in addressing structural dynamics problems. Four examples are discussed. The first is a comparison of the transfer functions taken from COMSAT's Intelsat IVA spacecraft test data. That test used several excitation techniques and the frequencies and damping values for the modal response are compared. The second example discusses the effort to derive mass and stiffness matrices from transfer functions computed from a high level random test on NASA's Pioneer Venus multiprobe spacecraft. The

third illustrates the effects of using different reference points in computing transfer functions and the meaning of the results. The fourth uses Intelsat IVA data to illustrate the use of transfer functions as a quality control tool in the detection of spacecraft failures.

#### DISCUSSION

By taking the ratio of the spectral power of the input and reference measurements, it is possible to compute transfer functions for many diverse sources of excitation such as random, transient, and sine sweeps. The excitation shapes must conform to the following limitations:

- 1) It must be possible to generate an electrical or mechanical signal of the desired shape.
- 2) It must have an energy spectrum covering the frequency range of interest.
- 3) For amplitude dependent (nonlinear) systems, the excitation power available must drive the system to the desired amplitude range.
- 4) The input and response signals must be amenable to the analysis equipment available.

\*This article is based on work performed at Hughes Aircraft Company under Intelsat Contract IS-774. The views expressed in the article are not necessarily those of INTELSAT.

The first constraint does not present a practical limitation since most available systems have several excitation strategies built in and many other strategies could be improvised. Pure random excitation is always available using a noise generator and band limiting analog filters. The second limitation of energy spectrum is important, particularly with hammer testing and other similar excitations where the frequency spectra are not easily controllable. With the hammer impact excitation method, variations in the hammer weight and head compliance can vary the input spectra. The third limitation may occasionally require limited frequency range excitation when there is a severe power limit. For example, random excitation may require dividing the frequency range of interest into narrow bands to achieve the desired response levels. The fourth limitation is best illustrated where a combination of high frequency and a long signal time places a severe demand on the analysis equipment.

Some of the excitation methods for computing transfer functions currently being used are:

- 1) Slow swept sine
- 2) Fast swept sine (frequently termed "chirp" varying from 10 octaves per minute and faster)
- 3) Random (Several strategies have been employed with random, the simplest being

a noise generator and others being computer controlled signals such as periodic random and pseudorandom.)

- 4) Transient (This could be computer controlled shock spectra type transients or hammer impact type testing.)

This paper presents transfer functions taken from a full-scale communication satellite vibration test using several of the above excitation methods. The desire is to measure and compare the resonant frequencies and damping as a function of excitation method and excitation amplitude in order to assess the usefulness of similar data taken from other programs.

#### INTELSAT IVA SPACECRAFT TEST

As part of an INTELSAT/COMSAT Laboratories spacecraft test improvement program, an Intelsat IVA communication satellite (Fig. 1) was subjected to several base excitation sources in the lateral direction (Ref. 1). That spacecraft was extensively instrumented and the transfer functions from the base acceleration to selected response locations were computed.

Five response points on the spacecraft were selected for the comparison (Fig. 2): the top of the spacecraft, accelerometer 1X, the upper and lower feeds, accelerometers 2X and



FIG. 1 - INTELSAT IVA Y-1 SPACECRAFT

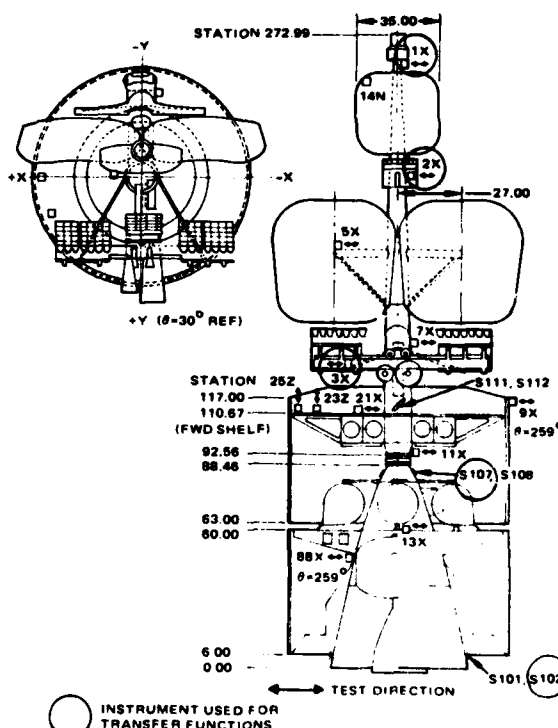


FIG. 2 - INTELSAT IVA Y-1 INSTRUMENTATION

3X, the moment at the despin bearing assembly, strain 107, and the base moment, strain 102. In all cases, the reference measurement was the base input acceleration. The use of the base accelerometer produces transfer functions and related modal data for the base fixed cantilever case.

#### Excitation Methods

1) Low level random. This test used a General Radio noise generator and Rockland tunable bandpass filters. The resulting random signal was fed to the shaker power amplifier and the input and response signals recorded for later analysis. The base acceleration had an energy bandwidth from 5 Hz to 30 Hz and an amplitude of approximately 0.06-g rms. While the input energy of the drive signal to the shaker power amplifier is flat, the response is not due to shaker and spacecraft dynamics. That variation is seen in the base accelerometer power spectrum plot in Fig. 3. This is the quality control test used at Hughes Aircraft Company prior to and following all spacecraft tests to detect any small change in the transfer function and thus an indication of possible structural failure.

2) Notched swept sine test. This is the currently used method at Hughes Aircraft Company to qualification test flight spacecraft. The base input acceleration level is specified but with the stipulation that selected spacecraft response levels are not to be exceeded. These limit response values are obtained from coupled booster-spacecraft analyses. Two notched sine tests were run, a low level and high level at 4 octaves per minute.

3) High level, narrow band random dwell. One of the spacecraft test methods considered during the study was the application of a high level random input applied simultaneously at each of the critical structural frequencies. The base input spectrum was selected such that the resulting structural response was representative of flight data experience. The

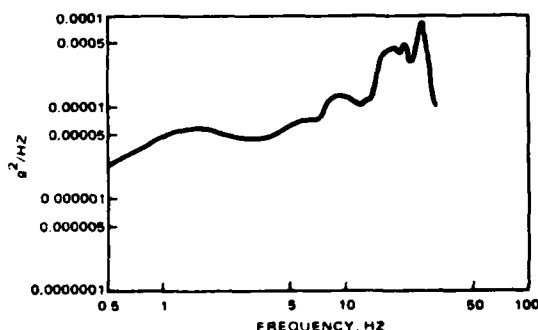


FIG. 3—BASE ACCELERATION FOR RANDOM BURST TEST 011

strategy was to adjust the random input at each frequency such that the desired response spectra would be generated. The base input amplitude was 0.18-g rms and the spectrum is shown in Fig. 4. The transfer function computation was done in a manner similar to the random test.

4) Transient input. Another excitation used was a transient which was representative of coupled booster-spacecraft analysis results. This transient was computed for and controlled at an intermediate point on the spacecraft (2IX, Fig. 2). This test, like the narrow band random test, is also frequency limited and only the lower frequencies are comparable. These transfer functions are of interest since they are used by the transient test software to update the control pulses.

#### Data Reduction Methods

The transfer functions were computed using the band selectable Fourier analysis package developed by Hewlett-Packard. This package is termed "zoom" in their literature and allows selection of narrow frequency ranges of interest for detailed analysis. The appendix describes the approach in detail.

One particular difficulty in obtaining good transfer functions was the short time records available. The tests were run to obtain comparative test data for the various approaches or, in some cases, the required data for spectral analyses. In retrospect, where possible, much longer time records would have been taken if transfer function analysis had been anticipated. This would have allowed a narrower zoom or increasing the number of averages for computing each transfer function. While realizing practical limitations, it is advantageous to compile a large quantity of data for transfer function computations.

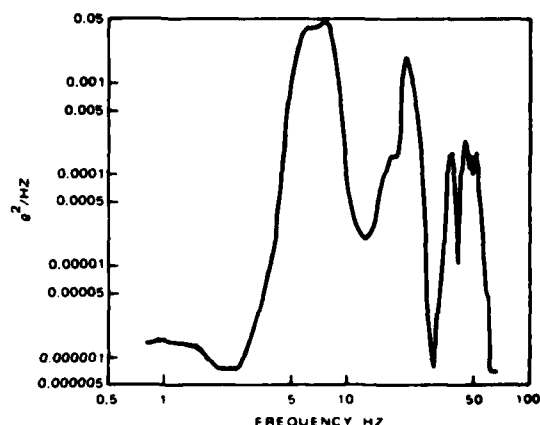


FIG. 4—BASE ACCELERATION FOR RANDOM DWELL TEST 3069



## Data Presentation

The transfer functions computed using traditional methods and the zoom method are compared as follows. The real and imaginary transfer functions for the spacecraft tip location for three of the methods are plotted in Figures 5, 6, and 7 using the traditional approach (nonzoom). Fig. 8 shows the transfer functions using the zoom approach. The Hewlett-Packard modal fit program was used on the zoom transfer functions which covered the first four frequencies; a quantitative comparison is given in Table 1. Modal data are not shown for all four frequencies for test 3071 since the data for all of the five locations did not result in usable transfer functions.

Table 1 illustrates the variation in frequency and damping values between the various methods. The table shows that the frequencies are repeatable for comparable amplitude excitations. As the amplitude goes up, and test

3031 was the highest amplitude test, the frequencies tend to go down and the damping increases. Inspection of the individual modal fit data indicates repeatable and similar fits for the random dwell data, and as the excitation energy diminished for the higher modes as on test 3071, the modal fits were poor and

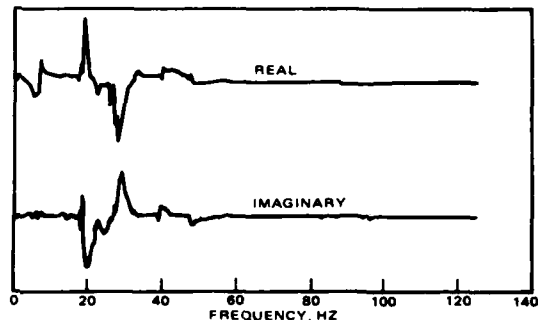


FIG. 6—SWEPT SINE (4 OCTAVE/MINUTE) TEST TRANSFER FUNCTION (BASEBAND METHOD)

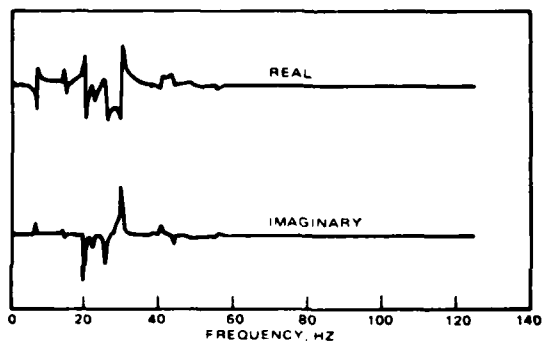


FIG. 5—RANDOM EXCITATION TRANSFER FUNCTION

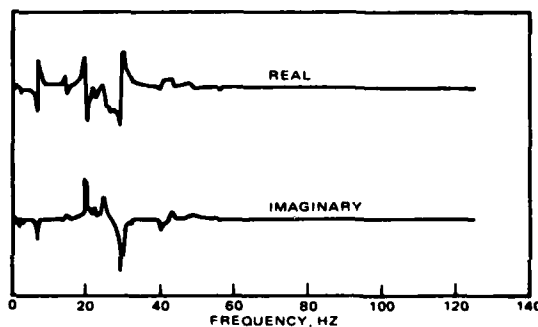


FIG. 7—RANDOM DWELL TRANSFER FUNCTION (BASEBAND METHOD)

TABLE 1  
Comparison of Intelsat IVA Y-1 Spacecraft Frequencies and Damping  
Based on Transfer Function Computations

Test	Type				
011	Random				
3010	1/3 level swept sine, 4 oct/min				
3031	Full level swept sine, 4 oct/min				
3069	High level random				
3071	Direct transient				
Test	011	3010	3031	3069	3071
f <sub>1</sub> Hz	7.28	7.04	6.81	7.05	6.93
ξ <sub>1</sub> %	0.64	1.84	1.32	1.35	1.34
f <sub>2</sub> Hz	14.38	14.26	13.97	14.46	*
ξ <sub>2</sub> %	0.90	1.73	2.65	1.06	
f <sub>3</sub> Hz	14.95	14.79	14.68	14.73	*
ξ <sub>3</sub> %	0.51	1.34	4.07	1.48	
f <sub>4</sub> Hz	20.29	20.10	19.75	19.93	19.95
ξ <sub>4</sub> %	0.67	0.82	1.88	1.54	1.12

\*Insufficient energy in the frequency region for all measurement locations.

the input to response coherence was also poor. For future use of this type analysis, the low level random test will yield frequencies and

mode shapes that are representative of that amplitude, but the damping value cannot be used in a projection to high amplitude loadings.

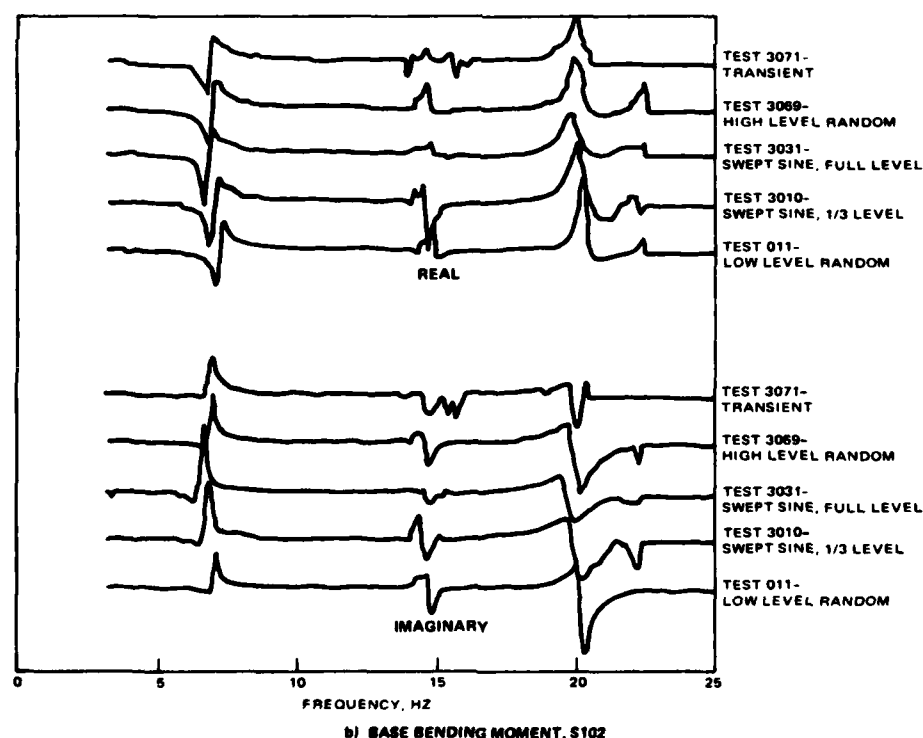
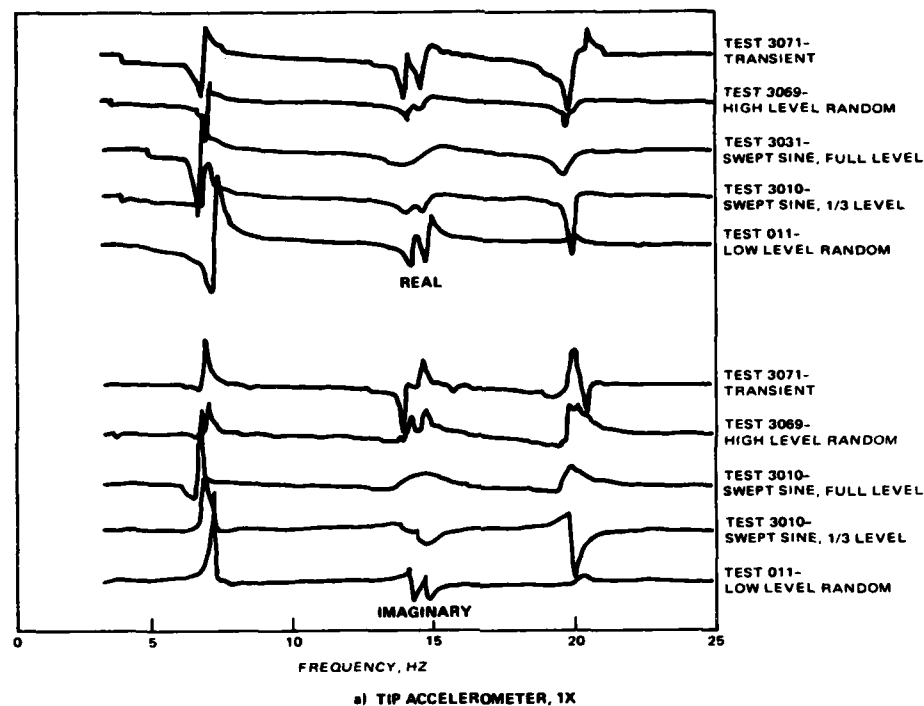


FIG. 8-INTELSAT IVA Y-1 SPACECRAFT TRANSFER FUNCTIONS

# Mass, Stiffness, and Damping Matrix Computation

During a recent spacecraft program, the vibration test frequencies and analytically predicted frequencies were considerably different. To save time and money, it was decided to use high level random vibration test data to develop transfer functions and, from those, the associated mass and stiffness matrices. The transfer functions were computed using the qualification level random test data supplied to Dr. Mark Richardson of Hewlett-Packard for computation of the matrices as described in Ref. 2. Table 2 lists the modal data using this procedure. Currently, the matrix computation program is not commercially available. Fig. 9 shows a view of the spacecraft and the accelerometers used. The available accelerometer data were reviewed and several were selected to be representative of motion of major masses of the spacecraft. The transfer functions relative to the shaker armature current were computed using band selectable Fourier analysis. The modal data and the mass and stiffness matrix were computed. It was necessary to adjust

the mass matrix to remove the shaker armature and fixture weights and also to develop a free stiffness matrix. The resulting stiffness matrix, Table 3, was checked by applying loads that had been applied to the structure during static tests. There was a 13 percent difference in the computed deflection and the measured deflection from the static test which was a considerable improvement over the original analytic model.

TABLE 3  
Mass and Stiffness Matrices

M =	$\begin{bmatrix} 674.8 & -21.8 & 20.79 \\ -21.8 & 1134 & -352.2 \\ 20.79 & -352.2 & 901.7 \end{bmatrix} \times \frac{1}{386}$
K =	$\begin{bmatrix} 9.1923 & 0.02949 & -9.22179 \\ 0.02949 & 5.8077 & -5.83719 \\ -9.22179 & -5.83719 & 15.05898 \end{bmatrix} \times 10^4$

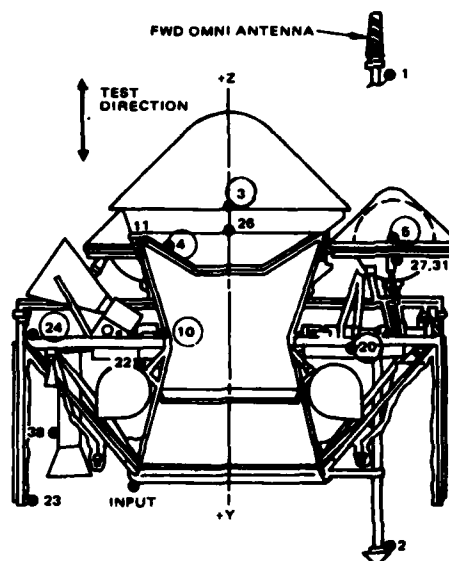


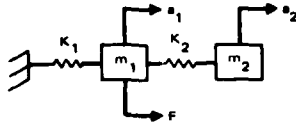
FIG. 9-PIONEER VENUS ACCELEROMETER LOCATIONS DATA USED FOR MASS AND STIFFNESS COMPUTATIONS

TABLE 2  
Modal Fit Data Used in Computing Mass and Stiffness Matrices (Hewlett-Packard Data)

Average Modal Frequencies and Damping						
Mode	Matrix Frequency (Hz)		Damping Factor (%)		Damping Coefficient (rad/sec)	
1	7.0342		9.5630		4.2480	
2	24.1202		0.7577		1.1484	
3	40.7786		3.1479		8.0695	
Amplitude Units, g/lb-sec						
	Mode 1		Mode 2		Mode 3	
	Amplitude	Phase	Amplitude	Phase	Amplitude	Phase
1	0.1060E-01	17.1	0.8810E-02	354.3	0.7951E-01	176.4
2	0.1142E-01	18.1	0.2703E-01	173.8	0.0000E+00	.0
3	0.1142E-01	18.1	0.2401E-01	172.3	0.6139E-02	158.6
4	0.1180E-01	15.9	0.2313E-01	173.2	0.2417E-02	217.4
5	0.5702E-03	183.8	0.5287E-03	175.8	0.1052E-02	168.7
6	0.8714E-02	11.3	0.3758E-02	168.1	0.4800E-02	201.7
7	0.1077E-01	17.1	0.4898E-02	355.6	0.1990E-01	348.9

### Alternate References for Transfer Functions

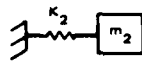
When transfer functions are computed for complex structural systems, care must be exercised in the selection of measurements which will reveal the desired information from the test. For the simple system shown



excited by  $F(t)$  it is possible to construct the transfer functions in the following ways to produce the modal sets shown.

$H(\frac{a_1}{F})$  and  $H(\frac{a_2}{F})$  will yield the frequencies and modes for the complete system.

$H(\frac{a_2}{a_1})$  will yield the frequency and mode for  $K_2, M_2$ , i. e.,



there will be only one frequency in this  $H(\omega)$ .

In each of these cases, the result has the effect on the system of setting the reference measurement used for the transfer function to zero. A common example of the above is the use of a sting shaker for modal testing. When the accelerometer response to force input transfer functions is used, the mass of the shaker armature and the armature flexures are not

part of the system. Note that if armature voice coil current is used, it is part of the system and will affect the results. With this introductory discussion, it is possible to consider the various possibilities used for reference points during spacecraft testing.

When a complete spacecraft is mounted on a slip table and shaker excited in the lateral axis, there are several choices for the transfer function reference. The following methods list the reference and the resulting set of modes.

1) Shaker voice coil current (proportional to force input). As stated, this has the effect of a zero force input; the modal set includes the first mode of the armature and spacecraft on the armature flexures. It is not particularly useful since the armature and flexure dynamics are not well known and therefore difficult to separate from spacecraft dynamics.

2) Base acceleration. This fixes the base lateral motion (sets it to zero) and since the slip table restrains rotation, the resulting modes are base fixed (cantilever). Base acceleration is the method used for base fixed modal studies done in conjunction with a qualification vibration test. Where several base (control) accelerometers are available, transfer functions between them can show the frequency where they are in phase and therefore the upper useful frequency of this method. Fig. 10 compares transfer functions for Intelsat IVA data using the base acceleration reference and the armature current reference. Note that there appears to be an additional mode at 6 Hz and that the higher frequency modes are shifted slightly due to the difference in the structural system that each represents.

For an axial vibration test on NASD Japan's Geostationary Meteorological Satellite program, the transfer functions referenced to

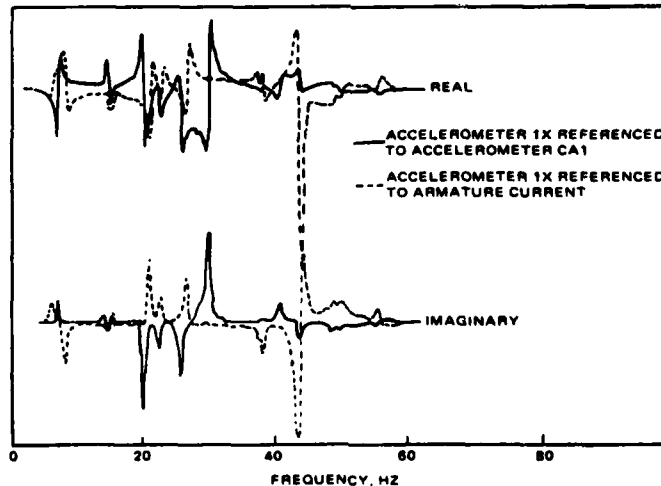


FIG. 10. COMPARISON OF TRANSFER FUNCTION USING TWO DIFFERENT REFERENCES

an intermediate spacecraft location were useful in determining a local resonant frequency. The shelf resonance was obtained by using shelf attach point accelerometer 14Z to edge accelerometer 20Z transfer functions. The resulting shelf frequency (56 Hz) is not apparent in either of the base referenced transfer functions (see Figures 11 and 12) as expected since they represent a different (base fixed) structural system.

Care has to be taken in order that the motion of the reference point is well known to avoid misleading conclusions. Many times the base of a structure will both translate and rotate making this base fixed approach incorrect since the input due to the rotation cannot be accounted for in the transfer function.

#### Failure Detection

During spacecraft qualification tests at Hughes, in each test axis, a low level random test was run prior to the first qualification test and another at the end of all testing in that axis. These two tests are analyzed for transfer functions and overplotted to detect any structural changes. During the Intelsat IVA test discussed above, a debonding of a portion of the lower feed structure occurred and the resulting shift in frequencies is shown in Fig. 13. That structure was repaired and the two fits of transfer functions prior to the test and following repair are shown in Fig. 14, indicating a successful complete repair. In several cases this valuable technique indicated a structural problem that was detected only after extensive examination by the inspectors.

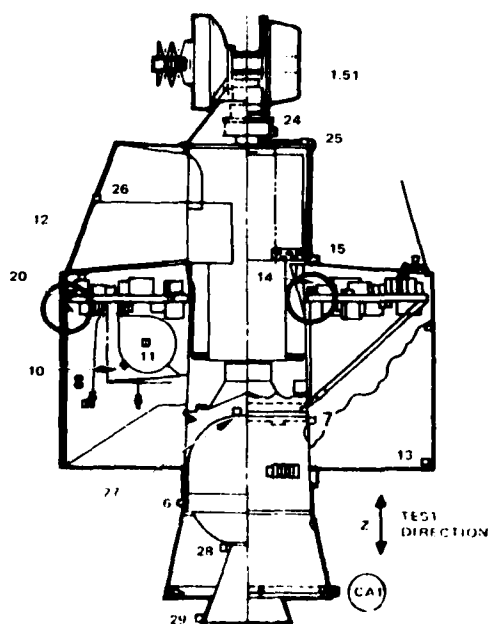


FIG. 11-GMS SPACECRAFT ACCELEROMETER LOCATIONS

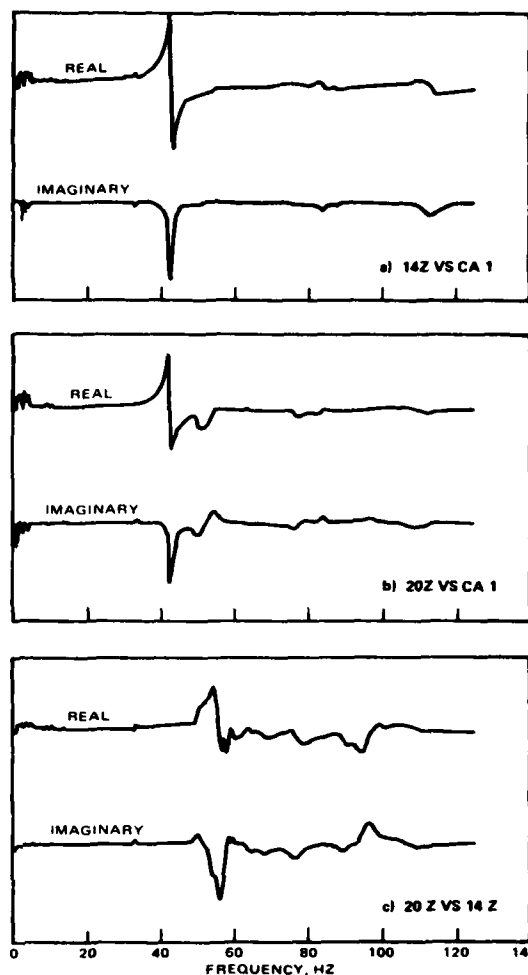


FIG. 12-GMS TRANSFER FUNCTION

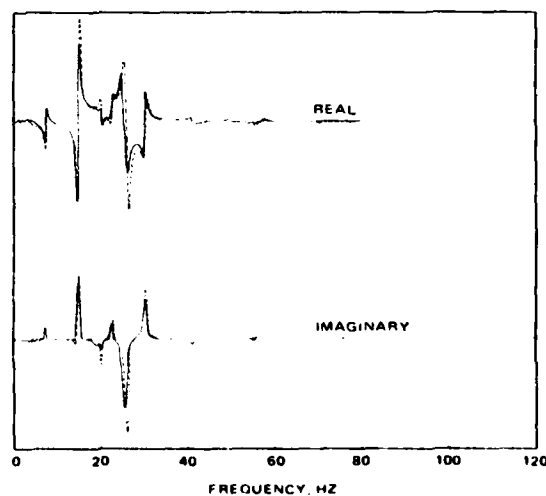


FIG. 13-RANDOM EXCITATION TRANSFER FUNCTION ILLUSTRATING FREQUENCY SHIFT CAUSED BY STRUCTURAL FAILURE TEST 011 VERSUS TEST 012

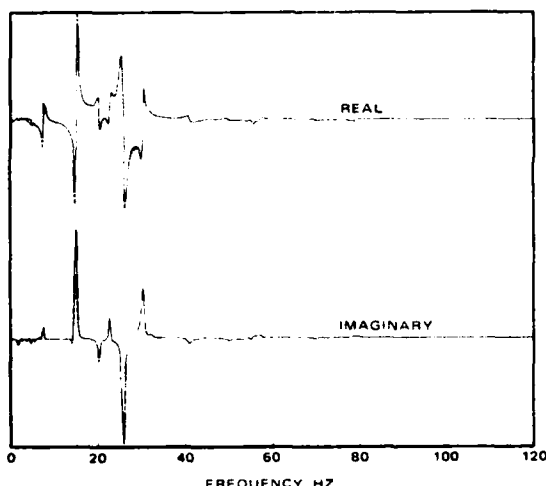


FIG. 14—RANDOM EXCITATION TRANSFER FUNCTION ILLUSTRATING FREQUENCY AGREEMENT FOLLOWING SPACECRAFT REPAIR TEST 011 VERSUS TEST 013

### Summary

- Band selectable Fourier analysis is an important extension in measuring transfer functions of dynamic systems. It is particularly useful when computing transfer functions for systems that have been excited using swept sine or transient signals.
- For the Intelsat IVA spacecraft, the higher level excitations produced lower modal frequencies and higher damping.
- The use of transfer functions computed from a low level random test before and after high level testing is a very effective quality control tool.
- The use of available vibration test data to develop a simple dynamic model for use in analytical analyses has been demonstrated. That technique could prove powerful in understanding the behavior of dynamic systems by providing test based mass and stiffness matrices.
- Use of alternate reference points for computing transfer functions has proved very useful in revealing structural dynamic information. Often the information, such as a local component or structural resonance, is not apparent until that approach is used.

### References

1. J.R. Fowler, D.T. DesForges, and R.J. Zuziak, Hughes Aircraft Company, and P.R. Schrantz, COMSAT Laboratories, "Alternatives to Notched Swept Sine Testings for Spacecraft and Other Large Systems," Proceedings, Institute of Environmental Sciences, April 1977.
2. Ron Potter and Mark Richardson, Hewlett-Packard Company, "Mass, Stiffness and Damping Matrices From Measured Modal Parameters," Instrument Society of America Paper 74-630.

### APPENDIX

Calculations of transfer functions from long time records, such as sine sweeps, can be accomplished in several ways.

The method employed to calculate the transfer functions shown in this paper involves band selectable or "zoom" transforms. Normally resolution is increased when the zoom transform is used; in this situation information spreading caused by the filtering of the zoom algorithms is taken advantage of.

A baseband measurement on a sine sweep will yield only a portion of the transfer function. This occurs because of the limit imposed by block sizes available, in combination with the sweeping input. That is, the total transfer function is made up from a number of averages from blocks taken as the sweep takes place. Windowing must be applied to each of the blocks. This windowing can cause voids in the spectral estimates in the composite (averaged) power spectra, and leads to unsatisfactory transfer functions.

Using zoom techniques, these voids become dips whose effects are divided out in the transfer function calculations. The reason this happens is the filtering that occurs in the zoom process. Information is spread over more sample points by the filtering, so that when the window is applied the information is not lost, only diminished. Parameters that can be controlled are the frequencies displayed, the sampling frequency, and the number of averages. The sampling frequency can be adjusted to give any desired information spreading (within the bounds of the ability to store data points). The idea here is to oversample the data stream, to provide more data points. Ultimately the investigator should overlap process the sweeps, in which case even better results are obtained.

LOAD TRANSFORMATION DEVELOPMENT CONSISTENT  
WITH MODAL SYNTHESIS TECHNIQUES

R. F. Hruda and P. J. Jones  
Martin Marietta Corporation  
Denver, Colorado

A method is presented for the development of component internal load transformations consistent with modal synthesis procedures. The resulting load transformations account for component interactions across statically indeterminate interfaces. A unique approach of obtaining these transformations is presented which, for large systems, would be more economical than the more laborious obvious techniques usually employed. Further, a modified modal coupling procedure is employed which offers advantages over previous techniques.

INTRODUCTION

An accepted practice used in developing structural dynamic models is to form modal data for components and subsequently use modal synthesis techniques to develop modal data of the total system. This practice is applied to complicated structures subjected to transient loading conditions where the final desired product often is internal structural loads. Detailed treatment of various techniques of modal coupling have been published, but development of consistent load transformations has generally been lacking.

This paper presents methodology for development of internal load transformations for a component that can be used with any inertial modal coupling technique. A variation of generally accepted modal coupling techniques of components with redundant interfaces is also discussed. Utilization of the subject load transformations in structural response analyses employing the coupled modal properties produce loads results exactly the same as if the total system was modeled as one structure. The unique feature of this development is that, for the individual component, no knowledge of the adjoining component is required other than geometry of the interfaces. The load transformation for the component is developed relative to: 1) interface deflections, and 2) unit loads applied to the component with fixed interfaces. Through the transformation developed in the

modal coupling procedure, the resulting load transformations are then expressed in terms of inertial loads (accelerations) which can then be utilized in a transient response analysis accounting for effects of adjoining structure through redundant interfaces.

Formation of the load transformation using finite element techniques is examined and two methods of development are presented, one being unique in that by-products of the development are required matrices for modal synthesis techniques. Development of related equations is detailed. An example case is presented for a transient response analysis comparing exact results obtained from a model and load transformation of a total system to results obtained using the subject component load transformations and modal synthesis techniques. Effects of modal truncation on loads results is also noted.

The versatility of the proposed method is obvious relative to the application to a loads analyses of a spacecraft that must be compatible with several boost vehicle systems. Redundant structural interfaces between spacecraft and booster in the past have been treated by either simplification using an approximation of a determinate interface and neglecting the interface feedback effects on loads, or by developing spacecraft load transformations utilizing structural compliance of the booster at the interfaces. The latter approach while offering a reasonable approximation of the

actual loading situation has a disadvantage in that the spacecraft model and load transformation become booster dependent requiring separate models for each booster vehicle considered. The proposed load transformation method offers significant advantages since it is mathematically correct and eliminates booster dependence.

#### MODAL COUPLING AND LOAD TRANSFORMATIONS

It is assumed that a large structural analysis is to be performed such that some technique of modal coupling is required. An elementary member loads equation is written as

$$\{L\} = [k\psi] \{h_B\} \quad (1)$$

where  $k$  = finite element stiffness kernel,  
 $\psi$  = geometric compatibility transformation  
 $h_B$  = discrete displacements of the composite component

The loads equation is shown here to point out that the basic data required to obtain loads (once the finite elemental stiffnesses have been defined) is an accurate definition of the displacements. The definition of the displacements is a function of the technique of the modal coupling.

Consider, as an example, two components, A and B, as shown in Figure 1, which could be thought of as a booster (component-A) and a payload (component-B).

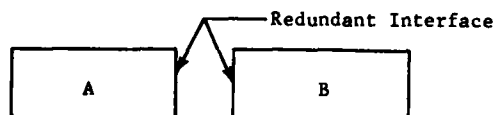


Figure 1. Components A and B

To obtain payload member loads via equation (1), an accurate definition of  $h_B$  must now be developed. For the two independent components, we may write

$$\begin{bmatrix} M_A \\ M_B \end{bmatrix} \begin{Bmatrix} \ddot{h}_A \\ \ddot{h}_B \end{Bmatrix} + \begin{bmatrix} K_A \\ K_B \end{bmatrix} \begin{Bmatrix} h_A \\ h_B \end{Bmatrix} = \begin{Bmatrix} F_A \\ F_B \end{Bmatrix} \quad (2)$$

where  $M$  = mass matrix,

$K$  = stiffness matrix,

$F$  = externally applied forces, and

$h$  = total discrete motion (displacement).

It is now desired to tie A and B together at the A/B interface. An inertial coupling technique is chosen to accomplish this as follows.

$$1. \text{ Let } h_A = I_A \bar{h}_A + T_A h_A I/F$$

$$\text{and } h_B = I_B \bar{h}_B + T_B h_B I/F$$

where typically,

$$\begin{bmatrix} I_A \\ I_B \end{bmatrix} = \begin{bmatrix} I \\ 0 \end{bmatrix} \begin{cases} \text{non-interface dofs} \\ \text{interface dofs} \end{cases}$$

$\bar{h}_B$  = non-interface relative (to interface) motion

$T_B$  = constraint modes (Ref. 1)

$$2. \text{ Tie A and B together via constraint equation}$$

$$\{h_B I/F\} = \{h_A I/F\} = \{h_I\} \quad (3)$$

Combining steps 1 and 2 into matrix form:

$$\begin{Bmatrix} h_A \\ h_B \end{Bmatrix} = \begin{bmatrix} T_A & I_A \\ T_B & I_B \end{bmatrix} \begin{Bmatrix} \bar{h}_A \\ \bar{h}_B \end{Bmatrix} \quad (4)$$

Substituting (4) into (2) and premultiplying by (4)-transposed yields inertially coupled equations of motion

$$\begin{bmatrix} T_A^T M_A T_A + T_B^T M_B T_B & T_A^T M_A I_A & T_B^T M_B I_B \\ I_A^T M_A T_A & I_A^T M_A I_A & 0 \\ I_B^T M_B T_B & 0 & I_B^T M_B I_B \end{bmatrix} \begin{Bmatrix} \ddot{h}_I \\ \ddot{h}_A \\ \ddot{h}_B \end{Bmatrix} + \begin{bmatrix} T_A^T K_A T_A + T_B^T K_B T_B & T_A^T K_A I_A & T_B^T K_B I_B \\ I_A^T K_A T_A & I_A^T K_A I_A & 0 \\ I_B^T K_B T_B & 0 & I_B^T K_B I_B \end{bmatrix} \begin{Bmatrix} h_I \\ h_A \\ h_B \end{Bmatrix} = \begin{Bmatrix} T_A^T F_A + T_B^T F_B \\ I_A^T F_A \\ I_B^T F_B \end{Bmatrix} \quad (5)$$

Next, use the bottom row of (5) to obtain an expression for  $\bar{h}_B$ .



$$\begin{aligned} \left[ \bar{h}_B \right] &= \underbrace{\left[ I_B^T K_B I_B \right]^{-1}}_{E_B} * \\ &\left( \left\{ \begin{array}{c} \ddot{h}_I \\ \ddot{h}_B \end{array} \right\} - \left[ \begin{array}{c|c} I_B^T M_B T_B & I_B^T M_B I_B \end{array} \right] \left\{ \begin{array}{c} \ddot{h}_I \\ \ddot{h}_B \end{array} \right\} \right) \\ &\equiv 0 \end{aligned} \quad (6)$$

or

$$\bar{h}_B = - E_B I_B^T M_B I_B \ddot{h}_B - E_B I_B^T M_B T_B \ddot{h}_I \quad (7)$$

Assuming there exists a set of normal elastic modes (constrained at the interface) for component B,

$$\ddot{h}_B = \phi_B \ddot{\xi}_B \quad (8)$$

Substituting equation (8) into (7) yields

$$\bar{h}_B = - \left[ E_B I_B^T M_B \right] \left[ \begin{array}{c|c} I_B \phi_B & T_B \end{array} \right] \left\{ \begin{array}{c} \ddot{\xi}_B \\ \ddot{h}_I \end{array} \right\} \quad (9)$$

Now equation (1) may be expanded by first substituting the second row of equation (4) into (1)

$$\left\{ L \right\} = \left[ k \psi \right] \left[ I_B \right] \left\{ \bar{h}_B \right\} + \left[ k \psi \right] \left[ T_B \right] \left\{ h_I \right\} \quad (10)$$

and then substituting equation (9) into (10),

$$\begin{aligned} \left\{ L \right\} &= \left[ k \psi \right] \left[ I_B \right] \left[ E_B \right] \left[ I_B^T \right] \left[ -M_B \right] \left( \left[ I_B \right] \left[ \phi_B \right] \left[ T_B \right] \right) \left\{ \begin{array}{c} \ddot{\xi}_B \\ \ddot{h}_I \end{array} \right\} \\ &+ \left[ k \psi \right] \left[ T_B \right] \left\{ h_I \right\} \end{aligned} \quad (11)$$

$$= \left[ LT1 \right] \left\{ \begin{array}{c} \ddot{\xi}_B \\ \ddot{h}_I \end{array} \right\} + \left[ LT2 \right] \left\{ h_I \right\} \quad (12)$$

Equation (5) could now be used to obtain an expression for  $h_I$  in terms of applied forces and accelerations (similar to what was done for  $h_B$  in equation (7)), however, expansion of  $h_I$  is superfluous for this discussion; suffice to point out that  $h_I$  will in fact be written in terms of applied forces and system accelerations and will not be left as a displacement term. So, in equation (12) let

$$\left\{ h_I \right\} = f(F, \ddot{h})$$

and finally, equation (12) may be written as

$$\left\{ L \right\} = \left[ LT1 \right] \left\{ \begin{array}{c} \ddot{\xi}_B \\ \ddot{h}_I \end{array} \right\} + \left[ LT2 \right] * f(F, \ddot{h}) \quad (13)$$

Equation (13) satisfies the formation of a loads equation/transformation. However, to complete this section, more discussion on "modal" coupling is in order.

Equation (5) represents the discretely coupled equations of motion of the system. To switch to a modally coupled equation, the following expression may be used.

$$\left\{ \begin{array}{c} h_I \\ \bar{h}_A \\ \bar{h}_B \end{array} \right\} = \left[ \begin{array}{c|c|c} \phi_I & & \\ & \phi_A & \\ & & \phi_B \end{array} \right] \left\{ \begin{array}{c} \xi_I \\ \xi_A \\ \xi_B \end{array} \right\} \quad (14)$$

where  $\phi_A$  = cantilevered modes of component-A, based on  $\bar{M}_A = I_A^T M_A I_A$  and

$$\bar{K}_A = I_A^T K_A I_A$$

$\phi_B$  = cantilevered modes of component-B, based on  $\bar{M}_B = I_B^T M_B I_B$  and

$$\bar{K}_B = I_B^T K_B I_B$$

$\phi_I$  = free-free\* modes of total composite system reduced to the interface dofs, based on

$$M_I = T_A^T M_A T_A + T_B^T M_B T_B, \text{ and}$$

$$K_I = T_A^T K_A T_A + T_B^T K_B T_B$$

\*Note - if either component-A or component-B is in reality constrained to ground at dofs other than I/F dofs, then the modes,  $\phi_I$ , will reflect the composite structure constraint (i.e.,  $\phi_I$  will be constrained modes). It should be noted that if the composite system is free-free, then  $\phi_I$  contains the rigid body modes. If the interface is determinant, then  $K_I = 0$ , and  $M_I$  is simply a rigid body mass matrix, and  $\phi_I$  is only rigid body modes. Substituting (14) into (5) and premultiplying by (14) transposed yields the inertially modal coupled equations of motion,

$$\begin{aligned} &\left[ \begin{array}{c|c|c} I & \phi_I^T T_A^T M_A T_A \phi_A & \phi_I^T T_B^T M_B T_B \phi_B \\ \phi_A^T T_A^T M_A T_A \phi_I & I & \\ \phi_B^T T_B^T M_B T_B \phi_I & & I \end{array} \right] \left\{ \begin{array}{c} \ddot{\xi}_I \\ \ddot{\xi}_A \\ \ddot{\xi}_B \end{array} \right\} \\ &+ \left[ \begin{array}{c|c|c} \omega_I^2 & & \\ & \omega_A^2 & \\ & & \omega_B^2 \end{array} \right] \left\{ \begin{array}{c} \xi_I \\ \xi_A \\ \xi_B \end{array} \right\} = \left\{ \begin{array}{c} \phi_I^T (T_A^T F_A + T_B^T F_B) \\ \phi_A^T F_A \\ \phi_B^T F_B \end{array} \right\} \end{aligned} \quad (15)$$

Equation (15) may be used in the form shown for further transient analyses, or the modal mass and stiffness coefficients may be used in another eigensolution to form

$$\begin{Bmatrix} \epsilon_I \\ \epsilon_A \\ \epsilon_B \end{Bmatrix} = [\phi_C] \begin{Bmatrix} \epsilon_C \end{Bmatrix} \quad (16)$$

Equation (16) may now be substituted into (15), then premultiplied through by (16) transposed to yield diagonal coefficient equations of motion of the form

$$\begin{Bmatrix} I \\ \phi_C^T \end{Bmatrix} \begin{Bmatrix} \epsilon_C \\ \omega_C^2 \end{Bmatrix} \begin{Bmatrix} \epsilon_C \end{Bmatrix} = \begin{Bmatrix} \phi_I^T (T_{FA}^T + T_{FB}^T) \\ \phi_{FA}^T \\ \phi_{FB}^T \end{Bmatrix} \quad (17)$$

A damping term may be included in the above equation using generally accepted practices.

#### UNIT LOAD SOLUTION

The procedure outlined for development of the load transformations in equation (11) involves direct matrix multiplication which can be cumbersome for large matrices. An alternate approach is available through a unit load solution, which is a feature of most finite element programs. Examining the terms of equation (11) reveals that

$$[K\psi] \begin{Bmatrix} I_B \\ E_B \end{Bmatrix} \begin{Bmatrix} I_B^T \end{Bmatrix} \quad (18)$$

is actually a coefficient matrix which yields member loads due to inertial and/or applied forces on component B with a fixed interface. This portion of the overall LT1 transformation is often a most cumbersome matrix to form due to potentially very large payload models now being generated. However, as an alternate to the explicit formation of  $K\psi E_B$ , a unit load solution can be employed. Applying unit loads successively to each of the non-interface degrees-of-freedom, yields a column of the transformation for each unit load.  $M_B$  and  $\phi_B$  are readily available, however  $T_B$  (the constraint modes) and the other coefficient of equation (11) LT2 or

$$[K\psi] \begin{Bmatrix} T_B \end{Bmatrix} \quad (19)$$

are, again, somewhat cumbersome to form. Expression (19) represents member loads due to unit interface displacements. This portion may be formed by applying unit loads to each of the degrees-of-freedom of the interface, one at a time, each time with the other interface degrees-of-freedom being fixed. For each applied unit load, a column in the above matrix is formed which can be normalized to unit deflection at the interface. Another feature of the unit load solution in this application is that in addition to formation of the load transformation, the constraint modes matrix  $T_B$  is obtained as a by-product. Each column of  $T_B$  is the displacement at each non-interface degree-of-freedom for a unit interface deflection. This matrix is also required for modal coupling as discussed previously and again direct formation requires large matrix inversions and multiplications.

#### EXAMPLE PROBLEM

The subject load transformation methodology was used with the modal coupling procedure on the component models of an example problem shown in Figure 2.

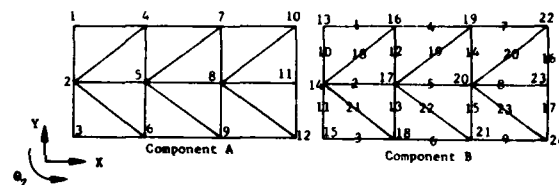


FIGURE 2. COMPONENT MODELS FOR EXAMPLE PROBLEM

An "exact solution" for comparison was obtained using the total system model as shown in Figure 3.

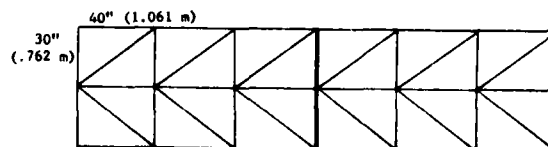


FIGURE 3. TOTAL SYSTEM FOR EXAMPLE PROBLEM

Component B represents a payload while component A represents a boost vehicle. The redundant interface is indicated at joints 10/13, 11/14, 12/15. Pinned jointed trusses with 2 degrees-of-freedom at each joint were used. The truss members were assigned axial stiffness of 40 lbs/in. (7000 N/m). Mass of 0.10 lbs sec<sup>2</sup>/in. (17.5 Kg) was assigned to joints 7, 8, 10 and 11 and 0.01 lbs sec<sup>2</sup>/in. (1.75 Kg) to all other joints.

#### Load Transformation for Component B Using Unit Load Solution

The inertial load dependent portion of the

component B load transformation (expression (18)) was formed using unit load solutions with the interface joints 13, 14 and 15 fixed in all degrees-of-freedom. Figure 4 shows structural deflections and member loads for typical unit load applications. The displacement dependent portion of the component B load transformation (expression (19)) was formed using unit load solutions with the results normalized to unit interface displacements. For each of these load conditions all interface degrees-of-freedom were restrained except for the degree-of-freedom where the unit load was applied. Continuing this procedure for all interface degrees-of-freedom completes the load transformation. Figure 5 shows structural deflec-

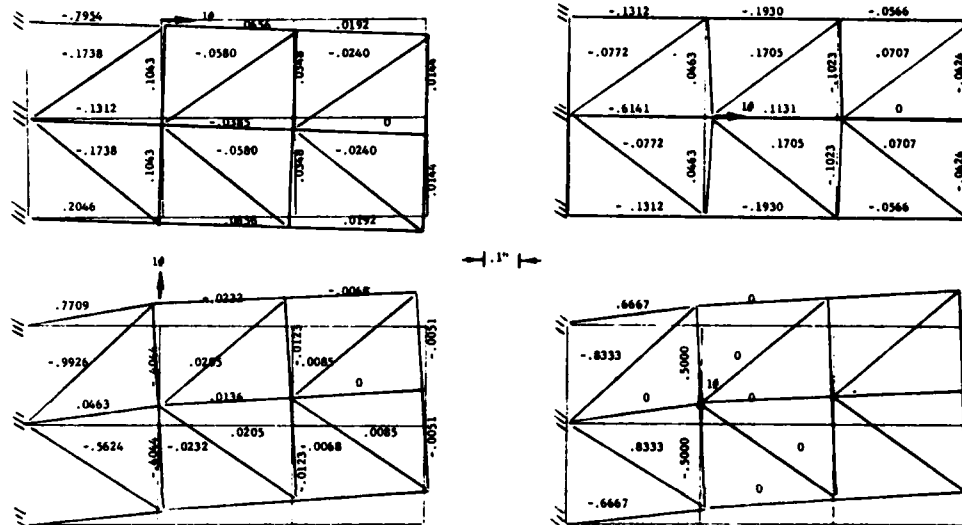


FIGURE 4 - TYPICAL STRUCTURAL DEFLECTIONS/MEMBER LOADS FOR UNIT APPLIED LOADS

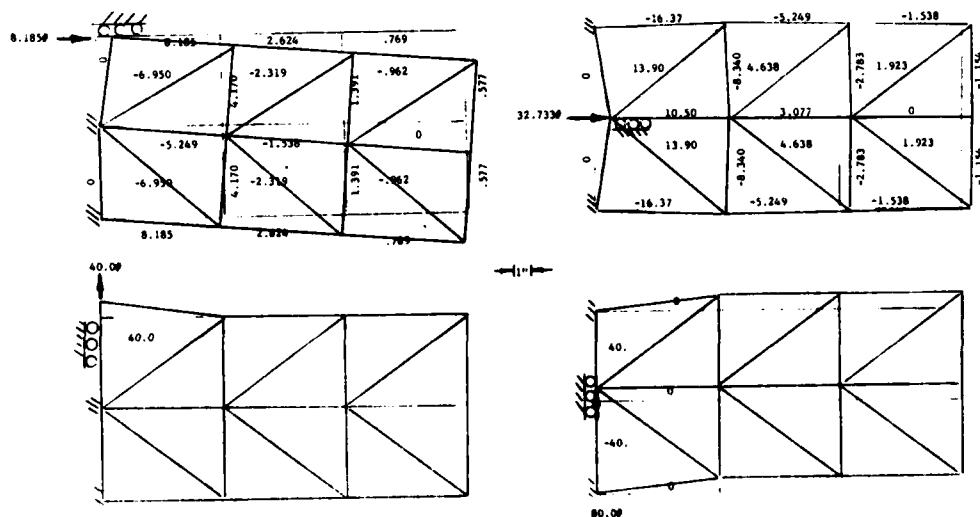


FIGURE 5 - TYPICAL STRUCTURAL DEFLECTIONS/MEMBER LOADS FOR UNIT INTERFACE DEFLECTION

tions and member loads for the unit interface deflection cases. The deflected shapes shown, as previously indicated, represents the constraint modes of component B.

#### Transient Response Analysis and Loads Comparison

A transient response analysis was conducted on the combined system (Figure 2) to affect an "exact solution".

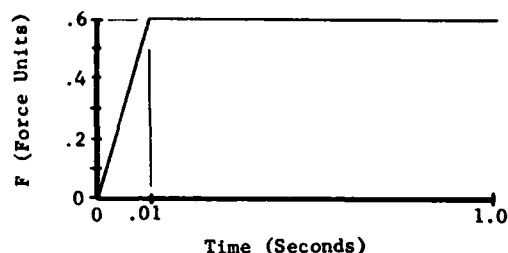


FIGURE 6. FORCING FUNCTION

The force time history shown in Figure 6 was applied to the X degree-of-freedom at joint 2 on component A to simulate a booster thrust transient condition.

For the "exact solution" composite system free-free stiffness and mass matrices,  $K_{AB}$  and  $M_{AB}$ , were obtained by discrete coupling of the component stiffness and mass matrices. Free-free modes,  $\phi_{AB}$ , and frequencies,  $\omega_{AB}^2$ , were generated using  $K_{AB}$  and  $M_{AB}$ . A transient analysis was then run using the form

$$\begin{bmatrix} I \end{bmatrix} \left\{ \ddot{\xi}_{AB}(t) \right\} + \begin{bmatrix} 0.2 \omega_{AB} \end{bmatrix} \left\{ \dot{\xi}_{AB}(t) \right\} + \begin{bmatrix} \omega_{AB}^2 \end{bmatrix} \left\{ \xi_{AB}(t) \right\} = \begin{bmatrix} \phi_{AB}^T \end{bmatrix} \left\{ F(t) \right\} \quad (20)$$

Note that all modes of the A/B system were kept in generating the above coefficient matrices. The member load time histories were then determined using the form

$$\begin{aligned} \left\{ L(t) \right\} &= \begin{bmatrix} K_B \end{bmatrix} \begin{bmatrix} \psi_B \end{bmatrix} \begin{bmatrix} E_{AB} \end{bmatrix} \left( \left\{ F(t) \right\} \right. \\ &\quad \left. - \begin{bmatrix} M_{AB} \end{bmatrix} \begin{bmatrix} \phi_{AB} \end{bmatrix} \left\{ \ddot{\xi}(t) \right\} \right) \end{aligned} \quad (21)$$

These "exact solution" results are tabulated in Table 1.

The modally coupled equations of motion were generated next. Referring to Figure 2,

the initial uncoupled equations of motion for component A and component B were written (see equation (2)). The two components were constrained at their interface dofs to obtain constrained modes and frequencies,  $\theta$  and  $\omega^2$ , and from the component free stiffness matrices, constraint modes,  $T$ , were obtained. Using  $K_I$  and  $M_I$  (see equation (14)),  $\theta_I$  and  $\omega_I^2$  were also obtained. Having this information, equations (4) and (14) were combined

$$\begin{Bmatrix} h_A \\ h_B \end{Bmatrix} = \begin{bmatrix} T_A \theta_I & I_A \theta_A \\ T_B \theta_I & I_B \theta_B \end{bmatrix} \begin{Bmatrix} \xi_I \\ \xi_A \\ \xi_B \end{Bmatrix} \quad (22)$$

and applied to equation (2) to form equation (15). The "modal modes" of equation (16) were then obtained and used to form the final modal equations of motion, including damping, rewritten here.

$$\begin{aligned} \begin{bmatrix} I \end{bmatrix} \left\{ \ddot{\xi}_C(t) \right\} + \begin{bmatrix} 2 \zeta \omega_C \end{bmatrix} \left\{ \dot{\xi}_C(t) \right\} + \begin{bmatrix} \omega_C^2 \end{bmatrix} \left\{ \xi_C(t) \right\} &= \begin{bmatrix} \phi_C^T \end{bmatrix} * \\ \begin{bmatrix} \phi_I^T & \phi_A^T & \phi_B^T \end{bmatrix} \begin{Bmatrix} T_A^T F_A(t) \\ F_A(t) \\ 0 \end{Bmatrix} \end{aligned} \quad (23)$$

(1% damping was assumed)

Note that the size of this modal system is dependent on the number of component modes (columns) kept in equations ((14) or (16)). Since modal truncation is known to affect the accuracy of the final results, member loads were calculated for two cases: 1) using all (42) available component modes to insure that any member load discrepancy from the exact solution was not a function of modal truncation, and 2) using only 30 modes (frequency cutoff at 15.0 Hz) to insure that the use of the subject loads transformations are not critically sensitive to modal truncation (as can be a modal displacement dependent loads transformation). Loads results are tabulated in Table 1 providing a comparison between the "exact solution" and the proposed load transformation methodology consistent with modal synthesis techniques.

TABLE 1.  
COMPARISON OF LARGEST VALUES OF  
MEMBER LOADS (FORCE UNITS)

Member No.	Exact Solution	Modal Synthesis Method	
		All (42) Modes	30 Modes
1*	.0956	.0956	.0950
2*	-.0597	-.0597	-.0581
3*	-.1919	-.1919	-.1990
4	.0811	.0811	.0812
5	-.0690	-.0690	-.0664
6	-.1232	-.1232	-.1238
7	-.0581	-.0581	-.0561
8	-.0667	-.0667	-.0647
9	-.1229	-.1229	-.1265
10*	.0825	.0825	.0824
11*	-.0666	-.0666	-.0674
12	-.0616	-.0616	-.0632
13	-.0766	-.0766	-.0722
14	.0457	.0457	.0477
15	-.0506	-.0506	-.0491
16	.0337	.0337	.0359
17	-.0314	-.0314	-.0298
18*	-.0656	-.0656	-.0677
19	-.0562	-.0562	-.0535
20	-.0602	-.0602	-.0557
21*	.0959	.0959	.0906
22	.0650	.0650	.0641
23	.0609	.0609	.0614

\* Members connected to interface joints (refer to Figure 2)

Examination of the Table 1 comparison shows that where all the modes are retained, precisely the same loads results are obtained with the proposed methodology as with the exact solution. Truncation of the modal information shows some minor deviation from the "exact results", consistent with normal expectations of modal coupling. The importance of the latter comparison is to show that the load transformation methodology results do not diverge as a result of modal truncation. This is to say that where large systems are involved which require modal synthesis, modal truncation is also required and minor errors are expected. The load transformation methodology does not represent a further compromise.

#### CONCLUSION

It should be noted that LT1 and LT2 of equation (13) can be formed by a payload developer without knowledge of the booster interface structure other than interface geometry. Further, due to the final form of LT1 and LT2, it does not matter whether or not there are more components with further redun-

dant load paths (eg., other booster stages) behind component A. Similarly, the booster developer can make changes to the interface properties for an evolving boost structure without impacting the payload model. Including the LT2 affects into the loads computations assures the additional payload loads due to applied and/or inertial loads on the lower structure, i.e., LT2 is a "feedback" term which potentially produces the additional loads.

Utilization of the modal coupling technique employing "interface modes" reduces the amount of work the booster contractor must do for each payload study by eliminating the requirement for "cascading" the effect of the payload and upper stages for conditioning of the uncoupled booster modal analyses (Reference 1). The interface modal information can be used even if the payload structure does not tie to all interface points or degrees-of-freedom. The effects of truncation of modes using the "interface" modal coupling method are still being investigated; especially for the case where degrees-of-freedom are not used by the adjoining structure.

#### REFERENCES

1. Benfield, W. A., and Hrudu, R. F., "Vibration Analysis of Structures by Component Mode Substitution", AIAA Journal, Vol. 9, No. 7, July, 1971, pages 1255-1261.

# REDUCED SYSTEM MODELS USING MODAL OSCILLATORS FOR SUBSYSTEMS (RATIONALLY NORMALIZED MODES)

F. H. Wolff and A. J. Molnar  
Westinghouse R&D Center  
Pittsburgh, PA 15235

This paper develops a method of using modal oscillators to represent complex structural subcomponents which can be applied to unidirectional models. It is shown that the oscillator mass must be the effective mass to guarantee the correct total system characteristics. Furthermore, when the modes are normalized in a specific way the effective mass and generalized or modal mass are identical.

## INTRODUCTION

Finite element methods using matrix techniques are being used extensively for dynamic analysis of complex structures. For linear elastic structures matrix reduction schemes and modal solutions using reduced numbers of modes are valuable methods for obtaining dynamic solutions of large mechanical systems. Many of these systems involve interaction between subcomponents which in themselves are quite complex.

This paper reviews and extends a method of reducing a class of complex structural subcomponents (unidirectional models) into modal oscillators which are dynamically equivalent to the subcomponent mode they represent. These oscillators can then be attached to the main structure to become part of the overall system model. If the overall system model is linear, reduction or modal methods can be repeated to further reduce the total system.

A brief review of applicable normal mode theory is presented which includes modal effective mass, unity participation factors, rationally normalized modes, restrictions, etc. Two illustrative examples are presented.

## DISCUSSION

The distinguishing feature of a normal mode is that the system can vibrate freely in that mode alone and during such vibration the ratio of the displacements of any two masses is constant with time. The ratios define the char-

acteristic shape of that mode. Since each mode can be arbitrarily multiplied by a constant, there are several normalizing schemes which are employed. For example, modes are often normalized such that the maximum amplitude in each mode is unity or sometimes the normalization is such that the generalized mass is unity. However, for these normalizing techniques the modal response ( $q$ ) has no physical significance. Furthermore, the mode shape amplitudes of two distinct modes relative to each other have no physical meaning.

F. J. Heymann [1] gave a terse treatment of "rationally normalizing" mode shapes. His work is extended in this paper to demonstrate that when modes are normalized such that participation factors are unity, a necessary and sufficient condition is established for "dynamic equivalence" between the modal oscillator and the physical mode it represents. That is, the energies (kinetic and strain), external work, momentum, and inertia reactions are preserved between the system response in a specific mode and the equivalent modal oscillator. This paper shows that if the modes are normalized such that the participation factors are unity the modal generalized mass is automatically the modal effective mass which satisfies the dynamic equivalence condition.

Modal oscillators are particularly convenient to use when only a few modes of vibration are required to describe the vibratory response of a structure or some subcomponent of the structure. For example, in seismic analysis usually the low frequency modes (0 to

30 Hz) are of concern, consequently, the higher frequency modes can be omitted. Also, in force excited systems where the location and nature of the externally applied forces are known only selected modes may be required.

An example is given where modal oscillators were used to represent the lateral vibration modes of steam turbine blades which are excited by torsional oscillations of the main rotor. Moreover, the mass of the oscillator (which must be the effective mass of the lateral modes calculated to a fixed base) is converted to the corresponding rotary inertia which is dependent upon the rigid body effects of the rotor radius. Finally a combined system torsional model is illustrated.

#### MODAL OSCILLATOR MODELS OF SUBCOMPONENTS

The use of modal oscillators to represent subcomponents is developed for a lumped parameter unidirectional model (Fig. 1A).

Following a modal transformation (assuming the subcomponent has a fixed support at A, Fig. 1A)

$$\{x^s\} = [\Phi^s] \{q^s\} \quad (1)$$

where

$\{x^s\} = \{x_j^s: j=1, N\}$  is the absolute displacement vector of the mass points of the subcomponent

$[\Phi^s] = [\phi_{j,a}^s: j=1, N \text{ \& } a=1, N]$  is the modal matrix

$\{q^s\} = \{q_a^s: a=1, N\}$  is the normal mode displacement vector

The equations of motion of subcomponent (s) can be written in terms of normal mode coordinates. For the  $a^{\text{th}}$  mode

$$MG_a^s \ddot{q}_a^s + KG_a^s q_a^s = FG_a^s + \left\{ (\omega_a^s)^2 \sum_{j=1}^N m_j^s (\phi_{j,a}^s) \right\} Z \quad (2)$$

where

$Z$  = the subcomponent connection (support) motion of point A,

$\ddot{q}_a^s$  = the subcomponent  $a^{\text{th}}$  modal acceleration,

$q_a^s$  = the subcomponent  $a^{\text{th}}$  modal displacement,

$\omega_a^s$  = the subcomponent  $a^{\text{th}}$  modal natural frequency,

$\phi_{j,a}^s$  = the amplitude of subcomponent mass point  $j$  in the  $a^{\text{th}}$  mode,

$MG_a^s = \sum_{j=1}^N m_j^s (\phi_{j,a}^s)^2$  = the  $a^{\text{th}}$  mode generalized mass,

$KG_a^s = (\omega_a^s)^2 MG_a^s$  = the  $a^{\text{th}}$  mode generalized stiffness,

$FG_a^s = \sum_{j=1}^N \phi_{j,a}^s F_j$  = the  $a^{\text{th}}$  mode generalized force.

The coefficient of the support motion ( $Z$ ) term can also be expressed as

$$(\omega_a^s)^2 \sum_{j=1}^N m_j^s \phi_{j,a}^s = (\omega_a^s)^2 MG_a^s P_a^s = P_a^s KG_a^s \quad (3)$$

where

$$P_a^s = \frac{\sum_{j=1}^N m_j^s \phi_{j,a}^s}{\sum_{j=1}^N m_j^s (\phi_{j,a}^s)^2} \quad (4)$$

is the participation factor for mode  $a$ . Therefore, Eq. (2) becomes

$$MG_a^s \ddot{q}_a^s + KG_a^s q_a^s = FG_a^s + KG_a^s P_a^s Z \quad (5)$$

In order for Eq. (5) to be the equation of motion of a modal oscillator the participation factor must be unity ( $P_a^s = 1.0$ ). This can be illustrated by examining the equation of motion for the system shown in Fig. 1B. In matrix form the equations are

$$\begin{bmatrix} M_1 & 0 & \dots & 0 \\ 0 & M_j & \dots & 0 \\ \vdots & \vdots & \ddots & \vdots \\ 0 & 0 & \dots & M_M \end{bmatrix} \begin{bmatrix} \ddots \\ \vdots \\ \vdots \\ \vdots \end{bmatrix} + \begin{bmatrix} 0 & 0 & \dots & 0 \\ 0 & 0 & \dots & 0 \\ \vdots & \vdots & \ddots & \vdots \\ 0 & 0 & \dots & 0 \end{bmatrix} \begin{bmatrix} X_1 \\ X_j \\ \vdots \\ X_M \end{bmatrix} + \begin{bmatrix} 0 & 0 & \dots & 0 \\ 0 & 0 & \dots & 0 \\ \vdots & \vdots & \ddots & \vdots \\ 0 & 0 & \dots & 0 \end{bmatrix} \begin{bmatrix} q_1^s \\ q_a^s \\ \vdots \\ q_N^s \end{bmatrix} = \begin{bmatrix} F_1 \\ F_j \\ \vdots \\ F_M \end{bmatrix} \quad (6)$$

$$\begin{bmatrix} K_1 + K_2 & -K_2 & \dots & 0 \\ -K_2 & K_2 + K_3 & \dots & 0 \\ \vdots & \vdots & \ddots & \vdots \\ 0 & 0 & \dots & K_M + \sum_{a=1}^N KG_a^s \end{bmatrix} \begin{bmatrix} X_1 \\ X_j \\ \vdots \\ X_M \end{bmatrix} + \begin{bmatrix} 0 & 0 & \dots & 0 \\ 0 & 0 & \dots & 0 \\ \vdots & \vdots & \ddots & \vdots \\ 0 & 0 & \dots & 0 \end{bmatrix} \begin{bmatrix} q_1^s \\ q_a^s \\ \vdots \\ q_N^s \end{bmatrix} = \begin{bmatrix} F_1 \\ F_j \\ \vdots \\ F_M \end{bmatrix} \quad (7)$$

Taking the equation (row) corresponding to the  $a^{\text{th}}$  mode of subcomponent (s) from Eq. (6).

$$MG_a^s \ddot{q}_a^s + KG_a^s \dot{q}_a^s = FG_a^s + KG_a^s x_m \quad (7)$$

Comparing Eq. (7) to Eq. (5) with the attachment constraint

$$x_m = Z$$

requires

$$KG_a^s = KG_a^s P_a^s$$

or

$$P_a^s = 1.0 \quad (8)$$

Also dividing Eq. (5) thru by  $P_a^s$  gives the equation of an oscillator whose coordinate is ( $q_a^s/P_a^s$ ); i.e.,  $1/P_a^s$  is in effect a scale factor for a modal oscillator. In cases where there is prescribed base motion the scaled modal oscillator equation gives the correct results; however, when the modal oscillator is attached

to another structure which is not scaled,  $P_a^s$  must be unity to obtain the proper total system model.

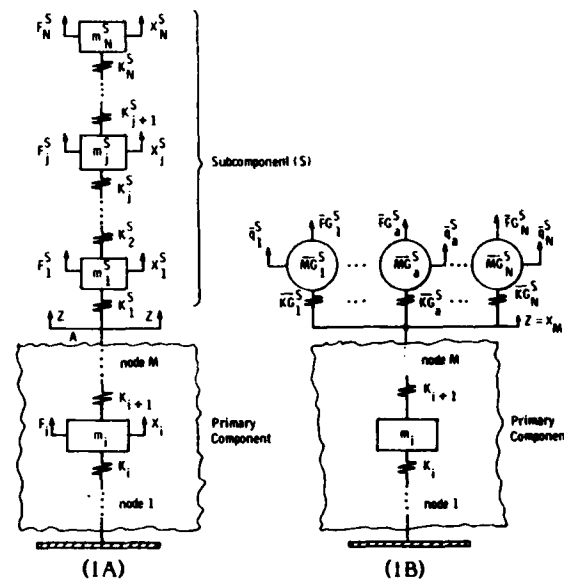


Fig. 1 - Unidirectional lumped parameter multi-degree-of-freedom system (1A) and "Dynamically Equivalent" model using modal oscillators for subcomponent (1B)

## RATIONAL NORMALIZATION OF NORMAL MODES

It can be shown that arbitrarily normalized mode shapes satisfy the eigenvalue problem [2]: however, in order to satisfy Eq. (8) ( $P_a^s = 1$ ) a normalizing factor  $\alpha_a^s$  is needed which will guarantee this condition. Consider newly scaled mode shapes

$$\bar{\phi}_{j,a}^s = \alpha_a^s \phi_{j,a}^s \quad (9)$$

The new participation factor becomes

$$P_a^s = \frac{\sum_{j=1}^N m_j^s \bar{\phi}_{j,a}^s}{\sum_{j=1}^N m_j^s (\bar{\phi}_{j,a}^s)^2} = \frac{\alpha_a^s \sum_{j=1}^N m_j^s \phi_{j,a}^s}{(\alpha_a^s)^2 \sum_{j=1}^N m_j^s (\phi_{j,a}^s)^2}$$



Applying condition (Eq. (8)) gives

$$\alpha_a^s = \frac{\sum_{j=1}^N m_j^s \phi_{j,a}^s}{\sum_{j=1}^N m_j^s (\phi_{j,a}^s)^2} = P_a^s \quad (10)$$

or the normalizing factor is the participation factor. The rationally normalized mode shapes become

$$\bar{\phi}_{j,a}^s = P_a^s \phi_{j,a}^s \quad (11)$$

The generalized mass corresponding to the rationally normalized mode shape is

$$\begin{aligned} \bar{M}G_a^s &= \sum_{j=1}^N m_j^s (\bar{\phi}_{j,a}^s)^2 = (P_a^s)^2 \sum_{j=1}^N m_j^s (\phi_{j,a}^s)^2 \\ &= \frac{\left( \sum_{j=1}^N m_j^s \phi_{j,a}^s \right)^2}{\sum_{j=1}^N m_j^s (\phi_{j,a}^s)^2} = ME_a^s \quad (12) \end{aligned}$$

which is the effective mass for mode a. Furthermore, the effective mass which is invariant

$$\begin{aligned} \bar{M}E_a^s &= \frac{\left( \sum_{j=1}^N m_j^s \bar{\phi}_{j,a}^s \right)^2}{\sum_{j=1}^N m_j^s (\bar{\phi}_{j,a}^s)^2} \\ &= \frac{(P_a^s)^2 \left( \sum_{j=1}^N m_j^s \phi_{j,a}^s \right)^2}{(P_a^s)^2 \sum_{j=1}^N m_j^s (\phi_{j,a}^s)^2} = ME_a^s \quad (13) \end{aligned}$$

has been shown by others [1, 3] to satisfy "dynamic equivalence" between an oscillator and the system in the mode the oscillator represents. Therefore, the modal oscillator

for mode (a) with effective mass and unity participation factor of subcomponent(s) is "dynamically equivalent" to mode (a) of subcomponent(s).

$$\bar{M}G_a^s \ddot{\bar{q}}_a^s + \bar{K}G_a^s \bar{q}_a^s = \bar{F}G_a^s + \bar{K}G_a^s Z \quad (14)$$

## SHOCK AND SEISMIC RESPONSE SPECTRA ANALYSES

For a system which is base excited only

$$Z = |Z| f(t) \quad (15)$$

with amplitude  $|z|$ , the equation of motion is

$$\bar{M}G_a^s \ddot{\bar{q}}_a^s + \bar{K}G_a^s \bar{q}_a^s = \bar{K}G_a^s Z = \bar{K}G_a^s |Z| f(t) \quad (16)$$

from which the static response is

$$\bar{q}_a^s (\text{static}) = |Z| \quad (17)$$

Therefore, the ratio of the static response of mass point is in any two modes u and v is identically the ratio of the rationally normalized mode shape amplitudes

$$\frac{x_{j,u} (\text{static})}{x_{j,v} (\text{static})} = \frac{\bar{\phi}_{j,u} \bar{q}_u (\text{static})}{\bar{\phi}_{j,v} \bar{q}_v (\text{static})} = \frac{\bar{\phi}_{j,u}}{\bar{\phi}_{j,v}} \quad (18)$$

because

$$\bar{q}_u (\text{static}) = \bar{q}_v (\text{static}) \quad (19)$$

In other words, the rationally normalized mode shapes determine the relative importance of the modes of vibration for the static response. Of course, for the total dynamic response the resonance or dynamic load factor must be included. However, when motion is suddenly applied to the base

$$Z(t) = \begin{cases} |Z| & \text{for } t > 0 \\ 0 & \text{for } t \leq 0 \end{cases} \quad (20)$$

The dynamic load factor [4] is 2 for all modes such that the rationally normalized mode shapes are the sole indication of what modes are important.

For a response spectrum analysis such as used in seismic calculation, the modal response can be read directly from the spectrum when the modes have been rationally normalized. This eliminates the need for using participation factors to evaluate important base

excited modes in shock or response spectra analyses; mode shape amplitudes and natural frequencies determine what modes are important.

# NUMERICAL EXAMPLE TO ILLUSTRATE EFFECTIVE MASS IS REQUIRED TO GIVE CORRECT OVERALL SYSTEM FREQUENCIES

The model of Fig. 2 is used to show that the effective mass is required to obtain the

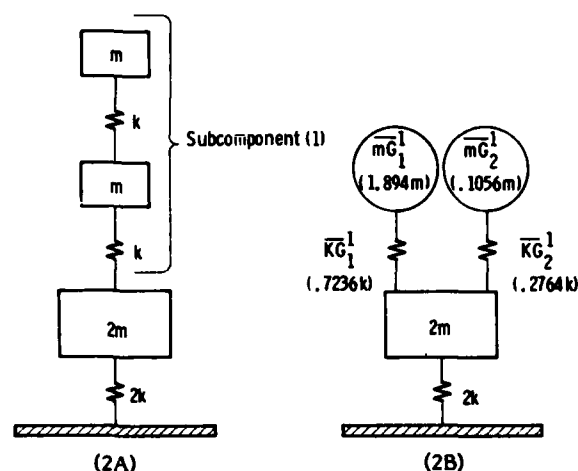


Fig. 2 - Model to illustrate effective mass (generalized mass with unity participation factor) is required to obtain correct system frequencies when modal oscillators represent subcomponent

correct overall system natural frequencies when a subcomponent is modeled with oscillators. The frequency equation for the two mass subcomponent of Fig. 2A is

$$\omega^4 - \frac{3k}{m} \omega^2 + \frac{k^2}{m^2} = 0 \quad (21)$$

which gives

$$\omega_1^2 = 0.382 \frac{k}{m}, \quad \omega_2^2 = 2.618 \frac{k}{m} \quad (22)$$

for the eigenvalues. One set of arbitrarily normalized mode shapes is

$$[\Phi] = \begin{bmatrix} 0.618 & -1.618 \\ 1.0 & 1.0 \end{bmatrix} \quad (23)$$

Therefore, the generalized parameters corresponding to mode shapes of Eq. (23) is

$$MG_1 = m((0.618)^2 + (1)^2) = 1.3819m;$$

$$KG_1 = 0.382 \frac{k}{m} 1.3819m = 0.5279k;$$

$$MG_2 = m((-1.618)^2 + (1)^2) = 3.6179m;$$

$$KG_2 = 2.618 \frac{k}{m} 3.6179m = 9.4717k;$$

$$P_1 = \frac{m(0.618 + 1)}{1.3819m} = 1.1708;$$

$$P_2 = \frac{m(-1.618 + 1)}{3.6179m} = -0.1708 \quad (24)$$

If the mode shapes are rationally normalized

$$[\bar{\Phi}] = \begin{bmatrix} P_1 \phi_{1,1} & P_2 \phi_{1,2} \\ P_1 \phi_{2,1} & P_2 \phi_{2,2} \end{bmatrix} = \begin{bmatrix} 0.7236 & 0.2764 \\ 1.1708 & -0.1708 \end{bmatrix}$$

the generalized parameters are

$$\bar{MG}_1 = m((0.7236)^2 + (1.1708)^2) = 1.8944m$$

$$= ME_1; \quad \bar{KG}_1 = 0.7236k;$$

$$\bar{MG}_2 = m((0.2764)^2 + (-0.1708)^2) = 0.1056m$$

$$= ME_2; \quad \bar{KG}_2 = 0.2764k;$$

$$\bar{P}_1 = \frac{m(0.7236 + 1.1708)}{1.8944m} = 1.0;$$

$$\bar{P}_2 = \frac{m(0.2764 - 0.1708)}{0.1056m} = 1.0 \quad (26)$$

The total system of Fig. 2A has the characteristic equation

$$\begin{vmatrix} 3k-2m\omega^2 & -k & 0 \\ -k & 2k-m\omega^2 & -k \\ 0 & -k & k-m\omega^2 \end{vmatrix} = 0$$

or

$$\omega^6 - 4.5 \frac{k}{m} \omega^4 + 5 \frac{k^2}{m^2} \omega^2 - \frac{k^3}{m^3} = 0 \quad (27)$$

which gives

$$\begin{aligned} \omega_1^2 &= 0.2554 \frac{k}{m}, f_1 = 0.0804 \sqrt{\frac{k}{m}} \\ \omega_2^2 &= 1.3555 \frac{k}{m}, f_2 = 0.1853 \sqrt{\frac{k}{m}} \\ \omega_3^2 &= 2.889 \frac{k}{m}, f_3 = 0.27 \sqrt{\frac{k}{m}} \end{aligned} \quad (28)$$

The "dynamically equivalent" modal oscillator model of Fig. 2B has the characteristic equation

$$\begin{vmatrix} 2k + 0.7236k + 0.2764k - 2m\omega^2 & -0.7236k & -0.2764k \\ -0.7236k & 0.7236k - 1.8944m\omega^2 & 0 \\ -0.2764k & 0 & 0.2764k - 0.1056m\omega^2 \end{vmatrix} = 0$$

or

$$\omega^6 - 4.5 \frac{k}{m} \omega^4 + 5 \frac{k^2}{m^2} \omega^2 - \frac{k^3}{m^3} = 0 \quad (29)$$

which yields the same natural frequencies as the original model (Fig. 2A).

On the other hand, consider what happens if the generalized parameters corresponding to arbitrarily normalized mode shapes (Eq. (24)) are used. The frequency equation is

$$\begin{vmatrix} 2k + 0.5279k + 9.4717k - 2m\omega^2 & -0.5279k & -9.4717k \\ -0.5279k & 0.5279k - 1.3819m\omega^2 & 0 \\ -9.4717k & 0 & 9.4717k - 3.6179m\omega^2 \end{vmatrix} = 0$$

or

$$\omega^6 - 9 \frac{k}{m} \omega^4 + 6.5 \frac{k^2}{m^2} \omega^2 - \frac{k^3}{m^3} = 0 \quad (30)$$

which gives uncorrect total system frequencies.

$$\begin{aligned} \omega_1^2 &= 0.218 \frac{k}{m}, f_1 = 0.074 \sqrt{\frac{k}{m}} \\ \omega_2^2 &= 0.5574 \frac{k}{m}, f_2 = 0.1188 \sqrt{\frac{k}{m}} \\ \omega_3^2 &= 8.2244 \frac{k}{m}, f_3 = 0.456 \sqrt{\frac{k}{m}} \end{aligned} \quad (31)$$

## MODELING TURBINE BLADE, DISC EFFECTS IN TORSIONAL MODELS OF TURBINE-GENERATOR SYSTEMS

Oscillator models are particularly useful when crucial modes of vibration can be clearly identified; e.g., to investigate the torsional vibrations of a turbine-generator system due to phase unbalance in the electrical load distribution system. Phase unbalance causes a 120 hz oscillating component of generator air gap torque; therefore, system modes at or near 120 hz are of primary concern.

Since turbine blades (or blade groups) and discs (axial direction) are mechanical components which have frequencies and vibration modes of the total rotor. The dynamics of the blades, etc. can be conveniently incorporated in a lumped parameter model by using oscillators to represent the important modes of the blades. The dynamic effects of the subcomponents on the total torsional system modes can be represented by using a model oscillator attached to the main rotor model which contains the effective modal inertia of a blade or blade group mode (a),  $IE_a$ , and a spring constant,  $IE_a(\omega_a)^2$ . The effective subcomponent inertia of higher modes is considered to be following the rotor; hence, this inertia is lumped with the rotor to conserve the total inertia.

Any structure such as a turbine blade group can be discretized into nodes with lumped mass and stiffness (finite elements); accordingly, the equations of motion (Fig. 3) can be expressed in matrix form for relative motion

$$[M]\{\ddot{u}\} + [K]\{u\} = -[M][X] + R[M]\{\ddot{\theta}_R\} \quad (32)$$

for rotor angular acceleration  $\{\ddot{\theta}_R\}$  where

$$\{u\} = \{Y\} - [R][I] + [X]\{\theta_R\} \quad (33)$$

and

$[X]$  = matrix of distances from blade root to nodes

$\{Y\}$  = absolute displacement of nodes

$\{u\}$  = relative displacement of nodes

$[I]$  = identity matrix

$R$  = radius of turbine disk

$$MG_a = \sum_j M_j \phi_{j,a}^2 \quad (37)$$

The effective inertia is then

$$IE_a = \frac{[R \Gamma_a + \lambda_a]^2}{MG_a} \quad (38)$$

For rationally normalized mode shapes the modal oscillator is dynamically equivalent to the blades vibrating in mode (a) and attached at a radius R on the rotor. Since the participation factor corresponding to rationally normalized mode shapes is unity, Eq. (36) becomes

$$\ddot{q}_a + (\omega_a)^2 q_a = -\ddot{\theta}_R \quad (39)$$

Once having the modal oscillator model of a blade or blade group, the combined rotor and blade dynamics can be investigated as a torsional system as illustrated in Fig. 4. The equations of motion for the 2 inertia model of Fig. 4 can be written as

$$\begin{bmatrix} I_R & 0 \\ 0 & IE_a \end{bmatrix} \begin{bmatrix} \ddot{\theta}_R \\ \ddot{\bar{q}}_a + \ddot{\theta}_R \end{bmatrix} + \begin{bmatrix} K_R + (\omega_a)^2 IE_a & -(\omega_a)^2 IE_a \\ -(\omega_a)^2 IE_a & (\omega_a)^2 IE_a \end{bmatrix} \begin{bmatrix} \theta_R \\ \bar{q}_a + \theta_R \end{bmatrix} = \begin{bmatrix} \text{Torq} \\ 0 \end{bmatrix}$$

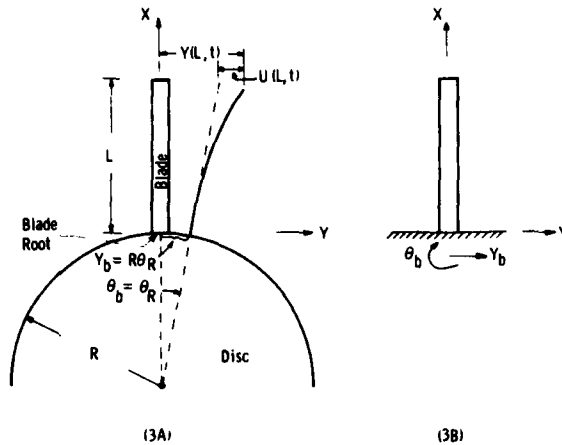


Fig. 3 - Schematic of a turbine blade and disc

After the normal mode transformation

$$\{u\} = [\Phi] \{q\} \quad (34)$$

is applied, the modal equations of motion become

$$\begin{aligned} & \{\ddot{q}\} + [\omega^2] \{q\} \\ & = -[MG]^{-1} \left[ [\Phi]^T [M] [X] \right. \\ & \quad \left. + R [\Phi]^T [M] \right] \{\ddot{\theta}_R\} \end{aligned} \quad (35)$$

where the generalized mass matrix is

$$[MG] = [\Phi]^T [M] [\Phi]$$

or for any particular mode (a)

$$\begin{aligned} & \ddot{q}_a + (\omega_a)^2 q_a \\ & = - \left\{ \frac{\Gamma_a}{MG_a} R + \frac{\lambda_a}{MG_a} \right\} \ddot{\theta}_R = -\beta_a \ddot{\theta}_R \end{aligned} \quad (36)$$

$$\Gamma_a = \sum_j M_j \phi_{j,a}$$

$$\lambda_a = \sum_j M_j X_j \phi_{j,a}$$

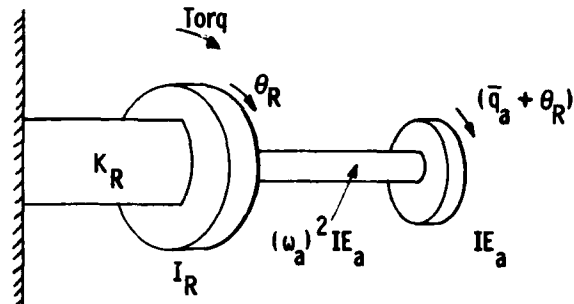


Fig. 4 - Torsional model for rotor and blade or blade group

The physical displacements (relative to rotor) of the blade or blade group at any node i in mode (a) are given from Eq. (34)

$$u_{i,a} = \bar{\phi}_{i,a} \bar{q}_a(t) \quad (41)$$

To include additional blade modes in the torsional model, parallel modal oscillators are added representing desired modes.

Fig. 5 shows the cross section of a specific low pressure turbine design which contained blade groups (L, L-1, L-2) having natural frequencies near 120 hz. Fig. 6 illustrates the lumped parameter model of a turbine-generator unit used to investigate responses to phase unbalance. Both the first  $(L-1)_1$  and second  $(L-1)_2$  modes of the L-1 blade groups were included in the model.

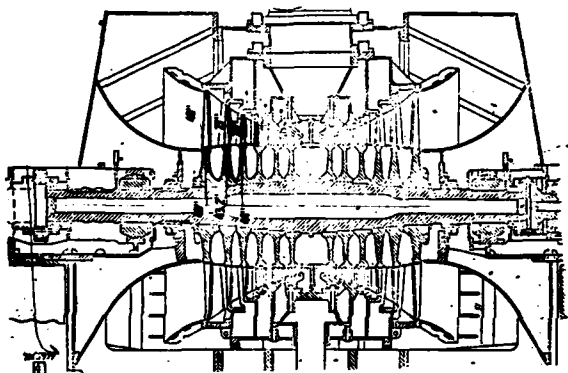


Fig. 5 - Cross section of a typical LP turbine

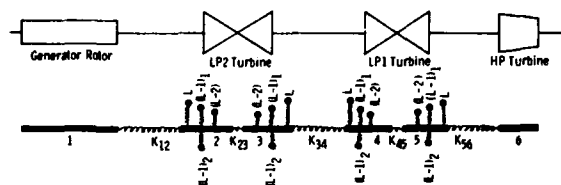


Fig. 6 - Turbine generator model used for a Typical System Analysis

## CONCLUSIONS

The analyst is in constant search for modeling techniques which lead to simplified representations of complicated systems while

maintaining the physical properties. Simplified models not only reduce time, cost, and effort in analyses but also give insight to the physical phenomena. This paper establishes a modal oscillator which is dynamically equivalent to a particular mode of vibration of a system or subcomponent of a system. In summary the following conclusions may be stated:

- (1) Oscillators may be used to model subcomponents any time there is a single attachment node.
- (2) The mass of the subcomponent oscillator must be the effective mass in order to obtain the correct total system characteristics.
- (3) Scaling the mode shapes such that the participation factor is unity has been labeled rational normalization of modes and guarantees that the generalized mass equals the effective mass; therefore, the subcomponent modal oscillator becomes dynamically equivalent to a specific mode of the subcomponent.
- (4) Rational normalization of the modes gives physical significance to the amplitudes of the mode shapes.
- (5) Rational normalization of modes eliminates participation factors as a criterion for determining important base excited modes of vibration.
- (6) Rational normalization of modes allows the modal response to be read directly from shock or seismic response spectra.

## REFERENCES

1. Heymann, F. J., "Derivation and Implications of the Navy Shock Analysis Method," Shock and Vibration Bulletin No. 37, 1968.
2. Frazer, R. A., W. J. Duncan, and A. R. Collar, "Elementary Matrices," London: Cambridge University Press, 1963.
3. Belsheim, R. O. and G. J. O'Hara, "Shock Design of Shipboard Equipment - Part I: Dynamic Analysis Method," Bureau of Ships, Navy Department, Navyships 250-423-30, May 1961.
4. Biggs, J. M., "Introduction to Structural Dynamics," McGraw-Hill Book Co., 1964.

## CHARACTERIZATION OF TORPEDO STRUCTURAL MODES AND RESONANT FREQUENCIES

C. M. Curtis, R. H. Messier, B. E. Sandman  
Naval Underwater Systems Center  
Newport, R.I. 02840

and

R. Brown  
Bolt, Beranek and Newman  
Cambridge, Mass.

A typical torpedo can be described as an assembly of complex structures contained within a ribbed shell of variable shape and thickness. For this reason, the generality embodied in the finite element method lends itself well to the construction of an analytical model of a torpedo structure.

In the present study a torpedo shell is modeled with plate and beam elements while internal components are represented as discrete masses on spring mounts. Analytical procedures and test data were used to formulate the various internal component models. Upon completion of the modeling, validation of the finite element model was gained through comparison of an eigenvalue analysis with the results of test data obtained during full-scale vibration of a torpedo. This investigation establishes a validated modeling technique which provides the basis for the prediction of transient shock response of torpedo vehicles under an input time history via time-space integration of the assembled set of dynamic equations.

### BACKGROUND

The structural elements and internal components of a torpedo are subjected to severe environmental conditions. The ability to withstand various forms of shock or explosive loading is a most critical aspect of torpedo design which directly influences the functional capacity of the vehicle and its components. Shipboard shock waves transmitted to stowage configurations, in-water explosive loading, and water-entry shock are forms of severe dynamic loading which can alter or destroy the vital functions of the component parts of a torpedo. Thus, with regard to torpedo component structural design, reduced levels of shock sensitivity are criteria of major importance. The identification of shock wave transmissibility and amplification factors is required for

the effective design of shock isolation mechanisms in proposed and existing undersea weapon systems. A coordinated effort of experimental and theoretical analyses provides the basis for establishing torpedo shock design factors. By experimental validation of theoretical modeling for torpedo shock dynamics, a confidence level is determined for the theoretical evaluation of proposed design modifications for shock mitigation in existing and conceptual underwater ordnance.

### INTRODUCTION

In order to analytically simulate the dynamic response of a torpedo and its internal components under shock loading, physical properties of stiffness and mass must be characterized for each element or section of the

structure. Since a complete torpedo configuration is composed of various complex structural elements, analytical modeling presents a formidable task. For this reason the dynamic model of a typical torpedo structure was composed using the finite element method. The torpedo hull is divided into primary structural elements such as beams and plates. The internal components are modeled as discrete masses with spring mounts. The complete structural model is constructed by coupling the various component elements together in the appropriate configuration with continuity requirements enforced at the nodal points of connection. An eigenvalue analysis is performed to determine the resonant characteristics of the relatively low-order torpedo structural vibration modes. The analytical predictions are compared to experimental results and good agreement is exemplified. Thus, a validated model is provided as the basis for the prediction of transient response under various forms of shock loading.

#### THEORETICAL MODELING AND ANALYSIS

##### A. Basic Description and Illustration of Finite Element Model

###### 1. Shell

In application of the finite element method one of the key decisions which must be made with respect to the mathematical model concerns the amount of detail to be included or, in other words, the "finess of the mesh". The degree of subdivision and the numbers of elements and grid points required to accurately model an occurrence depends strongly on the type of finite element being used in the modeling. Basic to the mathematical formulation of any finite element is the interpolation function, which describes an assumed form for the spatial variation of stress through the element. Some elements incorporate a linear stress variation and these are referred to as high-order elements. With a linear variation in stress through each element, a rapidly varying stress distribution can be accurately modeled with fewer elements than would be necessary if constant stress or lower-order elements were used. Accordingly, high-order elements are generally used in static continuum mechanics problems where the spatial variation of stress throughout the structure is difficult to predict, a priori. However, in the case of a structural dynamics calculation, the

use of high-order elements results in relatively many grid points and degrees of freedom, and their use is generally avoided for economy reasons in that class of problem.

In the modeling of a torpedo for shock and vibration analysis, the major concern was accurate representation of basic beam modes of the structure, since the results of previous test series indicated that these modes dominate the low frequency dynamic response of the torpedo. Accordingly, the decision was made to employ constant stress, linear displacement elements in the modeling. This approach was consistent with accurate characterization of the bending modes and lower shell modes, yet ensured feasibility of the dynamic analysis on economic grounds through limitation of the total number of degrees of freedom in the model.

Figure 1 presents a computer-generated plot of the finite element model for a torpedo. The shell is modeled with triangular and quadrilateral plate finite elements. These elements incorporate a linear displacement, constant stress interpolation function, as mentioned previously, and have three and four node points per element, respectively. Figure 2a provides a graphic description of the individual elements and typical interpolation functions for displacement. Each node point for these elements is allowed 5 degrees of freedom, including three displacements and two rotations. In general, the rotational degree of freedom with vector direction perpendicular to the plane of the plate element must be constrained to be zero, as shown in Fig. 2b, accounting for the missing rotational degree of freedom from the classical description of a particle in space. This omission is made necessary by the fact that no stiffness term is generated for the in-plane rotational degree of freedom within the formulation of these elements. However, in cases where two plate elements are joined together at an angle, as in Fig. 3, the in-plane rotational degrees of freedom along the junction may be left unconstrained due to the fact that in-plane rotational degrees of freedom for those nodes become bending degrees of freedom on the opposite element.

The complete shell model including control vanes, damping vanes, internal bulkheads, and shroud required 208 grid points (1248 degrees of freedom) and 375 plate elements for a model consistent with accurate repre-

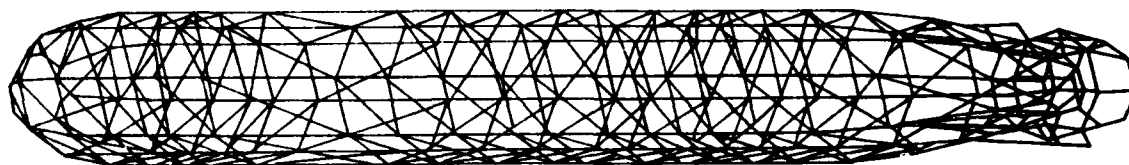


Fig. 1 - Torpedo finite element model

displacement interpolation functions

$$u = q_1x + q_2z + q_3$$

$$w = q_4x + q_5z + q_6$$

$$v = \gamma_x X + \gamma_z Z + q_7X^2 + q_8XZ + q_9Z^2 + q_{10}X^3 + q_{11}XZ^2 + q_{12}Z^3 + q_{13}$$

QUADRILATERAL PLATE FINITE ELEMENT

displacement interpolation functions

$$u = q_1x + q_2z + q_3$$

$$w = q_4x + q_5z + q_6$$

$$v = \gamma_x X + \gamma_z Z + q_7X^2 + q_8XZ + q_9Z^2 + q_{10}X^3 + q_{11}XZ^2 + q_{12}Z^3 + q_{13}$$

TRIANGULAR PLATE FINITE ELEMENT

Fig. 2a - Triangular plate finite element

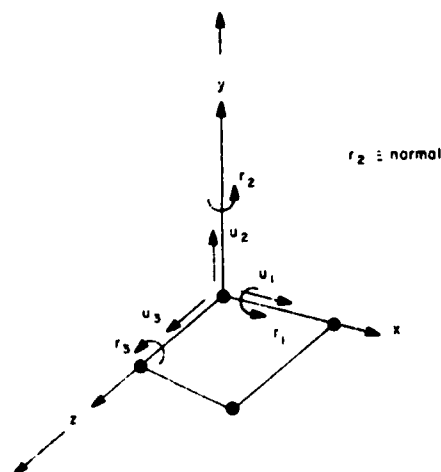


Fig. 2b - Typical grid-point degrees of freedom

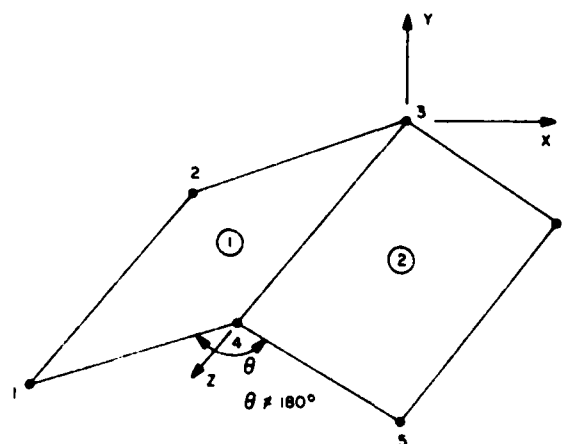


Fig. 3 - Non-coplanar plate finite elements



sentation of the basic bending modes and lower shell modes. Since the stiffness of a shell structure is obviously related to the shell thickness, full account of the variation in thickness along the length of the torpedo was taken in the model. Furthermore, the torpedo is a ring-stiffened shell structure, with many stiffeners and built-up sections along the length. These effects were included in the model through use of beam finite elements. Figure 4 depicts a beam finite element. Each beam element has two node points with 6 degrees of freedom per node. Stiffness terms corresponding to bending in two planes, tension/compression, and torsion are generated within the finite

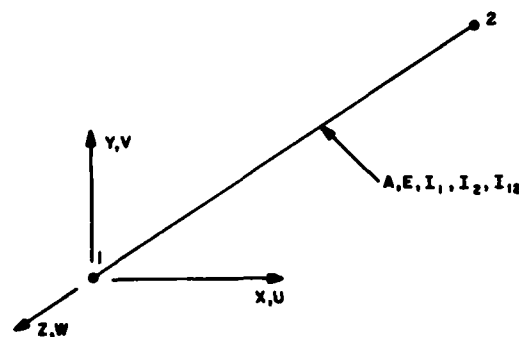


Fig. 4 Beam finite element description

## 2. Internal Components

The main purpose for development of the finite element model for a torpedo was to predict the shock response of the weapon. Included in this prediction must be the acceleration levels seen by the internal components of the vehicle during shock loading. Accordingly, the internal components were modeled using beams and lumped masses having the translational and rotary inertia properties of the various parts. These bodies were permitted the normal 6 degrees of freedom of a particle in space, three translations and three rotations. Figure 6 depicts a lumped mass with the calculations necessary to determine the inertia properties. The component models were attached to the torpedo

element computer program for the beam elements. The torpedo stiffeners were simulated by distribution of beam elements around the shell circumference at appropriate points, as shown in Fig. 5.

The torpedo shell sections were clamped together with joint bands. These bands were not included in the torpedo model, based upon the assumption that, together with the built-up sections which they clamp together, the bands form a short region with higher stiffness in both bending and tension than the basic shell. This assumption is justified by calculations of the joint band bending and tension stiffnesses presented in the Appendix.

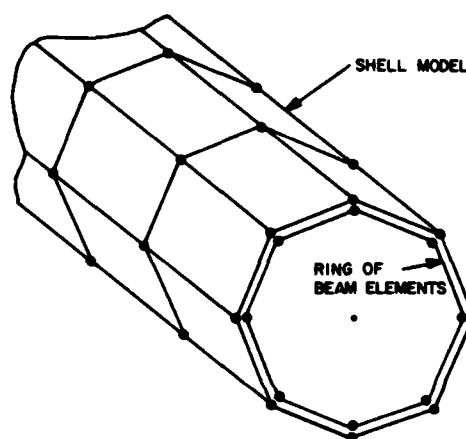


Fig. 5 - Distribution of beam finite elements around circumference of shell model

shell model using linear springs, as shown in Fig. 7. The nose package, control package, and engine were modeled using this procedure. Figure 8 summarizes the modeling procedure for the engine. The tankage sections were simulated by applying a distributed mass loading to the plate finite elements modeling those sections, as shown in Fig. 9. It was believed at the outset of the program, and verified by the experimental results, that this approach to the modeling of the internal components would provide accurate representation of the basic bending modes of the torpedo and resulting acceleration levels to the internal parts. The calculated acceleration levels could then be used as input for a shock specification to be met by designers of the actual components.

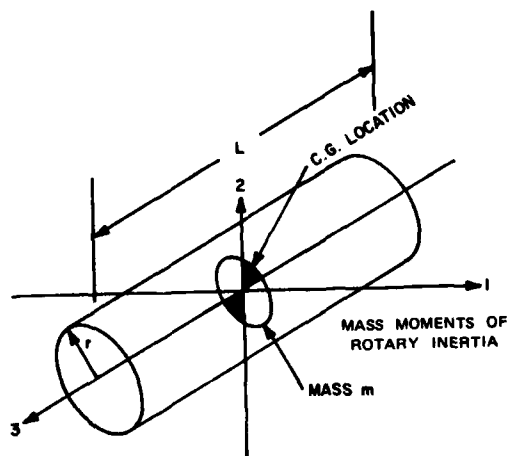
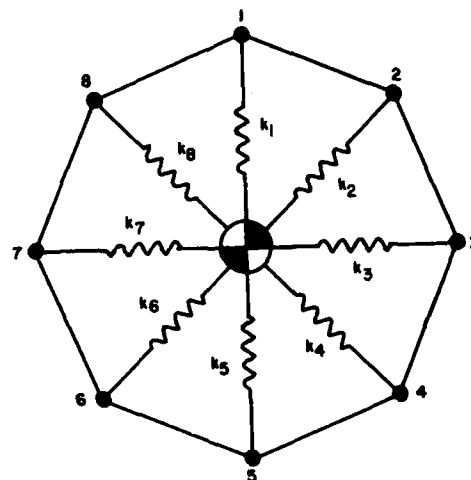


Fig. 6 - Lumped mass calculations for cylindrical mass



$k_i$  = SPRING CONSTANTS

Fig. 7 - Linear springs connecting lumped mass to shell model

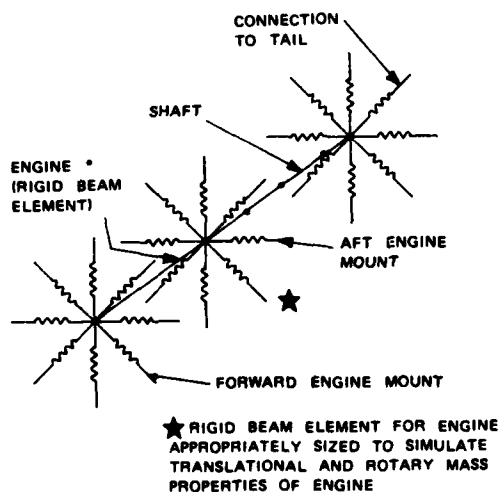


Fig. 8 - Modeling procedure for a torpedo engine

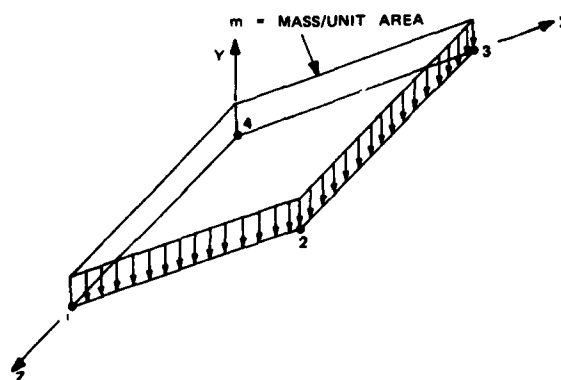


Fig. 9 - Distributed mass loading on a quadrilateral plate element

## B. Mathematical Composition of Dynamic Stiffness Matrix and Determination of Eigenfrequencies and Eigenvectors

The natural frequencies and eigenvectors for the torpedo model were calculated using the NASTRAN finite element computer program. The following is a brief description of the matrix equations for free vibrations of the structure:

$$[M] \{\ddot{x}\} + [K] \{x\} = 0 \quad (1)$$

$[M]$  = mass matrix for the structure

$[K]$  = structural stiffness matrix

$\{\ddot{x}\}$  = acceleration vector

$\{x\}$  = displacement vector

Assuming

$$\{x\} = \{x_o\} \sin \omega t, \quad (2)$$

the mode shapes for free vibration being  $\{x_o\}$ , and substituting Eq. (2) into Eq. (1),

$$-[M] \{x_o\} \omega^2 \sin \omega t + [K] \{x_o\} \sin \omega t = 0$$

which becomes, upon rearrangement and elimination of the  $\sin \omega t$  term:

$$([K] - \omega^2 [M]) \{x_o\} = 0 \quad (3)$$

Equation (3) presents the classic eigenvalue problem wherein a non-trivial solution  $\{x_o\}$  exists only for those values of  $\omega$  which result in vanishing of the determinant of the dynamic stiffness matrix.

$$|[K] - \omega^2 [M]| = 0 \quad (4)$$

Those values of  $\omega$  satisfying Eq. (4) are the natural frequencies of free vibration for the system described by Eq. (1). The  $\{x_o\}$  solutions of Eq. (3) are the mode shapes associated with those frequencies.

Equation (4) is solved within the NASTRAN computer program using a tridiagonalization technique known as Given Method [1].

As described earlier, each grid point in the structural model has generally 6 degrees of freedom in space. In the generation and assembly of the master stiffness matrix  $[K]$  by the NASTRAN program, each degree of freedom must have associated with it a stiffness term. The torpedo model contains 208 grid points and consequently 1248 degrees of freedom. In general, therefore, one would expect the matrix  $[K]$  to be of size 1248 x 1248. In actuality, however, the matrix is quite sparse with terms grouped near the diagonal of the matrix, since relatively few degrees of freedom are connected to each other through elements. This results in a stiffness matrix similar to that depicted in Fig. 10. Similar considerations hold in the generation of the structural

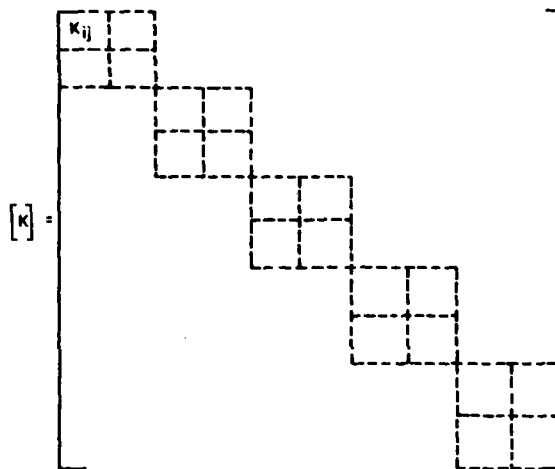


Fig. 10 - Stiffness matrix with terms grouped about the diagonal

mass matrix  $[M]$ . The NASTRAN program does not compute mass moments of (rotary) inertia independently for a model, and these are usually negligible for continuous structures except in cases where large rotary masses actually exist in the real structure. As mentioned earlier, rotary masses occur in the modeling of the internal components of the torpedo, and these were computed separately and included in the finite element model. For the continuous segments of the model (shell, stiffeners, etc.) a diagonal mass matrix was generated and assembled by the program based upon lumping of the mass associated with each element at the connected grid points. Thus, as shown in Fig. 11, a quadrilateral plate element is divided into four regions, and the mass of each region computed and lumped at the nearest grid point.

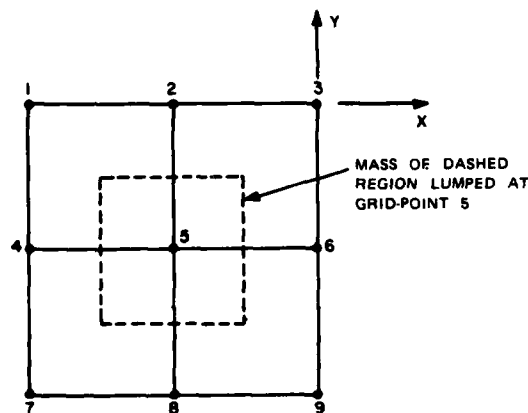


Fig. 11 - Lumping of mass at grid points in forming structural mass matrix

The Givens Method of tridiagonalization does not permit the inclusion of massless degrees of freedom in the system to be solved. Accordingly, since rotary inertia terms were not computed for the continuous parts of the model, the corresponding degrees of freedom (rotations) were not included in the so-called solution set. These degrees of freedom were omitted through the use of a static condensation scheme called the Guyan Reduction. In general, all rotational degrees of freedom on the shell and stiffeners were omitted from the solution set. However, rotational degrees of freedom were retained for all internal components of the torpedo.

#### EXPERIMENTAL ANALYSIS AND NUMERICAL RESULTS

##### A. Description of Experimental Configuration, Instrumentation, and Procedures

#### 1. Test Configuration and Instrumentation

The basic purpose of the experiment was to identify the resonant frequencies and corresponding mode shapes for a torpedo configured in a simulated stowage environment. It was desired to perform the experiments inexpensively and in an uncomplicated fashion. Figure 12 shows a general block diagram for the equipment used during the experiments. The equipment is divided into three major groups based on their functions: the driving system which provides the signals and force necessary to drive the carriage; the torpedo with vibration tables and lashing straps; and the vibration measurement system consisting of accelerometers, preamplifiers, and other signal processing and recording instruments. Each group is discussed separately in the following paragraphs.

The drive system consisted of three hydraulic vibration generators driven by sinusoidal signals provided by power amplifiers and oscillators. The motion of each vibration generator was measured by a velocity transducer, and these signals were fed to servo-units which provided in-phase controlled motion of each generator. The transducers and servo system were also used to provide a "motion" program during frequency sweeping operation. By using this program the table motion could be controlled as either constant displacement, velocity, or acceleration throughout the frequency range. A switch-over from one condition to another could also be programmed at selected frequencies. A frequency range of 5 Hz to 500 Hz was possible with this system.

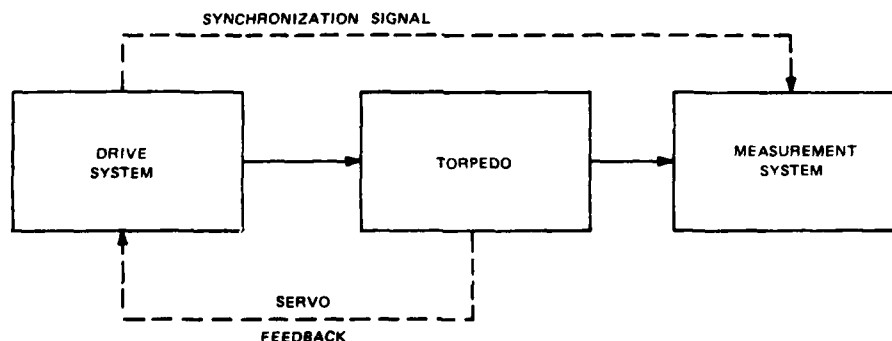


Fig. 12 - Block diagram showing general features of the experimental setup

The torpedo and the location of the vibration tables and lashing straps are all shown in Fig. 13. In the torpedo configuration, the warhead explosive was replaced with an inert filler of the same density and the fuel tanks were filled with water. Aside from these modifications, all internal hardware and components were the same as an actual torpedo. The lashing straps, however, were of different construction from the types used on a submarine, and were more flexible. The dolly motion was simulated using three vibration tables which floated on an oil film and were driven horizontally by the hydraulic vibration generators. The three tables were synchronized to provide in-phase, horizontal input motion to the torpedo.

The instrumentation system measured the accelerations and mode shapes of the torpedo and table system. A total of seven accelerometers were used. Three accelerometers were

employed to measure the motion of the motor internal to the torpedo. As shown in Fig. 13, these motor accelerometers were mounted to measure axial motion on each side of the motor, and to measure horizontal motion on the starboard motor side. Rocking motions could be determined by measuring the phase between the axially-oriented accelerometers. Additional accelerometers were mounted on the torpedo exterior to measure motion at the torpedo nose, midsection, and tail. These accelerometers helped isolate "beam-like" modes of the torpedo vibration response. A hand-held accelerometer was pressed on the torpedo exterior at various locations to map out the modal motion in detail. The final accelerometer was mounted on the middle vibration table directly below the accelerometer on the torpedo mid-section. This accelerometer was used to measure vibration transfer across the lashing straps, and to provide a phase-reference signal. Figure 13 shows all accelerometer locations.

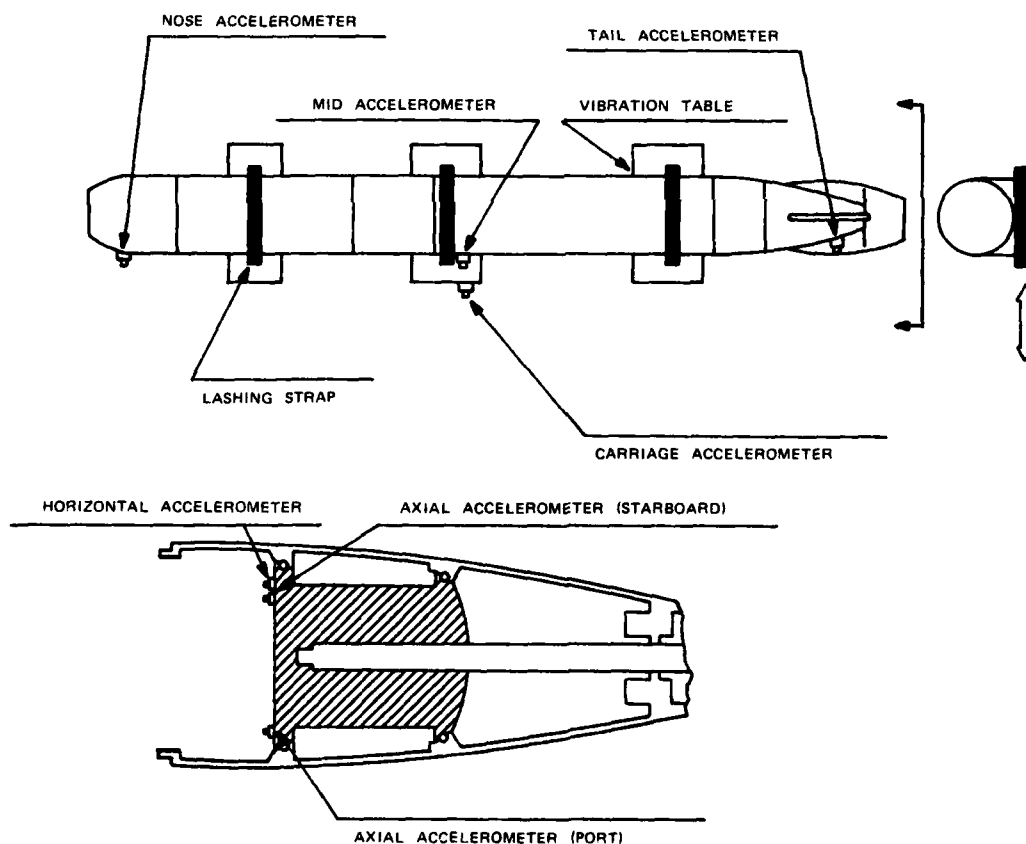


Fig. 13 - Top view of torpedo lashed to three vibration tables showing accelerometer locations. Also shown are the locations of the accelerometers on the engine configuration.

All of the accelerometers were BBN type 510, and had a sensitivity of -40 dBV/g. The accelerometers weighed only 28 grams and thus did not load down shell motion at the frequencies employed in these tests. These accelerometers also had an integrally mounted preamplifier with a low output impedance. This minimized cable noise and crosstalk, and made the sensitivity independent of cable length.

Post-accelerator instrumentation was employed to amplify, filter, and display the accelerations. A block diagram showing signal flows and operations is shown in Fig. 14. The accelerometer output voltages were amplified to levels necessary for subsequent conditioning by instrumentation amplifiers. The amplified voltages were then fed to a Mechanical Impedance/Transfer Function Analysis (MZ/TFA) system which performed two basic functions: first, it provided 10 Hz bandwidth tracking filters on each accelerometer voltages. This permitted measurements of low signal levels by increasing signal-to-noise ratios. Harmonics produced by non-linearities in the drive system and by the torpedo response were also attenuated by the tracking filters. Secondly, the MZ/TFA system was able to accurately measure the phase between the fundamental components of any two accelerometers. Amplitude and phase results were displayed on front panel meters.

In order to synchronize the tracking filters, a signal at the frequency of the drive signal and between 1.0 and 1.2 volts (rms) was required. This signal was supplied by the drive system oscillator, and fed through an automatic level regulator acting in a voltage leveling mode. This level regulator kept the voltage output constant at 1.1 volts despite fluctuations at the input. Unfortunately, synchronization of the remainder of the MZ/TFA system was not possible at the time these experiments were performed. Because of this, several convenient features such as differentiation of displacements, input-output ratio, and phase plotting could not be used. Quantities were recorded manually.

## 2. Experimental Procedure

A swept-sine procedure was employed. Several preliminary sweeps from low to high frequency were made to isolate the resonant frequencies of the torpedo. Both motor- and shell-mounted accelerometers were monitored.

The usable frequency range was limited at the low end to about 7 Hz. Although the drive system was capable of 5 Hz, a severe, "rocking" resonance at 7 Hz interfered with the servocontrol system, producing unstable operation below this frequency. The upper limit of the usable frequency range was determined by poor signal-to-

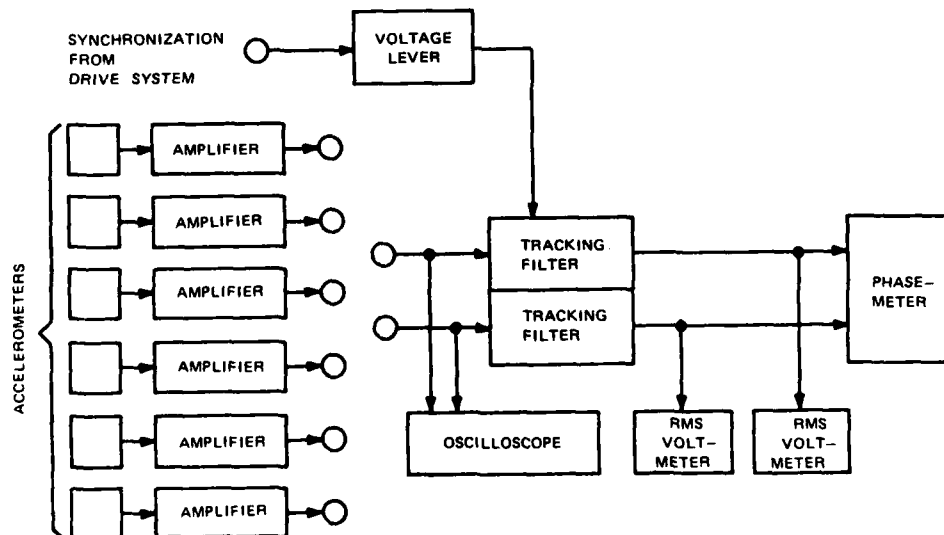


Fig. 14 - Block diagram of post-accelerator instrumentation signal processing, and display equipment

noise ratios. Due to the strap flexibility, the acceleration transmitted to the torpedo by the vibration tables was attenuated. Thus, acceleration levels on the torpedo decreased as the frequency was swept upward. At 200 Hz and higher, adequate signal-to-noise ratios could not be obtained.

The vibration levels on the driving tables were held to a constant displacement at low frequencies, and held to a constant acceleration level at the higher frequencies. The crossover frequency was determined automatically by the actual levels

employed so that a smooth crossover was obtained. Several levels were tried, but best results were obtained with an acceleration level of 1.2 g's (peak), and a 0.025 cm (peak-to-peak) displacement level. These levels determined a crossover frequency of about 48 Hz. They were also within a safety envelope of 3 g's (peak) acceleration and 0.25 cm displacement (peak-to-peak).

The motion at a resonant frequency was mapped out using the hand-held accelerometer. The response at the resonant frequency was peaked by alternately sweeping up and down in

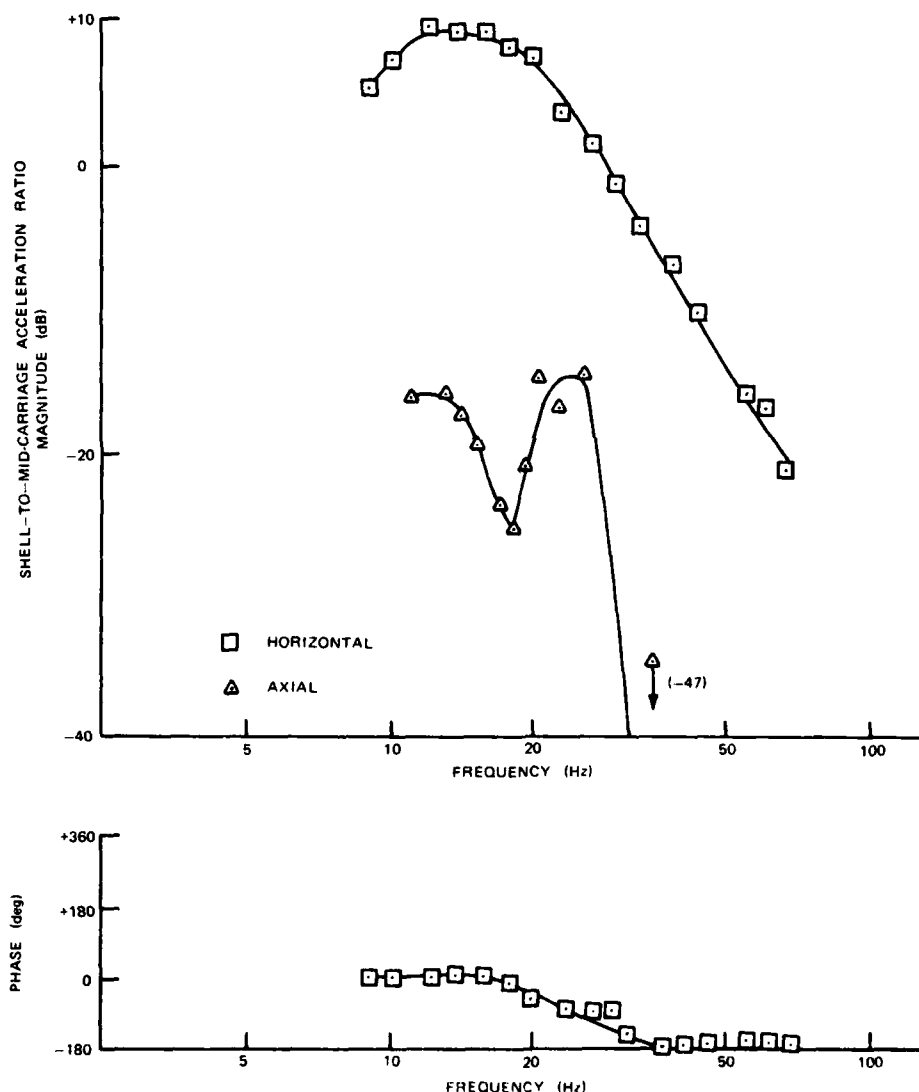


Fig. 15 - Results of sine-sweep tests showing the motor accelerations compared to the mid-carriage accelerations

frequency until a maximum acceleration was obtained. A fixed accelerometer with an adequate signal was selected as a phase reference. Then the magnitude and phase of accelerations along the torpedo shell were measured and recorded. The general mapping procedure was a tracing along the length of the torpedo with several circumferential tracings at interesting locations. Enough measurements were taken to map out the vibration field satisfactorily (generally about 50 points). This procedure could not be used for internal component monitoring. Hence, the only motion monitored was the fixed accelerometers on the forward part of the engine.

## B. Illustration and Discussion of Experimental Results

### 1. Resonant Frequencies

The results of the swept-sine tests are shown in Figs. 15 and 16. Figure 15 presents the magnitude and phase of motor motion, and Fig. 16 presents the magnitude and phase of the torpedo shell motion. All acceleration magnitudes are normalized to the middle vibration table phase. Magnitudes are plotted in decibels. The results are plotted as functions of frequency. The points represent values calculated from voltmeter readings.

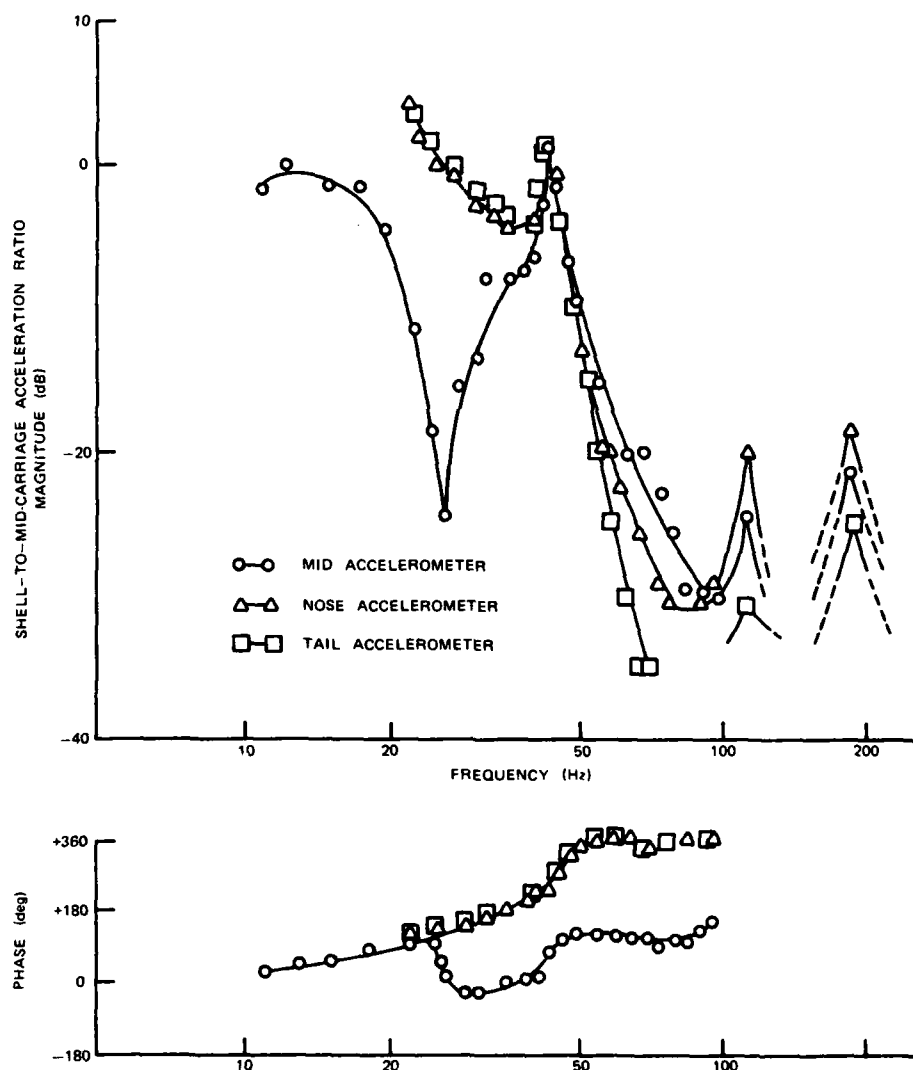


Fig. 16 - Results of sine-sweeps tests. Torpedo shell accelerations compared to midcarriage accelerations



Aside from the normal calculation accounting for accelerometer sensitivity and the amplifier gains, the effect of the crossover from constant acceleration motion to constant displacement motion had to be properly figured. Above the crossover frequency, a simple ratio of magnitudes sufficed. However, below the crossover frequency, the table accelerations were calculated according to the equation:

$$a_T = (f/f_c)^2 a_c \quad (5)$$

where  $a_T$  = the table acceleration

$f$  = the frequency

$f_c$  = the crossover frequency

$a_c$  = the table acceleration at the crossover frequency

For the data presented,  $a_c = 1.2$  g (peak) and  $f_c = 48.4$  Hz. This corresponds to a displacement of 0.0254 cm (peak-to-peak). The

accelerations calculated from this equation were compared to the accelerations measured on the middle vibration table and they agreed, as shown in Fig. 17. No correction was necessary for the phase measurements, since all phase angles were measured with respect to the middle vibration table accelerometer.

All told, five natural modes were identified experimentally in the frequency range of 5 Hz to 200 Hz. The frequencies, names, and brief descriptions of these motions are listed in Table 1. A description of the measurements and identification process follows for each of the modes.

No measurements were possible in the 5 Hz to 9 Hz frequency range because of a violent, rocking-type resonance about 7 Hz. It was impossible to control carriage motion in this range and no measurements could be taken safely. However, visual observation from an adjoining control room was possible for brief periods.

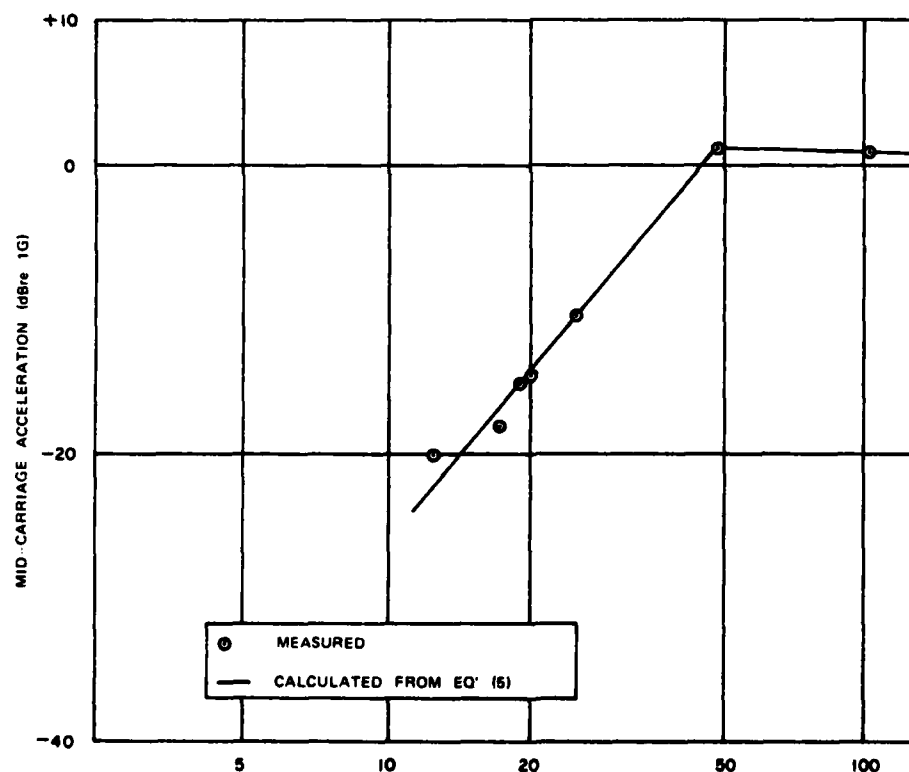


Fig. 17 - Midcarriage acceleration level as measured by midcarriage accelerometer compared to the calculated acceleration. The accelerations calculated using equation (5) were used to account for the constant displacement portion of sine sweep tests below 48.4 Hz.

TABLE 1

Brief Summary of the Experimentally Determined Resonant Motions of a Torpedo in Simulated Stowage Environment

SUMMARY OF RESONANT CHARACTERISTICS FOR TORPEDO ON SIMULATED DOLLY		
NAME	(Hz) FREQUENCY	DESCRIPTION
STRAP	7	RIGID BODY TYPE TORPEDO MOTION; LASHING STRAP STRETCHING
MOTOR	25.5	TORPEDO FLEXURE, LARGE MOTOR MOTION, HIGH DAMPING
BEAM	44.2	TORPEDO FLEXURE; 2 NODES; LITTLE MOTOR MOTION; LOW DAMPING
BEAM	115.0	SAME AS ABOVE; 3 NODES
BEAM	188.0	SAME AS ABOVE; 4 NODES

From this observation it appeared that the resonance involved rigid body motion (translation and rotation about the longitudinal axis) of the torpedo combined with stretching of the lashing straps.

The first appearance of resonant motion above this frequency was a highly damped resonance at about 25.5 Hz. This resonance was not particularly apparent either visually or on voltmeter readings. Probably, two reasons caused this. First was the high damping which limited the resonant motion and the sharpness of the resonance. Secondly, since accelerometers were monitored during a constant displacement sine-sweep, a bias proportional to the frequency squared was present. This further obscured any peaking. The basic clue to the presence of the resonance is the 90° phase shift between motor acceleration and carriage acceleration as seen in Fig. 15. Furthermore, above 25.5 Hz, the motor response decreases at a rate of 40 dB per decade.

The motion at this resonance involves motor and tail motions of approximately equal magnitude but opposite phases. The motion at the torpedo nose is about the same magnitude and in phase with the tail. Also, the axial motion of the motor, although low, peaks near this frequency. Axial accelerations on the motor were so low that a reliable phase comparison be-

tween the axially mounted accelerometers was impossible. Hence, a measurement of the "rocking" component of motor motion was not made. A curious feature of the motion is the sharp null in horizontal acceleration at the mid-section. An illustration of the motion is shown in Fig. 18a. Since torsional motion is not measured by the accelerometers, it may also be present. No mapping of the motion by the hand-held accelerometer was done. The percentage of critical damping was estimated from the slope of the phase curve to be approximately 100%. This large damping could arise from the rubber motor mounts and flexible coupling.

The remaining three resonances that were discovered are apparent as peaks in the torpedo shell frequency response, Fig. 16. The resonant frequencies were 44.2 Hz, 115 Hz, and 188 Hz, and each was a higher order motion involving the entire torpedo in flexure. Hence, they were named "beam" modes. Each of these modes was carefully mapped out using the hand-held accelerometer. The results of the mapping are plotted in Figs. 18b, 18c, and 18d. Each mode was quite peaked, indicating a relatively small loss factor. By measuring the "1/2-power" points on the response curves, the percentage of critical damping was estimated to be 6%, 7%, and 5%, respectively.

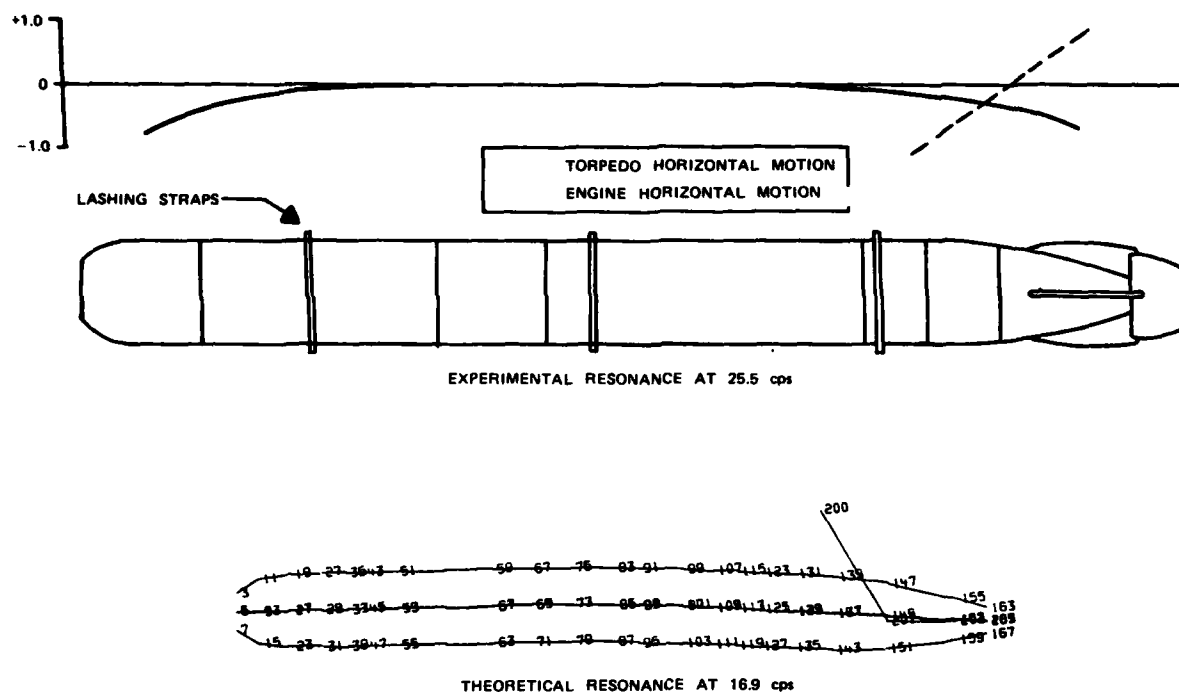


Fig. 18a - Experimental and theoretical resonance - predominant motor motion

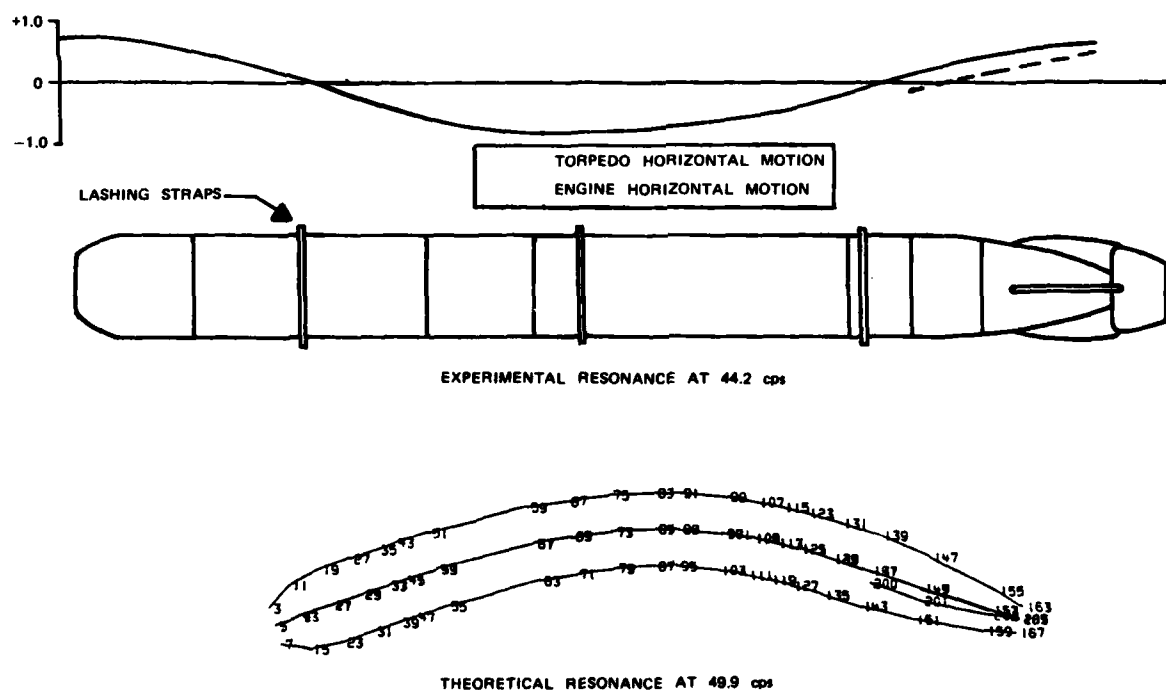


Fig. 18b - Experimental and theoretical resonance - beam motion of hull

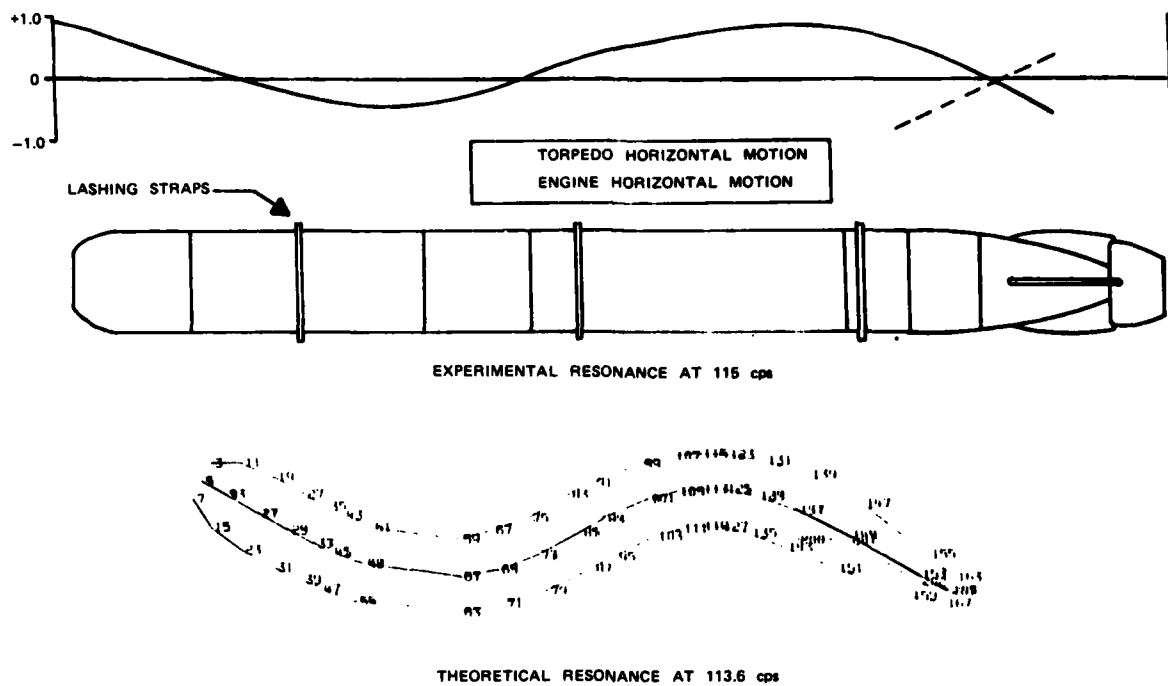


Fig. 18c - Experimental and theoretical resonance - beam motion of hull

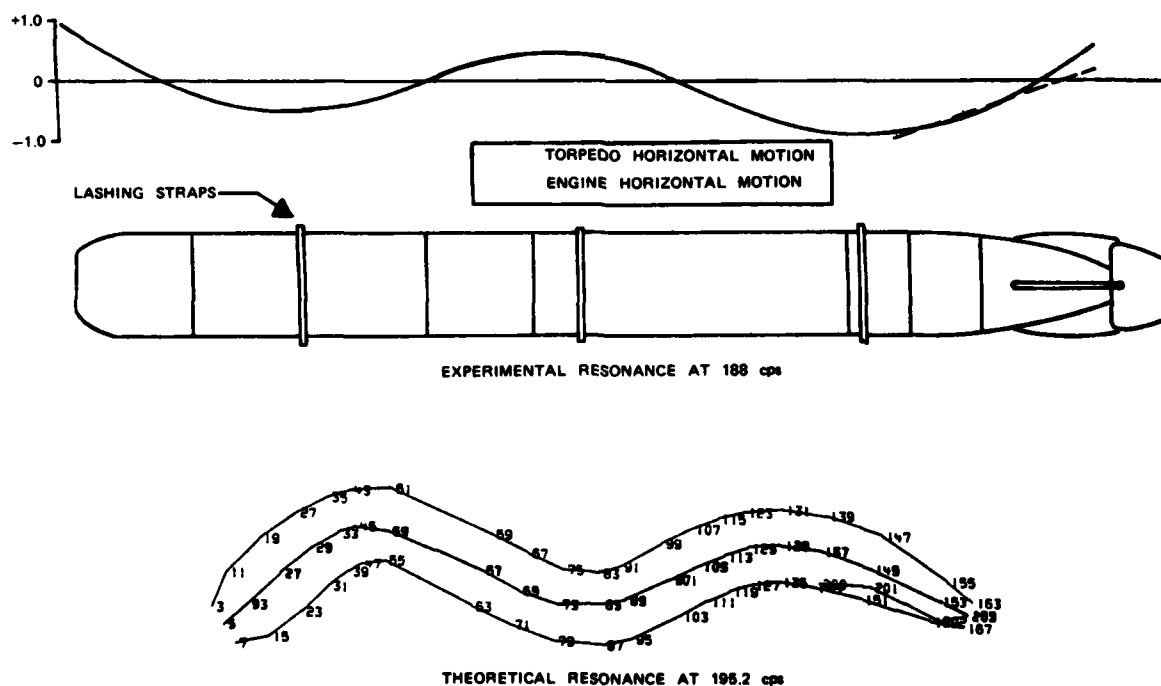


Fig. 18d - Experimental and theoretical resonance - beam motion of hull

Above 200 Hz, several peaks were noticed during frequency sweeps. However, acceleration levels were low and signal-to-noise ratios were poor. Since these higher frequency modes would not presumably affect the torpedo's shock response significantly, a detailed mapping or identification of these modes was not attempted.

### C. Correlation of Finite Element Analysis with Experimental Results

#### 1. Compliance of Mounts

In the initial prediction of modes and resonant frequencies, the degree and nature of the constraints imposed by the carriage configuration in the experiment was under considerable question. Thus, the finite element eigenvalue analysis was performed assuming negligible external constraint upon the displacement field. In addition to rigid body modes, this condition provided the free-free modes and frequencies of torpedo vibration. By the indicated low experimental frequency of rocking and translatory motion (Table 1), and the subsequent comparison of theory and experiment, the unconstrained condition was determined to be an excellent representation in regard to characterizing the normalized modes and frequencies of the torpedo as they occurred in the experimental configuration. It is noted that for an unconstrained configuration, the eigenvalue analysis predicts both horizontal and vertical modes of vibration which differ slightly due to minor magnitudes of structural asymmetry. However, the limitation to horizontal excitation in the experiment resulted in appearance of only horizontal modes in the frequency response spectrum. Thus, the comparison of results is presented in terms of horizontal mode shapes and frequencies.

In addition, the magnitude of the spring constants for proper representation of the motor mounts was determined to be a critical parameter in the analysis of torpedo vibration. Since the mass of the motor is sizeable, the stiffness of the attachment to the hull has a major influence upon modes and frequencies of vibration. For this reason static and dynamic tests were performed on an afterbody equivalent to that used in the full vehicle test configuration. Static deflection tests were performed by boring holes through the hull to provide access for leading probes. Dynamic shaker tests were then conducted to determine the

fundamental mode and frequency of motor vibration. Subsequently, the finite element eigenvalue analysis was exercised, with the motor mount spring constants determined by the static experimental test. Excellent results in the agreement of theory and experiment were obtained, and validation of the afterbody-motor portion of the theoretical model was achieved for an isolated configuration. Unfortunately, due to the inaccessibility of the motor in the complete torpedo configuration, measurement of the motor mount compliance was not possible. With the lack of any alternative, the mount stiffnesses measured in the isolated afterbody and motor assembly were adjusted in magnitude to provide reasonable agreement of the fundamental motor resonance in the finite element model of the full vehicle test configuration. It is noted that wear and fatigue imparted to the full vehicle during prior range exercises are possible sources of error in the structural equivalence of the two motor mount assemblies.

#### 2. Discussion of Results

The finite element eigenvalue analysis predicted mode shapes and frequencies for both horizontal and vertical plane vibration. Horizontal and vertical modes were obtained with similar forms, but slightly different frequencies, since the torpedo contains internal equipment rails that are mounted horizontally along the interior of the hull and act as stiffening members. By the comparison of theory and experiment, it was concluded that the additional stiffness due to the equipments rails is a negligible quantity which leads to nearly identical horizontal and vertical plane mode shapes. In addition, torsional and axial resonances were predicted by the analysis. Since the torpedo was excited experimentally only in the horizontal plane, the comparison of theory and experiment is made solely on the basis of transverse motion. The comparison of theoretical and experimental mode shapes and frequencies is illustrated in Figs. 18a through 18d. Fig. 18a shows the experimentally and theoretically determined frequencies for motor resonant response. The finite element grid points, 200 and 201, are essentially at the same location as the forward and aft accelerometers on the motor in the experimental test configuration. Thus, the motion of the motor shown experimentally (dashed line) is compared to the line connecting node points 200 and 201 in the element grid. The agreement in

the frequency of resonance represents that obtained by a step correction of the stiffness of the motor mounts in the finite element model. The lack of exact knowledge concerning the conditions and properties of the motor mounts in the complete torpedo configuration led to disparity of theoretical and experimental motor resonances. Thus, the single step correction of mount stiffness was made to provide improved agreement.

Figures 18b-18d show the comparison of theory and experiment for remaining modes of vibration. It is seen that the modes are essentially free-free type beam modes. Although the theoretical frequencies generally tend to be higher than those observed in the test configuration, the mode shapes are in excellent agreement. The high values of frequency are expected since the breakdown into finite elements produces a relatively "stiff" structural model. A refinement of the element size in addition to a more accurate specification of both motor mount and equipment mount stiffnesses would improve the results. However, in regard to low-frequency shock loading, the current characterization is viewed to be an adequate representation in order to produce reasonable estimates of response.

## CONCLUSIONS

A finite element model of a torpedo vehicle was assembled in order to facilitate the study of shock-loaded response. The investigation presented in this paper provides a basic phase in the validation of the model. By comparison of the theoretical and experimental results, it is shown that the model is capable of predicting resonant mode shapes exhibited by an actual torpedo configuration. The overall agreement between theory and experiment is excellent. The structural stiffness and damping of the motor mount assembly are critical parameters, since the mass of the motor is a sizeable quantity. Thus, a refinement of the stiffness matrix for the motor mounts, based upon more detailed experimental information, would improve the agreement between theory and experiment. In general, the prediction of the response of masses internal to the hull requires detailed knowledge of the mounting characteristics. Within the limitations of the current study, the prediction of resonant characteristics with a reasonable level of confidence is demonstrated, and the basis for shock response simulation is formulated.

## ACKNOWLEDGEMENT

The authors would like to thank J. Higson and M. Martino of NUSC for their assistance in the modeling and analysis presented in this study.

The authors of this paper would also like to express their appreciation to NAVSEA (Code 031) for supporting this investigation.

## REFERENCES

1. W. Givens, "Numerical Computation of the Characteristic Values of a Real, Symmetric Matrix," Oak Ridge National Lab., ORNL-1574, 1954.
2. R. H. Messier, "Analysis of Torpedo Joint Bands in Bending," NUSC TM No. SB22-4340-72, 28 August 1972.

## APPENDIX

### Calculation of Bending and Tension Stiffness For Torpedo Joint Bands

The method used in the calculation of these stiffness terms was originally developed and presented in Ref. 2.

### Tension Stiffness

The basic assumption in this calculation is that the joint bands are lubricated so that tensile loading on the joint results in expansion of the band diameter and thus sliding of the band up the inclined planes provided by the band seat, as shown in Figure A-1.

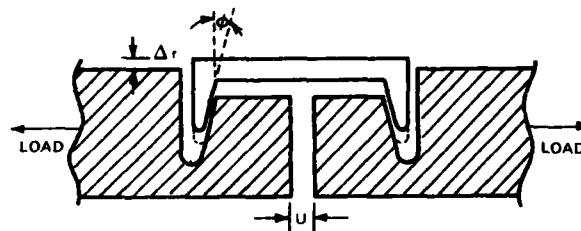


Fig. A-1

Tensile loading produces an axial displacement of the mating surfaces,  $u$ , which is uniform around the circumference. The change in radius of the band,  $\Delta r$ , results in circumferential strain in the band.

$$\epsilon_c = \frac{\Delta r}{r}$$

$$\tan \phi = \frac{u}{2\Delta r}$$

$$\Delta r = \frac{u}{2 \tan \phi}$$

$$\epsilon_c = \frac{1}{2 \tan \phi} \frac{u}{r}$$

$$\sigma_c = \frac{E}{2r \tan \phi} u + \frac{2P}{A_b}$$

where:

E is the Young's modulus of the band material  
r is the radius of the band  
P is the preload on the clamp band bolts  
A<sub>b</sub> is the cross-sectional area of the band

This stress distribution may now be integrated to find the force distribution on the band. In particular, equilibrium of one-half of the band can be considered, as in Fig. A-2.

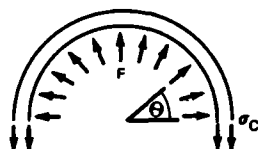


Fig. A-2

$$2 \int F \sin \phi \sin \theta \, ds = 2 \sigma_c A_b$$

where F is the force per unit length of band which is constant by symmetry for the tension case.

$$ds = r \, d\theta$$

$$2 \sigma_c A_b = 2 F r \sin \phi$$

$$\sigma_c = \frac{E}{2r \tan \phi} u + \frac{2P}{A_b}$$

$$\frac{EA_b u}{r \tan \phi} + 4P = 2 F r \sin \phi$$

$$F = \frac{EA_b u}{2r^2 \tan \phi \sin \phi} + \frac{4P}{2r \sin \phi}$$

It therefore follows that the spring constant, k, for the clamp band joint is:

$$k = \frac{EA_b}{2r^2 \tan \phi \sin \phi} 2\pi r$$

$$= \frac{\pi EA_b}{r \tan \phi \sin \phi}$$

For the bands,

$$E = 10.5 \times 10^6 \text{ psi } (7.24 \times 10^{11} \text{ dyn/cm}^2)$$

$$A_b = .985 \text{ in}^2 (6.35 \text{ cm}^2)$$

$$r = 10.5 \text{ in } (26.67 \text{ cm})$$

$$\phi = 15^\circ$$

$$k = 4.5 \times 10^7 \text{ lb/in } (7.88 \times 10^{12} \text{ dyn/cm})$$

Using an average shell thickness of 0.4 inches (1.02 cm) for the torpedo, the extensional spring constant for the shell is:

$$k_{\text{shell}} = AE/L; L=230 \text{ in } (584.2 \text{ cm})$$

$$= 1.23 \times 10^6 \text{ lb/in } (2.15 \times 10^{11} \text{ dyn/cm})$$

Thus the clamp band joints are stiffer in tension than the torpedo shell, and neglecting their effect is therefore justifiable.

A similar development for bending at the clamp band joints yields:

$$k_{\text{bending}} = \frac{3}{2} \frac{(4A_b E r)}{(4+\pi) \tan^2 \phi}$$

$$= \frac{6A_b E r}{(4+\pi) \tan^2 \phi}$$

$$= 1.27 \times 10^9 \text{ in.-lb/rad } (1.43 \times 10^{15} \text{ dyn-cm/rad})$$

For the torpedo shell, bending stiffness is:

$$k_{\text{bending of shell}} = \frac{0(EI/L)}{0(\quad) = \text{order of } (\quad)}$$

$$= 0(7.0 \times 10^7), (7.9 \times 10^{13} \text{ dyn-cm/rad})$$

Thus the bending stiffness of the clamp band joints will be a minimum of one order of magnitude greater than the bending stiffness of the torpedo shell, and their effect can therefore be neglected, since the region of influence is very small.

# LAGUERRE FUNCTION REPRESENTATION OF TRANSIENTS

G. R. Spalding  
Wright State University  
Dayton, Ohio

This paper discusses Laguerre functions and their use in modeling the dynamic response of highly damped systems. Laguerre functions of varying time constant are generated from the Laguerre polynomials. By sampling at the axis crossings of the  $n^{\text{th}}$  order Laguerre polynomial, system response can be represented by a finite set of orthonormal vectors. These vectors provide both a representation that is exact at the measurement points and interpolation functions that can be suited to the application.

## INTRODUCTION

This paper presents an introductory discussion of the Laguerre polynomials and their application to modeling the dynamic response of systems. These polynomials are particularly well suited to highly damped motions. Further, because they obey a summation as well as an integral orthogonality, they are an ideal means of representing measured response data. In so doing they provide the measurement locations, as well as flexibility both in the weighting of measurement points and in the form of the expansion functions.

The Laguerre polynomials are a special case of the Jacobi polynomials, as are the Chebyshev, and as such enjoy many of the computational advantages of this class of functions. Although they have been a part of the literature of theoretical physics for nearly a century, they were given particular engineering significance in the nineteen thirties when Lee [1] demonstrated that they could be generated by conventional analog circuits. In the early nineteen fifties, Wiener [2] brought them to prominence with his work on the synthesis of nonlinear systems. Since that time they have received little attention from the engineering community.

The application that prompted the writer's initial use of the Laguerre polynomials was the identification of time-varying coefficients in second-order models. A simplified form of such

a model is

$$\frac{d^2u}{dt^2} + \beta(t) \frac{du}{dt} + u = f(t) \quad (1)$$

This can be converted to an integral equation [3] having the form

$$u(t) - g(t) = \int_0^\infty u(\tau) \frac{d}{d\tau} [g(\tau, t) \beta(\tau)] d\tau \quad (2)$$

where  $\beta(\tau)$  is to be estimated on the basis of completely accurate measurements made upon  $u(t)$ . The function  $g(\tau, t)$  is known. If  $u(t)$  is measured at  $N$  points in time, it can be represented exactly as

$$u(\tau_i) = \sum_{n=0}^{N-1} a_n \phi_n(\tau_i) \quad (3)$$

where the  $\tau_i$  are the measurement points and correspond to the roots of

$$\phi_N(\tau) = 0 \quad (4)$$

and the  $\phi_n(\tau)$  are a set of Laguerre functions. It is these functions that this paper discusses.

## THE LAGUERRE FUNCTIONS

The Laguerre polynomials are a complete set of functions, orthonormal over



the interval zero to infinity with respect to the weighting function  $e^{-t}$ .

$$\int_0^{\infty} L_n(t) L_m(t) e^{-t} dt = \begin{cases} 1 & n=m \\ 0 & n \neq m \end{cases} \quad (5)$$

The  $n$ th polynomial can be computed from the general expression

$$L_n(t) = \frac{1}{n!} e^t \frac{d^n}{dt^n} (t^n e^{-t}) \quad (6)$$

or, from the recurrence relation,

$$\begin{aligned} (n+1)L_{n+1}(t) \\ = (1+2n-t)L_n(t) - nL_{n-1}(t) \end{aligned} \quad (7)$$

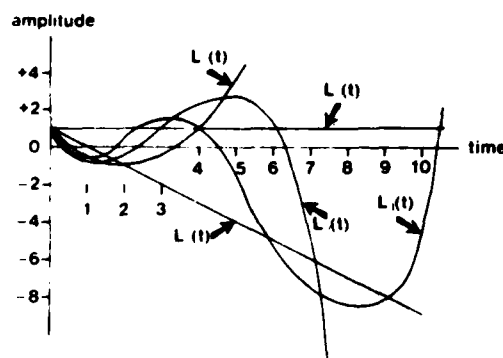
A function  $f(t)$  can be represented as

$$f(t) = \sum_{n=0}^{\infty} a_n L_n(t) \quad (8)$$

where

$$a_n = \int_0^{\infty} f(t) L_n(t) e^{-t} dt \quad (9)$$

Figure 1 shows the first five Laguerre polynomials plotted over their range of greatest interest. With the exception of  $L_0(t)$ , these functions are unbounded and consequently only suitable to represent functions that increase with time.



Amplitude vs Time - Laguerre Polynomials ( $t=0$ )

Figure 1

To obtain a bounded series, an alternate form, generally called the Laguerre functions, is defined by incorporating the weighting function into the polynomial form, i.e.,

$$\phi_n(t) = L_n(t) e^{-t/2} \quad (10)$$

Then

$$\int_0^{\infty} \phi_n(t) \phi_m(t) dt = \begin{cases} 1 & m=n \\ 0 & m \neq n \end{cases} \quad (11)$$

and the  $n$ th Laguerre function is defined by

$$\phi_n(t) = \frac{1}{n!} e^{t/2} \frac{d^n}{dt^n} (t^n e^{-t}) \quad (12)$$

The recurrence relation remains the same as for the polynomials, namely,

$$\begin{aligned} (n+1)\phi_{n+1}(t) \\ = (1+2n-t)\phi_n(t) - n\phi_{n-1}(t) \end{aligned} \quad (13)$$

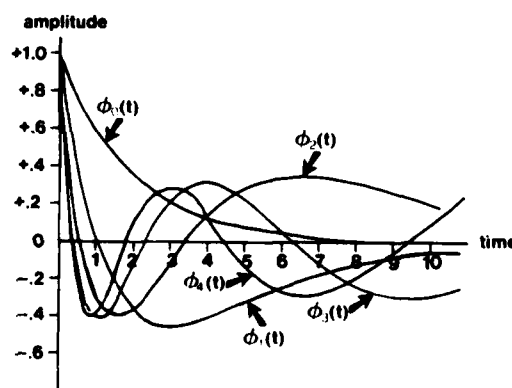
The series expansion of  $f(t)$  is

$$f(t) = \sum_{n=0}^{\infty} b_n \phi_n(t) \quad (14)$$

and the coefficients are obtained from

$$b_n = \int_0^{\infty} f(t) \phi_n(t) dt \quad (15)$$

Figure 2 shows the first five of these functions. Note that they decay with time and are asymptotic to zero amplitude.



Amplitude vs Time - Laguerre Functions ( $t=-.5$ )

Figure 2

In order for equations (8) or (14) to represent  $f(t)$  exactly, an infinite number of terms is required. Further, to obtain the coefficients accurately,  $f(t)$  must be known for all  $t$ . When

representing a measured function,  $f(t)$ , only a finite expansion can be obtained, based on knowledge of  $f(t)$  at a finite number of discrete values of  $t$ . The proper reference for such data, whether temporal or spatial, is a finite-dimensional vector space, rather than a truncated infinite-dimensional function space. Either the  $L_n(t)$  or the  $\phi_n(t)$  can be used to construct such a space.

As an example, a four-dimensional space will be generated using the  $\phi_n(t)$ . Using equation (13) and defining  $\phi_{-1}(t) \equiv 0$ , the first four recurrence relations are

$$\begin{aligned}\phi_1(t) &= (1-t)\phi_0(t) \\ 2\phi_2(t) &= (3-t)\phi_1(t) - \phi_0(t) \\ 3\phi_3(t) &= (5-t)\phi_2(t) - 2\phi_1(t) \\ 4\phi_4(t) &= (7-t)\phi_3(t) - 3\phi_2(t)\end{aligned}\quad (16)$$

Restricting  $t$  to the discrete values  $t_i$  where  $t_i$  are the roots of  $\phi_4(t)$ , namely,

$$\phi_4(t_i) = 0, \quad (17)$$

the recurrence relations in matrix form are

$$\begin{bmatrix} 1-t_i & -1 & 0 & 0 \\ -1 & 3-t_i & -2 & 0 \\ 0 & -2 & 5-t_i & -3 \\ 0 & 0 & -3 & 7-t_i \end{bmatrix} \begin{bmatrix} \phi_0(t_i) \\ \phi_1(t_i) \\ \phi_2(t_i) \\ \phi_3(t_i) \end{bmatrix} = 0. \quad (18)$$

The  $t_i$  are the eigenvalues of the square matrix, and the  $\phi_n(t_i)$  ( $n=0,1,2,3$ ) are the corresponding eigenvectors. The symmetry of the square matrix assures the orthogonality of the vectors.

In general, the coordinates of an  $N$ -dimensional vector space are

$$\phi_0(t_i), \phi_1(t_i), \dots, \phi_{N-1}(t_i),$$

where the  $t_i$  are the  $N$  roots defined by

$$\phi_N(t_i) = 0. \quad (19)$$

The coordinate vectors are normalized by

$$\lambda_k^2 \sum_{n=0}^{N-1} \phi_n^2(t_k) = 1. \quad (20)$$

This yields the orthonormal modal matrix

$$M = \begin{bmatrix} \lambda_1 \phi_0(t_1) & \lambda_2 \phi_0(t_2) & \dots & \lambda_N \phi_0(t_N) \\ \lambda_1 \phi_1(t_1) & \lambda_2 \phi_1(t_2) & & \vdots \\ \vdots & \vdots & & \vdots \\ \lambda_1 \phi_{N-1}(t_1) & \dots & \dots & \lambda_N \phi_{N-1}(t_N) \end{bmatrix} \quad (21)$$

For symmetric matrices,

$$M M^T = M^T M = I, \quad (22)$$

where  $M^T$  is the transpose of  $M$ . Using (22) produces the summation (or discrete) orthogonality relationships

$$\sum_{k=1}^N \lambda_k^2 \phi_n(t_k) \phi_m(t_k) = \begin{cases} 1 & n=m \\ 0 & n \neq m \end{cases} \quad (23)$$

Thus, if  $f(t)$  is measured at  $N$  discrete times,  $t_i$ , and represented by

$$f(t_i) = \sum_{n=0}^{N-1} b_n \phi_n(t_i), \quad (24)$$

the  $b_n$  are obtained from

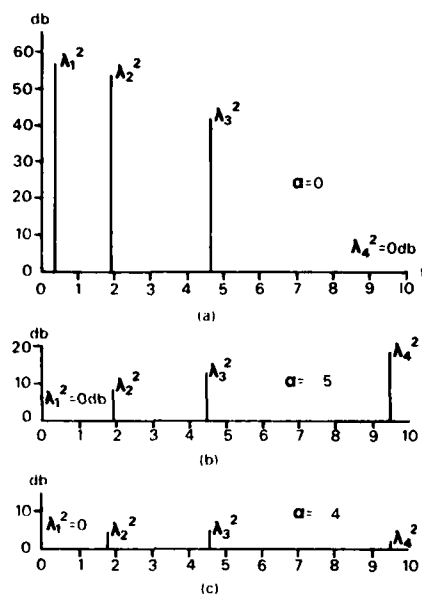
$$b_n = \sum_{i=1}^N \lambda_i^2 f(t_i) \phi_n(t_i). \quad (25)$$

Four points are emphasized as a result of this development:

1. The use of the sample times  $t_i$  assures independent measurements.
2. The concepts presented hold not only for the  $\phi_n(t)$  and the  $L_n(t)$  but also for more general Laguerre functions that will be presented below.
3. The integrations, generally used to evaluate coefficients, are replaced by simple summations.
4. The representation of  $f(t)$ , at the measurement points, is exact.

#### VARIABLE WEIGHTING

Referring to equations (24) and (25), it is apparent that the  $\lambda_k^2$  act to weight the measured values. For example, Figure 3a shows the weights for the  $L_4(t_i) = 0$  system. As this system exhibits increasing amplitude with time, the weighting decreases with time. In contrast the functions associated with the  $\phi_4(t_i) = 0$  system decrease with time, and thus the weighting increases with time, as shown in Figure 3b.



Measurement Weighting vs Time

Figure 3

The distribution of weights can be controlled by incorporating various portions of the exponential weighting into the expansion functions. Defining

$$\psi_n(t) = L_n(t)e^{\alpha t}, \quad (26)$$

the orthogonality condition is

$$\int_0^{\alpha} \psi_n(t) \psi_m(t) e^{\beta t} dt = \begin{cases} 1 & m=n \\ 0 & m \neq n \end{cases}, \quad (27)$$

where

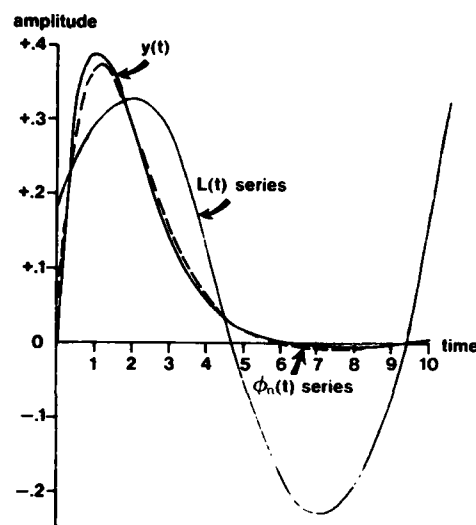
$$2\alpha + \beta = -1.$$

The weights associated with an  $\alpha$  of  $-0.4$  are presented in Figure 3c.

The  $\alpha$  exponent not only varies the weighting but also changes the form of the expansion functions. The expansions will always be exact at the measurement points, but interpolation between points will depend upon the  $\alpha$  value. To illustrate, the response of the system

$$\frac{d^2 y}{dt^2} + 1.8 \frac{dy}{dt} + y = \delta(t) \quad (28)$$

was represented by a four-term expansion



Amplitude vs Time for a Pulse and Two Representations

Figure 4

of  $\phi_n(t)$  ( $\alpha = -0.5$ ) and then, for contrast, by a four-term expansion of  $L_n(t)$  ( $\alpha = 0$ ). The results are shown in Figure 4. Both approximations are exact at the four measurement points. The  $\phi_n(t)$  expansion provides good interpolation between points; the  $L_n(t)$  interpolation is very poor.

## CONCLUSIONS

It is important to note that the Laguerre functions are not suited to pulses containing lightly damped oscillations. The representation of such functions would require an excessive number of terms in the series. In such cases, high frequency vibrations can often be separated from the basic pulse and modeled separately.

It is also necessary to adjust the time scale of the functions to be represented to coincide with the scale of the expansion functions. When using the interpolation property, it is particularly important to match the time constant of the problem to that of the expansion functions.

Finally, although the complete solution of the problem raised in the Introduction is outside the scope of this paper, the use of the Laguerre functions in obtaining the solution can be indicated.

The integral in equation (2) can be approximated to an arbitrarily high degree by a Gauss-type quadrature formula based on the Laguerre polynomials [4], i.e.,

$$\int_0^{\infty} u(\tau) \left\{ \frac{d}{d\tau} [g(\tau, t) \beta(\tau)] \right\} d\tau \\ \approx \sum_{k=1}^N \lambda_k^2 u(\tau_k) \left\{ \frac{d}{d\tau} [g(\tau, t) \beta(\tau)] \right\}_{\tau=\tau_k} \quad (29)$$

If equation (3) is put into the right-hand side of (29), then equation (2) becomes

$$u(t) - g(t)$$

$$= \sum_{n=0}^{N-1} a_n \sum_{k=1}^N \lambda_k^2 \phi_n(\tau_k) \left\{ \frac{d}{d\tau} [g(\tau, t) \beta(\tau)] \right\}_{\tau=\tau_k} \quad (30)$$

The inner sum of (30) is the discrete Laguerre transform of the quantity in braces (see equations 24 and 25). Thus, designating

$$\sum_{k=1}^N \lambda_k^2 \phi_n(\tau_k) \left\{ \frac{d}{d\tau} [g(\tau, t) \beta(\tau)] \right\}_{\tau=\tau_k} = K_n(t), \quad (31)$$

the inverse transform is

$$\left\{ \frac{d}{d\tau} [g(\tau, t) \beta(\tau)] \right\}_{\tau=\tau_k} = \sum_{n=0}^{N-1} K_n(t) \phi_n(\tau_k) \quad (32)$$

Equation (30) is now

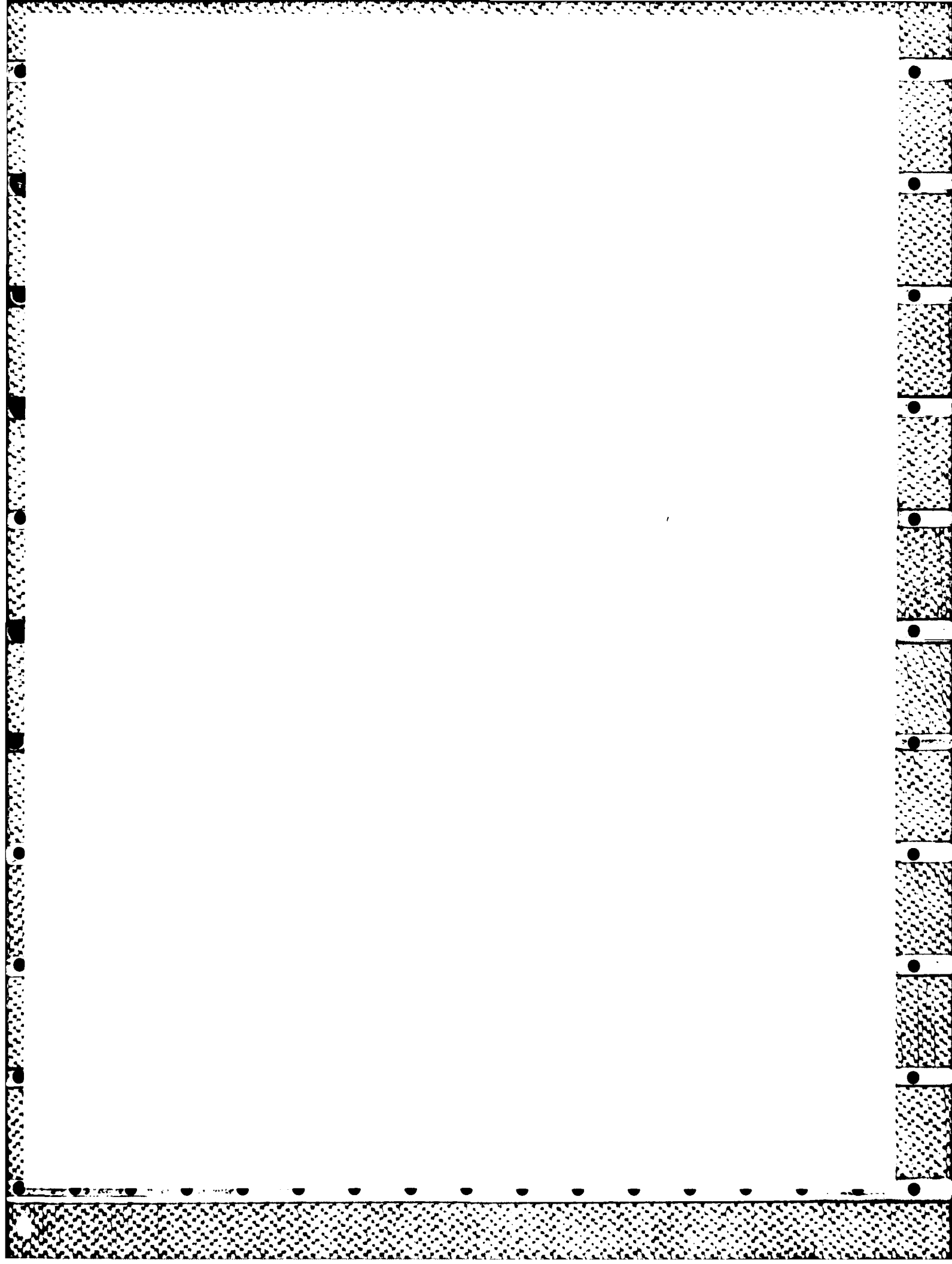
$$u(t) - g(t) = \sum_{n=0}^{N-1} a_n K_n(t) \quad (33)$$

This equation can be solved for  $K_n(t)$  because  $g(t)$  is known and  $u(t)$  is measured. The  $a_n$  are the expansion coefficients of  $u(t)$ . Once the  $K_n(t)$  are known, they are used in equation (32), which can then be solved for  $\beta(\tau)$ .

The important point is that use of the Laguerre polynomials, particularly for highly-damped, sampled data, provides a discrete approach which is highly accurate (for the number of samples) and computationally simple.

#### REFERENCES

1. Y.W. Lee, "Synthesis of Electrical Networks by Means of the Fourier Transforms of Laguerre's Functions," *Journal of Mathematical Physics*, June 1932, pp. 82-113.
2. N. Wiener, *Nonlinear Problems in Random Theory*, M.I.T. Press, 1958.
3. G.R. Spalding, "Distributed System Identification: A Green's Function Approach," *Transactions of the A.S.M.E. Journal of Dynamic Systems, Measurement and Control*, Vol. 98, June 1976, pp. 146-151.
4. L. Fox and I.B. Parker, *Chebyshev Polynomials in Numerical Analysis*, Oxford University Press, 1968, pp. 28-29.



**END**

**FILMED**

**12-84**

**DTIC**